Factors affecting perceived image quality in visual displays: chromatic aberration and accommodation, flicker fusion and visual fatigue.

Maydel Fernandez Alonso

A thesis presented for the degree of

Doctor of Philosophy

Biosciences Institute

Faculty of Medical Sciences

Newcastle University

December 2021

Abstract.

The aim of this thesis is to investigate how properties of the early human visual system interact with different types of display technologies and illuminations to determine the quality of the image perceived.

The longitudinal chromatic aberration (LCA) of the eye creates a chromatic blur in the retina that serves as an important cue for accommodation. While this mechanism can work optimally in daylight, the effects of modern narrowband illuminants are not completely known. In Chapter 2, we show that LCA causes a dioptric shift in the monochromatic accommodation response curve, while also affecting the slope and resulting visual acuity. In Chapter 3, we show that for two narrowband illuminants, observers accommodate in between the two, decreasing contrast for both, suggesting that these spectra are not optimal to maximise retinal image quality.

The relationship between luminous intensity and the maximum frequency of flicker that can be detected defines the limits of our temporal-resolving ability. It is known that critical flicker fusion (CFF) increases as a linear function of log retinal illuminance over four orders of magnitude, but as brighter displays are developed, it becomes important to expand the existing empirical data. In Chapter 4, we show that the CFF increases linearly with luminous intensity over 4 orders of magnitude, where saturation is reached.

In Chapter 5, we evaluate the impact that the screen luminance of mobile displays and ambient illuminance have on blink patterns and visual discomfort. While the research on the visual effects of prolonged computer display use is extensive, hand-held devices have not been as widely studied. The results show that lower screen contrast leads to decreased blinking activity and increased visual discomfort. Understanding the impact these factors have on ocular health can be valuable to design hardware and software features that minimise visual fatigue.

Acknowledgements.

I would firstly like to thank my supervisor Jenny Read. Her support and guidance throughout the last few years have been invaluable, and her passion for science and human vision have been a great example to have.

I would also like to thank our collaborators Gordon Love and Abigail P. Finch from Durham University for their contributions, as well as Anya Hurlbert for all her support and advise. I would also like to acknowledge the European Training Network on Full Parallax Imaging (Project number 676401) for funding part of this PhD, as well as the members of this network for the training opportunities provided.

También quiero agradecerles a mis amigas Ailec y Mónica por siempre estar ahí para mí, en las buenas y en las malas.

Finalmente quisiera agradecerles a mis padres Celia y Omar por todo su apoyo incondicional a través de los años, y por despertar en mi la curiosidad y la pasión por la ciencia y los conocimientos. Sin ustedes no estaría aquí hoy.

Table of Contents.

List of tables.

List of figures.

Chapter 1. The human visual system and the accommodation response.

In this chapter we introduce some basic concepts about the human visual system that are relevant to the work discussed in later chapters. It covers in particular the accommodative response of the visual system. In each of the chapters, the literature relevant to the topic in question is presented in more detail.

1.1. The anatomy of the human eye.

In Figure 1 we show a diagram of the human eye and its main structures. Light enters the eye through the pupil, after passing through the tear film, the cornea, and the aqueous humour, and it continues through the crystalline lens and the vitreous humour until it arrives to the retina. The iris controls the amount of light that enters the eye, increasing or decreasing the diameter of the pupil accordingly. This light is refracted by the cornea and the crystalline lens. While most of the refractive power of the eye is given by the cornea, the flexible nature of the crystalline lens is what allows us to bring into focus objects placed at different distances in the environment.

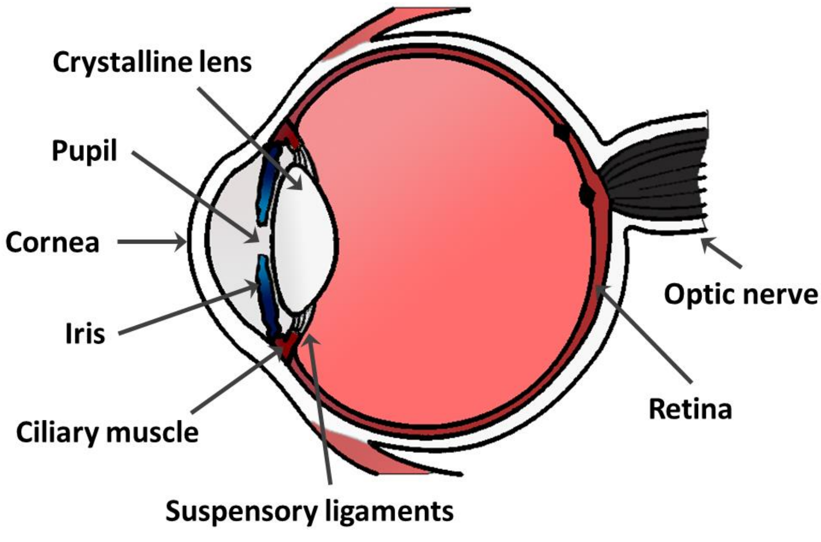

Figure 1. Basic anatomical structures of the human eye.

The crystalline lens is controlled by the ciliary muscle and attached to it by the suspensory ligaments or zonular fibres. When the ciliary muscle is relaxed, the lens is flat and allows us to focus on objects placed at farther distances. When the ciliary muscle contracts, the lens becomes thicker and increases its curvature, allowing to refract light coming from nearer distances. This process is called accommodation (see Figure 2). The range of distances for which the crystalline lens can bring an object into focus is the accommodative range and it is known to decrease with age due to the hardening of the crystalline lens. More details are given about the accommodation process in the following section.

After passing through the structures of the eye, light arrives to the retina. The retina is a light-sensitive multi-layered tissue that covers a portion of the inner surface of the eye and is responsible for transducing light information into electrical impulses that travel to the central nervous system via the optic nerve. The photoreceptors are the cells responsible for detecting the light reaching the retina, and they are the last neural layer within the tissue. This means that light must travel through the preceding layers before reaching them. In the fovea, these preceding layers are spread apart, allowing light to reach the photoreceptors directly, and they are also more tightly packed together, allowing for higher spatial resolutions to be perceived in this area. The fovea occupies about 5 degrees centrally in the visual field.

There are three main types of photoreceptors in the retina: rods, cones and intrinsically photosensitive retinal ganglion cells (ipRGCs). Rods are specialised for vision in lower light levels and are found concentrated in the peripheral areas of the retina. On the other hand, cones are more sensitive to higher light levels, being active during daytime vision, and crucially, they respond differently to light of different wavelengths. There are three types of cones according to their spectral sensitivity: S, M and L, responding to short-wavelength (~420 nm), middle-wavelength (~530 nm) and long-wavelength light (~560 nm), respectively. L and M cones are more prevalent in the retina, while S cones are significantly sparser, with the central fovea being composed exclusively of L and M cones. While each type of cell individually cannot distinguish between a change of intensity and a change in the wavelength composition of the light, the visual system is able to extract this information by comparing the signal received from the three types of cone cells. Thus, the different spectral sensitivities of the three cones are what allow us to perceive colour in our environment. Finally, ipRGCs are a type of retinal ganglion cell that express a light sensitive protein called melanopsin. This allows them to respond to light, and it has been shown they play an important role in pupil size control and human chronobiology, although whether they play a role in vision is still an area under active investigation.

Ganglion cells are one of the types of neurons that compose the remaining layers of the retina, together with bipolar cells, horizontal cells and amacrine cells. The bipolar cells transmit information from the cones and rods to the ganglion cells, while the amacrine and horizontal cells make lateral connections along these layers. Finally, the axons of the ganglion cells compose the optic nerve, that transmits information to the central nervous system.

1.2.The accommodation response.

When we fixate on an object, the lenses of the eyes automatically accommodate to the correct distance, adjusting their optical power to bring the images into focus in the retinas. The optical power required to accomplish this is inversely proportional to the distance of the target; that is, the closer the object is, the more optical power is required to bend the light rays coming from it. For this reason, the optical power of the lens is measured in dioptres (D), a unit that is equal to the reciprocal of the focal distance measured in metres.

If we express the distance of a target in dioptres, the optical power required to bring the image into perfect focus will follow a one-to-one correspondence with the distance. However, the accommodative response will not always match the accommodative demand. Studies characterizing the accommodation function of the human eye consistently find that the eye has a “resting state”, usually at around 1.5 D, where the response is the same as the demand presented by the stimulus, and where the eyes tend to return to when there is no input of light (Toates, 1972). Away from this state of tonic accommodation, the response will be less than the required for perfect focus (under-accommodation) for nearer objects, and will be greater than required (over-accommodation) for stimuli beyond this distance (Howard, 2012). A typical stimulus-response curve is showed in Figure 2. The dashed line shows the accommodative response required for perfect focus at each distance, while the continuous line shows the actual accommodative response typically found for one participant. The blue dot represents the tonic or resting state of accommodation.

Human ocular accommodation is possible thanks to the constant communication and negative feedback loop that exists between the visual cortex and the accommodative apparatus that controls the shape, and hence the optical power, of the crystalline lens (Artal, 2017). When fixation is changed from one distance to another, the new image formed in the retina will be out-of-focus or blurred. When the magnitude of blur is above the threshold of detection of the visual system (i.e. beyond the depth of focus of the eye), neural signals will be generated to activate the accommodation control apparatus and alter the optical power of the lens. This change in optical power then causes further changes in the retinal image that are processed by the visual cortex. This continues in an iterative fashion until the quality of the retinal image reaches a certain optimal state, after which accommodation will remain relatively stable or in a steady-state until a new change in retinal image contrast is detected.

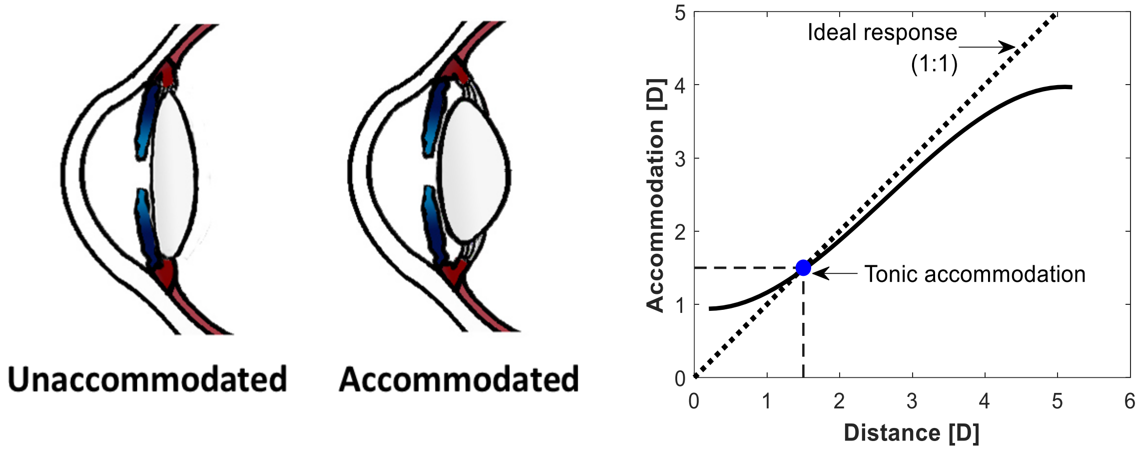

Figure 2. The accommodation response of the eye. Diagram representing an unaccommodated and accommodated eye (left), and typical accommodation stimulus-response curve (right).

During steady-state accommodation, the refractive power of the lens will experience small variations or micro-fluctuations. It has been suggested that these micro-fluctuations result in part from the flexible nature of the human crystalline lens and ocular muscles (Charman & Heron, 1988); however, the fact that the micro-fluctuations of both eyes correlate in phase and magnitude (Campbell & Westheimer, 1960; Campbell, 1960), indicates that they do not arise exclusively from the system's instabilities. Indeed, evidence seems to suggest that the low-frequency components of these micro-fluctuations are under neural control and that they help to maintain the steady-state accommodation response (Charman & Heron, 1988).

When the fixation distance changes, there are two challenges the accommodative system has to solve in order to reinstate clear vision. First, it needs to determine the direction of accommodation, that is, should the optical power increase or should it decrease to bring the new target into focus. Secondly, it needs to determine the magnitude of the response, that is, by how much the optical power needs to increase or decrease to obtain a clear image.

One of the main cues available in the blurred retinal image is defocus. This optical aberration causes that, as the object gets further away from the focal point, there will be a progressive loss of contrast in its retinal image, which will be more pronounced for the finer details or higher spatial frequencies contained in the image.

A very useful concept for understanding the effects of defocus on the retinal image is the Point Spread Function (PSF). It describes the response of an optical system to an infinitely small point of light. Even for an ideal eye that is free of aberrations, the in-focus retinal image will be degraded due to the diffraction of light at the edges of the pupil. Adding defocus will cause further spreading of the PSF (see Figure 3, left). The wider this function is, the lower the image-resolving ability of the eye will be, in particular for higher spatial frequencies.

To further understand this frequency-dependant effect, there is another useful concept that is used to evaluate the performance of imaging systems: The Optical Transfer Function (OTF). While the PSF allows us to quantify the effects of defocus on retinal image quality in the spatial domain, the OTF expresses these effects in the frequency domain. In particular, it quantifies how the contrast and phase of different spatial frequencies will be altered when imaged through an optical system. A common simplification is to disregard the phase effects and take only the contrast information, which is known as the Modulation Transfer Function (MTF). Thus, the MTF quantifies the attenuation of luminance modulation in the retinal image as a function of the spatial frequency of the object being imaged. In Figure 3 (right), we illustrate the effect that defocus has on retinal image contrast for an aberrations-free (diffraction-

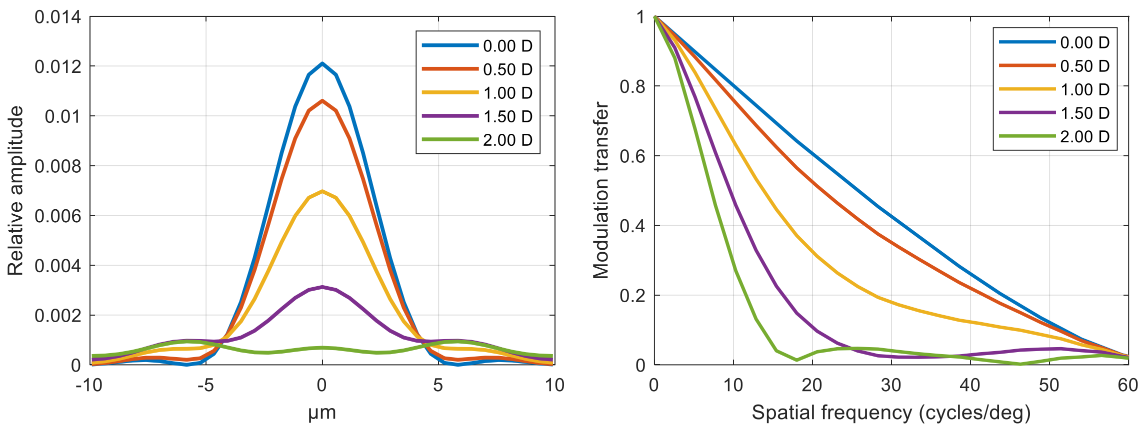

Figure 3. Representation of the Point Spread Function (left panel) and the Modulation Transfer Function (right panel), of an aberrations-free eye with different magnitudes of defocus, as indicated by the legend. The calculations were done for a diffraction-limited eye with a pupil diameter of 2 mm, and for a source with wavelength of 550 nm, using the Image System Engineering Toolbox for Biology – ISETBIO (Cottaris et al., 2019).

limited) eye. As observed, increasing defocus reduces the contrast of the retinal image, but the magnitude of the attenuation is unequal across different spatial frequencies, with it being more pronounced at higher values.

The accommodation system operates to maximise the contrast of the retinal image by adjusting the power of the crystalline lens. For this, it needs an error signal that can be minimised and used to assess when then optimal contrast has been reached. The effects of defocus on retinal image contrast and the spatial-frequency dependant effects previously discussed, can provide such a signal (Labhishetty et al., 2021). From the defocused retinal image, the visual system can extract information about the magnitude of the change in accommodation that is needed to bring an object into focus. However, pure defocus cannot give information about the direction of this change because, in a diffraction-limited eye, the loss in contrast will be the same for an object placed 1 dioptre in front or 1 dioptre beyond the focal point. In this sense, defocus is an even-error cue to accommodation, that is, it provides information about magnitude, but not the sign of the refractive error (Artal, 2017).

The accommodative negative feedback loop and the micro-fluctuations that are characteristic of the accommodative response have been proposed as a mechanism that, when combined with defocus, allows the system to determine the change in refractive power that is needed and its direction. Indeed, when the eye is focusing on a target, a single step or micro-fluctuation of accommodation in each direction could indicate whether the retinal image contrast could be improved by either an increase or decrease in refractive power. It has been shown that defocus values as small as ±0.12 dioptres can trigger an accommodative response (Kotulak & Schor, 1986), even when the blur caused by this stimulus is below the threshold for visual detection. Micro-fluctuations can vary in value between 0.04 and 0.2 dioptres (Kotulak & Schor, 1986), thus, making it possible that the visual system uses this mechanism to derive the error signal needed for the accommodative control system. However, some have postulated that this mechanism on its own would be too slow to allow for the quick and consistently accurate changes in accommodation that are possible in natural viewing (Charman & Heron, 1988), making it plausible that the system integrates this error signal estimation with other odd-error cues available.

There are several other factors that have been proposed that can indicate the sign of the accommodative error. Firstly, the visual system has access to other depth cues that indicate the distance of the target, so it can determine whether it is placed in front or beyond the focal point. In this sense, accommodation can be driven by binocular disparity (vergence-driven accommodation) and by other proximal cues (Howard, 2012). However, accommodation can also occur monocularly and in the absence of target proximity cues, meaning that these are not necessary for accommodation to occur. As a second possible factor, the optical imperfections of the human eye such as astigmatism and higher-order aberrations can serve as a directional cue for accommodation. When defocus is combined with these optical aberrations, the retinal images formed by an object in front and by an object behind the focal point can differ, which would allow the visual system to decode the sign of the refractive error. The results from a few studies seems to support this idea (Fincham, 1951; Campbell & Westheimer, 1959; Wilson et al., 2002; Cholewiak et al., 2018), although more research is needed to elucidate how strong of a role they play in accommodative control.

Finally, the longitudinal chromatic aberration of the human eye has been found to be every important odd-error cue for accommodation. This is discussed in more detail in the following section.

1.2.1. Longitudinal Chromatic Aberration as a cue to accommodation.

The refractive index of the eye decreases with an increase in wavelength. This means that its focal length is dependent on wavelength, so for a broadband light, the shorter wavelengths come into focus in front of the retina and the longer wavelengths behind the retina. This difference in the defocus of light along the axial axis of the eye is known as longitudinal chromatic aberration (LCA).

Several studies have measured the defocus caused by the LCA of the eyes. The “chromatic eye” model by Thibos et al. (1992), is the one that best predicts the data collected from multiple studies (Marimont & Wandell, 1994). It describes the refractive error of the eye as a function of wavelength through the following equation:

$$D(\lambda) = p - \frac{q}{\lambda - c} \qquad (Equation\ 1)$$

where λ is the wavelength of light in micrometres and D(λ) is the refractive error in dioptres. For the three parameters of the equation we took the values used by Marimont & Wandell (1994), such that p = 1.7312, q = 0.63346, c = 0.21410, and the reference wavelength that is kept in-focus is 580 nm. The total defocus across the entire visible spectrum is approximately

2 dioptres. An illustration of the LCA of the eye as well as a graphical representation of this equation is provided in Figure 4.

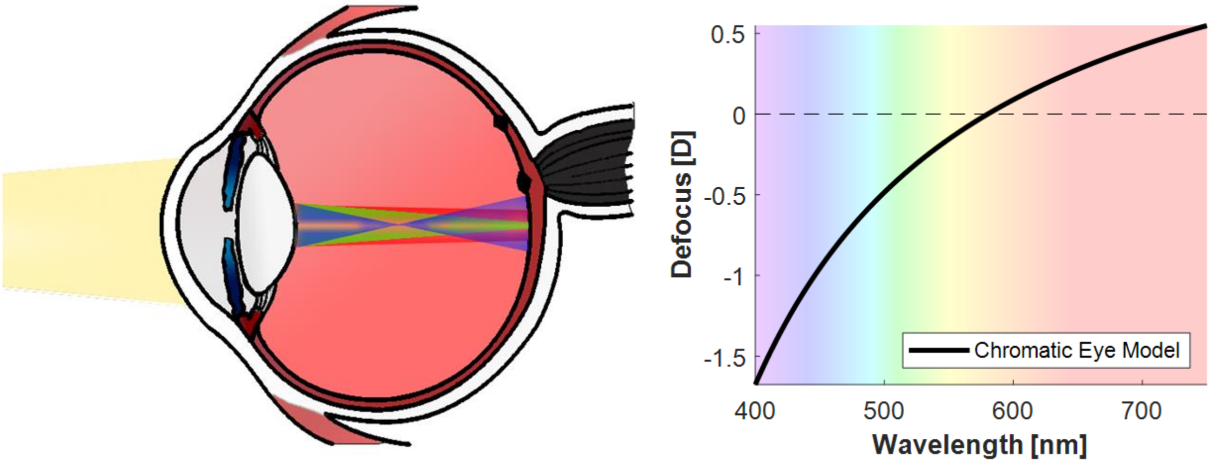

Figure 4. The longitudinal chromatic aberration of the eye. Diagram showing the change in refractive index with wavelength (left), and the defocus caused by LCA as a function of wavelength according to the chromatic eye model (right).

The defocus caused by LCA has several implications for visual perception in polychromatic light. While fixating on a target, the eye can only accommodate for one wavelength of the light coming from that point. This means that wavelengths shorter and longer than the one in focus, will create blur in the retina. Some studies have provided evidence that image quality can be reduced in polychromatic light compared to monochromatic light (Campbell & Gubisch, 1967; Aggarwala et al., 1995), and that contrast sensitivity is greater if chromatic aberration is corrected with achromatic lenses or reduced by using monochromatic light (Yoon & Williams, 2002; Williams et al., 2000; Artal et al., 2010).

The variation in defocus for different wavelengths will also mean that there is a greater depth of field in polychromatic light, that is, there is a greater range of accommodation values for which the image will appear acceptably sharp in the retina. Evidence from previous studies suggest that depth of field is indeed greater in polychromatic light than when chromatic aberration is corrected (Campbell, 1957) or minimised by using monochromatic light (Campbell & Gubisch, 1967). More recent studies have showed results with similar values (Marcos et al., 1999), with the depth of field in polychromatic light found to be 1.4 times larger than in monochromatic light (Campbell & Gubisch, 1967; Marcos et al., 1999). However, Marcos et al. (1999) suggested that the impact of this increase would be minimal, due to the reduced sensitivity of the visual system at long and short wavelengths of light.

An increased depth of field in polychromatic light has been proposed as a possible explanation for the non-linearity of the human accommodation function. A steady-state error is typically found when accommodation is measured for different distances with white light, and it has been proposed that this could be explained by a change in the component wavelength that is brought into focus at different distances (Ivanoff, 1949). For nearer distances, short wavelength components would be brought into focus, while for further distances, long wavelength components would be the ones in focus. Due to the increased depth of field, the image formed in the retina would remain acceptably sharp in both conditions. However, evidence already exists against this idea (Bobier et al., 1992; Labhishetty et al., 2021).

In addition to reducing retinal image contrast and increasing the depth of field, the LCA of the eye could be an odd-error cue to accommodation. In polychromatic light, depending on whether the target the observer wants to attend to is placed in front or beyond the current focal point, different wavelength components of its retinal image will have greater defocus. When the object is placed in front of the focal point, the long wavelength components will have more defocus than the short wavelengths; and when the object is placed beyond the focal point, the shorter wavelengths will have greater defocus. Several studies have tested this hypothesis, and there is now considerable evidence that LCA helps the accommodation system respond correctly by providing a direction signal.

Fincham (1951) found that 60% of his subjects had difficulty or could not accommodate at all when their chromatic aberration was minimized by using monochromatic light or neutralized by an achromatic lens. Fincham's findings were corroborated by Campbell & Westheimer (1959), who devised an experiment in which the participants had to adjust the position of a monocularly viewed out-of-focus target within an optical system, while they introduced changes in the illumination. They concluded that most subjects do use chromatic aberration as a directional cue for accommodation, although they can use other cues when chromatic aberration is not available. Other researchers have used high-speed optometers to measure the refractive error of the eye while they introduce changes in the illumination of the fixation target. Evidence from these studies shows that both dynamic and steady-state accommodation are more accurate in polychromatic or white light than in monochromatic light (Kruger & Pola, 1986; Kruger et al., 1993; Kotulak et al., 1995; Aggarwala et al., 1995; Aggarwala et al., 1995). Furthermore, correcting LCA in white light with an achromatic lens has a similar effect to accommodating in monochromatic light (Aggarwala et al., 1995), that is, it increases phase lag (i.e., the angular difference between stimulus and response phase) and decreases accommodative gain (i.e., the ratio of response to stimulus amplitude). Some of these studies have also measured dynamic and steady-state accommodation while reversing the LCA of the eyes with special lenses (Kruger et al., 1993; Aggarwala et al., 1995; Kruger et al., 1997). In those cases, the accommodative response was inhibited and severely disrupted, with some participants not being able to maintain focus in those conditions (Kruger et al., 1997). Overall, there is a substantial amount of evidence that indicates the visual system does indeed uses LCA as an odd-error cue for accommodation; and although some participants are able to take advantage of other directional cues, the polychromatic blur caused by LCA seems to be advantageous in increasing the speed and accuracy of dynamic accommodative responses.

1.2.2. Accommodation and modern visual displays.

The human visual system has the ability to extract the three-dimensional structure of a scene from two-dimensional retinal projections. To do this, it relies on a large number of visual cues (*i.e.,* variations in the properties of the retinal images) that in the natural world correlate with a change in depth. Understanding the mechanisms by which the visual system extracts and integrates this information has been of great interest to vision scientists, but it is also a relevant problem for the design, assessment, and use of visual display systems.

An ideal visual display would be one that provides images that are indistinguishable from those provided by a real environment. This means that such a display would need to deliver consistent information from all the visual depth cues that are available in the natural world. Creating realistic three-dimensional experiences has been a very active area of research and development, and as technology has progressed, engineers have been able to integrate a larger number of depth cues into visual displays.

In recent years, stereoscopic 3D displays (S3D) have experienced numerous improvements, with significantly enhanced image quality over previous generation technology. S3D displays provide a compelling sensation of depth to the viewer by projecting slightly different images to each eye. This technology makes use of binocular disparity, as well as other depth cues that are available in conventional displays (e.g., linear perspective, texture gradient, occlusion), to recreate scenes. In addition, some S3D displays include head tracking to provide motion parallax, that is, to update the images correspondingly as the eye translates. However, there is one type of depth cue that remains to be quite challenging in the development of digital displays: the focus cues. This is where S3D displays fall short and where new display technologies currently in development could have significant advantages in terms of realism and visual performance.

Our understanding of how stereo and focus cues affect viewer experience has grown substantially in the past few years, greatly thanks to the rising number of new technologies that support them. Both focus and stereo cues share a few similarities: they have both a retinal component and an associated oculo-motor response, and they are what we refer to as depth cues based in triangulation (Banks et al., 2016). The retinal component of stereo cues is binocular disparity, the difference in location between the retinal projections of an object seen by the two eyes. Blur is the retinal component of focus cues, and it results from the defocus caused by light rays passing through different parts of the pupil. They are cues based in triangulation precisely because they result from integrating information from different vantage points: disparity derives from the different positions of the two eyes and blur from light rays entering different parts of the pupil. Both of these components have an oculo-motor response associated to them. Binocular disparity triggers vergence, which is the simultaneous movement of both eyes in opposite directions to fixate on a target, and blur in the retinal image triggers accommodation.

It has been stated before that focus cues – retinal-image blur and accommodation – are weak and imprecise cues for indicating depth (Mather & Smith, 2002), and thus, do not have a significant effect in seeing three-dimensionally. In this sense, stereo cues – binocular disparity and vergence – have been considered the pre-eminent cues to depth perception. Estimating the 3D structure of a scene from binocular disparity is indeed very precise, and does not depend on regularities of the environment, like perspective-based cues for example; but our visual system only encodes disparities up to approximately one degree from the point of fixation (Read, 2012), so away from that, other cues are necessary to estimate depth.

Held *et al.* (2012) used a novel volumetric display to present images at different distances and compared different conditions where the distance was indicated only by binocular disparity, only by retinal-image blur, or by both cues consistently. When disparity was the only available cue, estimations of distance close to the fixation plane were highly precise, but as the objects were placed away from it, the estimations became highly inaccurate. On the other hand, when retinal-image blur was the only accessible cue, the thresholds for distance estimation remained roughly constant, and while they were higher than those based on disparity near the fixation plane, a few centimetres away from that, distance judgements based on retinal-image blur became more accurate. This study provided evidence that disparity and blur are complementary cues to depth.

Other studies have provided evidence that accommodation can also be used by the visual system to extract information about depth. As the eye looks around a natural scene, neural commands are sent to the ciliary muscles to change the focal power, and thereby minimize blur for the fixated target. The efferent signal to these muscles controlling the crystalline lens could be used as a cue for depth because the focal power required to focus the image depends directly on the distance from the eye to the fixated object. Mon-Williams & Tresilian (2000) used a manual pointing task to examine distance estimates in the absence of any other depth cue apart from accommodation. They found that the observers' estimates correlated with the target distance, but the accuracy was poor and variability high. Similarly, Fisher & Ciuffreda (1988) measured both subjective distance estimates and the refractive state of the participant's eyes while introducing variations in the accommodative demand in the absence of any other depth cue. They found that apparent distance correlated with accommodation, although it tended to exceed it, and that there was considerable intersubject variability in the accuracy of the distance judgements. These findings suggest that accommodation can act as a source for depth estimation in the absence of other cues, although its contribution to depth perception in multiple-cue conditions is not yet clear.

The evidence that focus-cues are indeed an important source for depth perception has significant repercussions for visual displays. In current stereoscopic displays, the focal distance remains constant, thus, as the eye looks around a virtual scene, its accommodative state stays the same. This means that both the neural commands that control accommodation and the blur gradient that is formed in the retina specify a flat scene, while stereoscopic cues indicate variations in depth, creating a conflict between the information conveyed by both cues. This mismatch has additional implications for visual perception, not only because of the discrepancy in the specified depths, but because of the neural link that exists between accommodation and vergence oculo-motor responses. Furthermore, as both responses are neurally coupled in the visual system, that is, stimulating one will evoke a corresponding change in the other (Fincham & Walton, 1957), a conflict between these cues creates discomfort and fatigue in the viewer and limits visual performance (Banks et al., 2008; Shibata et al., 2011; Kim et al., 2014). For these reasons, recent years have seen a growing amount of interest and effort to develop visual displays that can provide correct focus cues. However, in order generate content that recreates the accommodative stimulus of natural viewing conditions, we need to understand which components of such stimulus drive accommodation.

Chapter 2. The effect of longitudinal chromatic aberration on the accommodation stimulus-response curve.

2.1. Introduction.

One of the main differences between digital displays and the natural environment is in the spectral distribution of the light they emit or reflect. While daylight is composed of a smooth spectrum and natural objects tend to have broad spectral reflectance functions (Krinov, 1947), most digital displays take advantage of the fact that human vision is trichromatic and make use of only three lights or primaries to show us different images. These primaries – red, green, and blue– give rise to a spectral distribution with multiple narrowband peaks rather than a smooth spectrum, with modern displays increasingly making use of particularly narrowband light sources such as Light Emitting Diodes (LEDs) and lasers. As these lights differ significantly from the natural light the human visual system evolved to accommodate under, it is important to understand how they affect the accommodative response of the eye in order to be able to improve or maximise the quality of the image perceived in these displays.

Narrowband primaries might in particular, affect the way the visual system makes use of the LCA of the eye to aid accommodation. As discussed previously, the polychromatic blur caused by LCA in broadband light serves as an important cue to accommodation (Fincham, 1951; Kruger et al., 1993). This blur would be significantly reduced when accommodating under the individual narrowband primaries of a display. Furthermore, LCA would cause a shift in the best-focus distance for each individual wavelength, so observers would need to adjust their response accordingly.

Previous studies have demonstrated that both reduced spectral bandwidth and removing the LCA of the eye as a cue can negatively impact the accuracy of the dynamic accommodation response of the eye. Kruger et al. (1993) measured the accommodation responses of 25 participants to a sinusoidally moving target illuminated by either white broadband light or a narrowband light of 10 nm spectral bandwidth, while the LCA of the eye was either normal, removed, or reversed (i.e., blue light would come into focus behind the retina and red light in front). They found that accommodative gain decreased, and phase lag increased, when the LCA of the eye was neutralised as well as when the target was illuminated by monochromatic light. Furthermore, reversing the sign of LCA severely disrupted the accommodation response of observers and their ability to track the object while moving in depth. In a later study, Aggarwala et al. (1995) showed to eight participants a sinusoidally moving target illuminated by lights of 10 nm, 40 nm and 80 nm of spectral bandwidth and similar peak wavelengths around 550 nm, as well as a broadband white light with a smooth spectral distribution. Their results indicated that as the spectral bandwidth of the light increased, accommodative gain increased and phase lag decreased, with the broadband white light enabling significantly more accurate dynamic responses than even the 80 nm spectral bandwidth light. These authors performed another similar study where the sinusoidally moving target was illuminated either by one of ten narrowband lights of 10 nm spectral bandwidth and peak wavelengths between 430 nm and 670 nm that were viewed through an achromatizing lens, or by a white broadband light that was viewed with and without the achromatizing lens (Aggarwala et al., 1995). They found that accommodative gain tended to be higher and phase lag lower when the target was illuminated by white light with LCA intact (i.e., without using the achromatizing lens); however, their results also indicated that there was great inter-subject variability in the accommodative responses to the stimuli between the six observers that took part. Two subjects showed a decreased gain when accommodating to shorter wavelengths but accommodated reasonably well to longer wavelengths, two others showed a decreased gain and slightly increased phase lag when accommodating to the longer wavelength lights when compared to shorter wavelengths, and the two final subjects showed a decreased gain for all monochromatic stimuli and in particular, a severely disrupted accommodative response to longer wavelengths, with considerably decreased gains and increased phase lag. These last two subjects were also the most affected by the removal of the LCA cue in white light, with other participants showing a more modest effect. The authors concluded that narrowband illumination was a poor stimulus for accommodation and suggested that visual displays that used narrowband primaries were likely to reduce the ability of the eye to maintain accurate focus, albeit there was significant variability between observers, as some of the subjects seemed to be able to track some of the monochromatic targets moving in depth and accommodate to them reasonably well.

Other studies however, have not found evidence that the absence of LCA has a detrimental effect on accommodative responses, particularly when the targets are stationary. Bobier et al. (1992) measured the accommodation stimulus-response curves of six subjects for a broadband target when the LCA of the eye was normal, neutralized, increased, and reversed.

They found that the slopes of the accommodation functions did not change in any of the subjects for any of the conditions tested, with only one subject showing an effect on the reversed LCA condition, with a lower intercept and steeper slope. Thus, it seems that neither removing or increasing LCA had a significant effect on the accommodation response of participants, and even when the sign of chromatic blur produced by LCA was reversed, participants were able to maintain their steady-state accommodation responses. Furthermore, when looking at the variability of the responses under broadband and narrowband illumination for stationary targets, Atchison et al. (2004) found that none of their five observers had significantly more intra-trial variability in their accommodation when looking at targets illuminated by narrowband red or blue light, than when observing targets illuminated by broadband white light, suggesting that they were able to maintain focus just as well under reduced spectral bandwidth.

It is possible that these differences in results reflect the fact that LCA might be a more useful cue to dynamic accommodation than to steady-state responses. This would mean that the visual system uses LCA to detect when a change in accommodation is required, as well as the direction of the change, but once it is focused on a target, it is able to maintain accommodation via other cues or mechanisms. Kotulak et al. (1995) found evidence that this might be the case. They measured both dynamic and steady-state responses to stimuli of varying spectral bandwidth and found that increasing bandwidth caused an increase in the gain of dynamic responses (although no differences in phase lag), but that it had no effect on the steady state-error of accommodative responses to stationary targets. However, a set of later studies by Kruger et al. (1997) provided evidence contrary to this. In a first experiment, eight participants viewed stationary square-wave grating targets placed at distances of 0, 2.5 and 5 dioptres, and under three conditions of illumination: monochromatic light (550 nm ±10 nm bandwidth), white broadband light with normal LCA, and white light where the LCA of the eye had been reversed. They found that all subjects accommodated accurately in the normal LCA condition, 38% of the subjects had difficulty maintaining focus in monochromatic light at near and far (5 and 0 dioptres), and 88% of the subjects could not maintain focus at both near and far when LCA was reversed. They speculated that the detrimental effects of reduced spectral bandwidth on the steady-state accommodation response were only detectable at distances that were far away from the tonic state of accommodation, and that this was the reason for the differences in findings with previous studies, as those had used distances that were nearer the resting accommodative state of the eye. Furthermore, in another experiment they showed that accommodation responses to a stationary target changed when the relative contrast of the red, green, and blue primaries was altered, indicating that the visual system does use LCA as a cue to maintain the best point of focus. This agrees with more recent publications that have shown that presenting images that simulate the chromatic blur caused by LCA triggers a change in accommodation responses, even when other cues such as defocus, micro-fluctuations and higher order aberrations would be indicating that the best focus was already at the distance of the screen (Cholewiak et al., 2017, 2018). Thus, it seems that LCA is also an important cue for steady-state accommodation responses, and that the reduced spectral bandwidth of narrowband primaries in a display could impair the accuracy of this response, particularly at near and far distances.

As mentioned previously, in addition to a reduced spectral bandwidth, narrowband primaries of different peak wavelengths would also impose different accommodative demands due to the defocus caused by LCA. Multiple studies have shown that when accommodating to monochromatic or narrowband stimuli of different wavelengths, there is a dioptric shift in the accommodation response in the direction predicted by LCA, that is, higher accommodation for longer wavelengths and lower for shorter ones (Donohoo, 1985; J. V Lovasik & Kergoat, 1988; J. Lovasik & Kergoat, 1988; Charman, 1989; Seidemann & Schaeffel, 2002), albeit the magnitude of the dioptric shift has not always been up to the magnitude predicted by the LCA defocus (Donohoo, 1985). However, these studies have usually tested targets placed at only one or two fixed distances, rather than sampling the accommodation response at multiple points.

Only few studies to date have looked at the effect that narrowband light of different wavelengths has on the accommodation stimulus-response curve of observers. Charman and Tucker (1978) measured the accommodation of seven subjects at multiple target vergences for white light and for different narrowband illuminants. Most of their participants were experienced observers and were able to accommodate under monochromatic light as accurately as under white light; however, their one naïve observer was not initially able to accommodate to the narrowband targets, requiring further training in the task to be able to maintain accommodation for these stimuli. They also found that there was a dioptric shift in the accommodation responses of participants with wavelength, but no difference in their accuracy, such that the stimulus-response curves of one subject showed similar lags and leads for all colours tested. They did find however, that for blue light some observers had a slightly shallower slope, which they attributed to a combination of a small increase in LCA with accommodation (of ~3% per dioptre of accommodation), as well as reduced acuity for blue light in some subjects.

More recently, Jaskulski et al. (2016) measured the subjective depth of field of seven subjects for targets at distances of 0, 2 and 4 dioptres, and when illuminated under white light and monochromatic red, green and blue light. The measurements were performed in the paralyzed eye, while the higher order aberrations of the accommodated eye of each participant was simulated using an adaptive optics system (and from measurements obtained previously). They found that the slopes of the best focus position as a function of accommodative demand were lower than one, but similar between monochromatic and white light. Furthermore, they found no significant differences in the subjective depth of field under different monochromatic lights, and the depth of field for white light was greater at all distances by approximately 14%, although the differences were not statistically significant.

There are some limitations in these two studies that should be considered. Firstly, they both used a relatively small sample of mostly well-trained observers with experience in accommodation experiments, as described by the authors. We have seen so far that there can be significant inter-subject variability in the responses to monochromatic stimuli or to broadband stimuli when LCA has been removed or reversed (Aggarwala et al., 1995), which can explain some of the contradictory findings in the literature; and naïve observers can struggle to accommodate in monochromatic light without receiving training beforehand (Charman & Jill Tucker, 1978). This means that these findings might not be representative of the general population or the average untrained user of visual displays. Furthermore, Jaskulski et al. (2016) paralyzed the accommodative and pupil response of the eye and estimated accommodation from the subjective reports of perceived blur from the observers, which might not be a good indication of their real accommodative responses with natural pupil sizes.

Thus, in the experiments described in this chapter, we aimed to have a larger overall sample with a greater proportion of untrained observers. Furthermore, we allowed the accommodation and pupil size of observers to vary freely, in order to increase the ecological validity of the results and more closely match a real-life scenario of subjects viewing images in a digital display with narrowband primaries. Finally, we also concurrently measured visual acuity using a staircase procedure to explore the impact that any difference in accommodation to narrowband stimuli might have on the ability of subjects to resolve small targets, when compared to accommodation in broadband light where LCA is available as a cue.

As we have seen, there is evidence that both the dynamic and steady-state responses of the visual system might be negatively affected by the reduced spectral bandwidth of narrowband lights such as LED primaries. Our aim is to measure the accommodation stimulus-response curve under narrowband illuminants of different wavelengths and compare it to the accommodation function under broadband white light, as well as to determine the effect that any differences in accommodation might have on visual acuity.

2.2. Methods.

In this section we describe the methods used in three experiments where we measured the observers' accommodation response curve to different spectra. In experiments 1 and 2, the accommodation function was sampled by changing the physical distance of the stimuli, with the angular size of the diffuser and target changing concurrently in experiment 1 and being kept constant in experiment 2. In experiment 3, the accommodation function was measured by using trial lenses to simulate a larger range of optical distances, and the visual acuity of participants was measured concurrently.

The experiments were implemented in a sequential manner, such that the results of the previous stage informed the design and experimental setup of the following experiment. Here we briefly explain the rationale behind each of them. Experiment 1 had the simplest setup and served as a pilot study, allowing us to gain the first insights into the accommodation response of participants to different wavelengths. Since the same physical size of diffuser and fixation target was used at all distances, their angular size was changing concurrently as a result. To address this, in experiment 2, we changed the physical size of the diffuser and accommodative target as a function on distance, maintaining its angular size constant. However, the setup used for these two experiments limited the range of physical distances at which we could present targets, due to restrictions imposed by the measuring device. To circumvent this, in experiment 3 we used lenses to simulate a larger range of distances and measure the accommodation stimulus-response curve more fully. Furthermore, we wanted to concurrently measure visual acuity using a psychophysical procedure in order to understand the effects that the accommodative responses had on retinal image contrast. To do this, we needed a device capable of presenting spatial information dynamically, that used narrowband illumination or primaries, and that had a small enough pixel size such that visual acuity could be measured over a large range. We chose a smartphone display that used LED primaries, and that due to its high resolution and small physical size, allowed us to measure visual acuity thresholds as good as logMAR -0.66 (equivalent to 20/4), which is well beyond "normal" human visual acuity (logMAR 0 or 20/20).

In the following sections, more thorough detail is given about the methods used in each experiment. Experiments 1 and 2 used the same apparatus, thus, they are described together, while experiment 3 is described separately where necessary.

2.2.1. Participants.

Data were collected from 22 adults in total, with ages between 23 and 33 years old (mean 26.63, SD 7.26), out of which 13 were female and 9 were male. From this total sample, 2 participants took part in both experiment 1 and 2, and 2 participants took part in all three experiments. The data collected from 1 participant were excluded due to persistent sleepiness and having their eyes closed for a significant portion of the experiment. All but 3 participants were naïve as to the aim and hypothesis of the experiment. Table 1 shows the breakdown of the sample for each individual experiment.

Participants were recruited from students, staff, and the external pool of participants of the Biosciences Institute of Newcastle University for experiments 1 and 2, and only from students and staff of the Institute of Biosciences for experiment 3. The study was approved by Newcastle University Ethics Committee (reference number 15327/2016) and written consent was obtained from each subject.

In experiments 1 and 2, only participants that did not require visual correction (i.e., spectacles or contact lenses) to read or perform other daily activities were selected. The mean visual acuity of the sample was logMAR 0.03 with a range between logMAR -0.1 and 0.23. This means that the smallest characters they could read had a stroke width of 1.1 arcmin on average, with a range in the sample between 0.8 and 1.7 arcmin. In experiment 3, as recruitment was limited to staff and students, two of the ten participants normally used spectacles to read or perform activities at near distances (with corrections of approximately -0.7 D and -2.5 D) but performed the experiment without them, as they would change the intended accommodative demands.

Experiment	**Participants**	**Mean age (± SD)**	**Sex**	**Excluded**
Experiment 1	9	27.0 (± 2.7)	5 females, 4 males	1
Experiment 2	9	25.9 (± 2.5)	4 females, 5 males	0
Experiment 3	10	29.5 (± 2.4)	6 females, 4 males	0
Total	22	27.9 (± 2.9)	13 females, 9 males	1

Table 1. Sample description for experiments 1, 2 and 3. The total shows the number of unique participants for all three experiments.

2.2.2. Apparatus: Experiments 1 & 2.

The stimulus consisted of a Maltese cross printed on a transparent film and placed on top of a diffuser, which was mounted on a box containing six Light Emitting Diodes (LEDs) and centred to the right eye. The box was placed on a 2.5m long rail positioned at the height of participant's eyes, which allowed to change the physical distance of the stimulus. The stimulus was presented at six distances between 3 D and 0.5 D in steps of 0.5 D (corresponding to metric distances of 33.3 cm, 40 cm, 50 cm, 66.7 cm, 100 cm, and 200 cm).

For experiment 1, we kept constant the physical size of the diffuser (8.5 by 8.5 cm) and the Maltese cross (5 by 5 cm) across the different distances, thus, changing its angular size. The angular size of the diffuser changed between 14.5° and 2.4° in steps of 2.4° for the different distances, while the angular size of the Maltese cross changed between 8.6° and 1.4° in steps of 1.4°. For experiment 2, we kept the angular size of the diffuser and the Maltese cross constant across the different distances at 2.5° and 1.5° respectively. This was achieved by using stimuli that were of different physical size according to the distance at which they would be presented.

The refractive state of the eye and the pupil diameter was measured dynamically at 50 Hz using a photorefractor with pupillometry capabilities (the PowerRef 3 from PlusOptix, further details are given in section 2.2.4). Two Arduino Uno boards controlled the stimuli and were connected to the photorefractor to synchronise the recordings with the stimuli. A representation of the experimental setup is shown in Figure 5.

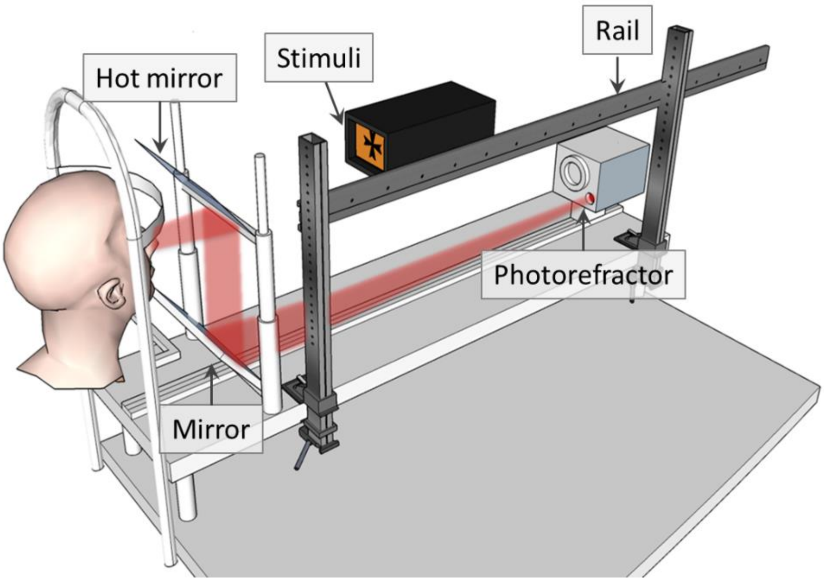

Figure 5. Diagram of the experimental setup.

The different spectra were created using six LEDs, five of which were narrowband and one white LED, with the latter being combined with the narrowband LEDs to create a broadband spectral distribution that approximated a D65 illuminant (see Figure 6). A driver circuit was built for each of the LEDs, and their luminance was controlled through pulse-width modulation from the Arduino Uno boards (at a frequency of 980 Hz). The circuit was designed such that the luminance of the LEDs varied minimally over time, by increasing the resistance and decreasing the current through each LED. During the first 10 seconds after each LED was turned on, the luminance remained constant for all LEDs except the red one, for which luminance decreased by ~0.7 cd/m2. Radiance measurements of the LEDs were taken with a CS-2000 Konica Minolta spectroradiometer at different duty cycles and over time. These measurements were used to calculate the luminance of the LEDs, as well as their peak wavelength and full width at half maximum (FWHM). The luminance and peak wavelength were calculated using the CIE physiologically-relevant luminous efficiency function (Stockman et al., 2008), and it was found to be a linear function of duty cycle for each LED. During the experiment, the luminance of the stimuli was kept constant at 10 cd/m^2. The peak wavelegth and FWHM were calculated by multiplying the radiance spectral distribution by the luminous efficicency function. While the chromatic aberration is a pre-perceptual phenomenon, the wavelenght-dependant sensitivity of the visual system will determine where the peak brightness and highest retinal contrast is reached during accommodation. For this reason, we used the luminance-weighted spectra to calculate the defocus caused by LCA for each LED. In practice, due to the lights being narrowband, this had a negligible in the peak wavelength and corresponding defocus values.

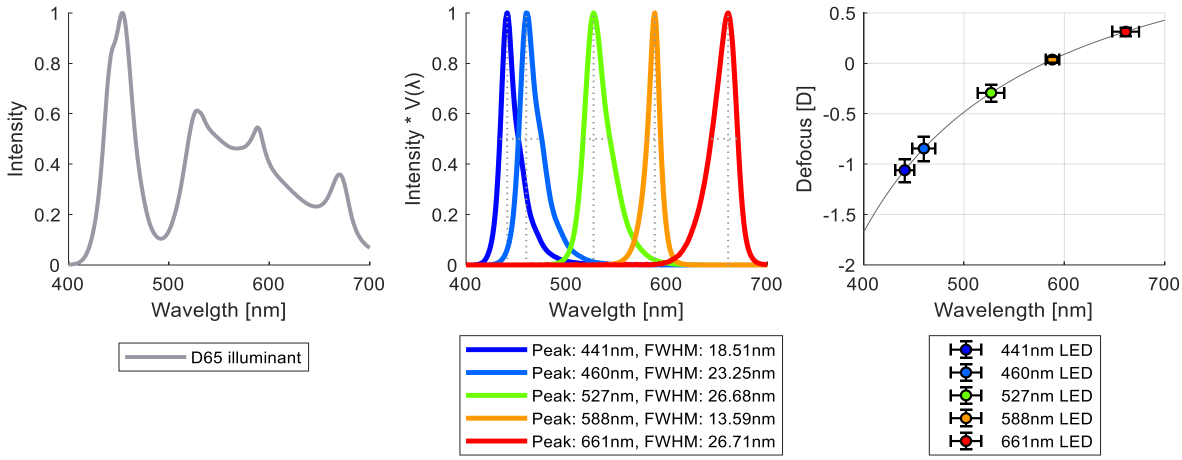

Figure 6. Normalised spectral distributions of the D65 broadband illuminant (left) and the narrowband LEDs (middle), and the defocus caused by LCA for the peak wavelengths of the LEDs calculated with Equation 1 (right), with horizontal error bars representing the FWHM and vertical error bars the corresponding spread in defocus.

2.2.3. Apparatus: Experiment 3.

The stimulus consisted of different Landolt C figures that were presented in an Active-Matrix Organic Light Emitting Diode (AMOLED) screen placed at a fixed distance of 1 m (1 D). The screen had a size of 6.84 cm by 12.2 cm, and a resolution of 1080 by 1920 pixels, and was from a OnePlus 3T mobile phone device.

To simulate the defocus caused by viewing the stimuli at different distances, 9 trial lenses were used with powers that ranged from -2 D to 7 D in steps of 1 D. The stimuli were viewed through the lenses, which were placed over the right eye in light-tight goggles. The left eye was covered by a 720 nm infrared filter that occluded the visual stimuli while allowing the refractive state and pupil diameter of the eye to be measured by the PowerRef 3 photorefractor. Accommodation and pupil control are yoked consensual responses (Spector, 1990; Marran & Schor, 2000). This means that even when only one eye is being stimulated, an equal pupil and accommodative response to the stimulus will be observed in the occluded eye, making it possible to measure these responses in the contralateral eye to where the stimuli are being presented.

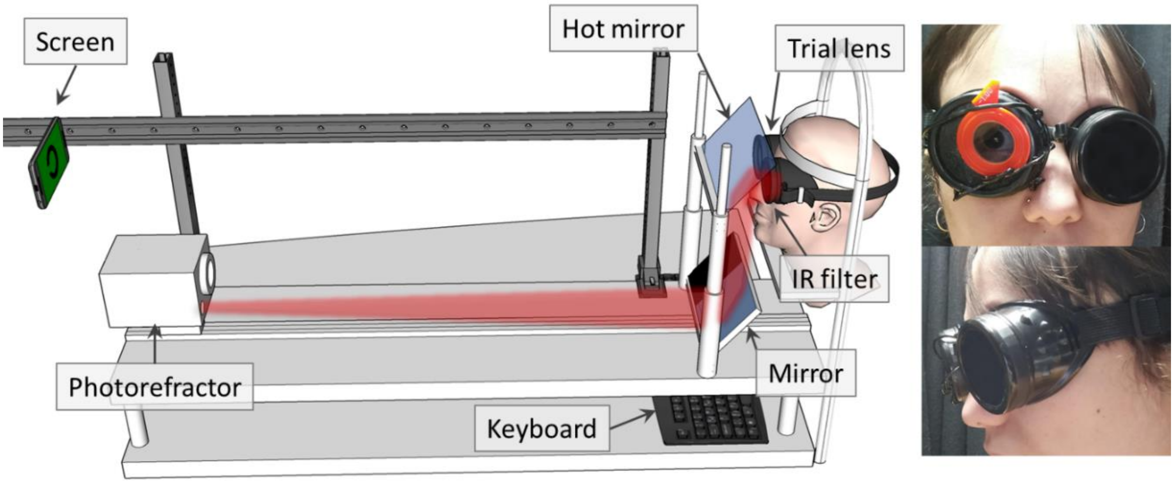

Figure 7. Representation and photos of the experimental setup.

A graphical representation and photos of the experimental setup are shown in Figure 7. The AMOLED screen and experimental routine were controlled from a computer running MATLAB (The MathWorks Inc., 2019), which was also connected to the photorefractor to synchronize the stimuli being presented with the recordings. The Landolt C figures were dynamically created using the Psychophysics Toolbox (Kleiner, M., Brainard, D. and Pelli, 2007). Figure 8 shows the spectral distributions of the screen primaries, as well as the defocus caused by the LCA of the eye for their peak wavelengths (Thibos et al., 1992).

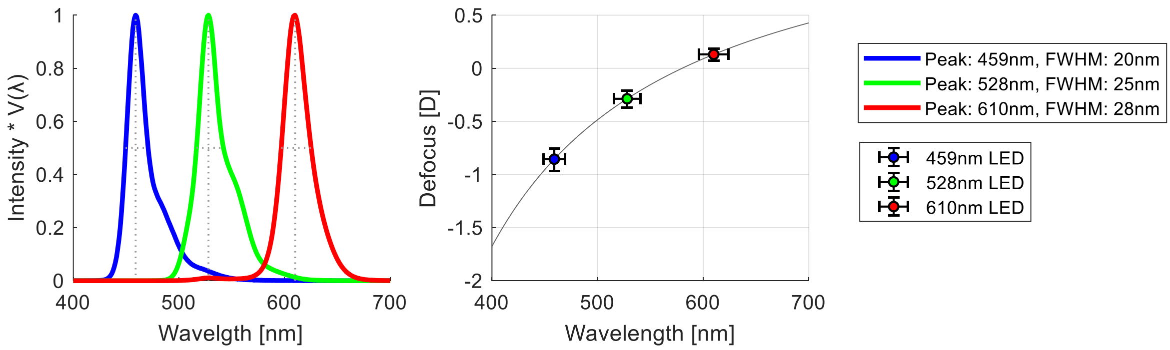

Figure 8. Normalised spectral distributions of the screen LED primaries (left), and the defocus caused by LCA for their peak wavelength as calculated with Equation 1 (right), with horizontal error bars representing the FWHM and vertical error bars the corresponding spread in defocus.

Radiance measurements of the screen primaries were taken with a CS-2000 Konica Minolta spectroradiometer at different intensities and over time. The peak wavelength and luminance of the LEDs were calculated using the CIE physiologically-relevant luminous efficiency function (Stockman et al., 2008). During the experiment, the three primaries of the screen were used at a fixed luminance of 15 cd/m^2 when used on their own to give narrowband illumination, and when they were combined to create a broadband illumination, each primary was given a luminance of 5 cd/m^2 for the same total luminance of 15 cd/m^2.

2.2.4. Photorefractor calibration.

The photorefractor used in these experiments consists of an array of nine infrared LEDs (peak wavelength of 850 nm) located eccentrically below an infrared camera that records at 50 Hz. Two mirrors reflect the infrared light into the retina (see Figure 7), which diffusely reflects this light back into the camera, and depending on the refractive state of the eye, the light reflected will vary in intensity vertically across the pupil. An inbuilt calibration factor then converts this slope of intensity across the pupil into a defocus value that indicates the refractive state of the eye.

This slope-based eccentric infrared (IR) photorefraction offers a convenient non-invasive way to measure refraction dynamically over a large range of dioptric values (-7 D to 5 D from the camera position at 1 D) and pupil sizes (~3 mm-8 mm); however, the accuracy of the results will largely depend on the calibration factor, which is often obtained from a sample of mostly Caucasian individuals. Previous studies have demonstrated that ethnic differences (Sravani et al., 2015) and further inter-individual differences (Bharadwaj et al., 2013; Ghahghaei et al., 2019) affect this calibration factor, reducing the accuracy of the results. They have also suggested how a correction factor specific to each individual can be quickly found and used to reduce these errors significantly (Bharadwaj et al., 2013; Sravani et al., 2015), that is independent of the viewing distance used (Ghahghaei et al., 2019).

To find this individual correction factor we followed the method described by Sravani et al. (2015). A fixation stimulus illuminated by the green LED is presented at 1 D from the participant and viewed monocularly through the opposite eye for which the calibration was being performed. The eye being calibrated (right eye in experiments 1 and 2, and left eye in experiment 3) was covered by an infrared filter, allowing to measure its refractive state while occluding the stimulus. A series of trial lenses from -4 D to 7 D in 1 D steps were also placed in front of this eye, and refraction was measured binocularly for at least 30 seconds for each of the lenses. This method allows to obtain the defocus measured by the photorefractor for objective values of defocus introduced for the calibrated eye through the trial lenses, while also accounting for the changes in accommodation by concurrently measuring the refraction of the left eye that views the stimulus. An individual correction factor was obtained by plotting the average differences in refraction between the two eyes as a function of the trial lens used and fitting a linear regression through the linear portion of this function (which was determined using a similar procedure to the one described later in section 2.3.1). The inverse of the resulting slope was then used to rescale all the refractive data obtained for this participant. An example of the results of the calibration procedure obtained for one subject are shown in Figure 9. In experiment 3, to account for the differences in refractive error between the two eyes, the average refractive difference with no trial lens (0 D) was obtained for each participant and subtracted from their data.

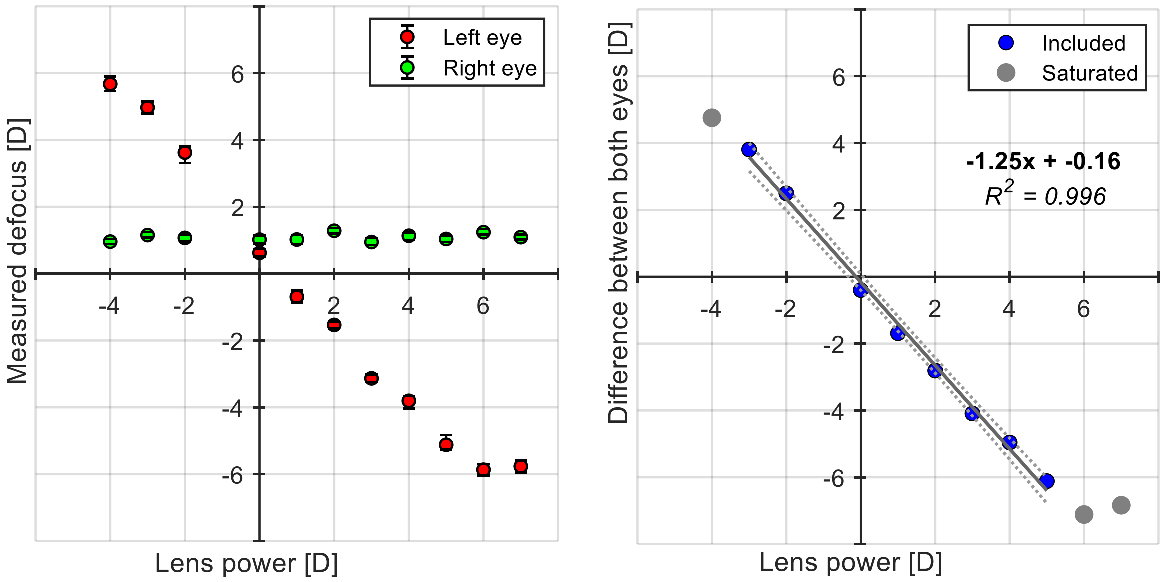

Figure 9. Results of the calibration procedure for one participant. The left panel shows the median and 25th and 75th percentiles of the measured defocus in both eyes as a function of the power of the lens used in front of the left eye. The right eye was uncovered and accommodating on a fixed target, while the left eye was covered by an infrared filter and different lenses. The right panel shows the difference in defocus between both eyes and the fitted linear regression. The steep slope indicates that the photorefractor overestimates the defocus in the left eye of this participant, measuring 1.25 dioptres for each 1 dioptre of real defocus. The inverse of this slope can be used to rescale the refraction measurements and correct the overestimation.

2.2.5. Design and procedure: Experiments 1 & 2.

At the start of the experimental session, participants read the information sheet and signed the consent form. Their visual acuity was then measured at near and far distances using a Snellen chart and a logMAR (logarithm of the Minimum Angle of Resolution) test, respectively. All participants had a visual acuity of logMAR 0.25 or better without the need for spectacle or contact lenses. That is, they could read characters that were smaller than 8.9 arcmin wide with a stroke width of 1.8 arcmin. The photorefractor calibration procedure was then performed.

During the experiment, their left eye was covered using an eyepatch and they sat with their head placed on a chinrest. They were instructed to fixate on the stimuli presented and to keep it in focus with as much effort as if they were reading a book. A button placed next to them allowed them to pause the task at any time, and frequent breaks were given throughout the experiment.

The distance of the stimuli was varied between experimental blocks, with the order of the distances being randomised between participants. In experiment 1, the size of the diffuser and fixation target was kept constant, while in experiment 2, it was changed according to the distance of the target to keep a constant angular size. Within each experimental block, the target was illuminated by the five narrowband illuminants and the broadband illuminant, with their order being randomised. In experiment 1, each illuminant was presented for 8 seconds and repeated at least five times at each of the six distances, for a total of 180 trials. In experiment 2, each illuminant was presented for 3 seconds and repeated 12 times each at each of the six distances, for a total of 432 trials. Between trials, the target was illuminated in both experiments with the orange (588 nm) LED to keep a constant luminance adaptation and to start at a relatively similar accommodation value before the target stimuli was presented. Both experiments took approximately one hour to complete.

2.2.6. Design and procedure: Experiment 3.

At the start of the experimental session, participants read the information sheet and signed the consent form. The photorefractor calibration procedure was then performed, and they were then given instructions for the visual acuity task. During the experiment, participants sat with their head placed on a chinrest, while wearing a pair of light-tight goggles that had an infrared filter over the left eye and allowed us to place different trial lenses over the right eye. Frequent breaks were given between experimental blocks and participants could pause the experiment at any time.

To measure visual acuity, we used a 4 Alternative Forced Choice (4-AFC) task with a best PEST staircase procedure of 24 trials (Kingdom & Prins, 2016). Each Landolt C was presented until the participant gave an answer, and the entire staircase procedure took between 20 and 30 seconds to complete. The background of the Landolt C targets was varied for each staircase according to the four illuminants used in the experiment (three narrowband and one broadband). The order of the illuminant was randomised within each experimental block, and a break of 5 seconds was given between each where no stimulus was presented. For each experimental block, a different trial lens was placed in front of the participant's right eye to add different values of defocus to the stimulus, and the order of the lenses was randomised between participants.

The distance of the stimuli in dioptres was calculated as a function of the physical distance of the screen in dioptres (P_{scrn}), the power of the different lenses placed in front of the eye (P_{lens}), and the distance from the eye to the lens (x_{lens}), such that:

$$P'_{scrn} = P_{scrn} \frac{1 + P_{lens}(x_{lens} - P_{scrn}^{-1})}{1 + P_{scrn}P_{lens}(x_{lens} - P_{scrn}^{-1})x_{lens}} \qquad (Equation\ 2)$$

Furthermore, the visual acuity thresholds obtained in degrees of visual angle were corrected for the small magnification the lenses produced, which was calculated as:

$$\frac{\theta'_{scrn}}{\theta_{scrn}} = \frac{1}{1 + P_{scrn}P_{lens}(x_{lens} - P_{scrn}^{-1})x_{lens}} \qquad (Equation\ 3)$$

The corrected thresholds in degrees of visual angle were then transformed to logMAR units by converting the values into minutes of visual angle and calculating the base-10 logarithm.

2.2.7. Data processing and analysis.

To analyse the refractive and pupil size recordings, the data points where the pupil was not found were identified as blinks and excluded, as well as 60 ms before and 120 ms after each blink. Blinks would on occasion cause big spikes in the refractive data, thus, any data points where reported refraction was greater than 25 D were also excluded. To allow time for the participants to accommodate, the first 1500 ms of refractive and pupil size data in each trial were excluded from further analysis in experiments 1 and 2. Similarly, the first 2000 ms of data in each trial were excluded in experiment 3. Finally, any trial with less than 1000 ms of measurements in experiments 1 and 2, or 2000 ms of measurements in experiment 3 were excluded as well. The calibration correction factor obtained for each participant was then applied to the refraction data, and the median accommodation and pupil size was obtained for each trial.

To perform the analysis on the slopes of the accommodation function, we first determined the linear portion of the accommodation response curve. For this, we calculated the gradient of the accommodation response for each illuminant at each distance, as well as the median gradient, and at any distances where the gradient decreased by 50% or more when compared to the median, the response was deemed to be saturated (further details of this procedure are given in section 2.3.1). These results were visually inspected, and some manual corrections were performed, although they mostly agreed well with the visual evaluation of the experimenter.

For the slope and within-trial response variability analyses (sections 2.3.2 and 2.3.4), the data of experiment 3 was divided in smaller subsets to improve the fit results. The trials in this experiment had a duration of between 20 to 30 seconds, so each one was divided in equal subsets of at least 5 seconds of duration. For all other analyses (i.e., sections 2.3.3, 2.3.5 and 2.3.6) the data were not divided.

Several linear mixed models were used to analyse the effect of distance and illuminant on the slope of the accommodation function (section 2.3.2), the effects of distance on the difference in accommodation to different wavelengths (section 2.3.3), the effects of illuminant and accommodation on response variability (section 2.3.4), the effects of the effects of accommodation on pupil diameter (section 2.3.5), and the effects of accommodative error on visual acuity (section 2.3.6). In all cases, the maximal random-effects structure without convergence issues. All models were fitted with the maximum likelihood estimation method, and all fits and corresponding residuals were visually inspected to verify that all assumptions were met. For the slope analyses (section 2.3.2), the median refraction data within each experiment were weighted by the number of valid measurements obtained within each trial as a proportion of the total number of measurements possible. That is, trials where fewer refractive measurements were obtained due to blinking or other factors, were assigned a lower weight in the model fits.

The data processing and most of the model fits were performed using MATLAB, while the model fits on visual acuity performed in section 2.3.6 and the post-hoc analyses were done using R (R Core Team, 2021), particularly the lme4 library (Bates et al., 2015) and the emmeans library (Lenth, 2021).

2.3. Results.

Figure 10 shows a typical accommodative response for the different illuminants used in experiments 1 and 2. As shown, a change in the refractive state of the eye occurs after approximately 300 ms from stimuli presentation, alongside pupil constriction for some of the illuminants presented. After 1000 ms, the refractive state of the eye remains relatively constant, while the pupil size slowly increases. For each trial presented, we excluded the first 1500 ms of refractive and pupil diameter measurements to obtain the steady-state response of the eye. For experiment 3, we excluded the first 2000 ms of data in both cases. The median responses over the remaining time of the trials were then calculated and used in all analyses presented here.

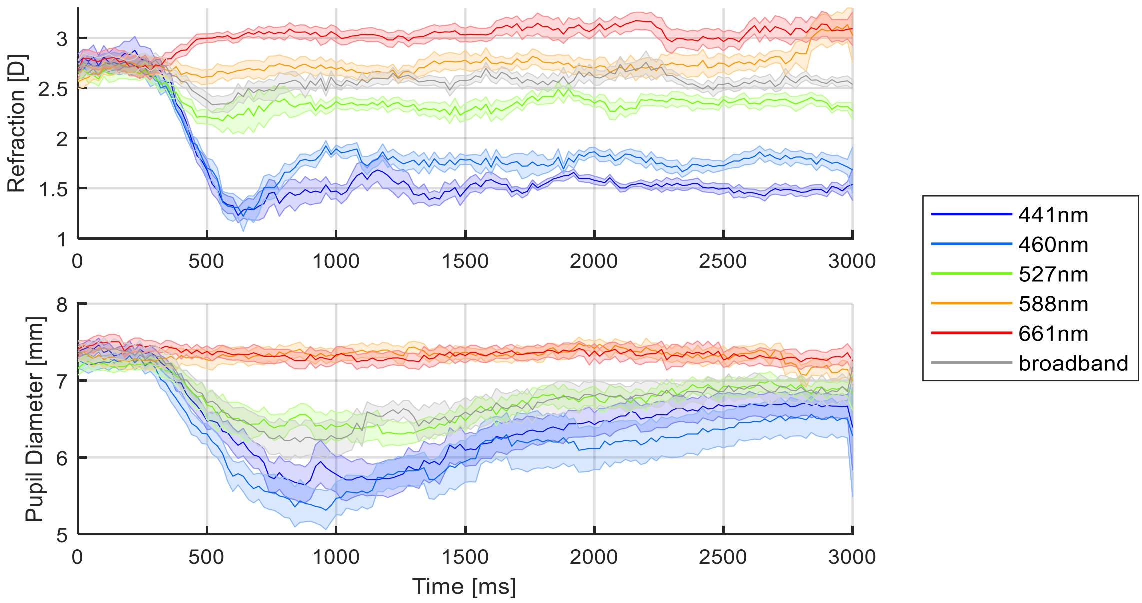

Figure 10. Average accommodation response of one participant to different illuminants presented at 33.3 cm (3 dioptres) and repeated 12 times each. The top panel shows the mean refractive state of the eye and the bottom panel the mean pupil diameter as a function of time. The continuous lines represent the mean, and the shaded areas represent the standard error of the mean. The time point of 0 ms represents the start of the trials, when the illuminant changed from the 588nm (orange) to the corresponding illuminant as indicated by the legend.

2.3.1. Determining the accommodative range of observers.

It is known that the accommodative range varies widely among individuals, particularly in a sample of observers with differences in age and refractive error. Within the accommodative range the response is expected to be quasi-linear with respect to the demand, while beyond it – that is, for demands higher than the near point of accommodation or lower than the far point – the response becomes saturated as the power of the crystalline lens can no longer increase or decrease, respectively. The slope of the accommodation response curve is usually assessed within this linear accommodative range; thus, it was important to determine the near and far point of accommodation for each individual observer in our sample.

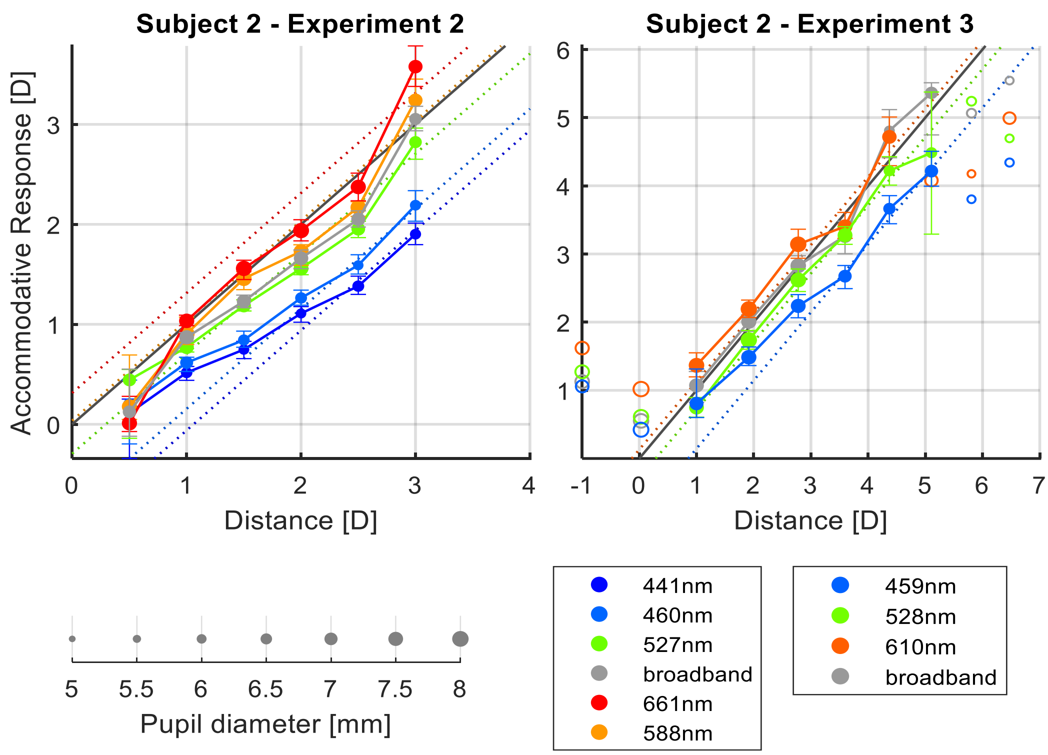

Figure 11. Median accommodation response as a function of distance in dioptres for one participant in experiments 2 and 3. The error bars represent the 25th and 75th percentiles of the response. The filled markers and continuous lines represent the portion of the response deemed to be within the accommodative range, while the unconnected open markers with no error bars are the saturated response. The colour of the markers represents the illuminant and the size the corresponding median pupil diameter, as indicated by the legend. The continuous black line represents the 1:1 ideal response, while the dotted coloured lines represent the 1:1 response corrected by the LCA defocus for each illuminant.

To do this, we calculated for each participant the gradient of the accommodation response as a function of distance in dioptres for each illuminant. At distances where the gradient dropped by 50% or more when compared to the overall median gradient, the response was determined to be saturated, while the distances where the gradient was maintained were taken to be within the accommodative range or linear portion of the accommodation response curve. This process was done for individual illuminants, such that the response to each could saturate at different distances (due to the differences in accommodative demand caused by LCA). The results of this process were visually inspected and agreed well with the evaluation of the experimenter (see Figure 11 for an example of the results for one subject). In all the analyses presented in following sections, the saturated portion of the accommodation response was omitted (i.e., only accommodative and pupil responses within the linear portion of the accommodation response curve were included), except for section 2.3.6, where some analyses include responses beyond the accommodative range, as detailed there.

2.3.2. Effects of LCA on the accommodation response curve.

The accommodation response curves of individual participants for each illuminant in the three experiments are shown in Appendix A, and an example of one subject in two of the experiments is provided in Figure 11. As shown, within the accommodative range of each subject, the response for a given illuminant is a quasi-linear function of distance, with the absolute value of accommodation changing in accordance with the defocus caused by LCA for each illuminant (i.e., at the same distance, observers accommodate less for shorter wavelengths and more for longer ones). An interesting feature of the data in most subjects is that the slope of the response seems to change for each illuminant, with a shallower slope observed for shorter wavelengths and a steeper slope for longer ones. This is illustrated in the examples provided in Figure 11, and it was widespread among our sample.

To quantify this effect, we fitted different linear mixed effects models, since they allow us to obtain slope and intercept estimates for each illuminant, as well as account for individual differences between observers. The fits were performed on the median accommodation response and only over the linear portion of the accommodation response curve (i.e., after excluding the saturated response). Three participants of experiment 3 (subjects 15, 21 and 22) were excluded from this analysis, as their response curves for most illuminants were only linear over 2 or 3 distances.

For each experiment, the linear mixed models were fitted with predictors of distance in dioptres, illuminant, and their interaction, and random intercepts and slopes of participant (i.e., the effect of distance, illuminant and their interaction were allowed to vary randomly among observers). Illuminant was used as a categorical predictor because the broadband illuminant with no peak wavelength was included, and because the change in slope with peak wavelength for the narrowband illuminants might not be linear (since the defocus caused by LCA as a function of wavelength is not linear). These models were compared in each case with a simpler model that contained no interaction term between distance and illuminant, so the effect of wavelength on accommodation would be constant regardless of distance and the slope for all illuminants would be the same. Results from the Likelihood Ratio Test (LRT) and the Akaike information criterion (AIC) comparison indicated that the model with the interaction term fitted the data better and had greater predictive power in all cases: for experiment 1 (χ^2 (55) = 177.6, p<0.001, ΔAIC= 67.6), experiment 2 (χ^2 (55) = 265.8, p<0.001, ΔAIC= 155.8), and experiment 3 (χ^2 (24) = 146.92, p<0.001, ΔAIC= 98.9). This provides further evidence that the effect of illuminant on accommodation changes as a function of distance.

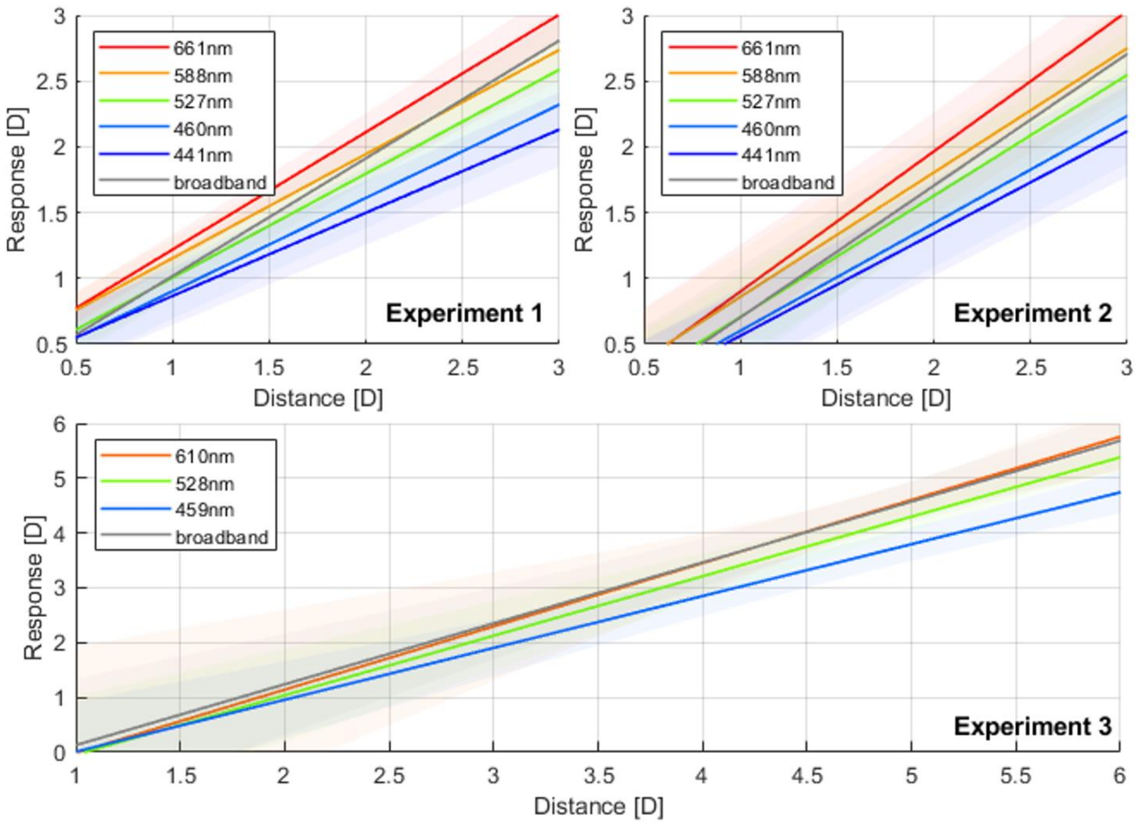

Figure 12. Estimated refraction as a function of distance for the linear portion of the accommodation response curve of all participants in experiment 1 (top left), experiment 2 (top right) and experiment 3 (bottom). The continuous line represents the estimated response and the shaded areas the 95% confidence intervals. The different colours represent the different illuminants used.

The results of the linear mixed models are illustrated in Figure 12 and presented in Table 2. In the latter, the estimated fixed effects coefficients have been used to obtain the slopes and intercepts of the accommodation response curves for each illuminant. The individual slopes and intercepts estimated for each subject (obtained from the estimated coefficients of the random effects of the model) are presented in Appendix B.

The results of experiment 1 show, as expected, that the slope of the accommodation response curve for narrowband illuminants becomes shallower as the peak wavelength decreases. Post-hoc pairwise comparisons (see Appendix B) revealed significant differences between the slopes estimated for all pairs of narrowband illuminants, except between the 588 nm and 527 nm illuminants. The intercepts of the narrowband accommodation functions, however, did not show any significant differences between them, with the exception of the 588 nm and 460 nm illuminants, with the latter being 0.17 dioptres lower ($t(5.39) = 5.36$, $p = 0.035$). Thus, as illustrated in Figure 12 (top left), the accommodation responses to narrowband illuminants are mostly similar at optical infinity, but as the stimulus nears the observer, the difference in accommodation to different wavelengths increases in correspondence with the defocus caused by LCA, i.e., accommodation at the same physical distance is higher for longer peak wavelengths and lower for shorter ones. This results in steeper slopes for longer wavelength illuminants, and shallower slopes for shorter peak wavelengths.

Experiment & Illuminant		Slope [D/D]							Intercept [D]			
		Est.	**95% CI**		**RE SD**	**t-ratio**	**df**	**p-value**	**Est.**	**RE SD**	**t-ratio**	**p-value**
1	661 nm	0.89	0.81	0.97	0.10				0.33	0.16		
	588 nm	0.79	0.74	0.84	0.04	-3.84	1246	*<0.001*	0.36	0.07	0.69	0.488
	527 nm	0.79	0.74	0.84	0.03	-4.15	1246	*<0.001*	0.21	0.08	-2.05	*0.041*
	460 nm	0.71	0.65	0.77	0.06	-5.90	1246	*<0.001*	0.19	0.19	-1.61	0.107
	441 nm	0.63	0.58	0.69	0.05	-9.07	1246	*<0.001*	0.23	0.24	-0.95	0.341
	broadband	0.90	0.84	0.95	0.05	0.08	1246	0.940	0.12	0.09	-3.67	*<0.001*
2	661 nm	1.07	0.91	1.22	0.23				-0.16	0.71		
	588 nm	0.94	0.88	1.01	0.07	-3.89	3157	*<0.001*	-0.08	0.10	1.43	0.154
	527 nm	0.92	0.84	1.00	0.10	-3.66	3157	*<0.001*	-0.21	0.23	-0.53	0.595
	460 nm	0.82	0.72	0.91	0.13	-5.07	3157	*<0.001*	-0.21	0.30	-0.46	0.648
	441 nm	0.78	0.69	0.86	0.11	-6.59	3157	*<0.001*	-0.21	0.26	-0.49	0.626
	broadband	1.00	0.93	1.07	0.08	-1.86	3157	0.063	-0.30	0.15	-2.02	*0.044*
3	610 nm	1.15	0.67	1.64	0.65				-1.16	3.24	-0.95	
	528 nm	1.09	0.81	1.36	0.36	-0.49	1774	0.624	-1.13	1.64	0.06	0.956
	459 nm	0.95	0.66	1.24	0.38	-1.40	1774	0.161	-0.93	1.84	0.33	0.744
	broadband	1.11	0.92	1.31	0.26	-0.43	1774	0.667	-0.98	1.24	0.38	0.702

Table 2. Linear mixed models of accommodation as a function of distance in dioptres and illuminant for each experiment. The estimated coefficients and their 95% confidence intervals (95% CI) have been used to calculate the estimated slopes (in dioptres/dioptres) and intercepts (in dioptres) for each illuminant. The random effects standard deviations (RE SD), t-ratios, degrees of freedom (df), and p-values are also shown. The t-tests compare within each experiment, the slope and intercept estimates of each illuminant with the estimates for the longest-wavelength illuminant.

For the broadband illuminant used in experiment 1, the accommodation response curve was found to have a similar slope to the longest wavelength illuminant (661 nm), with no significant differences between them. However, the intercept of the accommodation function for the broadband illuminant was the lowest of all illuminants, and post-hoc pairwise comparisons revealed that it was significantly lower than for the 661 nm illuminant by 0.20 dioptres ($t(4.03) = 6.18$, $p = 0.049$), and from the 588 nm illuminant by 0.24 dioptres ($t(3.75) = 8.21$, $p = 0.023$). Thus, as illustrated in Figure 12 (top left), this means that accommodation to the broadband illuminant at farther distances was closer to the responses to the shorter wavelength illuminants, but due to the steeper slope, accommodation progressively shifted towards longer wavelengths as the target neared, and at 3 dioptres, it more closely matched the responses to the 588 nm illuminant.

The results of experiment 2 show a similar pattern to the results of experiment 1, with the accommodation response to narrowband illuminants presenting a steeper slope as the peak wavelength increases. However, confidence intervals for corresponding illuminants are wider in experiment 2, and the standard deviations of the random slopes are larger when compared to experiment 1. This means that there was greater variability between the subjects that took part in experiment 2, and thus, less certainty of the estimated coefficients. In post-hoc pairwise comparisons (see Appendix B), the slope of the 661 nm illuminant was found to be significantly steeper than all the other narrowband illuminants; and while pairwise differences between the slopes of the 588 nm, 527 nm and 460 nm were not found to be significant, the 441 nm illuminant had significantly shallower slope than the 588 nm illuminant (by 0.17 D/D, $t(7.44) = 4.61$, $p = 0.017$) and the 527 nm illuminant (by 0.14 D/D, $t(7.48) = 3.98$, $p = 0.036$). Similarly to experiment 1, no significant differences were found in pairwise comparisons between any of the intercept estimates of the narrowband illuminants.

For the broadband illuminant in experiment 2, the slope of the accommodation response had a similar value to the slope for the longest wavelength illuminants, and indeed, post-hoc pairwise comparisons revealed no significant differences with the slope of the 661 nm, 588 nm and 527 nm illuminants. The slope for the broadband illuminant was, however, significantly steeper than the slope of the 460 nm illuminant (by 0.18 D/D, $t(7.60) = -4.60$, $p = 0.017$) and 441 nm illuminant (by 0.22 D/D, $t(7.56) = -5.87$, $p = 0.004$). The intercept for the broadband illuminant had the lowest estimated value when compared to the narrowband illuminants, and while an initial difference with the 661 nm illuminant was found, once p-values were corrected for multiplicity in post-hoc pairwise comparisons, this difference was not found to be significant ($t(7.23) = 2.09$, $p = 0.683$).

When comparing between experiment 1 and experiment 2, we see that the slope estimates for corresponding illuminants in the latter are steeper, while intercept estimates are lower. In experiment 2 there is also greater uncertainty in the slope and intercept estimates, with wider confidence intervals and higher standard deviation values in the random effects. It is unclear how the differences in the slope and intercept estimates could be a consequence of the differences in experimental design. In experiment 2 the physical size of the stimuli was reduced as it neared the observer, keeping the angular size the same, while in experiment 1 the physical size was kept the same and it was equal to the physical size of the target for the farthest distance in experiment 2. Thus, the greatest differences in the angular size of the stimuli between both experiments were present at the nearest distances; however, as illustrated in Figure 12 (top), at 3 dioptres of distance, the accommodation values for corresponding illuminants are similar between both experiments. If the changes in the angular size of the target were responsible for the differences in slope and intercept between experiments, the greatest differences should be observed at this distance; therefore, it is more likely that these differences are due to the variability between subjects as well as the within-subject variability across time.

The accommodation response curves for narrowband illuminants in experiment 3 show a similar pattern as experiments 1 and 2, with steeper slopes corresponding to longer wavelength and broadband illuminants. However, the confidence intervals are much wider, and the standard deviations of the random effects are higher, indicating greater variability between subjects. Post-hoc pairwise comparisons revealed a significant difference of 0.14 dioptres/dioptres between the 528 nm and 459 nm illuminant ($t(5.13) = 4.46$, $p = 0.023$), while the slope of the 610 nm illuminant was not found to be significantly different to the other two, despite having the highest estimated value, albeit also the widest confidence interval. The estimated slope for the “equal luminance” broadband illuminant used was found to have a similar value to the 610 nm and 528 nm illuminants and was significantly higher than the slope of the 459 nm illuminant by 0.16 dioptres/dioptres ($t(5.26) = 5.17$, $p = 0.012$). As observed in Figure 12 (bottom), the accommodation response for this illuminant seems to overlap with the response to the 610 nm over most of the distances tested. No significant differences were found between the intercept estimated for any of the illuminants used.

To illustrate how the change in slope for different illuminants affect the lags and leads of the linear portion of the accommodation response curve, we show in Figure 13 the accommodative error as a function of distance for each illuminant. We calculated the accommodative error by subtracting the demand from the predicted response, thus, a

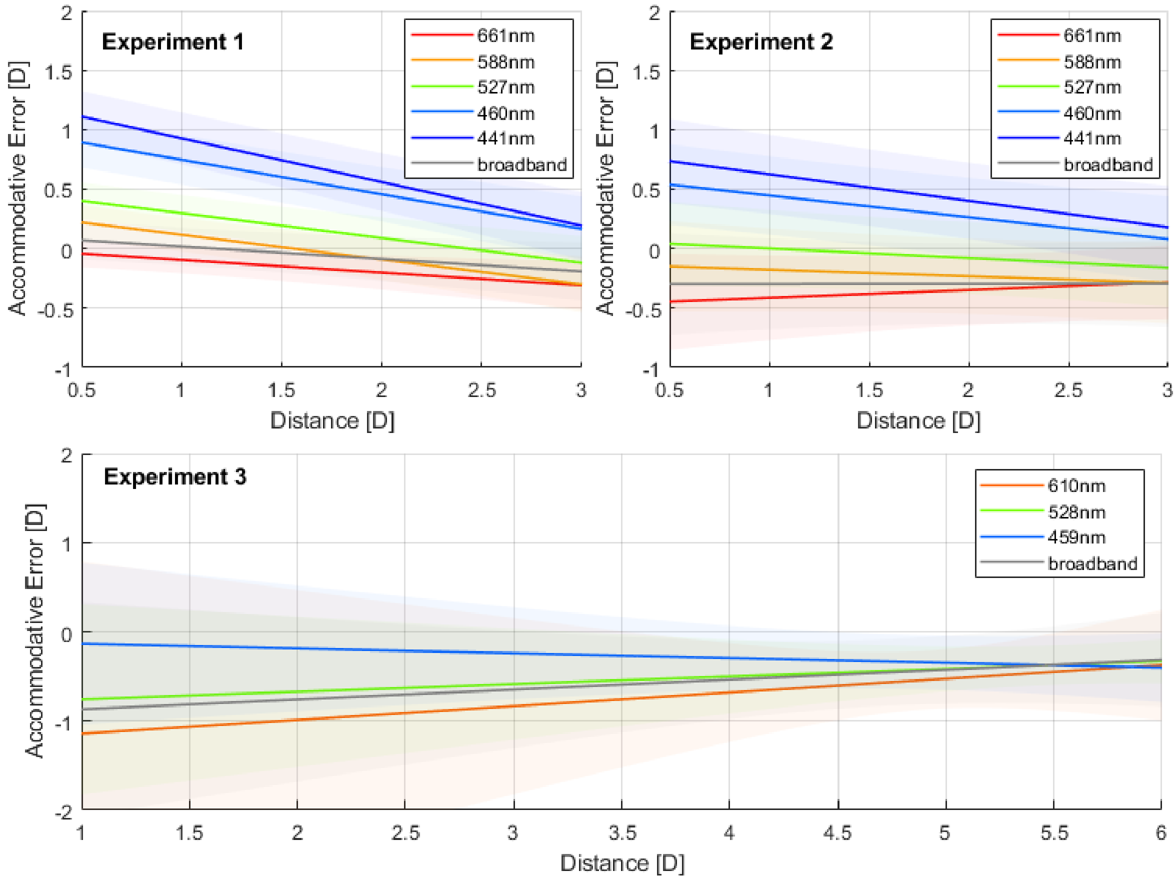

Figure 13. Accommodative error as a function of distance for different wavelengths, as predicted by the linear mixed effects models fitted to the data of each experiment. The continuous lines of different colours represent the predicted responses for different illuminants, as indicated by the legend, and the shaded regions represent the 95% confidence intervals.

negative error indicates the eye is under-accommodating or focusing farther away than where the target is (accommodative lag), and a positive error indicates that the eye is focusing nearer than the stimulus (accommodative lead). The accommodative demand is given by the distance of the stimuli and the defocus caused by LCA for the peak wavelength of the narrowband illuminant, which we calculated following the chromatic eye model by Thibos et al., (1992). As illustrated, the increased difference in the accommodative response to different wavelengths as the stimulus is placed nearer, corresponds with the change in demand caused by LCA. In other words, participants are increasingly compensating for LCA as the target is placed at nearer distances, causing the accommodative error to become both smaller and less dependent on wavelength. Furthermore, accommodation is more accurate for middle wavelengths over most distances, with a tendency to overaccommodate for shorter wavelengths and under-accommodate for longer ones, and the accommodative errors for all wavelengths and in all three experiments seem to approach a small negative value of approximately -0.5 D rather than zero, indicating a small accommodative lag at nearer distances.

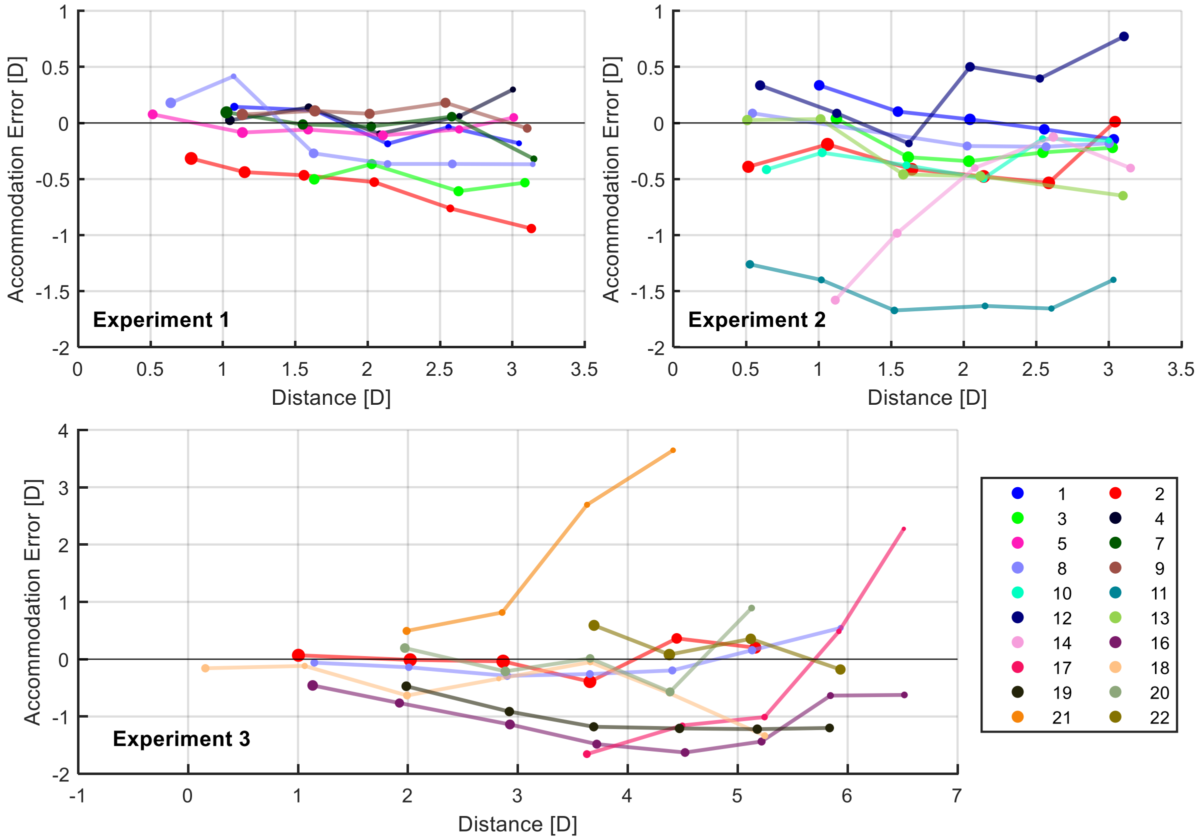

Figure 14. Median steady-state accommodative error as a function of distance for broadband stimuli in the three experiments. Each colour and continuous line represent one participant, as indicated by the legend, and the marker sizes represent the corresponding median pupil size.

While the fitted models indicate a very small accommodative lag at nearer distances, interestingly, not all subjects showed this lag in their response curves. In Figure 14 we present the median accommodative error as a function of distance for the broadband illuminants used in each experiment, and the individual accommodation response curves are shown in Appendix A (see Figures 4, 5, and 6). As illustrated, the accommodative error for the broadband illuminant as a function of distance remains relatively constant for most subjects in experiments 1 and 2, albeit there is greater variability in the latter, and in these experiments only distances of up to 3 dioptres were tested, which is a limited range to observe the typical accommodation lag.

In experiment 3, where distances of up to 6.5 dioptres were tested, we see that only two participants (subjects 16 and 19, see Appendix A) show an accommodative lag that increases with distance and reaches values of -1 to -1.5 D; while five participants (subjects 2, 8, 18, 20, and 22) do not present this lag, with accommodative errors that remain relatively constant and close to zero over the linear portion of the accommodation response curve. Finally, there are three participants that show atypical responses, with one (subject 15) having a very limited accommodation range of 2 dioptres and a relatively flat response curve, and two others (subject 17 and 21) with response curves that have a slope of ~2 dioptres/dioptres, with the accommodative error steeply increasing towards positive values as a function of distance.

2.3.3. Effects of distance on the accommodation response to different wavelengths.

As shown previously, the extent to which participants change their accommodative responses under illuminants of different wavelengths to compensate for the LCA of the eye, changes with the distance of the stimulus. To determine the rate of this change, we fitted a linear mixed model on the relative difference in accommodation between wavelengths, with predictors of distance in dioptres, the defocus predicted by the Chromatic Eye model, and their interaction, and random slopes and intercept of participant. The accommodation responses were centred around the response to the green illuminant (527 nm in experiments 1 and 2, 528 nm in experiment 3) for each subject at each distance and the defocus predicted by the Chromatic Eye model was set to be zero at 527.5 nm.

While in the previous analysis, illuminant was being treated as a categorical predictor, and no assumptions were being made about how it affected accommodation, here we are using the LCA defocus predicted by the Chromatic Eye model for the peak wavelength of the narrowband illuminants and examining how well it predicts the differences in accommodation between illuminants. A slope of 1 for this relationship would indicate that observers are fully compensating for the LCA of the eye when accommodating to the narrowband illuminants, while a slope of 0 would indicate that there are no differences in the accommodation response to different wavelengths (i.e., they are not correcting for the defocus caused by LCA). Furthermore, we are also exploring here how this relationship between LCA defocus and the difference in accommodation to different wavelengths changes as a function of distance.

Based on the previous results presented thus far, we would expect nearer distances to cause an increase in the effect that LCA has on the accommodation response.

The results of the fitted linear mixed model are shown in Table 3. A model that included experiment as a fixed effect as well as its interaction with distance and defocus was also fitted, however no significant effect of experiment was found, and a LRT and AIC model comparisons revealed that the model including experiment as a factor was not significantly better than the simpler model (ΔAIC = -45.85; χ^2 (8) = 5.26, p = 0.730). This means that the differences in the design of the three experiments did not influence the extent to which participants correct for LCA, once the individual differences between participants had been accounted for. Other fits including the median pupil diameter of participants as an interacting factor were also attempted, however this variable was not found to have a significant effect.

Parameter	Estimate	CI 95%		t-ratio	df	p-value	RE SD
Intercept	0.05	-0.03	0.14	1.19	5205	0.233	0.19
Distance [D]	-0.02	-0.05	0.00	-1.71	5205	0.088	0.05
LCA Defocus [D]	-0.26	-0.76	0.23	-1.04	5205	0.296	1.14
Distance [D] * LCA Defocus [D]	***0.28***	***0.08***	***0.47***	***2.82***	***5205***	***0.005***	***0.45***

Table 3. Linear mixed model results of accommodation to different wavelengths relative to the green illuminant, as a function of distance, the defocus caused by LCA, and their interaction. Coefficient estimates, their 95% confidence interval (CI 95%), and the random effects standard deviations (RE SD) are shown, as well as the t-tests results with degrees of freedom (df), t-ratios, and p-values. Parameters in bold italics are significant at the 0.05 level.

As seen in Table 3, the results agree with the previous slope estimations, with the effect of LCA on accommodation increasing by a factor of 0.28 for every dioptre of increase in the distance of the stimulus (95% CI between 0.08 and 0.47, t(5205) = 2.82, p = 0.005). This means that at a distance of approximately 4.5 dioptres, participants change their accommodation responses to compensate for the defocus caused by LCA to the full extent predicted by the Chromatic Eye model. Furthermore, we see that at a distance of 0 dioptres, participants do not significantly change their accommodation to different wavelengths (t(5202)= 1.04, p=0.296), albeit there is considerable variability between subjects at this distance, as indicated by the large standard deviation of the random effects and the wide confidence intervals. Finally, as the predictor was centred at 527.5 nm and the response was centred by the 527 nm and 528 nm illuminants, effectively removing the effect of distance, we see that distance has no significant effect on accommodation when LCA defocus is 0 (i.e., at 527.5 nm).

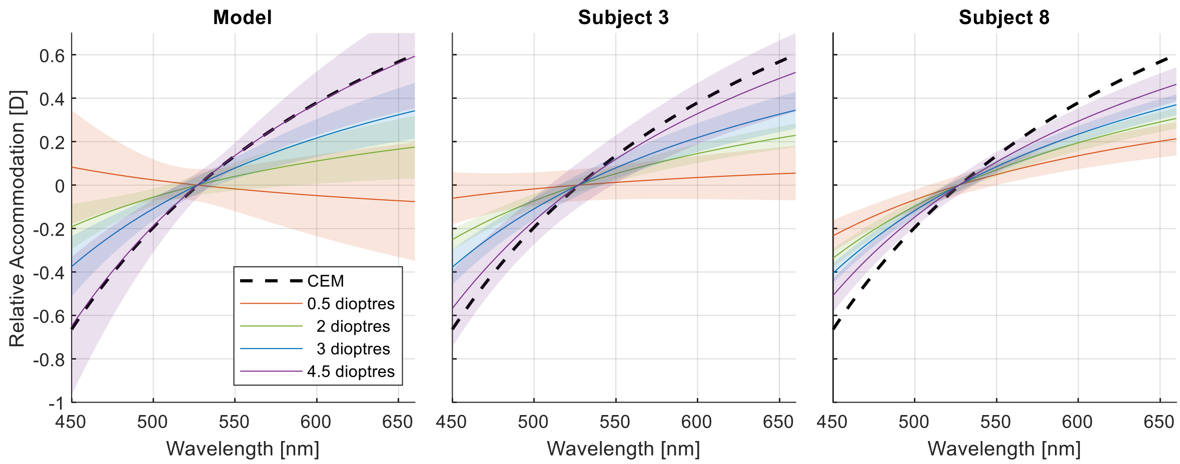

Figure 15. Relative changes in accommodation to different wavelengths as predicted by the linear mixed model (left), and for subjects 3 and 8 (middle and right). The response at each distance was centred by the 527 and 528nm illuminants, so it represents the relative difference in accommodation to these wavelengths. The black dashed line represents the defocus caused by LCA as predicted by the Chromatic Eye model (and centred at 527.5nm). The continuous coloured lines represent different distances as indicated by the legend, and the shaded regions represent the corresponding 95% confidence intervals.

An illustration of the results of the model plotted as a function of wavelength and at different distances is shown in Figure 15 (left), as well as the fitted responses of two subjects (middle and right). As observed, the confidence intervals are wider at the distance of 0.5 dioptres, reflecting the uncertainty of the predictions likely caused by the inter-observer differences being greater at this distance. This is illustrated in the differences between subject 3 and subject 8, as the latter shifted their accommodative responses to correct for LCA to a greater extent than the former when the stimulus was placed at 0.5 dioptres. However, we see that for nearer distances, their responses are more similar. In summary, distance had a significant effect on the dioptric shift observed in the accommodative responses of participants to narrowband illuminants of different wavelengths, however there was considerable inter-subject variability, particularly at further distances.

2.3.4. Variability in the accommodation responses to narrowband and broadband illuminants.

In our experiments we recorded the refraction of the eye dynamically at a frequency of 50 Hz, which allows us to assess the within-trial variability of the steady-state accommodation response over time for the different illuminants used. In other words, once participants accommodate to a target, how much does the response fluctuate over time, and are there any differences between narrowband and broadband illuminants, and between narrowband illuminants of different wavelengths? Furthermore, as fluctuations in accommodation are known to increase with increasing accommodative power, we also evaluated the effect of the mean refractive state as a predictor.

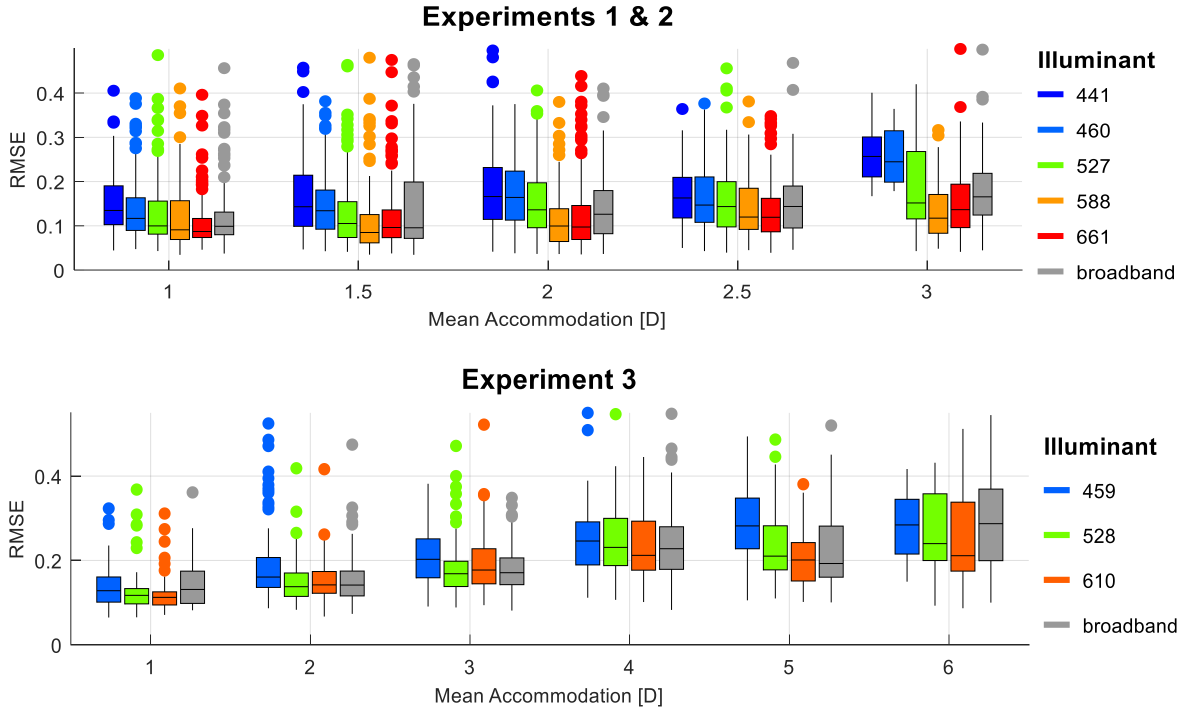

Figure 16. Distributions of the root-mean-square errors (RMSE) of an unconstrained linear fit through the within-trial accommodation response, as a function of mean accommodation and illuminant in experiments 1 and 2 (top) and experiment 3 (bottom). Each colour represents an illuminant as indicated by the legend. The mean accommodation values have been rounded and grouped for illustration purposes only. Note that each abscissa is on a different scale.

To obtain a measurement of intra-trial accommodation variability, we fitted a linear function through the refractive response measured in each trial as a function of time and obtained the root-mean-squared errors (RMSE). This approach has been used previously for similar purposes (MacKenzie et al., 2010) and has the advantage of penalizing larger fluctuations in accommodation more and maintaining the units of the response. In Figure 16 we illustrate the distributions of the RMSEs as a function of mean accommodation and illuminant. Since the same illuminants were used in experiments 1 and 2, the data obtained in both were combined. As shown, the within-trial variability seems to increase with increasing mean accommodative state, as well as appearing to be higher for shorter-wavelength illuminants than longer-wavelength ones, with no obvious differences observed between the latter and the broadband illuminants.

To quantify these differences, we fitted two linear mixed effects models on the RMSEs, with mean accommodation as a continuous predictor and illuminant as a categorical predictor, while maintaining the full random-effects structure. The results are shown in Table 4. Both models were compared with a more complex model that included an interaction between illuminant and mean refraction; however, the LRT and AIC comparison did not show that these models fitted the data significantly better or had greater predictive power, neither for experiments 1 and 2 ($\chi^2(55)$ =34.79, p= 0.985, ΔAIC=-75), nor experiment 3 ($\chi^2(3)$ =3.43, p=0.329, ΔAIC=-2.6). This means that there is no evidence in our data that the effect of illuminant on the within-trial accommodative response variability changes as accommodation increases.

Experiment	Parameter	Estimate	CI 95%		t-test	df	p-value	RE SD
1 & 2	Intercept	0.155	0.12	0.19	8.94	4420	*<0.001*	0.06
	460 nm	-0.008	-0.02	0.00	-2.06	4420	*0.039*	0.01
	527 nm	-0.023	-0.03	-0.01	-5.35	4420	*<0.001*	0.01
	588 nm	-0.050	-0.07	-0.03	-6.18	4420	*<0.001*	0.03
	661 nm	-0.043	-0.05	-0.03	-7.22	4420	*<0.001*	0.02
	broadband	-0.022	-0.03	-0.01	-4.63	4420	*<0.001*	0.01
	Refraction	0.020	0.01	0.03	4.21	4420	*<0.001*	0.02
3	Intercept	0.134	0.10	0.16	8.67	2190	*<0.001*	0.05
	528 nm	-0.028	-0.04	-0.01	-3.78	2190	*<0.001*	0.02
	610 nm	-0.031	-0.05	-0.02	-3.93	2190	*<0.001*	0.02
	broadband	-0.020	-0.03	-0.01	-2.81	2190	*0.005*	0.02
	Refraction	0.031	0.02	0.04	6.45	2190	*<0.001*	0.01

Table 4. Linear mixed model results of the root-mean-square errors (RMSEs) of an unconstrained linear fit through the within-trial accommodation response, as a function of refraction and illuminant, in experiments 1 and 2, and experiment 3. Coefficient estimates and their 95% confidence interval (CI 95%) are shown, as well as degrees of freedom (df), t-ratios p-values, and the random effects standard deviation (RE SD). The intercepts of the models are the corresponding shortest wavelength illuminants (441 nm in experiments 1 and 2, and 459 nm in experiment 3) at zero dioptres of refraction.

In both experiments we observe similar intercepts of 0.15 dioptres (95% CI from 0.12 to 0.19) in experiments 1 and 2, and 0.13 dioptres (95% CI from 0.10 to 0.16) in experiment 3, with the 441 nm and the 459 nm illuminants, respectively. This means that at zero dioptres of refractive power, the accommodation response of observers to targets illuminated by these short wavelength illuminants fluctuates on average by 0.13 and 0.15 dioptres around the central response over time. The effect of refraction on RMSE was similar in both experiments as well, with one dioptre of increase in accommodation causing an increase of 0.02 dioptres (95% CI from 0.01 to 0.03) in experiments 1 and 2, and an increase of 0.03 dioptres (95% CI from 0.02 to 0.04) in experiment 3.

When comparing between different illuminants, we see similar results in both datasets, with the highest within-trial variability in accommodation being observed for the shortest wavelength illuminants, and this variability decreasing as the peak wavelength of the illuminant increases. In experiments 1 and 2, the lowest RMSE was present with the 588 nm and 661 nm illuminants, with estimates of 0.11 dioptres for both (95% CI from 0.09 to 0.12 and from 0.10 to 0.12, respectively), followed by the 527 nm and the broadband illuminant with estimates of 0.13 dioptres of RMSE (95% CF from 0.12 to 0.14 for both), and finally, the highest RMSE was observed with the 460 nm and the 441 nm illuminants, with estimates of 0.15 dioptres for both (95% from 0.14 to 0.15 and from 0.12 to 0.19, respectively). A similar pattern of results is found for the model fitted to the data of experiment 3. In summary, we see that the within-trial variability of the accommodation response increases with increasing refractive power, and it is lowest for the longer wavelength illuminants (588, 610 and 661 nm) and highest for the shorter wavelength illuminants (441, 459 and 460 nm). We found no systematic differences between broadband and narrowband illuminants, with the intra-trial variability being similar for the middle-wavelength (527 and 528 nm) and broadband illuminants.

2.3.5. Accommodation and pupil size.

The median pupil diameter, centred to each participant, is illustrated as a function of accommodation and for the different illuminants used in Figure 17. To assess the effect of accommodation and of the different illuminants on the pupil diameter of participants, we fitted a linear mixed model for each experiment, with refraction in dioptres as a continuous predictor, and the illuminant as a categorical predictor, with random slopes and intercepts of participant. The latter were important as there was significant inter-individual variability in the median pupil diameter. The results are shown in Table 5. Note that for each experiment, the shortest wavelength illuminant was taken as the intercept of the model (441 nm for experiments 1 and 2, and 459 nm for experiment 3).

We found that pupil diameter significantly decreases as accommodation increases, although the rate of this change differs between experiments. In experiment 1 where the angular size of the stimuli increased as it was placed nearer the eye, pupil diameter decreased by 0.75 mm (95% CI from 62 to 89 mm) for every dioptre of increase in refraction. However, in experiments 2 and 3 where the angular size of the stimuli was kept constant, the slope was shallower, with pupil diameter decreasing by 0.16 mm (95% CI from 0.06 to 0.26 mm) and 0.18 mm (95% CI from 0.06 to 0.29 mm) for every 1 D of increase in refraction, respectively.

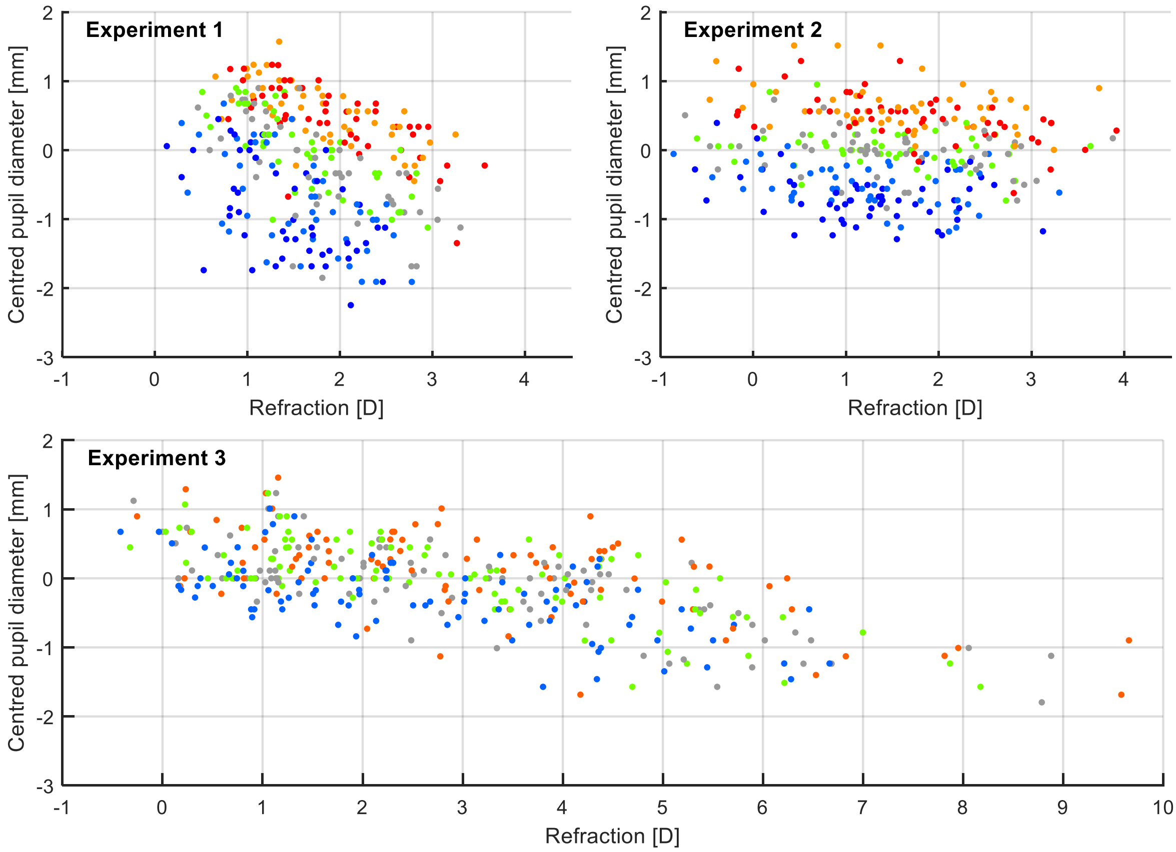

Figure 17. The centred to each participant median pupil diameter as a function of accommodation. Each panel represents the data obtained in one experiment and the colour of the points represents the illuminant used. As illustrated, pupil diameter decreases more steeply with increasing accommodation in experiment 1 (where angular size was not kept constant) than in experiments 2 and 3.

The different illuminants used had a significant effect in the pupil size, with the shortest wavelength illuminants corresponding to the smallest diameters, and pupil size increasing progressively for longer wavelengths, even though the luminance was equal in all cases. The largest difference in pupil diameter for stimuli of equal luminance was of 1.70 mm (95% CI: 1.38 to 2.01 mm) for experiment 1 between the 441 nm and 661 nm illuminants; of 1.40 mm (95% CI: 1.21 to 1.58 mm) for experiment 2 between 441 nm and 588 nm, and of 0.45 mm (95% CI: 0.30 to 0.59 mm) for experiment 3 between 459 nm and 610 nm. Thus, a change in the peak wavelength of the illuminant used can have a larger effect on pupil diameter than changes in accommodation, particularly when the angular size of the stimuli is kept constant. Finally, the median pupil size for the broadband stimuli used seems to approximately correspond with the pupil diameter of middle wavelength illuminants: 527 nm in experiments 1 and 2, and 528 nm in experiment 3.

Experiment	Parameters	Estimate	CI 95%		t-ratio	df	p-value
1	Intercept	6.11	5.79	6.42	38.09	1448	<0.001
	460 nm	0.22	0.11	0.33	3.95	1448	<0.001
	527 nm	0.97	0.67	1.27	6.34	1448	<0.001
	588 nm	1.66	1.39	1.94	11.98	1448	<0.001
	661 nm	1.70	1.38	2.01	10.57	1448	<0.001
	broadband	0.86	0.62	1.10	7.12	1448	<0.001
	Refraction	-0.75	-0.89	-0.62	-10.81	1448	<0.001
2	Intercept	5.28	4.80	5.76	21.68	3494	<0.001
	460 nm	0.23	0.16	0.30	6.22	3494	<0.001
	527 nm	0.75	0.59	0.90	9.48	3494	<0.001
	588 nm	1.40	1.21	1.58	14.67	3494	<0.001
	661 nm	1.26	1.11	1.41	16.22	3494	<0.001
	broadband	0.70	0.55	0.86	8.82	3494	<0.001
	Refraction	-0.16	-0.26	-0.06	-3.12	3494	0.002
3	Intercept	5.63	5.12	6.15	21.62	912	<0.001
	528 nm	0.30	0.18	0.42	4.81	912	<0.001
	610 nm	0.45	0.30	0.59	6.06	912	<0.001
	broadband	0.23	0.14	0.31	5.18	912	<0.001
	Refraction	-0.18	-0.29	-0.06	-3.02	912	0.003

Table 5. Linear mixed model results of pupil diameter for experiments 1, 2 and 3. Coefficient estimates, their 95% confidence interval (CI 95%) and standard errors (SE) are shown, as well as degrees of freedom (df), t-ratios and p-values. The intercepts of the models are the corresponding shortest wavelength illuminants (441 nm in experiments 1 and 2, and 459 nm in experiment 3) at zero dioptres of refraction.

2.3.6. Accommodative error and visual acuity.

In experiment 3, the visual acuity of participants was measured for each illuminant at each distance, which allowed us to assess the effect that the median accommodation response of participants while they performed the staircase procedure had on their visual acuity. In Figure 18, we present the visual acuity thresholds obtained for all participants as a function of the median accommodative error (top) and as a function of the median pupil diameter (bottom). Individual figures for each participant are presented in Appendix C.

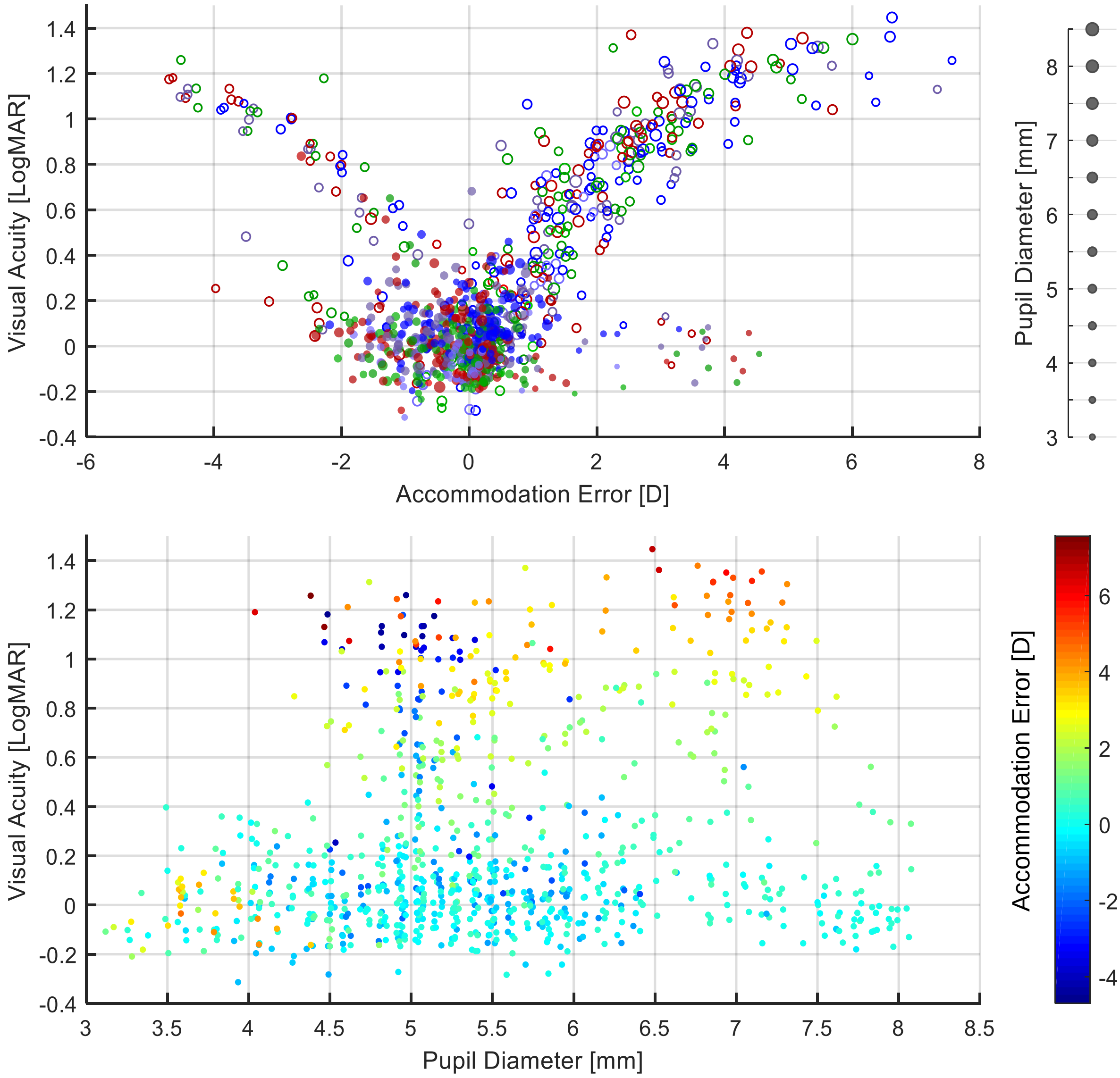

Figure 18. Visual acuity as a function of median accommodative error (top) and as a function of median pupil diameter (bottom). In the top panel, filled markers correspond to measurements over the linear portion of the accommodation response curve, and open markers measurements at distances where the function was saturated. The marker colours represent the illuminant used, and the marker sizes the corresponding median pupil size. In the bottom panel, the colour of the markers represents the median accommodative error.

Firstly, we analyse the results obtained over the linear portion of the accommodation response curve (see Figure 18 top, filled markers). As observed, over this portion, participants had visual acuity thresholds that were mostly concentrated between logMAR -0.2 and 0.2, which corresponds with better than normal to near normal vision. Median accommodative errors were mostly between -2 D and 1 D, with errors of larger magnitude mostly present for the portions where the response curve was found to be saturated. When looking at the individual results of each participant (see appendix C), we see that most of the data points with large negative errors of up to -2 D and low visual acuity thresholds belong to subjects 16 and 19, which were the two participants that presented the typical lags in their accommodation response curves. Thus, it seems that in these two subjects, such lags did not correlate with a worsening of visual acuity.

Another relevant feature of the data is the small cluster of trials in which participants obtained low visual acuity thresholds between logMAR -0.2 and 0.2 despite presenting positive accommodative errors of up to 4.5 D of magnitude. As illustrated in Figure 18 (bottom), one common feature of these trials is that the median pupil diameter of participants was mostly between 3 and 4 mm. Smaller pupil sizes improve depth of focus which can decrease the effect that accommodative errors have on visual acuity. Additionally, the infrared photorefractor used relies on measuring the variation in reflected light intensity across the pupil to estimate the refractive state of the eye. This means that smaller pupils offer less information which could lead to less accuracy in the measurements taken. For these reasons, and since at these small pupil sizes the measured accommodative error does not seem to correlate with visual acuity thresholds, data points where the median pupil diameter was below 4 mm were excluded from all analyses.

To further explore the relationship between accommodative error and visual acuity over the linear portion of the accommodation response curve, we fitted a linear mixed model with predictors of accommodative error magnitude, error sign, and their interaction, as well as illuminant, and random intercept and slopes of participant. The data used were the accommodative errors and visual acuity thresholds obtained within the accommodative range of participants (see filled markers in Figure 18), while excluding trials where the median pupil diameter was smaller than 4 mm. The estimated coefficients are shown in Table 6. We found that accommodative error magnitude was estimated to have a worsening effect on visual acuity, albeit the confidence intervals were wide, and the effect was not found to be significantly different from zero. The wide confidence intervals are likely reflecting the fact that the errors over the linear portion of the accommodation response curve were very small in magnitude for most subjects. In other words, subjects were accommodating successfully to the stimuli over a range of distances, resulting in small values of defocus and greater uncertainty in estimating its effect on visual acuity. However, the parameter estimates still indicate that the overall effect on visual acuity was detrimental, with thresholds worsening by logMAR 0.10 for each dioptre of increase in negative accommodative error (95% CI from -0.05 to 0.24, $t(8.37) = 1.51$, $p = 0.168$), and by logMAR 0.12 for each dioptre of increase in positive accommodative error (95% CI from 0.00 to 0.23, $t(6.44) = 2.36$, $p = 0.053$).

Visual acuity [logMAR] - Linear portion of the accommodation function							
Parameters	**Estimate**	**CI 95%**		**t-ratio**	**df**	**p-value**	**RE SD**
Intercept	0.04	-0.06	0.15	0.79	8.29	0.452	0.16
Error magnitude [D]	0.10	-0.02	0.21	1.69	8.66	0.126	0.17
Positive sign	0.01	-0.07	0.09	0.26	7.04	0.800	0.11
Illuminant: 528 nm	***-0.11***	***-0.17***	***-0.06***	***-3.95***	***8.72***	***0.004***	***0.08***
Illuminant: 610 nm	***-0.08***	***-0.14***	***-0.02***	***-2.72***	***8.70***	***0.024***	***0.08***
Illuminant: broadband	***-0.09***	***-0.12***	***-0.05***	***-4.53***	***9.09***	***0.001***	***0.05***
Error magnitude [D] * Positive sign	0.02	-0.10	0.14	0.31	9.70	0.761	0.16

Table 6. Linear mixed model results of visual acuity over the linear portion of the accommodation response curve, as a function of illuminant, accommodative error magnitude, accommodative error sign, and their interaction. The coefficient estimates, their 95% confidence intervals (CI 95%), t-ratios, degrees of freedom (df), p-values, and random effects standard deviations (RE SD) are shown.

A significant effect of illuminant on visual acuity was found. When accommodative error is zero, visual acuity for the 459 nm illuminant was estimated to be logMAR 0.04 (95% CI from -0.06 to 0.15). In comparison with this illuminant, visual acuity thresholds were lower for the 528 nm illuminant by logMAR 0.11 (95% CI from 0.06 to 0.17, $t(8.7) = 3.95$, $p = 0.004$), for the 610 nm illuminant by logMAR 0.08 (95% CI from 0.02 to 0.14, $t(8.7) = 2.72$, $p = 0.024$), and for the broadband illuminant by logMAR 0.09 (95% CI from 0.05 to 0.12, $t(9.1) = 4.53$, $p = 0.001$). Post-hoc pairwise comparisons of the estimated marginal means of visual acuity for each illuminant (i.e., the means averaged over the effects of accommodative error magnitude and sign), revealed that these differences were consistent and present across the small values of accommodative error found within the linear portion of the accommodation response curve. We found higher visual acuity thresholds for the 459 nm illuminant when compared to the

528 nm illuminant by logMAR 0.11 (95% CI from 0.02 to 0.20, $t(8.91) = 3.87$, $p = 0.017$), and by logMAR 0.09 when compared to the broadband illuminant (95% CI from 0.02 to 0.15, $t(8.74) = 4.34$, $p = 0.009$). Visual acuity was also lower for the 610 nm illuminant when compared to the 459 nm one by logMAR 0.08, although this difference was not significant (95% CI from -0.01 to 0.18, $t(8.91) = 2.66$, $p = 0.100$). This means that over the linear portion of the accommodation response curve and for equal values of accommodative error, visual acuity was worst for the shortest wavelength illuminant than for any of the other illuminants used. No significant differences were found in pairwise comparisons between the 610 nm, 528 nm and broadband illuminants.

To further explore the effect of accommodative error and the illuminants used we fitted linear mixed models on all the data obtained, that is, including distances that were nearer or farther away than participant's accommodative range (see Figure 18, both open and filled markers). Due to the complexity of the data and the observed differences between the effect of underaccommodation (negative errors) and overaccommodation (positive errors), the dataset was separated accordingly and fitted separately. For positive accommodative errors, visual acuity thresholds seem to saturate for error magnitudes greater than 5.5 D and at around logMAR 1.2; thus, these values (error magnitude > 5.5 D and visual acuity > logMAR 1.2) were excluded from the analyses to improve model convergence. As with the previous model, trials where the median pupil diameter was less than 4 mm were excluded, and the pupil diameter predictor was centred so that the intercept of the model was at 4 mm. Several models were fitted to both datasets, with different combinations of accommodative error magnitude, pupil diameter, illuminant and retinal illuminance used as separate or interacting predictors, while maintaining the full structure of the random effects. Through multiple comparisons, it was determined that for both datasets, a model with predictors of error magnitude, pupil diameter, their interaction, and illuminant, had the greatest predictive power and lowest Akaike Information Criterion. The results of the fits for both datasets are shown in Table 7.

For overaccommodation (see Table 7, top), we see that the accommodative error magnitude had a significant effect on visual acuity, with thresholds worsening by logMAR 0.21 for every 1 D increase in error for a pupil diameter of 4 mm (95% CI from 0.10 to 0.31, $t(4.38) = 3.84$, p=0.016). Furthermore, for every millimetre of pupil size increase, the effect of error magnitude on visual acuity significantly increases by logMAR 0.08 (95% CI from 0.02 to 0.13, $t(5.39) = 2.78$, $p = 0.036$). This means that when participants have larger pupil sizes, their visual acuity is more affected as defocus increases. No significant differences in visual acuity were found between illuminants, so the differences previously observed for small accommodative errors within the linear portion of the accommodation response curve, are not present for positive accommodation errors of larger magnitude.

Visual acuity [logMAR] - Overaccommodation							
Parameters	**Estimate**	**CI 95%**		**df**	**t-ratio**	**p-value**	**RE SD**
Intercept *(4 mm, 0 D, 459 nm)*	0.13	-0.06	0.32	4.52	1.31	0.252	0.29
Error magnitude [D]	***0.21***	***0.10***	***0.31***	***4.38***	***3.84***	***0.016***	***0.14***
Pupil Diameter [mm]	-0.07	-0.15	0.01	5.80	-1.80	0.123	0.10
Illuminant: 528 nm	-0.05	-0.11	0.01	10.09	-1.67	0.126	0.08
Illuminant: 610 nm	-0.01	-0.08	0.06	9.62	-0.23	0.822	0.09
Illuminant: broadband	-0.04	-0.09	0.01	13.18	-1.68	0.116	0.05
Error magnitude [D] * Pupil Diameter [mm]	***0.08***	***0.02***	***0.13***	***5.39***	***2.78***	***0.036***	***0.07***
Visual acuity [logMAR] - Underaccommodation							
Parameters	**Estimate**	**CI 95%**		**df**	**t-ratio**	**p-value**	**RE SD**
Intercept *(4 mm, 0 D, 459 nm)*	0.14	0.04	0.25	5.08	2.61	*0.047*	0.14
Error magnitude [D]	0.06	0.00	0.12	9.97	1.82	0.098	0.07
Pupil Diameter [mm]	-0.05	-0.12	0.02	7.09	-1.44	0.192	0.09
Illuminant: 528 nm	-0.07	-0.14	-0.01	7.31	-2.16	0.066	0.08
Illuminant: 610 nm	-0.04	-0.11	0.03	7.48	-1.21	0.264	0.09
Illuminant: broadband	-0.07	-0.14	-0.01	4.83	-2.15	0.086	0.08
Error magnitude [D] * Pupil Diameter [mm]	0.04	-0.02	0.11	3.53	1.31	0.268	0.09

Table 7. Linear mixed models' results of visual acuity for positive accommodative errors (top) and negative accommodative errors (bottom), as a function of error magnitude, pupil diameter, their interaction, and illuminant. The coefficient estimates, their 95% confidence intervals (CI 95%), t-ratios, degrees of freedom (df), p-values, and random effects standard deviations (RE SD) are shown.

For underaccommodation (see Table 7, bottom), we see that increases in error magnitude has a smaller effect on visual acuity that does not reach significance, with thresholds only worsening by logMAR 0.06 (95% CI from 0.00 to 0.12, $t(9.97) = 1.82$, $p = 0.098$) for every dioptre of increase in error and a pupil diameter of 4 mm. For 1 mm of increase in pupil diameter, the effect of accommodative error increases by logMAR 0.04 per dioptre, however, the confidence intervals are wide, and the effect is not significant (95% CI from -0.02 to 0.11, $t(3.53) = 1.31$, $p = 0.268$). Finally, visual acuity thresholds were higher for the 459 nm when compared to the 528 nm illuminant by logMAR 0.07 (95% 0.01 to 0.14, $t(7.31) = 2.16$, $p=0.066$) and the broadband illuminant by 0.07 (95% CI 0.01 to 0.14, $t(4.38) = 2.15$, $p = 0.086$); however, these differences only reach significance at the 0.10 level.

The differences in results between both models could be explained by the fact that the negative accommodative errors were found mainly over the linear portion of the accommodation response curve, as the nearest distance used was not sufficient to reach the upper limit of the accommodative range of most participants. Indeed, we can see the similarities between the results for the linear portion of the accommodation response curve and for all the negative accommodative errors data. On the contrary, most participants did reach the lower limit of their accommodative range before the farthest distances used, so there was a wider range of data for the positive accommodative errors fit. However, it is possible that some of the differing results found are due to inherent differences in the effect of the accommodative error sign, as we see that for one of the two participants that reached their upper accommodative limit, visual acuity thresholds increased with a shallower slope when underaccommodating to the stimuli (see Appendix C, Subject 2).

2.4.Discussion.

In this chapter we presented results of three experiments where we measured the steady-state accommodation and pupil responses of mostly untrained observers when looking at targets illuminated by different narrowband lights and placed at different distances. We found that most participants were able to accommodate under monochromatic light when the illumination of the target was changed abruptly and were able to maintain focus for the duration of the trials with similar accuracy as in white light, particularly at nearer distances (see Figure 10 to Figure 12). We found no systematic differences between broadband and narrowband illuminants in the variability of the accommodation response of observers over time, and the within-trial accommodative response fluctuated on average by similar amounts for the broadband and the green illuminants, regardless of the mean accommodative state (see Figure 16).

This finding contradicts some of the results reported by Kruger et al. (1997), as 38% of their sample had difficulty maintaining focus with narrowband targets placed away from the tonic state accommodation (at distances of 0 and 5 dioptres), while they could accommodate accurately to a broadband target at the same distance. These distances were included in our experiments, and we found no such impairment in steady-state accommodation. Instead, our results agree with those of Atchison et al. (2004) that accommodative responses to targets with reduced spectral bandwidth were not more variable than responses to broadband targets; as well as with the findings of Charman & Tucker (1978), which showed that participants can accommodate to narrowband stimuli of different wavelengths and maintain focus as accurately as in white light. It is notable that most of the participants in our sample were untrained naïve observers, as the one inexperienced observer of Charman & Tucker (1977) was not able to accommodate to the narrowband stimuli without additional training in the task. It is plausible that nowadays, with the increasing prevalence of narrowband LEDs as primaries in digital displays and as illumination sources, naïve observers have more experience accommodating to this type of stimulus and can make use of other cues to determine the sign and magnitude of the accommodative change, as well as to maintain focus. Some residual chromatic blur could still be present in our narrowband stimuli that could potentially serve as an accommodative cue since LEDs are not completely monochromatic (with a spectral bandwidth of ~20 nm). This would be especially true for shorter wavelengths, as the effects of LCA are greater towards the blue end of the spectrum (see Figure 6, right). However, we did not find that accommodation was more accurate for short wavelengths, and in fact, the slope of the accommodation response curve as a function of distance was shallowest for these illuminants and the variability of the response higher. Thus, there is no evidence that any residual chromatic blur within a single narrowband illuminant contributed to the subject's abilities to accommodate.

One of our main findings is that the slope of the linear portion of the accommodation stimulus-response curve becomes shallower as the peak wavelength of the narrowband illuminants decreases, which is caused by an increase in the difference in accommodation to different wavelengths as the target is placed at nearer distances (see Figure 12). In other words, the extent to which participants change their accommodation responses to compensate for the LCA of the eye increases as they accommodate to nearer targets. At a distance of ~0.5 dioptres there are no significant differences in the accommodation to different wavelengths, while at approximately 4.5 dioptres, participants change their accommodation responses nearly to the full extent that the chromatic eye model predicts (Thibos et al., 1992). This was a common finding in all three experiments, but there were considerable differences between participants, particularly at farther distances, as some subjects did change their accommodative responses to some extent to compensate for LCA even at 0.5 dioptres or farther.

Previously, Charman & Tucker (1978) had found some comparable results. They measured the accommodation response curves for six participants under red and blue light and found that the slope was shallower for blue (468 nm) in at least two of the subjects. However, for one of these subjects they measured the response to other narrowband illuminants (644 nm, 579 nm, 546 nm, 503 nm) and did not find a significant difference in the slope of the accommodation function other than for blue, albeit at distances of 1 and 2 dioptres this subject significantly underaccommodated for red (644 nm). They theorized that this change could be partly explained by an increase in the LCA of the eye as the power of the crystalline lens increases. They then took objective measurements of the LCA of the eye in this participant and observed that it increased by ~3% (0.03) per dioptre of accommodation, which they postulated could account for the results found for that subject (although some overaccommodation for blue and underaccommodation for red remained at the farthest distances tested of 1 and 2 dioptres, even after this adjustment). Across our sample, however, we found that the extent to which participants change their accommodation responses to correct for LCA increases by a much larger factor of 0.28 (95% CI from 0.08 to 0.45) per dioptre of increase in target vergence; thus, while an increase in LCA with accommodation might account for part of our results, it does not seem to fully explain them on its own. Charman & Tucker (1977) also proposed that the change in slope in blue light might be due to reduced acuity at shorter wavelengths; however, we found that the difference in slope was significant between other illuminants tested as well (e.g., red and orange), so it does not seem to be unique to blue light.

Previous studies had found an increase in LCA with accommodation (Nutting, 1914; Sivak & Millodot, 1974), as well as inter-individual differences in the LCA measured for different observers (Nutting, 1914; Wald & Griffing, 1947; Bedford & Wyszecki, 1957; Sivak & Millodot, 1974). Sivak & Millodot (1974) in particular, used an achromatizing lens that corrected for most of the LCA of the eye (Bedford & Wyszecki, 1957), and subjectively measured the difference in optimal focal distance between different wavelengths at distances of 0.6, 3.0 and 7.1 dioptres. They observed that the difference in accommodation as a function of wavelength increased in all subjects from a mean of 0.40 dioptres at the farthest distance, to 0.65 dioptres at the nearest, with some variability between observers. If we perform a linear fit on their data, we see that the rate of increase in LCA is of 0.036 (or 3.6%) per dioptre of accommodation, similar to the results of Charman & Tucker (1977).

The fact that participants accommodate with increased accuracy to different wavelengths as the target nears is perhaps a surprising result, if we consider our finding that pupil size decreases with increasing accommodation, increasing the depth of focus of the eye. Indeed, it has been observed that the steady-state accommodative response of the eye is more accurate for larger pupil sizes (Ward & Charman, 1985), thus, we would expect observers to compensate for LCA to a greater extent when pupil size is larger at farther distances. In addition to this, in the first experiment the angular size of the target increased as it was placed nearer the observer, which would have decreased the high spatial frequency content of the image and increase power at lower spatial frequencies. Previous studies have found that the steady-state accommodation response is more accurate for higher spatial frequencies and substantial in error for lower spatial frequencies (Charman & Tucker, 1977), so we would expect this factor to contribute to responses being less accurate at nearer distances, but the results of this experiment indicate otherwise.

One possibility that could explain these results is that, as LCA is significantly reduced in narrowband light, participants are making use of other cues to find the optimal focal distance for different wavelengths, and these cues might change with target vergence. Specifically, the micro-fluctuations of the crystalline lens have been found to increase in magnitude as accommodation increases due to the increased freedom of movement (Kotulak & Schor, 1986; Stark & Atchison, 1997; Day et al., 2006), covering an approximate range of 0.02 dioptres in both directions when the mean accommodation is 1 dioptre, and increasing to a range of up to 0.1 dioptres when the accommodative response is 4 dioptres (Kotulak & Schor, 1986b). These micro-fluctuations can serve as a cue to accommodation by providing negative feedback to the accommodative control mechanism (Kotulak & Schor, 1986), essentially functioning as sub-threshold blur detector (Kotulak & Schor, 1986b); thus, it is possible that the increased range of these micro-fluctuations at higher accommodation levels allows the visual system to find the focal distance for each wavelength more accurately when the colour of the target is changed and in the absence of the chromatic blur caused by LCA. However, this is only speculation on our part, as there is no evidence in the literature that the increased amplitude of micro-fluctuations can lead to higher accommodative accuracy, and on the contrary, consistent steady-state errors when accommodating to nearer targets are often found (Plainis et al., 2005).

Another factor that could be influencing these results is that accommodation might become less accurate as observers reach the far point of their accommodative range, which would happen at nearer physical distances for targets illuminated by shorter wavelength light. In other words, the typical lag of the accommodation response curve would start to occur at nearer distances for short than for long wavelength light, which would cause the slope estimate to be shallower. However, the analysis performed to determine the accommodative range of each participant for each individual illuminant, and the subsequent exclusion of the saturated points should have addressed this issue, at least partially. Overall, our results seem novel within the literature, albeit Charman & Tucker (1978) had some comparable findings with two of their subjects. It is not clear why participants increasingly correct for LCA at nearer distances when accommodating to narrowband stimuli, and more research is needed in this area to explain these results, as well as to further explore the individual differences between observers.

Another of our findings was that accommodation to white light tended to overlap with middle wavelengths over all distances tested (see Figure 10 to Figure 12). When the targets were illuminated by a white light with the highest luminous spectral power between 530 and 590 nm, accommodation was similar to the narrowband illuminants of similar peak wavelengths (527 and 588 nm) over all distances tested, although the slope as a function of distance was steeper than for the narrowband illuminants and closer to one, with accommodation slightly shifting from green towards orange as target vergence increased from 0.5 to 3 dioptres. In a third experiment where a broadband illuminant was created by using the three narrowband primaries at equal luminance, accommodation seemed to overlap with the red illuminant (610 nm), or between the red and green (528 nm) illuminants, over most distances tested.

Some previous studies have investigated the wavelength that comes into focus in the retina in broadband white light at different distances. Ivanoff (1949) found that with increasing accommodation, the wavelength that was kept in focus in the retina decreased, from ~600 nm at 0.5 dioptres, to ~500 nm at 2.5 dioptres. Similarly, Sivak & Millodot (1974) found that the wavelength in focus changed from 620 nm at a distance of 0.7 dioptres, to 530 nm at a distance of 7.1 dioptres. Ivanoff (1949) proposed that this change of wavelength-in-focus with distance could explain the lag and leads of the accommodative response by a process of "sparing of accommodation", that is, the visual system uses the LCA of the eye to accommodate as close as possible to the tonic or resting state, choosing to accommodate to shorter wavelengths at near distances, as they require the least refractive power, and to longer wavelengths for farther distances. If this were the case, one would expect to find much steeper stimulus- response curves for narrowband illuminants than for white light, which does not agree with our findings. Similarly, Charman & Tucker (1978) and Jaskulski et al. (2016) did not find that the stimulus-response curves for narrowband light of different wavelengths was steeper than for white light. Thus, no "sparing of accommodation" seems to be taking place, and it is possible that those earlier findings were due to the spherical aberration of the eye usually changing from positive at far, to increasing negative values as accommodation increases (Thibos et al., 2013; Del Águila-Carrasco et al., 2020). When spherical aberration is positive at far distances, the rays entering through the periphery of the pupil will come into focus in front of the retina, so the shorter wavelength content of that light will be more out of focus and longer wavelengths will come into focus closer to the retina. When accommodation increases and spherical aberration becomes negative, the peripheral rays will come into focus behind the retina, so the longer wavelength content will be more out of focus and shorter wavelengths more in focus. Thus, it is possible that the phenomenon observed by Ivanoff (1949) was due to the distribution of light in the retina changing due to a change in the sign of the spherical aberration of the eye, rather than by the visual system shifting the wavelength that is kept in focus in white light.

Our results seem to indicate that when accommodating to white light, the wavelength that is kept in focus is between 527 and 610 nm, which agrees with findings by DeHoog & Schwiegerling (2007) who reported that the best focus in white light occurred at equivalent values of monochromatic light between 590 and 610 nm. The slightly steeper slope closer to unity that we found for white light when compared to the green or orange illuminants, could be explained by the presence of the chromatic blur caused by LCA aiding accommodation to match the demand more accurately, albeit our results are not conclusive in that regard.

Another of our findings was that steady-state median pupil diameter decreases with increasing accommodative state and with decreasing peak wavelength in narrowband illuminants, even when luminance and angular size was equal (see Figure 17). The effect of wavelength can be explained by the contribution of the melanopsin photopigment present in some intrinsically-photosensitive retinal ganglion cells (ipRGCs) to steady-state pupil size control (Spitschan, 2019b, 2019a). While the stimuli were created to provide equal input to the luminance channel, pupil size control has a strong input from the ipRGCs (Spitschan, 2019a) in addition to the cone photoreceptors. The melanopsin photopigment is more sensitive to short wavelength light than the L and M cones, with a peak sensitivity at 480 nm (Al Enezi et al., 2011); thus, the shorter wavelength light used in our experiments would provide greater stimulation to the ipRGCs and the pupil control mechanism than the longer wavelength illuminants of equal luminance.

The literature investigating the effect of accommodation on pupil size offers a less clear picture to explain our results. While the near triad of accommodation, convergence and pupil constriction is a well-established fact, there is contradictory evidence on whether convergence or accommodation are responsible for the pupil response at near distances. Some studies have found that accommodation alone does not trigger a pupil response when convergence and other factors such as target size and alignment are controlled (Stakenburg, 1991; Phillips et al., 1992; Feil et al., 2017). However, one of these studies measured dynamic rather than steady-state pupil responses, and another did not directly measure accommodation, but inferred it from acuity measurements. Other studies have arrived to the opposite conclusion, finding that blur-driven accommodation and not fusional vergence, cause pupil constriction (Marg & Morgan, 1949; Wilson, 1973; Jones, 1989, cited on Phillips et al., 1992). As to the extent of the change, Marg & Morgan (1950) found that pupil diameter changed on average by 0.48 mm per dioptre of accommodative stimulus and did not change with convergence, although it is possible that factors such awareness of target proximity might have played a role (Phillips et al., 1992). On the other hand, O'Neill & Stark (1968) and van der Wildt & Bouman (1971) both reported measurements showing an increase of ~0.17 mm per dioptre of accommodation when describing the design and construction of equipment to measure accommodation, vergence and pupil diameter dynamically. While their experiments had more carefully controlled parameters, presenting the targets monocularly and maintaining constant target size, alignment along the axis of the eye, and luminance, their sample was limited to just one subject each. Here, we present results with a larger sample that show similar estimates, with steady-state pupil diameter decreasing by 0.16 to 0.18 mm per dioptre of accommodation for targets that were viewed monocularly, aligned with the axis of the stimulated eye, and with constant luminance and angular size. Furthermore, in one of our experiments the apparent distance of the target was also kept constant, with the accommodation being driven by placing lenses in front of the eye. Thus, our results provide further support to the idea that steady-state pupil constriction can be caused by accommodation alone, although the rate of change is smaller than reported in some of the previous studies.

Over the quasi-linear portion of the accommodation response curve, we found that accommodative errors (i.e., the difference between accommodative demand and the median response) had mostly magnitudes of up to 1 dioptre in either direction, although underaccommodation was more prevalent in our sample (see Figure 18). An interesting finding was that not all subjects presented the consistent lags in accommodation as the target nears that are often reported in the literature (Nakatsuka et al., 2003), and overall, there was great inter-subject variability in the shape and slope of the stimulus-response curve. Furthermore, the two subjects that did present significant lags of up to 1.5 and 2 dioptres of magnitude at near distances in the third experiment, did not have their visual acuity significantly impaired by those accommodative errors. In fact, over the linear portion of the accommodation response curve for all participants, we found that accommodative error did not have a significant effect on visual acuity thresholds.

It is possible that our measurements were not precise enough to capture the relationship between accommodative error and visual acuity for a relatively small range of errors. Accommodation was measured as participants performed the staircase procedure with targets of different spatial frequency being presented and pupil size allowed to change freely, so the accommodative response would not be the only factor affecting retinal image quality, and the median of this response might not be representative of the defocus of the retinal image when participants were viewing the smaller targets that were more critical to the thresholds obtained. The depth of field of the eye would also allow some of these accommodative errors to not have a detrimental effect on visual acuity. For pupil diameters between 4 and 6 mm, the depth of field can be between 0.4 and 0.5 dioptres, even for high spatial frequencies and monochromatic light (Marcos et al., 1999), albeit higher estimates have been obtained (Wang & Ciuffreda, 2006). Jaskulski et al. (2016) for example, found that the subjective depth of field for a pupil diameter of 3.8 mm and a target of logMAR 0.1 size, was approximately 1.19 dioptres for narrowband light, and slightly higher for polychromatic light. Of course, even the higher estimates are not enough to fully explain the results obtained, particularly in the two subjects that showed lags of significant magnitude.

Recently, Labhishetty et al. (2021) used several objective and subjective measurements to measure the accommodation of the eye. They found that, for target distances between 0 and 6 dioptres, objective measurements had higher accommodative errors than subjective measurements based on visual acuity. In particular, the measurements taken using a photorefractor gave the largest measured lags, with magnitudes between 0.5 and 1.5 dioptres. Despite these large errors, subjective measurements indicated that participants were accommodating accurately to the distance that maximised their visual acuity, with the subjective errors being much lower at ~0.15 dioptres. These results are comparable to ours, as we used a photorefractor to measure accommodation and found errors of considerable magnitude (mostly lags) that did not seem to have a detrimental effect on visual acuity. In particular, the two subjects that displayed the more typical large accommodative lags, maintained visual acuity thresholds close to logMAR 0 regardless of the magnitude of these errors.

It has been suggested that the consistent errors that are observed when accommodation is measured objectively with a photorefractor (i.e., lags and leads), might actually be the consequence of the spherical aberration of the eye, particularly its change in sign with accommodation (Plainis et al., 2005; Thibos et al., 2013). As mentioned previously, the eyes of most observers tend to exhibit positive spherical aberration when accommodating at far distances, which decreases steadily with increasing demand and becomes negative at nearer distances (Del Águila-Carrasco et al., 2020). This means that peripheral rays will come into focus in front of the retina at far distances and behind the retina at near. As photorefractors use the distribution of reflected light across the entire pupil to estimate the refractive state of the eye, they might put more weight on these marginal rays than the visual system does, leading to apparent leads and lags in accommodation, even when paraxial rays are focused correctly in the retina (Thibos et al., 2013). Thus, it is possible that the large accommodative lags observed in two of the subjects in our third experiment are due to their own spherical aberration and the method used to measure accommodation.

While accommodative errors were small over the linear portion of the accommodation response curve, and thus, did not have a significant effect on visual acuity, we did find differences caused by the illuminants used. Visual acuity thresholds were significantly lower for blue light when compared to the other three illuminants. When accommodative error was zero, the visual acuity for blue light was estimated to be logMAR 0.04, while for the red, green, and broadband illuminants it was logMAR -0.04, -0.07 and -0.05, respectively.

It is known that S-cones, which are more sensitive to short-wavelength light, are sparsely distributed in the retina, resulting in a lower spatial resolution when compared to the other two cone systems. However, luminance was kept the same for all illuminants used in this experiment, resulting in an equal input to the luminance (L+M) channel. In other words, all lights appeared as of equal intensity to the achromatic or luminance channel, which has a higher spatial resolution. This means that the differences in visual acuity cannot be explained by the differences in sensitivity to different wavelengths or the sparseness of the S-cones in the retina. The lower visual acuity for blue light can rather be explained by the blur caused by LCA for shorter wavelengths.

For a spectral distribution that is not completely monochromatic, the LCA of the eye will cause greater defocus at shorter wavelengths, which will in turn reduce retinal image contrast, particularly at higher spatial frequencies. The blue light used had a spectral bandwidth (full width at half maximum) of 20 nm around a peak wavelength of 459 nm, which would cause a difference in defocus of 0.21 dioptres. In comparison, even though the green and red illuminants had slightly larger spectral bandwidths (25 and 28 nm, respectively), there would only be a difference of 0.16 and 0.11 dioptres in defocus across the bandwidth of their respective spectral distributions. As this defocus is caused by the intrinsic change in refractive index of the eye with wavelength, the accommodative response alone cannot correct it. Furthermore, it seems that the smaller average pupil size for blue light is not sufficient to improve focus or the retinal contrast of the image. Indeed, it has been observed in the literature that, while visual acuity in blue narrowband light is lower under normal conditions, compensating for the LCA of the eye improves the thresholds so that they more closely match those obtained in green, red and white light (Domenech et al., 1994). Overall, however, our results indicate that the visual acuity thresholds for blue were still within the range of normal vision, and the differences with the other primaries of the display were small (~logMAR 0.09), such that it is unlikely to have a significant impact in most real-life applications.

The increased defocus caused by LCA for shorter wavelengths could also explain the increased variability of the accommodation response for these illuminants when compared to longer wavelength ones. It has been previously reported that the magnitude of the micro-fluctuations of accommodation increases with increasing blur in the image (Niwa & Tokoro, 1998) and with decreasing contrast (Denieul & Corno, 1986; cited in Charman & Heron, 1988), and correlate with the objective depth-of-focus of the eye (Yao et al., 2010). The higher defocus caused for narrowband LEDs of shorter peak wavelength would reduce retinal image contrast and increase the depth-of-focus, which could increase the magnitude of the micro-fluctuations of accommodation, resulting in the higher within-trial variability of the response observed. We did not find, however, an increased variability in the broadband illuminants used, even though defocus and depth-of-focus would be greater in this condition (Jaskulski et al., 2016). Niwa & Tokoro (1998) previously found that micro-fluctuations increase as the blur of the image increases, but only for small amounts of blur. As the magnitude of blur continues to increase, the magnitude of the micro-fluctuations starts to decrease again, and the amount of blur at which micro-fluctuations peak is lower for higher spatial frequencies. These changes were found in particular for the low-frequency components of micro-fluctuations, which are caused by the action of the ciliary muscles on the crystalline lens (i.e., are under neural control), and have been proposed to be of more significance to the accommodative control system (Charman & Heron, 1988). As blur increases, micro-fluctuations might increase in order to serve as an error signal to accommodation and improve the accuracy of the response. With higher depth-of-focus, the magnitude of the micro-fluctuations would need to be higher in order to provide the same amount of information for error detection to the accommodative control mechanism. Niwa & Tokoro (1998) postulate that when blur surpasses a certain threshold, it can no longer be discriminated and there is an overall reduction in micro-fluctuations, with this threshold being lower for higher spatial frequencies as they are more affected by defocus. Thus, it is possible that the higher defocus caused by LCA for the broadband illuminants is not detectable, causing the magnitude of the micro-fluctuations to be lower when compared to the short wavelength illuminants. It is important to note that these differences in response variability were found even after controlling for the mean accommodative state of the eye, as micro-fluctuations have been found to increase with increasing accommodation (Kotulak & Schor, 1986a; Stark & Atchison, 1997; Day et al., 2006), which we corroborated in this study.

Interestingly, visual acuity thresholds in white light did not differ significantly from those obtained with the narrowband green and red illuminants. The chromatic blur caused by LCA in broadband white light did not seem to impair visual acuity, even though for our broadband illuminant all three primaries were set at equal luminance (so the chromatic blur would not be attenuated by the reduced luminous sensitivity at longer and shorter wavelengths). Domenech et al. (1994) found comparable results: with normal LCA, the visual acuity in white was similar as for red and green narrowband light and compensating for the LCA of the eye did not significantly improve the thresholds for white light. More recently, Suchkov et al. (2019) also found that correcting the LCA of the eye did not cause the predicted improvement in visual acuity, but rather a slight decrease (albeit it was not statistically significant), and that doubling the LCA of the eye had a more detrimental effect than predicted from their simulations. Further evidence from these authors also shows that correcting for the LCA of the eye does not improve visual acuity in high contrast conditions, even when subjects are given time to adapt to the corrected LCA (Fernandez et al., 2020). Thus, it seems that the ability of the visual system to resolve small targets with precision is not impaired by the chromatic blur caused by LCA, at least in high contrast conditions.

Finally, when considering all the visual acuity measurements, including those obtained beyond the accommodative range of participants, we found that overaccommodation had a significant detrimental effect on visual acuity, and a statistically significant interaction with pupil diameter, such that visual acuity was more affected by defocus in larger pupils than in smaller ones. This is consistent with previous findings in the literature of an increased depth of focus with smaller pupil sizes (Marcos et al., 1999; Wang & Ciuffreda, 2006). No effect of illuminant was found, indicating that larger values of defocus affect broadband and narrowband targets equally, including blue light. This is also consistent with previous findings that indicate that depth of focus increases with decreasing acuity (Tucker & Charman, 1975), such that the small amount of blur caused by LCA for blue light would no longer have an impact on retinal image quality.

In summary, we found that narrowband illumination can be an adequate stimulus to accommodation when compared to white light, even in a sample of mostly untrained observers. We also found that the extent to which participants change their accommodative responses to compensate for the LCA of the eye increases at nearer distances and matches the predictions of the chromatic eye model from approximately 4.5 dioptres (22 cm) and nearer; a finding which is not fully explained by the previously reported increase in LCA of ~3% per dioptre of accommodation. This means that considering the spectral distribution of the display primaries and its effect on accommodation might be more relevant for displays that are used at nearer distances, such as mobile phones or computer monitors, than for those that are viewed farther away such as television or cinema screens. We found no detrimental effects on visual acuity for narrowband light, with only blue light causing a significant worsening of the thresholds due to the larger spread of defocus caused by LCA at shorter wavelengths for a display primary that is not completely monochromatic. However, visual acuity in blue light was still within the range of normal vision (~logMAR 0), and this small difference is unlikely to be relevant to real-life display applications where images with multiple spatial frequencies are used.

Chapter 3. Accommodation to pairs of narrowband illuminants.

3.1. Introduction.

As we have previously discussed, the Longitudinal Chromatic Aberration (LCA) of the human eye serves as an important directional cue to accommodation, both for dynamic and static responses. Previous evidence suggests that observers are able to use the chromatic blur caused by LCA to find the point of best focus (Kruger et al., 1993), and that in broadband white light they accommodate to wavelengths in the middle of the visible spectrum approximately around green and orange (Charman & Jill Tucker, 1978; J. Lovasik & Kergoat, 1988; DeHoog & Schwiegerling, 2007). In daylight, this strategy would lead to an optimal retinal image quality, as the spectral distribution of the light is smooth, and subjects would accommodate to wavelengths near the peak of their luminous sensitivity. However, most digital displays make use of three colour primaries that are relatively narrowband, leading to a spectral distribution with three distinct peak wavelengths. Accommodating to middle wavelengths when a target is illuminated by the red and blue primaries for example, could lead to suboptimal retinal image contrast, particularly for high spatial frequencies within the image (Ward, 1987); thus, it is possible that observers adopt a different strategy, such as using other available cues to find the best point of focus.

Some previous evidence suggests that LCA might improve the accuracy of the accommodative reflex, even when only two relatively narrowband lights are present. Fincham (1953) tested the accommodation reflex of trichromats and dichromats (lacking either the L or M cones) when a divergent lens was quickly introduced between the eye and targets illuminated either by a narrowband yellow light, or by a colour matched combination of green and red light. They found that trichromats accommodated much more accurately to targets illuminated by the red and green mixture than by the narrowband yellow light, while in dichromats there was no difference between both stimuli, and the accuracy of their responses was comparable to that of trichromatic subjects for narrowband yellow light. However, they did not report where subjects accommodated to for each stimulus, and only tested the red-green mixture at matched luminance values.

Most other studies to date that have looked at accommodation to mixed chromatic stimuli have done so by presenting different combinations of target and background colours using the primaries of visual displays (e.g., blue letters on a red background). These studies were particularly prevalent in the 80s and 90s and were driven by the development of colour video display terminals and their increased incorporation into work environments and daily life. Their findings were overall mixed.

Murch (1982) measured accommodation to mixtures of red, green, and blue primaries on a black background, as well as to letters of each individual colour on a black background. They found that while the monochromatic targets drove accommodation as predicted by the LCA defocus (i.e., greater accommodation for red, lower for blue, and green at an intermediate value), accommodation to their different mixtures on a black background was similar for all combinations. Similarly, Lovasik & Kergoat (1988) found that monochromatic letters on a black background elicited the expected difference in accommodation; however the responses to blue letters on a red background, blue letters on green background, and red letters on a green background, had all similar values and were not statistically different from one another. Furthermore, accommodation for the three mixtures was significantly higher than for all the monochromatic targets, including the red letters on a black background. While they were not able to find an explanation for these results, they reproduced these findings in another study (J. Lovasik & Kergoat, 1988), at two separate distances of 2.5 dioptres and 1.25 dioptres. Intrigued by these results, Charman (1989) performed a similar study, albeit using coloured paper illuminated by white light. They found great inter-subject variability in the results, with some favouring accommodating to red, others to blue, and a third and fourth group accommodated to whatever colour the background, or the target letter had, respectively. They also found that some participants accommodated to one colour in one trial, and the other on the next, but never within the same trial, and never accommodating in between. More recently, Atchison et al. (2004) found that accommodative responses to multicolour red-on-blue and blue-on-red targets were closer in value to the blue-on-black response than to red, and that they were not significantly more variable than the responses to a white target on a black background. These studies as a whole suggest that there might be considerable inter-subject variability when accommodating to mixed chromatic stimuli, as well as variability between samples and studies that could be caused by the differences in experimental conditions used. In particular, some of these results could be explained by the difficulty of the visual system has when accommodating to isoluminant or near-isoluminant targets (Atchison et al., 2004). More research in this area is necessary to elucidate if other factors such as the luminance of each colour in the mixture, target size and distance, could be influencing where participants accommodate.

Other studies have proven that accommodative responses can be elicited by simulating the effects of LCA with the three primary colours of a screen. Lee et al., (1999) showed observers sine gratings with simulated blur where the intensity profile of the red, green and blue primaries had been selectively altered to simulate 1 dioptre of defocus in front and behind the retina in an eye with LCA. They compared these conditions with a control in which 1 dioptre of defocus was simulated in an eye with neutralised LCA (i.e., there was no chromatic blur). They found that, when viewing these stimuli through a pinhole, most participants changed their accommodation responses in the direction indicated by the simulated chromatic blur with respect to the control condition. That is, accommodation was higher than in the control condition for hyperopic defocus, and it was lower than in the control for myopic defocus. These results were later replicated and found to be robust even when the three colour images were slightly misaligned (Stark et al., 2002). A similar study was conducted by Kruger, Mathews, et al. (1995), where they selectively manipulated the contrasts of the red, green and blue primaries to simulate a grating oscillating in focus at 1 dioptre in front and 1 dioptre behind the retina. They found that the dynamic accommodation responses of participants were strongly driven by this stimulus, and not by a similar luminance control trial with no chromatic blur. More recently, Cholewiak et al. (2017) developed a method to render simulated blur that incorporates the LCA of the eye and generates retinal images similar to those found for natural defocus. They showed that this method could be used to drive the accommodative response of observers at distances of up to 1.4 dioptres away from the screen, both when viewed through a pinhole and through a natural pupil (i.e., open and closed loop conditions). These results indicate that the visual system uses LCA as an important cue to accommodation, even when it is in conflict with other cues such as defocus or micro-fluctuations, and when it is detrimental for overall retinal image quality (as accommodating away from the screen would worsen the defocus of the image).

Another set of possibly relevant findings come from studies on multiplane displays. These are visual displays that seek to provide focus cues to the observer by placing multiple screens at different distances from the eye and driving accommodation continuously between the screens by changing the distribution of light across each plane according to the desired demand. This process is referred to in the literature as depth-filtering (Ravikumar et al., 2011), and evidence suggests that it can drive accommodation as intended (MacKenzie & Watt, 2010; MacKenzie et al., 2010), reducing the negative effects of the vergence-accommodation conflict (Hoffman et al., 2008). MacKenzie et al., (2010) found that monocularly, observers will accommodate between two planes when they are separated by distances of up to 1.1 dioptres, but that for greater separations the accommodation response deviates from the intended demand, and observers accommodated to one of the planes, rather than in between. These findings agreed well with the results of their simulations, which also suggested that the spatial frequency of the target plays an important role. For low and middle spatial frequencies of 2 and 4 cycles per degree (cpd), contrast is maximised when accommodating between the two planes for separations between planes of up to 1.1 dioptres. However, for higher spatial frequencies of 8 and 16 cpd, the response is expected to diverge from the intended demand at separations higher than 0.7 dioptres, as contrast is no longer maximised when accommodating between the two planes, but rather when accommodating to one of the planes or the other.

These findings could be potentially relevant to determining where participants accommodate when looking at targets illuminated by two narrowband lights of different peak wavelengths. Due to LCA, each wavelength will elicit a different accommodative demand, and by weighting their luminance within the mixture, it is possible that observers will accommodate between the two wavelengths when the difference in accommodative demand between the two is 1.1 dioptres or less. However, for wavelengths that have a greater difference in accommodative demand (e.g., 1.23 dioptres between 450 nm and 650 nm), observers might accommodate to the narrowband light with the highest luminance in order to maximize retinal image contrast. Furthermore, we could also expect that for targets of higher spatial frequency, this shift to one of the illuminants might occur for wavelengths with smaller differences in their accommodative demands (e.g., for 450 nm and 550 nm with a difference in defocus of 0.8 dioptres).

In this chapter we present three experiments that aim to offer some answers to the questions posed so far and establish where participants accommodate to when a target is illuminated by pairs of narrowband illuminants, and how this point changes as their relative luminance within the mixture changes. We also explore the role that the spatial frequency of the target might have on the accommodative responses to these mixed chromatic stimuli. Our results could offer valuable information on the different rules that the human visual system uses to accommodate in the presence of unnatural spectral stimuli. This could be relevant for understanding how retinal image contrast might be affected by defocus in displays with narrowband primaries, as well as for the design of visual displays that aim to drive accommodation by providing focus cues to the observers.

3.2.Methods.

In this section we describe the methods used in three experiments where we measured the accommodation responses of participants to pairs of narrowband lights. As previously, the experiments described in this chapter were designed and implemented in a sequential manner, such that the results of the previous stage informed the aims and experimental setup of the following one. Experiment 1 served as an exploratory study that allowed us to get an initial insight into the accommodation responses of participants to pairs of narrowband wavelengths. We focused on using luminance proportions closer to 50/50 for the pair of lights, as we assumed these would be the most informative. Furthermore, we used a longer trial duration in order to allow enough time for participants to accommodate to these stimuli. Since we observed that participants could accommodate to the targets quickly, in experiment 2 we reduced the duration of the trials, increased the number of repetitions and used a greater range of luminance proportions in order to observe more fully how steady-state accommodation changed from one light in the mixture to the other. Finally, we wanted to understand the role that the spatial frequency of the target had on the accommodation responses observed, so we used a separate experimental setup with a display that was capable of presenting spatial information dynamically.

The first two experiments used the same apparatus as experiments 1 and 2 described in Chapter 2, while the third experiment used the same apparatus as experiment 3 described that chapter. Any differences are detailed here, and experiment 3 is described separately where necessary.

3.2.1.Participants.

Data were collected from 14 adults in total, with ages between 23 and 32 years old (mean 26.8, SD 2.8), out of which 8 were female and 6 were male. From this total sample, one participant took part in both experiment 1 and 2, one participant took part in experiments 1 and 3, and one participant took part in all three experiments. All but 2 participants were naïve as to the aim and hypothesis of the experiment. Table 1 shows the breakdown of the sample for each individual experiment.

Participants were recruited from students, staff, and the external pool of participants of the Institute of Biosciences of Newcastle University. The study was approved by Newcastle University Ethics Committee (reference number 15327/2016) and written consent was obtained from each subject.

Experiment	Participants	Mean age (± SD)	Sex
Experiment 1	8	26.5 (± 2.4)	4 females, 4 males
Experiment 2	5	24.8 (± 2.4)	3 females, 2 males
Experiment 3	5	28.4 (± 2.9)	3 females, 2 males
Total	14	26.8 (± 2.8)	8 females, 6 males

Table 8. Sample description for experiments 1, 2 and 3.

3.2.2.Apparatus: Experiments 1 & 2.

The stimulus consisted of a Maltese cross printed on a transparent film and placed on top of a diffuser, which was mounted on a box containing six Light Emitting Diodes (LEDs) and centred to the right eye. The box was placed on a 2.5 m long rail positioned at the height of participant's eyes, which allowed to change the physical distance of the stimulus.

For experiment 1, the box was placed at a distance of 50 cm (2 dioptres), and the diffuser and Maltese cross had sizes of 8.5 cm by 8.5 cm (9.7° of visual angle), and 5 cm by 5 cm (5.7° of visual angle), respectively. For experiment 2, the box was placed nearer the observer at 33.3 cm (3 dioptres), and the sizes of the diffuser and Maltese cross were reduced to 1.5 cm by 1.5 cm (2.6° of visual angle), and 0.9 cm by 0.9 cm (1.5° of visual angle), respectively.

The refractive state of the eye and the pupil diameter was measured dynamically at 50 Hz using the photorefractor PowerRef 3 from PlusOptix. Two Arduino Uno boards controlled the stimuli and were connected to the photorefractor to synchronise the recordings.

The different pairs of narrowband stimuli were created using the five LEDs described previously in section 2.2.2. For convenience, the LEDs will be named according to their peak wavelength as: violet (441 nm), blue (460 nm), green (528 nm), orange (588 nm) and red (661 nm). In both experiments we tested 6 pairs of LEDs: green and violet, orange and violet, orange and blue, red and violet, red and blue, and red and green. The relative luminance of each LED within the pair was varied, while maintaining the total luminance at 10 cd/m^2.

In experiment 1, the luminance of the first LED was alternated so that they were presented at values of 10, 7, 6, 5, 4, 3, and 0 cd/m^2, while the luminance of the other LED in that pair concurrently increased to keep the total luminance constant. In experiment 2, the number of luminance steps were increased, and the first LED was tested at values of 10, 8.75, 7.5, 6.25, 5, 3.75, 2.5, 1.25, and 0 cd/m^2, while the luminance of the second LED simultaneously increased to keep the total luminance constant at 10 cd/m^2.

3.2.3. Apparatus: Experiment 3.

The stimuli were presented in an Active-Matrix Organic Light Emitting Diode (AMOLED) screen placed at a distance of 1 m (1 dioptre). The screen had a size of 6.84 cm by 12.2 cm, and a resolution of 1080 by 1920 pixels. The spectral distribution of the three primaries of the screen were described in section 2.2.3. For convenience, the three screen primaries will be named here according to their peak wavelengths as blue (459 nm), green (528 nm) and red (610 nm). They were tested in 3 pairs: green and blue, red and green, and red and blue. For each pair, the first LED was presented at luminance values of 10, 8.75, 1.25, 7.5, 6.25, 5, 3.75, 2.5, 1.25 and 0 cd/m^2, while the luminance of the second LED in the pair concurrently increased in similar steps, maintaining the total luminance at 10 cd/m^2.

Participants wore light-tight goggles, and the targets were viewed through the right eye, while the left eye was covered by a 720 nm infrared filter that occluded the stimuli but allowed the infrared light of the photorefractor to pass. To increase the accommodative demand of the stimuli, a lens of -4 D of power was placed in front of the right eye. This was changed for two subjects (17 and 23) to lenses of -3 D and -5 D, respectively, as they were having difficulties completing the task due to their own refractive errors.

The screen and experimental routine were controlled from a computer running MATLAB (The MathWorks Inc., 2019), which was also connected to the photorefractor to synchronize the stimuli being presented with the recordings. The images were dynamically created using the Psychophysics toolbox (Kleiner, M., Brainard, D. and Pelli, 2007).

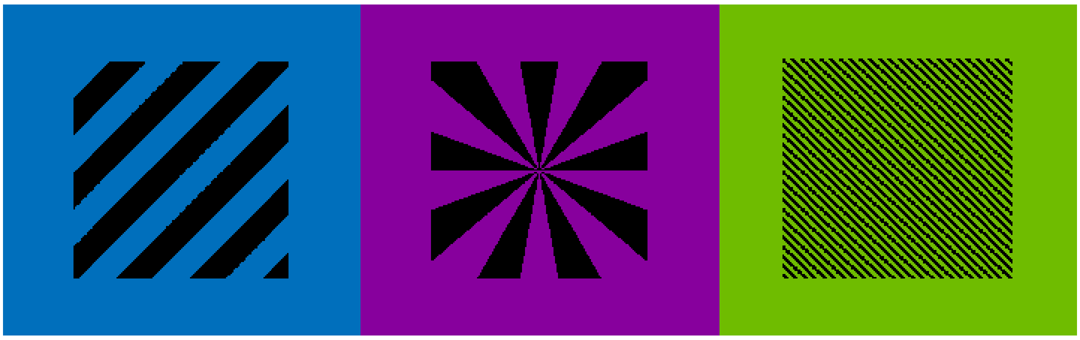

Figure 19. Illustration of the accommodative targets presented in experiment 3 (not to scale).

The images presented as accommodative targets had a size of 400 by 400 pixels (1.30 degrees of visual angle) and consisted of (a) a pinwheel pattern of 9 cycles, or diagonal square wave stripes of approximate spatial frequencies of 2.2 cpd, 9.0 cpd and 18.1 cpd, with either (b) left or (c) right orientation. The angular size and spatial frequency values were corrected by the small magnification factor caused by the lenses used (using equation 3). Some examples of these images are shown in Figure 19.

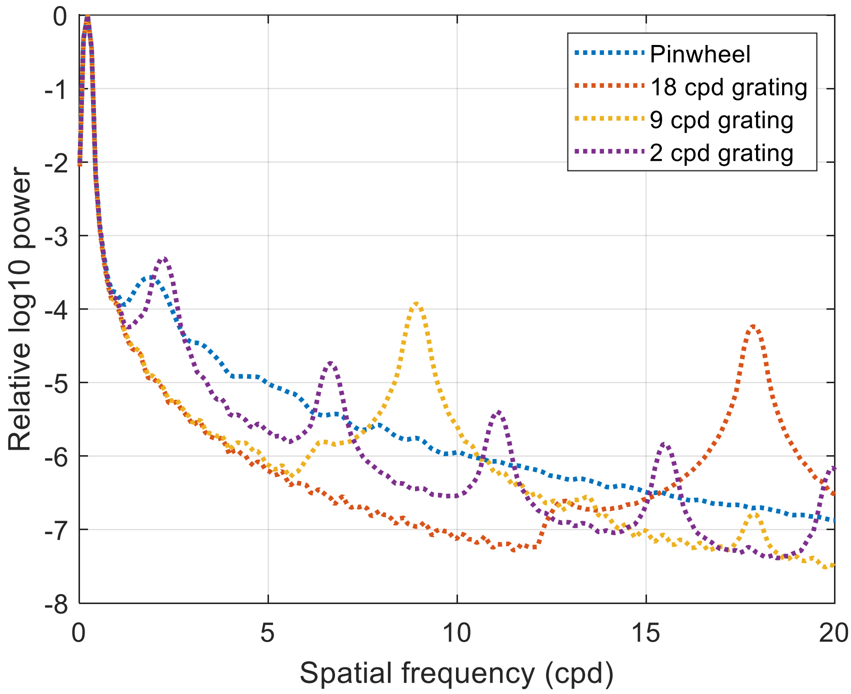

Figure 20. Spatial power spectrum of the different accommodative targets used, showing how much information is contained at each spatial frequency for the different images. The analysis was performed including the small patch that contained the images. The resulting spatial frequency values were corrected by the magnification effect caused by viewing the target through a lens of -4 dioptres of power (using equation 3). The image was created using code provided by Anton (2022).

In Figure 20, we show the spatial spectral density of the different accommodative targets, that is, how much power they contain at the different spatial frequencies. In this analysis we included the small patch that contained the targets within the screen, which shows here as the high power at the very low spatial frequencies that is equal for all targets. For the diagonal square wave gratings, we see that the highest power is at the intended spatial frequency, with other peaks following at the higher harmonics. Finally, for the pinwheel target, we see a peak at a low frequency, similar to the 2.2 cpd grating, but more power at higher frequencies when compared to this target. This analysis was performed in part by using the code provided by Anton (2022).

3.2.4. Design and procedure: Experiments 1 & 2.

At the start of the experimental session, participants read the information sheet and signed the consent form. Their visual acuity was then measured at near and far distances using a Snellen chart. All participants had a visual acuity of logMAR 0.25 or better without the need for spectacle or contact lenses. The photorefractor calibration procedure was then performed.

During the experiment, their left eye was covered using an eyepatch and they sat with their head placed on a chinrest. They were instructed to fixate on the stimuli presented and to keep it in focus with as much effort as if they were reading a book. A button placed next to them allowed them to pause the task at any time, and frequent breaks were given throughout the experiment. All experimental conditions (i.e., all pairs of narrowband illuminants and their luminance combinations) were presented within each experimental block, with the order being randomised each time. In experiment 1, each experimental condition was repeated five times, and presented for 8 seconds. In experiment 2, each experimental condition was repeated 12 times and the trial duration was of 2.5 seconds. Before each trial, the target was illuminated in both experiments with the orange (588 nm) illuminant for 2.5 seconds to keep a constant luminance adaptation and to start at a relatively similar accommodation value before the target stimuli was presented.

3.2.5. Design and procedure: Experiment 3.

At the start of the experimental session, participants read the information sheet and signed the consent form. The photorefractor calibration procedure was then performed, and they were given instructions for the task. They were asked to keep the stimuli presented on the screen in focus at all times, and to use the keyboard indicate which stimuli was being presented. The up-arrow key was used to indicate a pinwheel image was on the screen, while the left and right arrow keys were used to indicate a diagonal stripe pattern was present that had a left or right orientation, respectively. During the experiment, participants sat with their head placed on a chinrest, while wearing the pair of light-tight goggles. Frequent breaks were given between experimental blocks and participants could pause the experiment at any time.

All experimental conditions (i.e., all the target images presented under all the illuminant pairs at the different luminance combinations) were repeated four times, except for one subject who completed nine repetitions. Each trial had a duration of 3.5 seconds, or longer if participants had not given an answer. Before each trial, a fixation cross over a grey background of matched luminance was presented for 3.5 seconds to keep a relatively similar level of luminance adaptation and accommodation.

3.2.6. Data processing and analysis.

The data processing and analysis was performed using MATLAB. To analyse the refractive and pupil diameter recordings, the data points where the pupil was not found were identified as blinks and excluded, as well as 60 ms before and 120 ms after each blink. Blinks would on occasion cause big spikes in the refractive data, thus, any data points where refraction was greater than 25 D were also excluded. The calibration correction factor obtained for each individual participant (see section 2.2.4) was then applied to the refraction measurements.

To allow time for the participants to accommodate, the first 500 ms of refractive data for each trial and the first 1000 ms of refractive data for each pre-trial stimulus were excluded from further analysis in all experiments. Any trial with less than 500 ms of remaining measurements during the pre-trial or trial target presentation, were also excluded.

The accommodation values obtained for each trial were normalised using the median accommodation response to the corresponding pre-trial target. This was done by calculating for each participant the difference between the response to each pre-trial target, and the absolute median response to all pre-trial targets presented. These differences were then used to adjust the accommodation response to each corresponding trial. This normalisation was done under the assumption that participants will always accommodate to the same distance for the pre-trial target presented, and it allowed us to correct for any adjustments that participants made to their head or eye position over the long duration of the experiment. Overall, it reduced the variability of responses within subjects, but it did not alter the main findings presented in this chapter.

3.3.Results.

3.3.1.Accommodation to pairs of narrowband illuminants: Experiments 1 and 2.

In experiment 1 we showed observers a Maltese cross of 5.7 degrees of visual angle, placed at a distance of 2 dioptres and illuminated by different pairs of narrowband lights. The mean accommodation responses of all 8 participants that took part are presented in Figure 21. In experiment 2, we reduced the size of the accommodative target to 1.5 degrees of visual angle and increased the accommodative demand by placing it nearer the observers, at 3 dioptres of distance. The mean accommodation responses of the 5 participants that took part are presented in Figure 22. The individual responses of participants in all experiments are shown in Appendix D.

While there are differences between the results of both experiments, one common finding is that for mixtures of two narrowband lights, participants accommodate to an intermediate distance between the two, and as the luminance of one of the lights increases, accommodation more closely matches the accommodative demand of that illuminant.

One difference between the two experiments is that the accommodative differences between single narrowband illuminants of different wavelengths seem to be greater in experiment 2, more closely matching the change in accommodative demand created by the LCA of the eye. Participants tended to underaccommodate for red, overaccommodate for green, and considerably overaccommodate for blue and violet, with the responses being more accurate for the orange illuminant. Indeed, when analysing the differences in accommodation as a function of the predicted defocus for each wavelength caused by LCA (Thibos et al., 1992), we see that the slope of the response to the single narrowband illuminants is 0.37 (95% CI from 0.27 to 0.46, $t(186) = 7.69$, $p<0.001$). This means that, under these experimental conditions, subjects only shift their accommodation responses to correct for LCA at 37% of the amount predicted by the chromatic eye model. In experiment 2 the accommodative responses to single narrowband illuminants matched more closely the demand predicted by the LCA model, showing a greater dioptric shift between different peak wavelengths. The demand-response function for the single narrowband illuminants has a steeper slope than in experiment 1, albeit it's still shallower than the identity line at 0.48 (95% CI from 0.28 to 0.67, $t(206) = 4.82$, $p<0.001$). Interestingly, this affects the accommodative responses to the pairs of narrowband

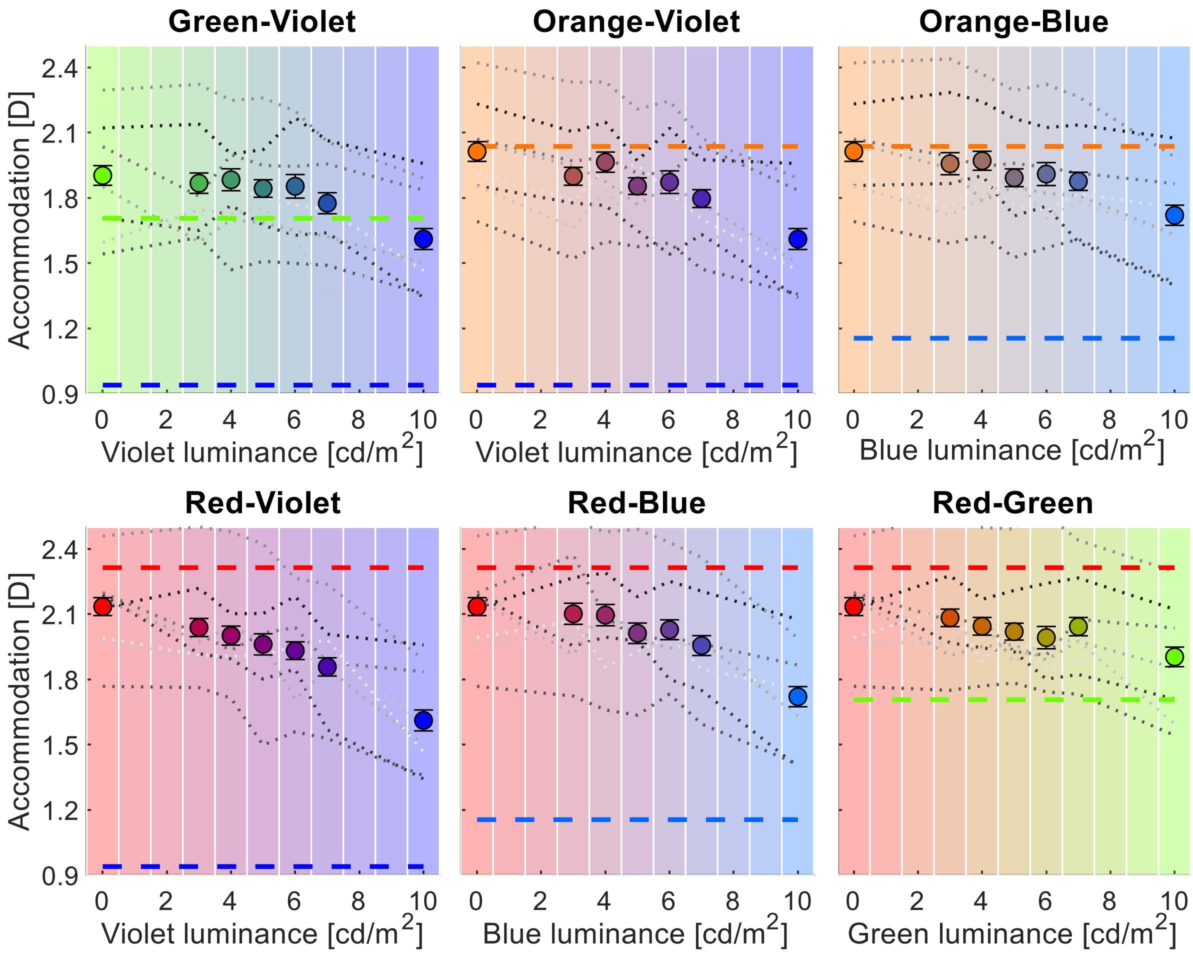

Figure 21. Mean accommodation responses of all participants in experiment 1 to each pair of narrowband illuminants. Each panel corresponds to one pair of illuminants. The abscissas represent the luminance of the shortest wavelength illuminant within the pair. The luminance of the other illuminant decreased in opposite steps, maintaining the total luminance at 10 cd/m^2. The markers and error bars represent the mean and standard error of the mean of the median accommodation responses in each corresponding trial. The dashed lines represent the expected accommodative demand for each illuminant in the pair, calculated as a function of the physical distance of the target (2 dioptres) and the defocus caused by LCA for the peak wavelength of the illuminant. The dashed lines in grayscale represent the median accommodation responses of individual participants.

illuminants as well; that is, in experiment 2 there is a greater difference in accommodation with changes in the proportion of luminance within the mixture than in experiment 1. Thus, it seems that either the smaller angular size of the target in experiment 2, its nearer physical distance, or a combination of both factors, increased the extent to which participants correct for the LCA of the eye. Given the results presented in the previous chapter, the nearer physical distance of the target seems to be the more likely explanation.

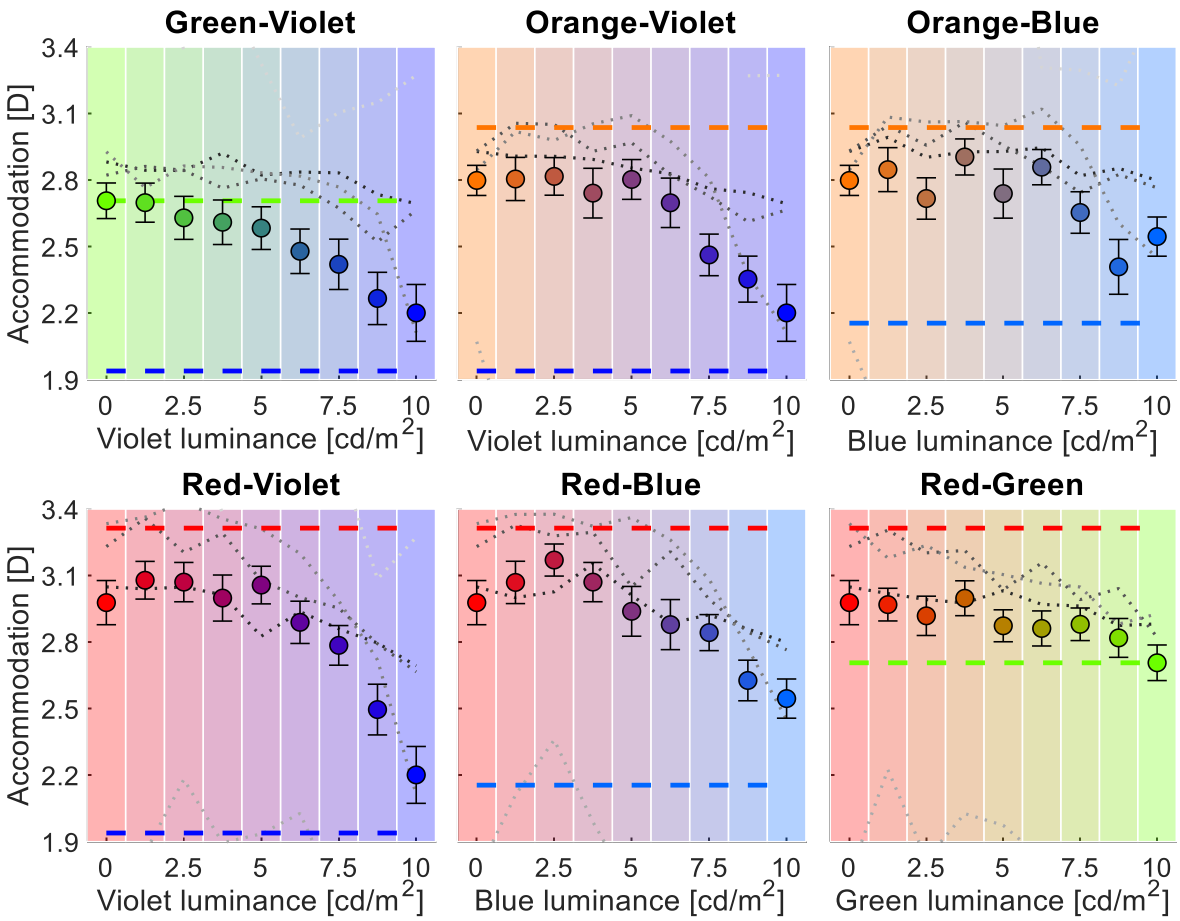

Figure 22. Mean accommodation responses of all participants in experiment 2 to each pair of narrowband illuminants. Each panel corresponds to one pair of illuminants. The abscissas represent the luminance of the shortest wavelength illuminant within the pair. The luminance of the other illuminant decreased in opposite steps, maintaining the total luminance at 10 cd/m^2. The markers and error bars represent the mean and standard error of the mean of the median accommodation responses in each corresponding trial. The dashed lines represent the expected accommodative demand for each illuminant in the pair, calculated as a function of the physical distance of the target (3 dioptres) and the defocus caused by LCA for the peak wavelength of the illuminant. The dashed lines in grayscale represent the median accommodation responses of individual participants (note that one participant is not shown in the plot due to falling outside of the limits of the ordinates).

Another feature of the results is that the accommodative responses do not seem to change linearly with the changes in luminance, but rather they seem to fall on a curve that increases in gradient as the luminance of the shortest wavelength illuminant increases. This seems to be particularly true for pairs that include the blue or violet illuminant, while it is not evident in the red-green mixtures; and the effect is much more pronounced in experiment 2 than in experiment 1. This pattern of responses is also present in individual observers (see Appendix D, and grayscale dashed lines in Figure 21 and Figure 22). It seems that participants favoured accommodating to the longer wavelength illuminant when presented with mixtures containing blue or violet, and only shifted their accommodation towards these illuminants when their luminance within the mixture was 50% or higher.

3.3.2. The effect of target spatial frequency: Experiment 3.

In experiment 3 we explored the role that the spatial frequency of the target has on the accommodative responses of participants. We presented stripe patterns of 2.2, 9.1 and 18.1 cpd, as well as a pinwheel pattern composed of multiple spatial frequencies, placed at approximately 4.4 dioptres. The mean accommodation responses of the 5 participants that took part are presented in Figure 23.

Firstly, we see greater differences between the accommodation responses to single narrowband illuminants of different wavelengths than in experiments 1 or 2. Accommodation to the single narrowband illuminants as a function of the predicted defocus for their peak wavelength presented steeper slopes for all targets: 0.69 for stripes of 2.2 cpd (95% CI from 0.54 to 0.84, $t(97) = 8.93$, $p<0.001$), 0.68 for stripes of 9.1 cpd (95% CI from 0.20 to 1.17, $t(94) = 2.81$, $p=0.006$), 0.76 for stripes of 18.1 cpd (95% CI from 0.56 to 0.97, $t(94) = 7.54$, $p<0.001$), and 0.75 for the pinwheel pattern (95% CI from 0.57 to 0.94, $t(95) = 8.19$, $p<0.001$). It is worth pointing out that the pinwheel pattern used in this experiment had an angular size of 1.30 degrees of visual angle, while the Maltese cross used in experiment 2 had an angular size of 1.50 degrees of visual angle, and both were targets composed of multiple spatial frequencies. However, despite these similarities, participants corrected for the LCA of the eye to a greater extent in experiment 3, with the slope being 0.27 dioptres/dioptres higher, which seems to suggest that the nearer distance of the target in this experiment was the cause of this increase. Furthermore, as previously discussed, this can also explain the difference in slope between experiment 1 and 2, as the target was placed nearer the observer by 1 dioptre in the latter, and the slope was 0.11 dioptres/dioptres higher.

Secondly, we see that the spatial frequency of the accommodative targets had a noticeable effect on the accommodative responses of participants. Although the estimated slope was higher for the highest spatial frequency target, the confidence intervals were wide and overlapped. However, despite the slope estimates not being significantly different, we see that the absolute accommodation values are higher for the two targets with the highest spatial frequency (9.1 and 18.1 cpd), when compared to the pinwheel and low spatial frequency

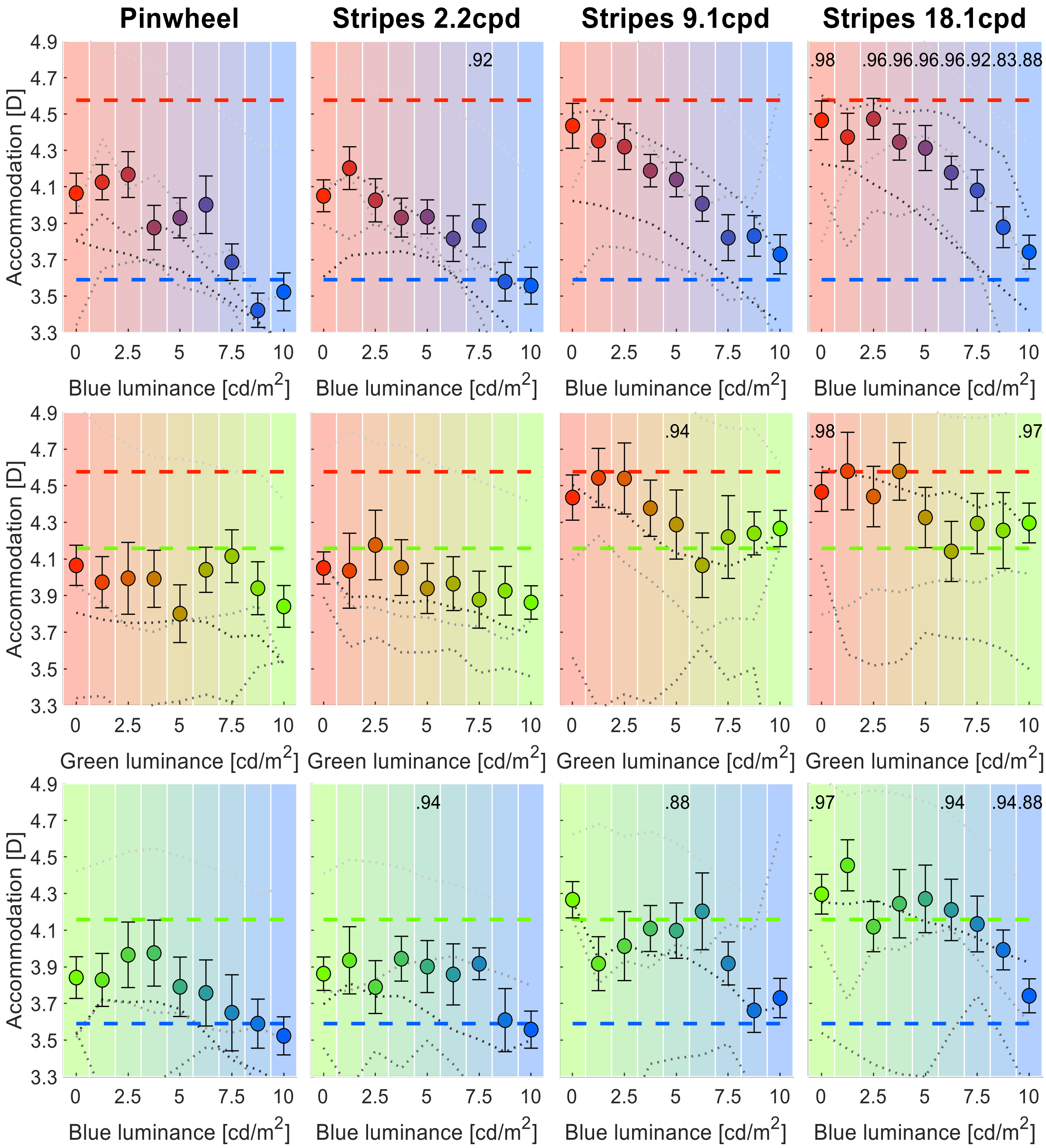

Figure 23. Mean accommodation responses of all participants in experiment 3 to each accommodative target presented under different pairs of narrowband illuminants. Each column of panels represents one type of accommodative target, and each row corresponds to one pair of narrowband illuminants. The abscissas represent the luminance of the shortest wavelength illuminant within the pair. The luminance of the other illuminant decreased in opposite steps, maintaining the total luminance at 10 cd/m². The markers and error bars represent the mean and standard error of the mean of the median accommodation responses in corresponding trials. The proportion of correctly identified targets is presented at the corresponding luminance values, only for proportions lower than 1. The dashed lines represent the expected accommodative demand for each illuminant in the pair, calculated as a function of the physical distance of the target (~4.4 dioptres) and the defocus caused by LCA. The dashed lines in grayscale represent the median accommodation responses of individual participants (note that some participants are not shown due to falling outside of the limits of the ordinates).

targets. To estimate these differences, we fitted some simple linear mixed effect models to the median accommodation responses obtained for each pair of illuminants, with a fixed categorical predictor of target and random intercepts of participant. The estimates of these models were used to perform post-hoc pairwise comparisons between the different targets for each pair of illuminants, and the results are shown in Table 9. As seen, accommodation was highest of the 18.1 cpd stripes pattern, followed by the 9.1 cpd stripes, and then the 2.2 cpd stripes and pinwheel pattern, which had similar estimates and no significant differences in median accommodation in any of the three pairs of illuminants.

contrast	**diff.**	**SE**	**95% CI**		**t-ratio**	**df**	**p-value**
			Red - Blue				
18.1 cpd - 2.2 cpd	***0.30***	***0.05***	***0.18***	***0.42***	***6.4***	***583***	***<0.001***
18.1 cpd - 9.1 cpd	0.12	0.05	0.00	0.24	2.6	583	0.052
18.1 cpd - pinwheel	***0.32***	***0.05***	***0.20***	***0.45***	***6.8***	***583***	***<0.001***
2.2 cpd - 9.1 cpd	***-0.18***	***0.05***	***-0.30***	***-0.06***	***-3.9***	***583***	***0.001***
2.2 cpd - pinwheel	0.02	0.05	-0.10	0.14	0.4	583	0.971
9.1 cpd - pinwheel	***0.20***	***0.05***	***0.08***	***0.33***	***4.3***	***583***	***<0.001***
			Red - Green				
18.1 cpd - 2.2 cpd	***0.39***	***0.06***	***0.23***	***0.54***	***6.5***	***388***	***<0.001***
18.1 cpd - 9.1 cpd	0.09	0.06	-0.06	0.25	1.5	388	0.422
18.1 cpd - pinwheel	***0.38***	***0.06***	***0.23***	***0.53***	***6.4***	***388***	***<0.001***
2.2 cpd - 9.1 cpd	***-0.29***	***0.06***	***-0.45***	***-0.14***	***-4.8***	***388***	***<0.001***
2.2 cpd - pinwheel	-0.01	0.06	-0.16	0.15	-0.1	388	0.999
9.1 cpd - pinwheel	***0.29***	***0.06***	***0.13***	***0.44***	***4.7***	***388***	***<0.001***
			Green - Blue				
18.1 cpd - 2.2 cpd	***0.34***	***0.06***	***0.19***	***0.50***	***5.7***	***373***	***<0.001***
18.1 cpd - 9.1 cpd	***0.19***	***0.06***	***0.04***	***0.35***	***3.2***	***373***	***0.007***
18.1 cpd - pinwheel	***0.36***	***0.06***	***0.21***	***0.52***	***6.0***	***373***	***<0.001***
2.2 cpd - 9.1 cpd	-0.15	0.06	-0.30	0.00	-2.5	373	0.058
2.2 cpd - pinwheel	0.02	0.06	-0.13	0.18	0.4	373	0.983
9.1 cpd - pinwheel	***0.17***	***0.06***	***0.02***	***0.32***	***2.9***	***373***	***0.021***

Table 9. Results of the pairwise comparisons between the median accommodation response to targets of different spatial frequency composition, for the mixtures created with the red and blue (top), red and green (middle) and green and blue (bottom) illuminants. The left column represents the pairs being compared, and the estimated differences (diff.), standard errors (SE) and 95% confidence interval (95% CI) are shown; as well as the t-test results against the null hypothesis that the difference is zero, with t-ratios, degrees of freedom and p-values. The rows in bold italics are significant at the 0.05 level. P-values were adjusted for multiplicity of testing using Tukey's method.

While some of the differences are not significant, in general, the picture emerges of an increase in median accommodative state with higher spatial frequency targets. The accommodative response to the 18.1 cpd stripes was between ~0.30 and 0.39 dioptres higher when compared to the 2.2 cpd stripes and pinwheel pattern; and accommodation to the 9.1 cpd stripes was between ~0.15 and 0.29 dioptres higher when compared to the low frequency and pinwheel patterns. This means that when subjects need to resolve a smaller target, their accommodation responses for all wavelengths and their mixtures increase, and when accommodating to a pinwheel pattern with multiple spatial frequencies, their responses are similar to those found with the low spatial frequency target.

In the results of this experiment, we can also see some similar finding to experiment 2. For the green-blue pair, the accommodative responses of participants remain at similar values to the responses given to green, despite the luminance of the blue light increasing. Accommodation only decreases when the luminance of blue surpasses 50 to 75% within the mixture. This preference for the longer wavelength illuminant in the pair can also be observed in the mean responses to the red-blue mixtures, and particularly in the responses of some individual subjects with at least one of the target patterns (e.g., see subjects 2, 8, 17 and 23 in Appendix D). However, this preference towards the longer wavelength illuminant in the pair does not seem to be present for the red-green mixtures tested.

Finally, as participants were asked to identify the target that was being presented, their errors can give us some insight into the effect that the stimuli presented, and their accommodative responses to it, had on their ability to perceive the targets. Overall, participants were able to discriminate the orientation of the stripes above chance level (50%) and no errors were made in the identification of the pinwheel pattern. Most subjects were at 100% in nearly all conditions, in any condition where errors were made, the proportion of correct responses are presented at the top of the corresponding panel in Figure 23.

Looking at the results of individual participants (see Appendix D), we see that there were two subjects (17 and 18) who made no errors on target detection, despite their accommodative responses being more variable between trials than for the other participants. They were also the two subjects with the smallest mean pupil sizes, so it is possible that the resulting increased depth of focus allowed them to resolve the targets correctly, despite their accommodation responses being less accurate in some trials. For the remaining three subjects

(2, 8 and 23), most of the mistakes were made for the high spatial frequency stripe targets and under the red-blue and green-blue pairs of illuminants, in particular when the luminance of the blue light was higher within the mix and when the blue illuminant was presented on its own. This seems to suggest that it is the presence of blue light that causes this increase in errors, rather than the presence of two distinct wavelengths with different accommodative demands. This is despite the fact that luminance was equal for all stimuli (thus, all targets provided equal input to the luminance or L+M channel), and that mixtures with blue light would benefit from the increased depth of focus caused by a smaller pupil size, as discussed in the previous chapter.

3.3.3.Accommodation response variability.

Thus far we have reported the median accommodative state of participants to the different mixtures of narrowband illuminants, finding that subjects accommodate to an intermediate point between the two accommodative demands weighted by the luminance of each light in the mixture. However, it is unclear whether this value truly reflects the steady-state accommodation, as it would be possible to obtain similar results if observers where switching their accommodation between the demands created by the two individual wavelengths. In this case, we would expect to see an increased variability in the within-trial accommodation response as a function of time for the mixtures of narrowband illuminants, but not when only a single illuminant is presented. To determine if this was the case, we fitted a linear function to the within-trial accommodation response as a function of time and calculated the root-mean-squared error (RMSE), in a similar analysis to the one described in Chapter 2. However, in this case the linear function fitted was constrained to have an intercept equal to the median and a slope of zero, so the RMSE reflects in this case how much the response fluctuates over time around the median. The results for experiment 1 are shown in Figure 24, for experiment 2 in Figure 25, and for experiment 3 in Figure 26.

Each figure shows the distributions of RMSE for the single narrowband illuminants (dark diamond markers) and for the mixtures (white round markers) as a function of the luminance of the shortest-wavelength illuminant in the mix, and for each pair of lights used (as well as target type in experiment 3). We see that there is no evidence for a systematically higher variability in the within-trial accommodation response to mixtures of narrowband lights when compared to the single narrowband illuminants. Observers do not seem to be switching

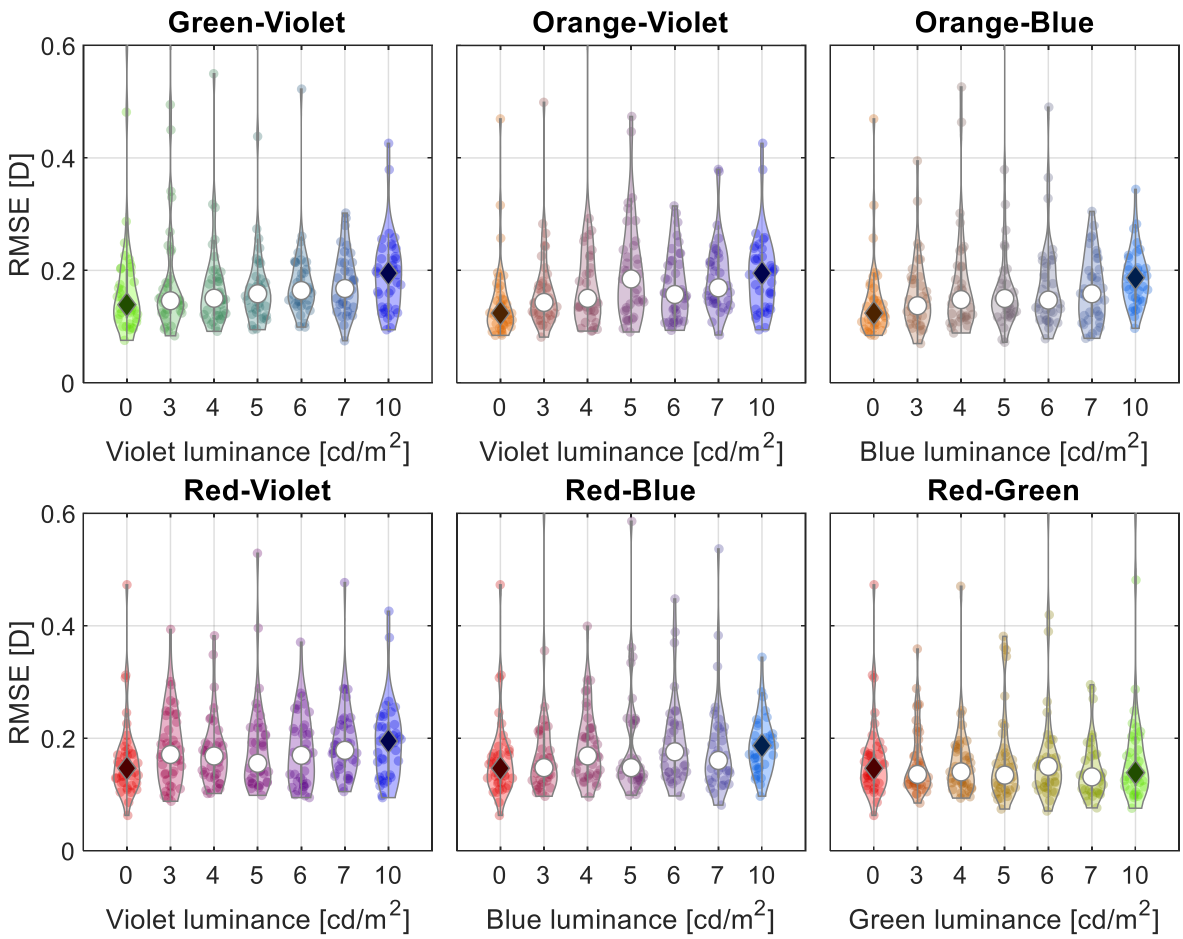

Figure 24. Distributions of the RMSE of the within-trial accommodation response as a function of time for Experiment 1. Each panel corresponds to one pair of illuminants as indicated by the title. The abscissas represent the luminance of the shortest wavelength illuminant within the pair. The luminance of the other illuminant decreased in opposite steps, maintaining the total luminance at 10 cd/m^2. The central markers represent the median, with white circular markers for the mixtures of two illuminants, and the diamond dark markers for the narrowband illuminants presented on their own.

between the accommodative demands created by the two wavelengths, and the response over time fluctuates by similar amounts from the median as the response to the single narrowband illuminants.

Some differences between lights of different peak wavelength, however, do become evident. In experiments 1 and 2, for mixtures that include the blue and violet illuminants, we see that the RMSE increases as the luminance of these lights increases, and it is generally highest when these illuminants are presented on their own. Thus, it seems that is the presence of these short-wavelength lights that causes the increase in RMSE, rather than the mixture of two illuminants of different peak wavelengths. In experiment 3, no systematic increase in RMSE

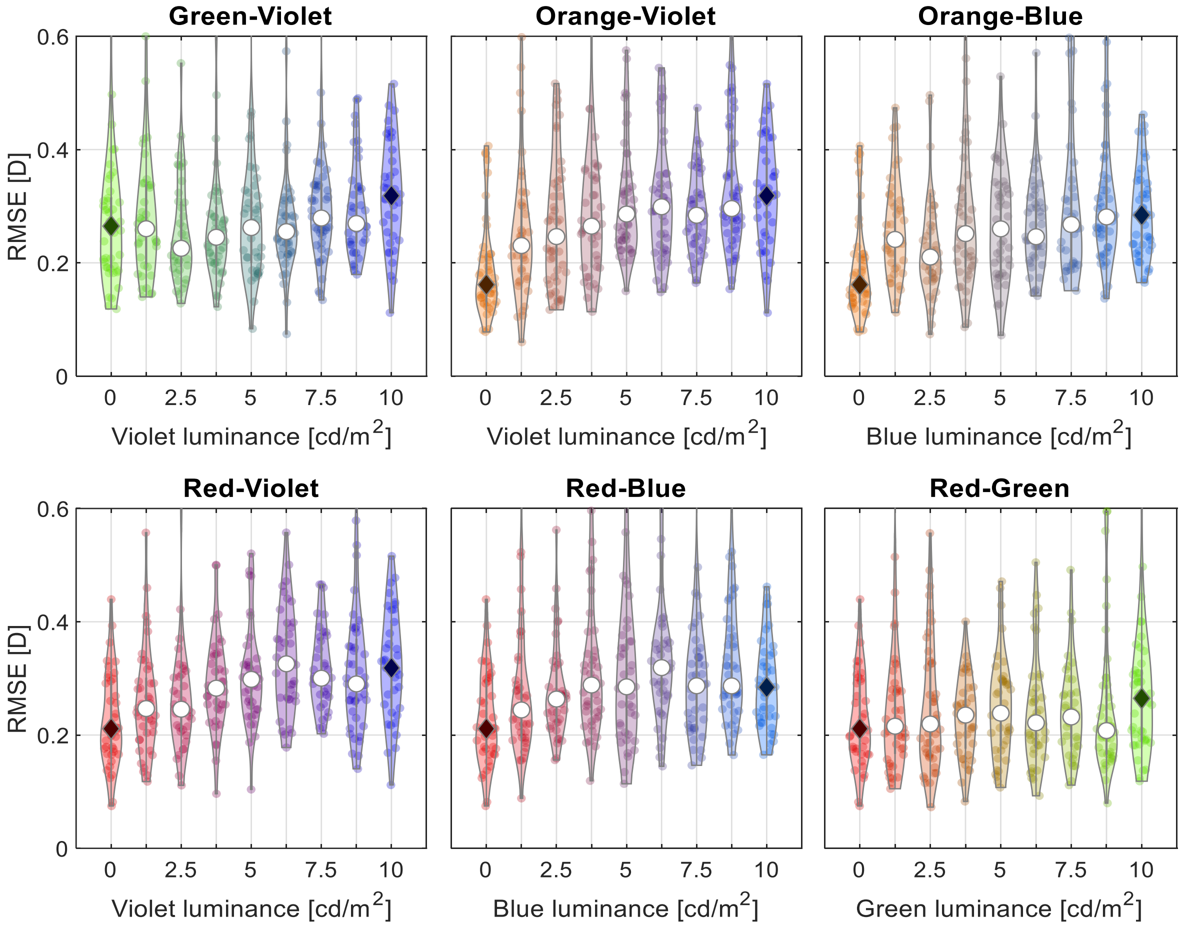

Figure 25. Distributions of the RMSE of the within-trial accommodation response as a function of time for Experiment 2. Each panel corresponds to one pair of illuminants as indicated by the title. The abscissas represent the luminance of the shortest wavelength illuminant within the pair. The luminance of the other illuminant decreased in opposite steps, maintaining the total luminance at 10 cd/m^2. The central markers represent the median, with white circular markers for the mixtures of two illuminants, and the diamond dark markers for the narrowband illuminants presented on their own.

with increasing blue light can be observed for the red-blue pair of illuminants; while some increase is present for the green-blue pair, particularly for the stripe targets. Overall, the greater fluctuation in the accommodation response for short-wavelength narrowband light, agrees with the results presented in the previous chapter. Furthermore, we also see that the variability of the response increases for nearer distances, with higher RMSE in experiments 2 and 3 (between ~0.2 and 0.3 dioptres) when compared to experiment 1 (between ~0.15 and 0.2 dioptres). This is likely caused by the increase in the accommodative state of the crystalline lens due to the higher refractive demand, as previously discussed.

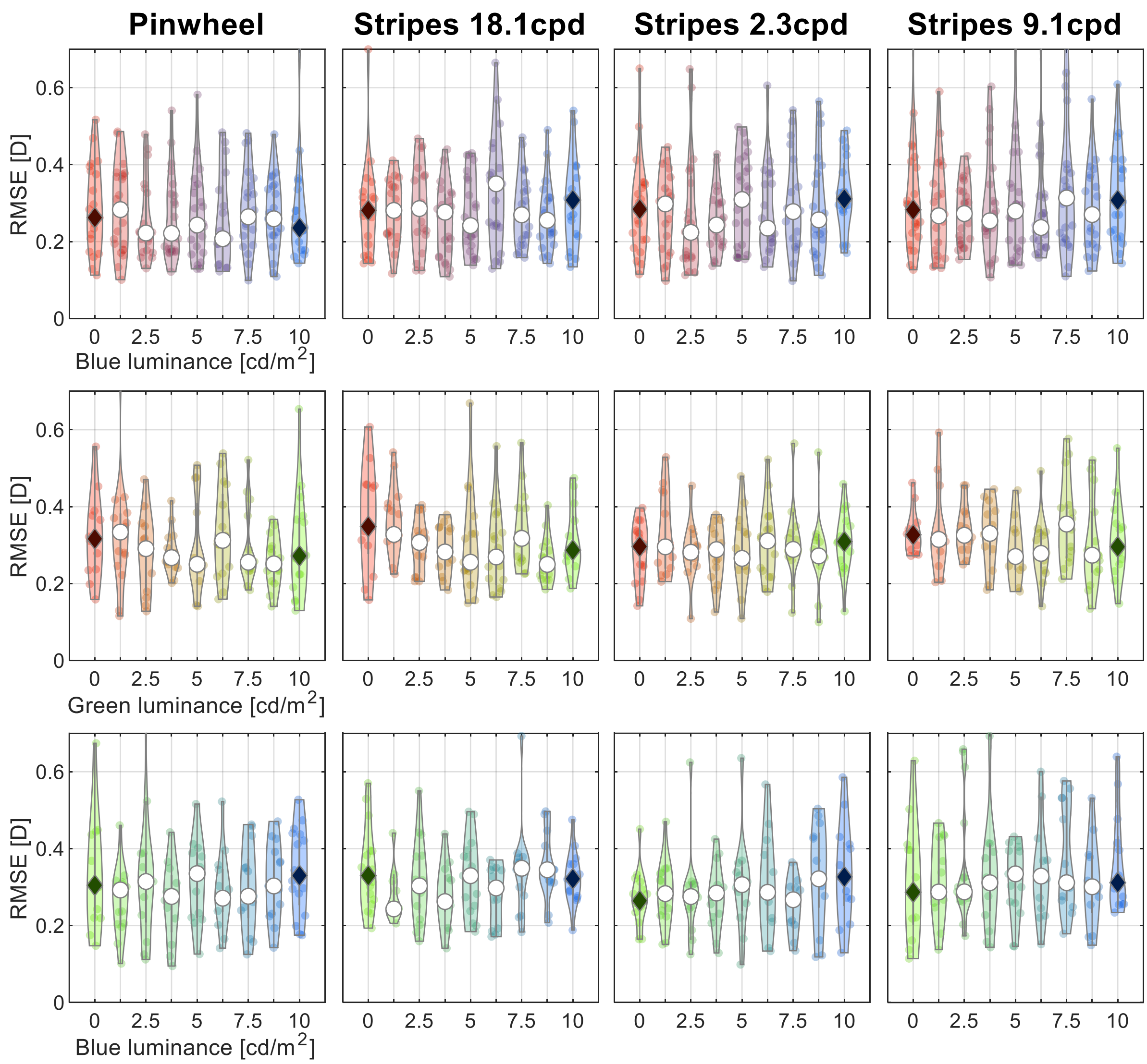

Figure 26. Distributions of the RMSE of the within-trial accommodation response as a function of time for Experiment 3. Each column of panels represents one type of accommodative target, and each row corresponds to one pair of narrowband illuminants. The abscissas represent the luminance of the shortest wavelength illuminant within the pair. The luminance of the other illuminant decreased in opposite steps, maintaining the total luminance at 10 cd/m^2. The central markers represent the median, with white circular markers for the mixtures of two illuminants, and the diamond dark markers for the narrowband illuminants presented on their own.

3.4. Discussion.

In the experiments presented in this chapter, we aimed to characterize where participants accommodate to when presented with targets illuminated by pairs of narrowband illuminants with different peak wavelengths, and how their responses change as the luminance of each light and the spatial frequency of the target vary. We found that participants accommodate to an intermediate point between the demands created by the two lights of different wavelengths, and that this point is weighted by the proportion of luminance of each light within the mixture. This finding was robust for all pairs of narrowband illuminants tested, and to changes in the distance, the angular size and the spatial frequency content of the target. Distance did have however, an important effect on the extent to which participants correct for the LCA of the eye as predicted by the chromatic eye model of Thibos et al. (1992), which agrees with findings previously reported and discussed in Chapter 2. Here we report that this effect is present for mixtures of these lights as well as for the individual narrowband illuminants. This means that, although the difference in accommodative demand between any two wavelengths will be independent of distance (or only expected to increase by ~3% per dioptre of accommodation), the difference in accommodative response will be significantly greater for nearer distances, and thus, there will also be a greater difference in accommodation to combinations of these wavelengths at varying proportions of luminance.

Research on multiplane displays had demonstrated that accommodative responses could be driven between two planes that were placed at a distance of up to 1.11 dioptres for targets with low and middle spatial frequency contents (MacKenzie et al., 2010). Beyond this distance, accommodation would remain in one of the planes rather than in between, and no longer correspond with the intended demand. However, in our experiments we found that for a target with multiple spatial frequencies, participants accommodated in an intermediate distance in between a 441 nm and a 661 nm light, even when these wavelengths have a difference in accommodative demand of 1.37 dioptres, albeit the difference in the actual responses of some of the subjects was considerably smaller. Furthermore, MacKenzie et al. (2010) also determined from their simulations and experimental results that for higher spatial frequencies of 8 and 16 cpd, this maximum distance between planes would be reduced to approximately 0.7 dioptres. This is in line with previous studies that have demonstrated that retinal contrast falls off much more quickly with defocus at high spatial frequencies than at low (Charman & Tucker, 1977; Labhishetty et al., 2021). But again, when presented with high spatial frequency targets of 9 and 18 cpd illuminated by narrowband lights of 610 nm and 459 nm peak, participants accommodated between the two even when these illuminants have a difference in accommodative demand of 0.99 dioptres. Thus, these results seem to suggest that the visual system is more tolerant of the potential detrimental effects on retinal image contrast caused by chromatic blur than by other types of defocus. However, it is not possible to completely rule out that participants are choosing to maximise contrast at low spatial frequencies, even when this would reduce contrast at high spatial frequencies, and when only the high spatial frequencies are task relevant. In experiment 3, the screen had a relatively small size, occupying a small area of the visual field, and the stimulus was contained in a square patch. This means that there were still lower spatial frequencies present that subjects could have used to accommodate, even when the task required them to resolve the high spatial frequencies in order to discriminate the orientation of the stripes. If this was the case, the results seen could be explained by the visual system always choosing to maximise contrast for the lower spatial frequencies contained in the scene, regardless of task demands.

We found that the spatial frequency of the target had a significant effect on the absolute accommodation values of participants, with the responses for all three primaries and their mixtures being highest for the stripe patterns of 18 cpd, followed by the 9 cpd targets, and accommodation was lowest for the stripe patterns of 2.2 cpd and the pinwheel targets which were composed of multiple spatial frequencies (although had higher power at lower spatial frequencies as shown in Figure 20). Charman & Tucker (1977) previously reported that the accommodation response increases as the spatial frequency of the target increases, more closely matching the demand, and that this effect becomes more prominent as the stimulus is placed at nearer distances. These and other authors have reported further similar findings (Charman & J. Tucker, 1978; Tucker et al., 1986; Tucker & Charman, 1987), and they have hypothesised that accommodation might be initially driven by middle and low spatial frequencies to a state that approximates the demand, and that higher frequencies then allow the observers to “fine tune” their response, particularly when the instructions given to them emphasize to keep the target in sharp focus (Ward, 1987). In our case, participants were presented with a pre-trial stimulus that allowed them to keep an approximately accurate accommodative response, and they were required to discriminate the orientation of the stripe patterns, therefore requiring to accommodate accurately to the higher spatial frequencies in order to improve retinal image contrast. While they were asked to keep all targets in sharp focus, at lower spatial frequencies retinal contrast is less affected by defocus, thus it is possible that the 2.2 cpd stripe patterns did not contain the necessary information that allowed them to increase the accuracy of their response further; although some evidence exists that the higher harmonics of square wave gratings (the stimuli we used) could aid accommodation accuracy even at low frequencies (Tucker & Charman, 1987). Another possibility is that participants only made the accommodative effort that was required to identify the orientation of the stripes, rather than keeping it at the best possible focus, as volitional effort has also been found to be an important factor in the accuracy of accommodative responses to different spatial frequencies (Owens, 1980; Ward, 1987). This might also explain why the accommodative responses to the pinwheel pattern that contained multiple spatial frequencies were more similar to those of the 2.2 cpd stripe pattern, even when it contained more power at higher spatial frequencies in comparison (see Figure 20); that is, subjects accommodated to this target enough to be able to identify it and provide a response, rather than making the image as sharp as possible.

Given these results, it seems then unlikely that the visual system would always choose to maximise contrast at low spatial frequencies in detriment of high spatial frequencies, even when only the latter ones are task relevant. However, we cannot completely rule out that when the point of best focus for low and high spatial frequencies are in conflict (such as with mixtures of two narrowband lights), the visual system chooses to maximise contrast for the former, while also increasing the overall gain of the response to improve accommodative accuracy when high frequencies are relevant to the task. That is, there could be separate processes in the accommodation control system to find the point of best focus and to increase gain when high spatial frequencies are present and task relevant.

The alternative explanation would be that chromatic blur is distinct from monochromatic defocus, such as that created by a display with multiple planes. Whatever mechanism allows the visual system to use LCA as a cue to accommodation by monitoring chromatic blur at luminance edges, could be indicating to maintain equivalent blur for each of the narrowband lights in the mixture weighted by their luminance. This strategy would be optimal for illumination with smooth spectral distributions such as daylight, although with artificial illumination such as mixtures of narrowband lights, it is detrimental to retinal image quality.

There is a growing body of research showing that, when available (i.e., when there are multiple wavelengths in the spectral composition of the illumination), LCA is a very strong cue to accommodation (Fincham, 1951; Kruger et al., 1993; Kruger, Nowbotsing, et al., 1995; Lee et al., 1999; Stark et al., 2002), used not only as a directional cue to drive dynamic responses (Fincham, 1951; Kruger, Mathews, et al., 1995), but also to maintain focus on stationary targets (Kruger et al., 1997; Cholewiak et al., 2017). It is remarkable that the visual system uses this cue even when it might reduce retinal image contrast, particularly at high spatial frequencies. An important caveat is that the higher order optical aberrations of some observers might reduce the detrimental effect of chromatic blur on image quality (McLellan et al., 2002); however we found similar results in all subjects in our sample.

More recent studies have provided strong evidence in favour of this hypothesis. Cholewiak et al. (2017) presented images to participants that simulated positive or negative refractive errors of up to 1.4 dioptres by differentially blurring the primaries of the screen at luminance edges, as LCA would on a real scene. They found that, even when looking at these targets through their natural pupil, observers made a change in their accommodative responses that corresponded with the sign and magnitude indicated by the LCA cue, and that their responses were as robust as those triggered by an actual change in the focal distance of the target. These results were quite notable, as accommodating away from screen through a natural pupil would worsen the defocus of the image, and all other cues such as micro-fluctuations and higher order aberrations would be indicating to the visual system that no change in accommodation was required. The authors later reproduced these results and proved that these images with simulated LCA defocus also triggered dynamic accommodation responses as strongly as a real change in the distance of the image (Cholewiak et al., 2018)

It has been proposed that the visual system makes use of LCA as a cue by monitoring chromatic blur at luminance edges via the L and M cones (Fincham, 1953; Stone et al., 1993; Rucker & Kruger, 2006), and the S cones at least for near distances (Rucker & Kruger, 2004). As for a specific neural implementation, Flitcroft (1990) proposed that the refractive error of the eye in polychromatic light could be estimated by comparing image quality between the different cone photoreceptors, via spatially band-pass chromatically opponent neurons such as double opponent cells, with both colour channels (red-green and blue-yellow) possibly playing a role. If this was the case, one would expect subjects with impaired colour vision such as dichromats and monochromats that lack one or two cone types, to show an impairment in using LCA as a cue. Indeed, there is evidence that the accommodative reflex under polychromatic illumination is impaired in dichromats lacking either the L or M cones when compared to normal trichromats (Fincham, 1953). More recently, Cholewiak et al. (2018) compared the responses between dichromats and normal trichromats using their rendering method that simulates the effects of LCA on a screen with no real change in defocus. They tested two protanopes and one deuteranope, lacking the L and M cones, respectively; and showed that while their accommodation changed in the correct direction indicated by the LCA cue, the magnitude of the change was reduced when compared to normal trichromats, and they showed very large oscillations and higher variability in their accommodative responses. These results indicate that the red-green (L-M) channel plays an important role in extracting the information on refractive error provided by LCA from the retinal image. However, since their accommodative responses still changed in the correct direction, it also suggests that the blue-yellow channel (S-(L+M)) alone still allows to extract some of this information, albeit not sufficiently to generate a steady accommodative response of the correct magnitude. In general, these results point to complex interactions in the role that different cone photoreceptor types and colour-opponent mechanisms might play in accommodation under polychromatic illumination, and more research is needed to elucidate them.

One important thing to note is that there are other cues the visual system can use to accommodate. Indeed, the dichromats tested by Cholewiak et al. (2018) showed normal accommodation responses when a real change in the defocus of the image was introduced. In other words, the visual system is able to use other cues to estimate the sign and magnitude of the refractive error and to direct the necessary change in accommodation. Thus, from our data we cannot completely rule out that these cues are playing a role in our experimental results, with the visual system either choosing to maximise retinal image quality at low spatial frequencies, using the chromatic blur in the stimuli caused by LCA to accommodate, or even a combination of these strategies.

Another of our findings was that, when presented with mixtures that include short wavelength light (~441-460 nm), some participants favour accommodating towards the longer wavelength illuminant (i.e., red, orange or green), only decreasing their accommodation responses when the blue light surpasses 50% of luminance within the mixture. Rucker & Kruger (2006) have previously shown that the L/M cone sensitivity ratio of observers influences their accommodative responses. Participants with higher L-cone contrast sensitivity relative to their M-cone sensitivity overaccommodated to the targets presented, showing a bias in their responses for maximising contrast at longer wavelengths. They also found a correlation between the refractive error of participants and their L/M cone ratio, with myopes being more likely to have a higher ratio than emmetropes or hyperopes. Most of the subjects in our sample were (self-reported) myopes, so it is possible that those that showed this bias towards longer wavelengths in their accommodation responses to some of the mixtures presented had a higher L/M cone sensitivity ratio than the rest. However, this bias was not apparent for the red-green mixtures tested, so other factors might be at play.

The bias towards longer wavelengths seemed to be more prevalent when the angular size of the target was reduced (in experiment 2 when compared to experiment 1) and seemed to increase for the higher spatial frequency patterns presented (in experiment 3). We also found that most errors in target identification were made at the highest spatial frequencies for red-blue and green-blue mixtures, as well as when the blue illuminant was used on its own. In Chapter 2, in which we used the same experimental setup, we reported that the visual acuity of observers was significantly reduced in narrowband blue light, even when accounting for accommodative error, when compared with red, green, and with a combination of the three primaries at equal luminance. This is likely caused by LEDs not being completely monochromatic and the greater defocus caused by LCA for a similar spectral bandwidth at shorter wavelengths. This likely also explains the increased variability in the within-trial accommodative responses to the short wavelength illuminants or to mixtures containing these lights that we reported here. Thus, it seems plausible that this preference for accommodating towards longer wavelengths when presented with mixtures that contain blue light, was a strategy used by observers to improve visual acuity, particularly when needing to resolve smaller targets.

Under natural illumination, accommodating to an intermediate point in the spectrum would lead to optimal image contrast, as the spectral distribution of daylight is smooth and broadband, and observers would accommodate close to the peak of their luminous sensitivity. However, our results suggest that the visual system maintains this strategy when accommodating to mixtures of narrowband illuminants, even when it might lead to suboptimal image sharpness. This means that visual displays that use narrowband primaries, particularly those that are used at near distances from the eye, might not be ideal to maximise the retinal image contrast of observers when presenting images with high spatial frequencies and illuminated by two of these narrowband primaries. Furthermore, these results could also be relevant for visual displays that aim provide correct focus cues to observers, as it has been shown that LCA is a very strong cue to static accommodative responses, thus it could be considered when designing these displays and incorporating it might ensure that accommodative responses are robustly driven as intended.

Chapter 4. Peripheral flicker fusion at high luminance: beyond the Ferry-Porter law.

4.1.Introduction

The interest in studying the temporal sensitivity of the human visual system has been closely related to the development of new visual display technologies. The introduction of the cinema at the end of the nineteenth century stimulated an early set of studies, while the beginning of widespread television use created another big push from the fifties onwards. The reason was that these display technologies could present a bothersome flicker artifact caused by the successive presentation of the different frames. The Critical Flicker Fusion (CFF) is the lowest frequency at which an intermittent light appears to be completely steady to the average human observer. The CFF is a very important concept for nearly all display technologies, determining the refresh rate at which they operate.

One early observation was that the frequency up to which flicker could be observed, increased linearly with the logarithm of the luminance. This was observed by Ferry in 1892 and Porter in 1902 (cited in Tyler & Hamer, 1993), and it is known as the Ferry-Porter Law. While other laws have existed that attempt to describe this relationship, Tyler & Hamer (1990) demonstrated in a seminal study that the CFF follows this law at photopic levels and up to $\log_{10}$ 4 Trolands of retinal illuminance. This linear relationship is maintained even when the spectral composition, size and eccentricity of the stimulus change (Tyler & Hamer, 1990; Hamer & Tyler, 1992; Tyler & Hamer, 1993), although the slope and intercept of the function will vary depending on these factors.

Changes in the spectral composition of the test stimulus will alter the slope of the linear function between log illuminance and CFF. When the CFF is measured for green (510-555 nm) and red flicker (630-660 nm) as a function of retinal illuminance in both the fovea and peripheral retinal areas, the slope of the linear function is significantly steeper for the green stimuli (Hamer & Tyler, 1992). The slope also varies as a function of the eccentricity of the target in the visual field. For stimuli of equal illuminance and size (scaled to match the anatomical density of receptors in different retinal areas), the slope of the CFF as a function of illuminance will get steeper as eccentricity increases up to 40° temporally (Tyler, 1987), and from there it will stay constant or decrease in some meridians. Finally, for a wide range of photopic luminance levels, the CFF increases linearly with the logarithm of the stimulus area, which is known as the Granit–Harper law (Brindley, 1964). Variations in the slope of the function reflect changes in the speed of the temporal response, while changes in the intercept reflect differences in the absolute threshold sensitivity. A stimulus of larger size would stimulate a higher number of cells in the retina, allowing for more light to be captured, and thus, increasing the absolute sensitivity to light. On the other hand, the steeper slope and decrease in the time constant in the periphery of the retina has been postulated to be due to an increase in the diameter of the cones inner and outer segments with eccentricity, which correlates with the generation of higher voltages in the phototransduction process, producing a proportional increase in sensitivity with increasing light intensity (Tyler, 1985). Finally, Hamer & Tyler (1992) hypothesized that the increase in slope for green when compared to red light reflects a faster temporal processing for transmitting information near the CFF in the M cone pathway, with flicker detection being determined by the receptor mechanism that is most sensitive to the wavelength composition of the stimuli.

Several models exist that can predict how the CFF and log illuminance function can vary depending on the size and eccentricity of the target (e.g., Tyler, 1989; Barten, 2009), with most predicting that the Ferry-Porter Law continues to hold as intensity levels increase logarithmically. However, no experimental data exist of peripheral flicker sensitivity at intensities higher than $\log_{10}$ 4 Trolands. If as predicted by these models, the CFF continues to rise linearly with log illuminance, this would mean that brighter displays would need very high refresh rates to avoid the perception of flicker, and even higher to reduce the visibility of other temporal artifacts. If on the contrary, the response saturates at higher intensities, there would be no need for increasingly higher refresh rates.

Currently, several manufacturers have consumer-ready television displays that can reach peak luminance values between 2,000 and 5,000 cd/m^2 (Byung-Wook, 2022). This would correspond with retinal illuminance values between $\log_{10}$ 4.1 and $\log_{10}$ 4.5 Trolands — assuming a pupil diameter of 3 mm and after correcting for the Stiles-Crawford effect (Barten, 2009). However, prototypes already exist of television screens that can reach up to 10,000 cd/m^2 (Archer, 2018; Morrison, 2018), which would amount to $\log_{10}$ 4.8 Trolands for a 3 mm pupil; and even novel micro-displays with intended applications in virtual and augmented reality, that can reach up to 3 million cd/m^2 (Chen, 2020) or $\log_{10}$ 7.3 Trolands. Although these high-luminance digital displays are not yet widely used or available to the public, mostly due to cost limitations, we can expect that, as these technologies continue to be developed, they will become more common place. This raises the need for extending the experimental data available on the human CFF at high illuminance values. Furthermore, these results would also be relevant for illumination sources that are temporally modulated, such as LEDs which are frequently controlled through pulse-width modulation.

Some studies that preceded the work of Tyler and colleagues had found a saturation in the log illuminance – CFF function. Notably Hecht & Verrijp (1933) found that in the fovea, the linear relationship held only up to approximately $\log_{10} 2$ Trolands, at which point it saturated and started to decrease. The maximum frequency of flicker detected before saturation was reached was between 50 to 60 Hz. Their results in other retinal eccentricities tested were similar, albeit paradoxically, they found that the slope was shallower in the periphery, and saturation was reached at lower illuminances. Indeed, most experimental results preceding the study by Tyler (1987) had shown a slower response and lower sensitivity to flicker in the periphery (Hecht & Verrijp, 1933; Hecht et al., 1933; Brooke, 1951; Tyler, 1989). However, Tyler & Hamer (1990) later showed that with more careful control of the experimental setup, and adjusting the size of the target to stimulate a similar number of photoreceptors at different retinal locations, the temporal response was indeed faster and sensitivity to flicker higher in the periphery.

In summary, the relationship between luminous intensity and the maximum frequency of flicker that can be detected defines the limits of the temporal-resolving ability of the human visual system and characterizing this relationship has very important theoretical and practical applications. The CFF has been demonstrated to follow the Ferry-Porter law and reach up to approximately 90 Hz at 10,000 Trolands (Tyler & Hamer, 1990); however, not much is currently known about the human CFF beyond these retinal illuminance levels. In this study, we aim to extend these measurements in the periphery at higher intensity levels than previously reported in the literature, and test whether the CFF continues to increase linearly with log intensity or if saturation is reached.

4.2. Methods.

4.2.1. Participants.

Data were collected from 5 adults with ages between 25 and 45 years old (mean 30.6, SD 8.26), out of which 2 were female and 3 were male. Due to the time requirements involved in the experiment, participants were recruited from postgraduate students and staff of the Institute of Biosciences at Newcastle University. The study was approved by the university's ethics committee (reference number 445487/2018) and written consent was obtained from each subject at the beginning of the first session.

4.2.2. Apparatus.

The experimental setup and apparatus were built following the one described in Tyler and Hamer (1990). A graphical representation and photos are provided in Figure 27.

The stimulus consisted of six high-power LEDs placed behind a diffuser with an angular size of 5.7 degrees. In a second task, this size was increased to 10 degrees. The diffuser was placed at 35 degrees of eccentricity from the right eye in the horizontal meridian, a retinal region chosen due to having a good homogeneity of receptors and peak temporal response (Tyler & Hamer, 1990). The target LEDs had a peak wavelength of 526 nm and were relatively narrowband (FWHM: 24 nm), which guaranteed maximum luminous efficiency, while avoiding any risks associated with high intensity short wavelength light. The visual field was surrounded by a high luminance white background, which was used to keep a constant light adaptation level throughout the retina. A fixation cross was placed immediately in front of the right eye to help participants keep the test stimulus in the right location.

To create different levels of retinal illuminance without interfering with the stimulus, Neutral Density (ND) filters were used. These were placed over the observer's eye during the experiment. Luminance measures of the stimulus were taken with a Konica Minolta LS-100 through all the filters used, and with no filter. To maximise retinal illuminance during the experiment, the participant's right pupil was dilated using eye drops of Cyclopentolate Hydrochloride at 1%, which also allowed to keep a constant pupil size throughout the experiment.

A computer running MATLAB (The MathWorks Inc., 2019) controlled the experimental routine, selecting the stimulus levels, and collecting and processing the participant's

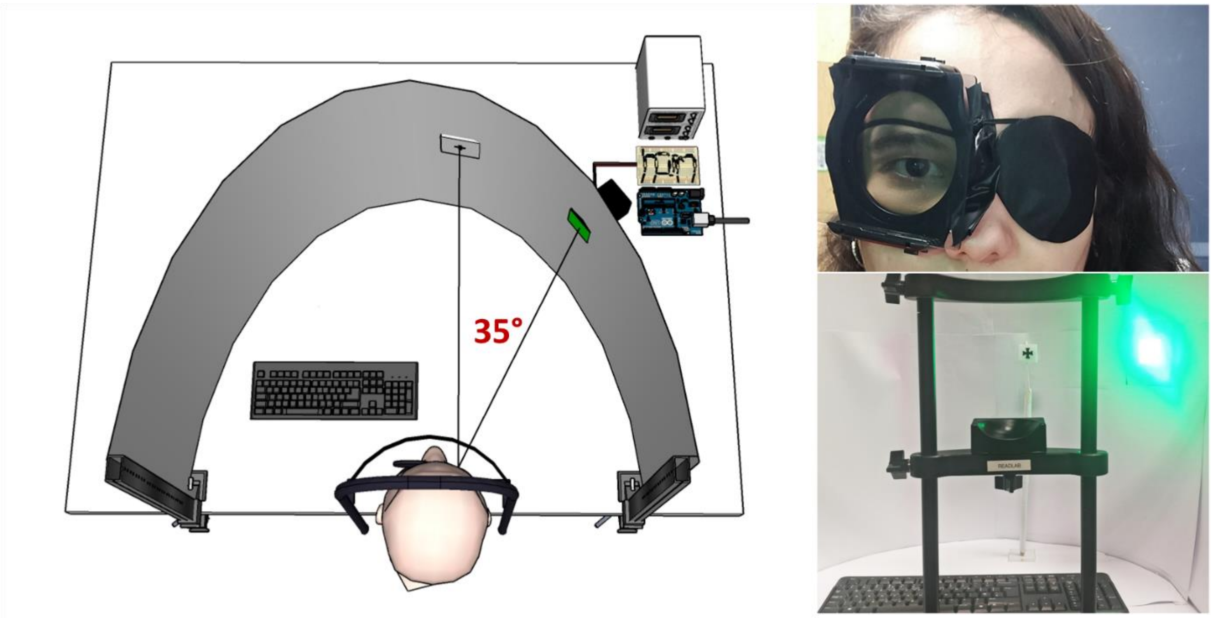

Figure 27. Graphical representation and photos of the experimental setup.

responses. The frequency of the flicker was set via an Arduino Uno connected to the computer, which modulated the voltage of the LED driver circuit in a 50% duty cycle square wave.

To modulate the high-power LEDs at the required frequencies with minimal wave distortion, a fast-switching driver circuit was designed and built. High power LEDs can have large junction capacitance, which added to the parasitic capacitance of the support circuitry, can slow the transitions, and increase the rise and fall times of the luminous output. This would result in a non-square luminance waveform and would cause the total luminance to vary when the half-period of flicker was less than the rise time of the LED. To address these issues, a custom circuit was designed and built that minimized the changes in voltage between the ON and OFF states of the LEDs. Rather than switching the voltage to zero in the OFF state, a voltage was selected that was as close as possible to the ON state voltage, while generating the lowest possible luminous output. This output was sufficiently low to be absorbed by the box and diffuser where the LEDs were encased, and several tests were carried out to confirm that the luminance in the OFF state was 0 cd/m^2. This reduction in voltage changes reduced the rise and fall time of the LEDs significantly, allowing the square waveform to be preserved (see Figure 28), and the total luminance to remain constant regardless of the frequency.

Several calibration procedures were carried out on the experimental setup. Firstly, to confirm that the frequency of flicker of the luminous output was equal to the input frequency,

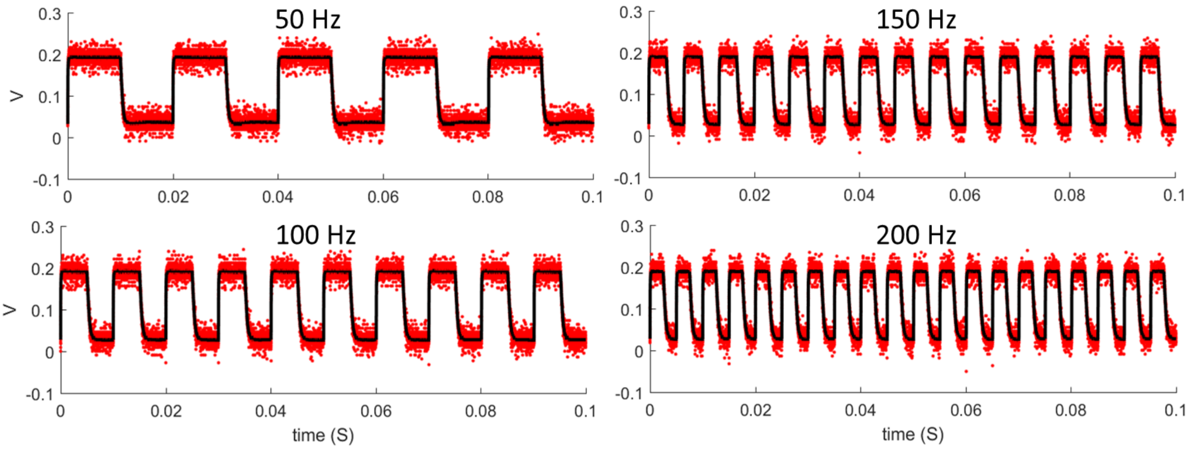

Figure 28. Luminous output measurements at four different frequencies. The red dots represent the raw individual measurements, while the black markers represent the average of these measurements at each time point.

luminance measurements were taken with a photodiode connected to an oscilloscope (PicoScope 2000). All frequencies between 20 and 200 Hz, in steps of 10 Hz, were tested for 100 ms with 32 repetitions at each frequency. Some examples of these measurements are shown in Figure 28. All repetitions were averaged, and the resulting period was obtained and fitted in a linear regression against the input period. The resulting slope was equal to 1 and the intercept 0.37 ms, thus, indicating a very good agreement between input and output. Secondly, to confirm that luminance did not vary with the frequency of flicker, measurements were taken with a Konica Minolta LS-100 at different frequencies between 40 Hz and 1000 Hz. No change in luminance with frequency was found and the standard deviation of the measurements were well within the instrument error. Thirdly, to assess if luminance changed over time, luminance measurements of the stimulus were taken over the course of 9 hours, simulating the scenarios where multiple participants would perform the experiment in one day. We found that luminance decreased by approximately 1300 cd/m^2 over the first 5 minutes, beyond which no further consistent changes were found, with only small random fluctuations around the mean of 23,250 cd/m^2 with a standard deviation of 204 cd/m^2. To account for the small decrease at the start, we ensured the experimental setup was turned on for at least 15 minutes before commencing data collection.

4.2.3. Task and design.

Flicker fusion thresholds were measured by a YES/NO task using the constant stimuli method. One threshold estimate was obtained for each retinal illuminance level in each experimental session. To obtain the estimate, 8 equally spaced frequencies were presented 30 times each, in addition to 30 supra-threshold frequency trials (500 Hz) or “no flicker” trials, all in a randomized order. Between trials, the frequency was set to 1000 Hz. Eight levels of retinal illuminance were evaluated for each participant, from 3 to 6.5 log Trolands approximately (actual values varied for each participant depending on their dilated pupil size).

A more advanced adaptive staircase procedure for YES/NO tasks was initially trialled: Lesmes et al. (2015) Quick Yes-No algorithm; however, after extensive testing, it was deemed to be unsuitable for our experiment, due to an overestimation of the threshold by approximately 15 Hz (±7 Hz) when compared to the more robust constant stimulil method. Further details can be found in Fernandez-Alonso et al., (2020).

4.2.4.Procedure.

Before the day of the experiment, potential participants received the information sheet with all the details of the experiment, including the possible side effects of the drug used. On the day of the experiment, participants were given the information sheet to read, a consent form to sign, and an additional information leaflet to take with them, which included all the prevention measures, possible side effects of the drug, and the steps to follow in case of an emergency. Once consent was obtained, their right pupil was dilated with two drops of Cyclopentolate Hydrochloride at 1%, and after a period of one hour, pupil diameter measurements were taken using the PowerRef 3, an infrared autorefractor with pupillometry capabilities.

Participants then sat in front of the experimental setup with their head fixated in a chinrest. They viewed the stimuli through their right eye, which had the mask holding the corresponding ND filter, while the left eye was occluded with an eye patch. A cross central to the right eye was used as a fixation point. Instructions for the task were given, as well as a few trials of practice in their first session. In each trial, the stimulus was presented for an unlimited duration, until participants gave a response. Each experimental session had an approximate duration of 3 hours, and frequent breaks were given between experimental blocks (every 20 minutes approximately). Participants completed between 3 and 8 sessions on separate days.

4.2.5. Threshold estimation and data analysis.

The CFF thresholds were obtained following the procedure described in Kingdom & Prins (2016) for YES/NO tasks, and using the Palamedes toolbox (Prins & Kingdom, 2018) and custom MATLAB code.

One of the main drawbacks of YES/NO tasks is their susceptibility to observer bias, that is, the proportion of hits and false alarms obtained are influenced by the decision criterion adopted by the observer. Signal Detection Theory (SDT) offers a framework and method for obtaining a criterion-independent measure of performance.

SDT states that due to the existence of internal noise, each stimulus level presented (including a null stimulus) will generate an internal response that will vary randomly from trial to trial. These internal responses are drawn from normal distributions with a given mean and variance, and the extent to which two distributions overlap, determines the discriminability between those two stimuli. In a YES/NO task, observers must determine if the internal response generated by the stimulus presented is drawn from the noise distribution (no flicker), or from one of the signal distributions (different frequencies of flicker). For this, they adopt a criterion of how strong the internal response must be before they give an affirmative answer. A looser criterion will result in many hits (correct "yes" responses) as well as many false alarms (incorrect "yes" responses), while a stricter criterion will result in fewer hits and fewer false alarms. Thus, by obtaining the proportion of hits for each frequency of flicker and the proportion of false alarms, it is possible to calculate the observer criterion (C) such that:

$$C = -\frac{z(pH) + z(pF)}{2} \qquad (Equation\ 4)$$

where *z(pH)* and *z(pF)* are the z-values for the proportion of hits and false alarms, respectively. Negative values of *C* indicate a bias toward "yes" (loose criterion), and positive values a bias toward "no" (strict criterion). Furthermore, it is also possible to estimate the sensitivity (*d'*) of the observer to each frequency of flicker, which is given by the distance between the means of the noise and the signal normalized to their standard deviations (which are assumed to be equal):

$$d' = z(pH) - z(pF) \qquad (Equation\ 5)$$

One problem encountered on some occasions was that d' would assume negative values whenever the proportion of hits for a specific frequency was lower than the proportion of false alarms. This would happen particularly in the higher frequencies (or lower periods of flicker) that were not visible to the observer. Since this is unlikely to be caused by a higher sensitivity to the null stimulus than to the frequency of flicker presented, and more likely the result of the relatively low number of trials at each level, whenever d' assumed negative values, it was set to zero.

Finally, from the calculated d', we obtained an unbiased measure of performance, i.e., the percentage of correct responses the observer would achieve if a neutral criterion (C=0) were adopted. This percentage, termed Pc_{max}, is calculated as:

$$Pc_{max} = \Phi(d'/2) \qquad (Equation\ 6)$$

Once Pc_{max} as a function of the period of flicker was obtained, it was fitted with a Quick psychometric function (PF) through a maximum likelihood procedure, to get estimates of the threshold, slope, and lapse rate (which was allowed to vary, but constrained between 0 and 0.03). Standard errors of the threshold estimates were obtained through parametric bootstrap analysis with 600 simulations. Goodness of fit measurements based on the likelihood ratio test were then obtained for all PFs fits, and those that were deemed to be poor (p<0.05) were discarded. This resulted in just one threshold estimate among all subjects being excluded.

Once CFF thresholds were estimated, retinal illuminance was calculated from the luminance and the measured pupil diameter, while correcting for the Stiles-Crawford effect using Barten (2009)'s method, such that:

$$I = \frac{\pi d^2}{4} L \left[1 - \left({}^{d}/_{9.7}\right)^2 + \left({}^{d}/_{12.4}\right)^4\right] \qquad (Equation\ 7)$$

where *I* is retinal illuminance in Trolands, *L* is luminance in cd/m^2, and *d* is the pupil diameter in mm.

The CFF thresholds as a function of log retinal illuminance for each participant were fitted with a two-segment piece-wise linear regression using the Segmented R library (Muggeo, 2003, 2017). These data were further analysed by fitting a linear mixed model using MATLAB, with predictors of log retinal illuminance and squared log retinal illuminance. For the data obtained with the 5.7° target size, random effects of participant in these two predictors and the intercept were included, as well as random effects of the different experimental sessions within participant on the intercept. For the 10° target size, due to the smaller number of subjects and sessions, only a random effect of experimental session within participant on the intercept was included. The residuals of the models were inspected with diagnostic plots to confirm that no assumptions were violated.

4.3.Results.

In Figure 29, we present an example of the results obtained for one participant at one intensity level. As shown, for each experimental session and at each retinal illuminance value tested, we obtained the proportion of hits as a function of the period of flicker, and the proportion of false alarms (see Figure 29, left). From these, we calculated *d'* (middle), and from there the proportion of correct responses if the observer were unbiased, which was fitted with a psychometric function to obtain a threshold estimate (right).

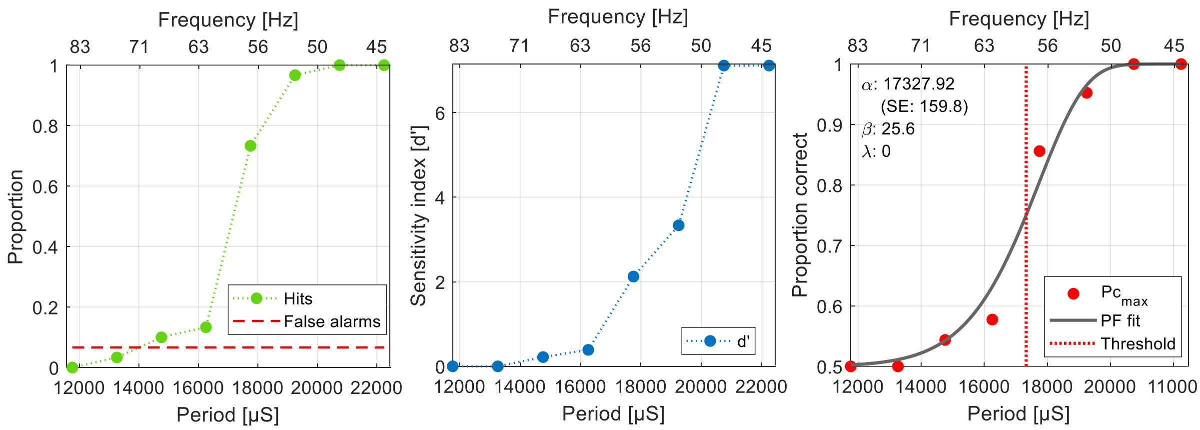

Figure 29. Example of the results obtained for one participant at one retinal illuminance level. The left panel shows the proportion of hits as a function of the period of flicker and the proportion of false alarms. The middle panel shows the calculated d' as a function of the period of flicker presented. The right panel shows the unbiased proportion correct (PC_{max}) as a function of the period of flicker, the Quick psychometric function fitted, and the estimated threshold. In all panels the corresponding frequency of flicker is displayed in the top abscissa.

The thresholds obtained as a function of $\log_{10}$ retinal illuminance (log I) for each participant in each experimental session are presented in Figure 30. For all subjects, the CFFs were measured for a test field size of 5.7 degrees of visual angle, while with two of the subjects we also collected data for a stimulus diameter of 10 degrees of visual angle. In general, we see that the CFF thresholds rise linearly with log I up to approximately $\log_{10}$ 4 Trolands, at which point it saturates between 80 and 90 Hz for the 5.7° stimulus. The larger stimulus diameter of 10° placed at the same eccentricity, increased the intercept of the function and accordingly the value at which it saturates (~100 to 110 Hz), but shows a similar slope. This means that the absolute sensitivity to flicker increases, but the rate at which it changes with increasing intensity is the same. We can also see that the point at which the response starts saturating is similar than for the smaller stimulus size within the same subject. Overall, there is considerable inter-subject variability in both the slope of the linear portion and the value at which the function asymptotes, as well as intra-subject variability between sessions for some participants.

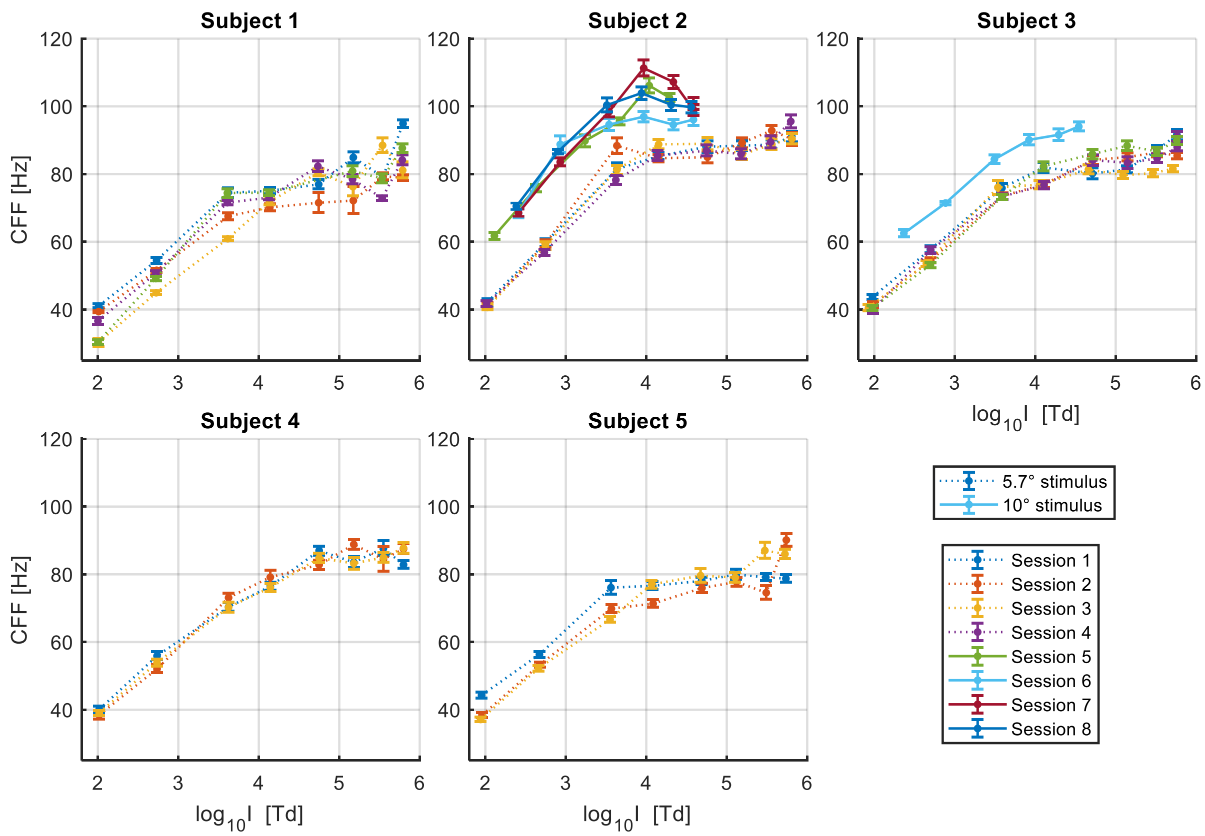

Figure 30. Estimated CFFs as a function of $\log_{10}$ retinal illuminance. Error bars represent the standard error of the CFFs obtained through parametric bootstrap analysis. Different sessions are represented with different colours. The dotted lines represent CFFs obtained for a stimulus of 5.7 degrees of visual angle, and the continuous lines for a stimulus of 10 degrees of visual angle.

Some outlier CFF estimates at the highest intensity values can be observed for a few subjects (e.g., subject 1 and 5). Given the CFF estimates obtained at lower illuminance values, as well as the estimates obtained at that level of intensity in other experimental sessions, it is unlikely that these reflect a real detection of flicker and are more likely to be caused by noise in the psychophysical measurements and by perceptual artifacts that become more salient at the highest intensity levels.

4.3.1.Segmented linear regression.

The apparent shape of the log illuminance – CFF function seems to vary between subjects. For some (e.g., subject 2, 3 and 4) the data could be well described by a sigmoid function, with the rate of change on CFF with log illuminance progressively decreasing at higher intensities until it reaches saturation. For other subjects (e.g., subjects 1 and 5) there seems to be a more sudden transition in the response. Since previous experimental data in the literature have shown this relationship to be linear up to $\log_{10}$ 4 Trolands, and to facilitate the comparison of results, we chose to firstly fit the data with a piece-wise linear function with two segments. For this, we used the Segmented R library, which allows us to estimate the breakpoint and its confidence intervals directly from the data without making any initial assumptions (Muggeo, 2003, 2017). The results for each individual participant and the average of the parameter estimates are shown in Table 10.

Size & Subject		Breakpoint [$\log_{10}$ Td]				Segment 1 Slope [Hz/decade]				Segment 1 x-Intercept [$\log_{10}$ Td]		Segment 2 Slope [Hz/dec.]	
		Est.	**95% CI**		**SE**	**Est.**	**95% CI**		**SE**	**Est.**	**SE**	**Est.**	**SE**
5.7°	1	3.61	2.85	4.37	0.4	21.4	12.9	29.8	4.2	0.36	0.47	6.3	1.1
	2	3.71	3.55	3.86	0.1	25.5	23.5	27.5	1.0	0.42	0.11	3.3	0.8
	3	3.73	3.51	3.96	0.1	20.7	18.6	22.7	1.0	-0.01	0.14	4.9	0.9
	4	4.45	4.22	4.68	0.1	18.2	16.6	19.8	0.8	-0.19	0.13	1.1	1.6
	5	3.63	3.15	4.11	0.2	19.2	15.3	23.2	1.9	-0.13	0.28	5.1	1.6
	Mean	**3.82**	**3.45**	**4.20**	**0.2**	**21.0**	**17.4**	**24.6**	**1.8**	**0.09**	**0.23**	**4.2**	**1.2**
10°	2	3.87	3.67	4.06	0.1	24.0	19.5	28.4	2.1	-0.54	0.26	-9.2	4.5
	3	3.73	3.27	4.20	0.1	19.5	15.1	23.9	1.0	-0.82	0.15	6.2	1.8
	Mean	**3.80**	**3.47**	**4.13**	**0.1**	**21.7**	**17.3**	**26.1**	**1.6**	**-0.68**	**0.21**	**-1.5**	**3.2**

Table 10. Segmented linear regression results of CFF as a function of $\log_{10}$ retinal illuminance for each size of stimuli and subject. The breakpoint is the value of log I at which the piecewise linear function separates. The estimated values (Est.), their standard errors (SE), and 95% confidence intervals (CI 95%) are shown. The slopes are in units of Hz/decade, and the x-intercept and breakpoint in units of $\log_{10}$ Trolands.

We see that the breakpoint (i.e., the point at which the rate of change in the response changes abruptly) had similar estimates in most participants and in the two stimulus sizes used, with estimated values between 3.61 and 3.87 $\log_{10}$ Trolands, and an average of 3.82 for the 5.7°

target (mean 95% CI from 3.45 to 4.20 $\log_{10}$ Trolands) and 3.80 for the 10° target (mean 95% CI from 3.47 to 4.13 $\log_{10}$ Trolands). This suggests that the CFF to log illuminance function starts to saturate at an approximately similar value regardless of target size. For one subject however, the estimated breakpoint is much higher at 4.45 $\log_{10}$ Trolands (95% CI from 4.22 to 4.68 $\log_{10}$ Trolands). This can be observed in Figure 30, where the CFF for this participant continues to increase relatively linearly at intensities where the responses of other observers have already saturated.

The slope of the first linear segment (i.e., the response at intensities lower than the breakpoint) shows further individual differences between observers, ranging from 18.2 Hz/decade to 25.5 Hz/decade, with an average of 21.0 Hz/decade for the 5.7° target size (mean 95% CI from 17.4 to 24.6 Hz/decade) and 21.7 Hz/decade for the 10° target size (mean 95% CI from 17.3 to 26.1 Hz/decade). Furthermore, we see that the estimated slope is consistent within participants across target sizes, with subjects 2 and 3 having similar estimated rates of increase with overlapping confidence intervals in both conditions. These results indicate that, as expected, the size of the target does not affect the slope of the CFF - log illuminance function.

Instead of the estimated y-intercept of the first linear segment, we report here the x-intercept instead which was calculated from the estimated slopes and y-intercepts. The x-intercept is a more physiologically relevant measurement, as it represents the threshold sensitivity to light under given experimental conditions. We see that the estimated x-intercept is, as expected, much lower for the 10° target size with estimates between -0.82 and -0.54 $\log_{10}$ Trolands, when compared to the 5.7° target size (with estimates ranging from -0.19 to 0.42 $\log_{10}$ Trolands); reflecting the increased sensitivity to the same amount of light when emitted over a larger area.

Finally, there is large variability in the estimated slopes for the second segment of the piece-wise linear regression, with estimates ranging between 1.1 and 6.3 Hz/decade for the 5.7° target, and between -9.2 and 6.2 Hz/decade for the 10° target. The fact that most estimated values are positive might be reflecting the fact that the change in the response is not completely abrupt but rather gradual for most subjects, as well as the existence of some outliers at higher intensities. However, it is unlikely that the CFF would continue to rise at the estimated rates, as the response seems to completely saturate at the highest retinal illuminance values. Thus, to better capture both the gradual nature of the change and the saturation of the response, we performed a further analysis fitting the data with a quadratic function, using the more robust linear mixed model method. This approach will also allow us to better capture the between-subject and within-subject (i.e., between-session) variability in the measured CFF thresholds.

4.3.2. Linear mixed model with quadratic term.

To better capture the relationship between CFF and log illuminance, we fitted a linear mixed-effects model to the thresholds obtained for each target size, with fixed effects of log illuminance and squared log illuminance. For the 5.7° target size, the intercept was allowed to vary randomly among subjects, with an additional random effect on the intercept of experimental session nested by subjects. More complex random effects structures that included the effects of log illuminance and squared log illuminance were tried but including these resulted in overfitted models, indicating that these structures were too complex to be supported by the data. For the CFF thresholds obtained with 10° target size, we fitted a mixed

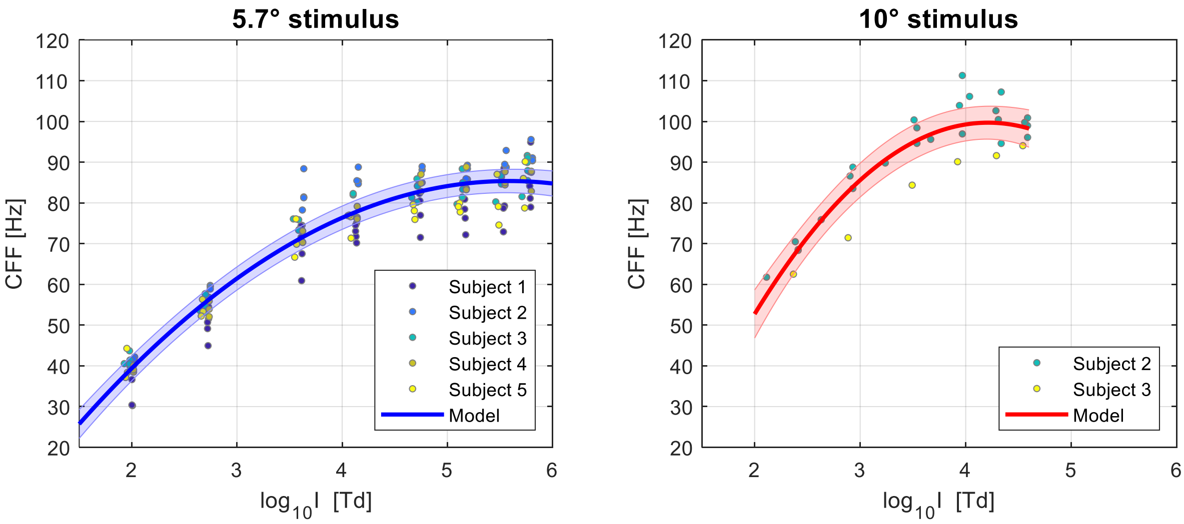

Figure 31. Quadratic linear mixed model results of CFF as a function of log_{10} retinal illuminance, for stimulus sizes of 5.7 (left) and 10 (right) degrees of visual angle. The continuous coloured lines represent the model fit and the shaded regions represent the 95% confidence intervals. The individual markers show the estimated thresholds for each subject over several experimental sessions, and the colour of the markers represents the participant as indicated by the legend.

model with the same fixed effects, but only a random effect of session nested within subject on the intercept. Thus, the intercept of the function could vary randomly for each experimental session done by each participant, but not the other parameters of the model.

Including a random effect of subject would not be advisable with only two subjects in this experimental condition; and allowing the effect of the other parameters to vary randomly by experimental session would add unsupported complexity to our model.

The results of the fitted models are shown in Table 11 and illustrated in Figure 31. For the 5.7° target we see that the more gradual nature of the change in the CFF – log illuminance relationship has been more accurately captured, with the response completely saturating at the highest intensity values and for frequencies of flicker below 90 Hz. However, the estimates of the model refer to the "average observer" given our sample, but as it can be seen, some subjects can perceive flicker at higher frequencies than this. Using the random effects of the model (i.e., the parameters obtained for individual observers) would allow to obtain estimates of the CFF at different light intensities for these more sensitive individuals.

Somewhat similar results are seen for the 10° target, albeit with higher CFF thresholds for equal values of intensity, as previously discussed. The function seems to saturate at approximately 100 Hz and at similar values of light intensity as with the 5.7° stimulus. Overall, however, the limited number of subjects and data in this experimental condition result in a poorer fit with larger standard errors, and thus greater uncertainty about the parameter estimates.

5.7° stimulus – CFF [Hz]									
								RE SD	
Parameter	**Est.**	**SE**	**95% CI**		**t-ratio**	**df**	**p-value**	**subject**	**session**
Intercept	-26.05	3.42	-32.80	-19.30	-7.63	157	<0.001	3.03	0.86
$\log_{10} I$	39.86	1.71	36.49	43.24	23.34	157	<0.001	-	-
$(\log_{10} I)^2$	-3.57	0.22	-3.99	-3.14	-16.58	157	<0.001	-	-

10° stimulus – CFF [Hz]								
								RE SD
Parameter	**Est.**	**SE**	**95% CI**		**t-ratio**	**df**	**p-value**	**session**
Intercept	-70.52	14.03	-99.26	-41.77	-5.03	28	<0.001	4.05
$\log_{10} I$	80.80	8.38	63.64	97.97	9.64	28	<0.001	-
$(\log_{10} I)^2$	-9.59	1.21	-12.07	-7.11	-7.92	28	<0.001	-

Table 11. Linear mixed model results of CFF as a function of $\log_{10}$ retinal illuminance and squared $\log_{10}$ retinal illuminance. The parameters estimate (Est.), their standard errors (SE) and 95% confidence intervals (95% CI) are shown, as well as the t-test results and the standard deviation of the different random effects included (RE SD).

Finally, one more factor to consider is that the way CFF thresholds were estimated here, and are usually estimated in the literature, might not be ideal when considering practical applications such as minimising the visibility of flicker on digital displays or illumination sources. As it is common in psychophysics, the CFFs reported here corresponded to the frequency at which subjects reported to see flicker in 50% of the trials of the YES/NO task (equivalent to 75% of correct responses when considering the trials where no flicker was presented). However, in a real-life scenario, an illumination source that leads to the percept of flicker 50% of the time could be very detrimental for the observer. Aiming for a lower visibility rate of flicker would mean threshold estimates of higher frequency than those presented thus far. Since in our experiments we measured the full psychometric function using the constant stimuli method, it is possible to offer estimates of the frequencies of flicker that would lead to only a 10% visibility rate of flicker (i.e., the lowest frequency at which participants report to not see flicker in 90% of the trials). This percentage was selected as it is an alternative threshold occasionally reported in the literature (Barten, 2009).

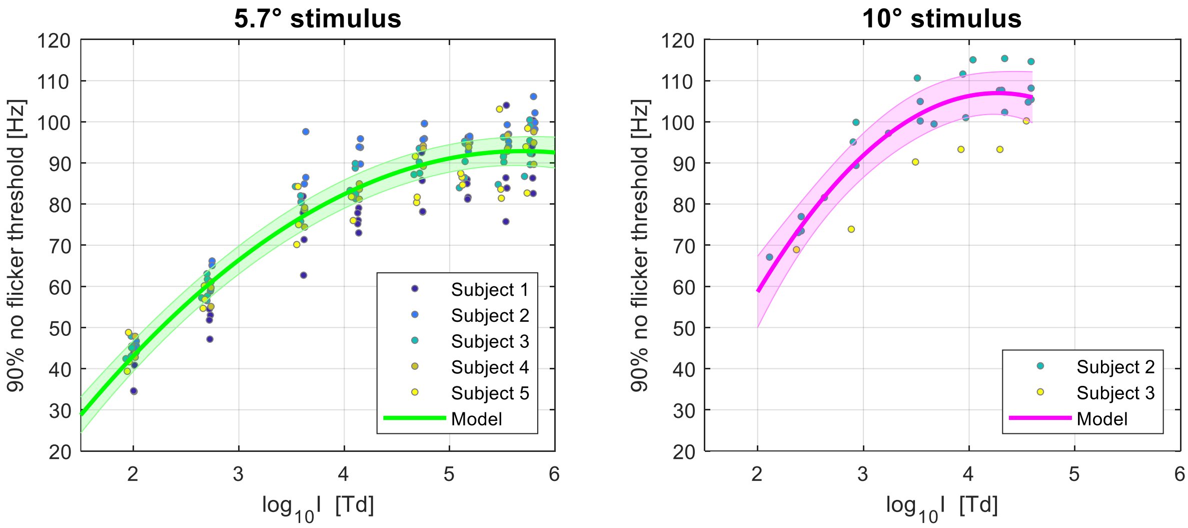

Figure 32. Quadratic linear mixed model results of the 90% "no flicker" threshold as a function of $\log_{10}$ retinal illuminance, for stimulus sizes of 5.7 (left) and 10 (right) degrees of visual angle. The continuous coloured lines represent the model fit and the shaded regions represent the 95% confidence intervals. The individual markers show the estimated thresholds for each subject over several experimental sessions, and the colour of the markers represents the participant as indicated by the legend.

In Figure 32 we illustrate these estimates for the 5.7° and 10° stimuli, as well as the linear mixed models fitted with the same parameters as the previous ones presented in this section. The estimates and full results of the model are shown in Table 12.

As expected, we observe higher values of frequencies that can be perceived when taking the lower visibility rate of 10%; albeit the effect is modest, with the frequency at which the models saturate increasing by ~5 Hz in both target sizes. The estimated parameters would allow to obtain frequency estimates at which flicker is only perceived 10% of the time for different values of retinal illuminance and for an average observer given our sample, being particularly relevant for capturing the saturation of the function at higher illuminance levels.

5.7° stimulus – 90% "no flicker" threshold [Hz]									
								RE SD	
Parameter	**Est.**	**SE**	**95% CI**		**t-ratio**	**df**	**p-value**	**subject**	**session**
Intercept	-25.36	4.47	-34.20	-16.52	-5.67	156	<0.001	3.60	0.71
$\log_{10} I$	41.53	2.28	37.03	46.03	18.22	156	<0.001	-	-
$(\log_{10} I)^2$	-3.65	0.29	-4.21	-3.08	-12.69	156	<0.001	-	-
10° stimulus – 90% "no flicker" threshold [Hz]									
								RE SD	
Parameter	**Est.**	**SE**	**95% CI**		**t-ratio**	**df**	**p-value**	**session**	
Intercept	-63.92	22.69	-110.39	-17.45	-2.82	28	<0.001	4.81	
$\log_{10} I$	80.03	13.60	52.18	107.89	5.89	28	<0.001	-	
$(\log_{10} I)^2$	-9.37	1.96	-13.39	-5.35	-4.77	28	<0.001	-	

Table 12. Linear mixed model results of the 90% "no flicker" threshold as a function of $\log_{10}$ retinal illuminance and squared $\log_{10}$ retinal illuminance. The parameters estimate (Est.), their standard errors (SE) and 95% confidence intervals (95% CI) are shown, as well as the t-test results and the standard deviation of the different random effects included (RE SD).

4.4. Discussion.

The relationship between light intensity and the temporal sensitivity of the human visual system has very important practical applications, particularly in the design of digital displays and illumination sources that are temporally modulated. This relationship is best described by the Ferry-Porter Law, which states that the CFF increases linearly with the logarithm of the retinal illuminance. This linearity has been shown to hold for a wide range of stimulus and up to $\log_{10}$ 4 Trolands (Tyler & Hamer, 1990); however, beyond this intensity, it is unknown if the CFF continues to rise linearly or if saturation is reached. In this study we aimed to extend the experimental data available on the peripheral CFF at higher light intensity levels than previously reported in the literature. For this, we built an experimental setup following the one described by Tyler & Hamer (1990), with careful control of the illumination source, the stimulus size and location, and the psychophysical method used to estimate the CFF (Fernandez-Alonso et al., 2020).

To analyse our results, we first fitted a piece-wise linear regression with two segments. For the slope of the first segment, we found results comparable to those of Tyler & Hamer (1990), with the CFF increasing by 19 to 25 Hz/decade with increasing retinal illuminance for both target sizes. Their sample showed rates of increase of ~20 Hz/decade for the same temporal retinal eccentricity of 35°. However, while these authors show that the linear increase continues up to $\log_{10}$ 4 Trolands, we found that saturation of the response can start at lower illuminances for some subjects. The estimated breakpoint or sudden change in the rate of the response was between $\log_{10}$ 3.6 and 4.4 Trolands among our sample. Beyond this, the response saturates, and the rate of increase of the CFF decreases dramatically.

The change in the rate of the response was in reality not a sudden transition, but rather a gradual change. To capture this, we fitted a linear mixed model with a quadratic term. We found that saturation happened gradually between ~ $\log_{10}$ 3.6 and $\log_{10}$ 4.6 Trolands, with the CFF reaching just below 90 Hz for the target of 5.7 degrees of visual angle, and approximately 100 Hz for the 10 degrees target. As expected, the thresholds were higher for the test field with larger area, but the speed of the response was the same, which was reflected in higher absolute values of CFF but similar slope estimates. This is anticipated to happen for a stimulus of larger area but equal retinal eccentricity and wavelength of light. In practical terms, as visual displays tend to have larger sizes than the stimuli used, we can expect the maximum frequency at which saturation occurs to be higher.

Another important practical consideration is that the way thresholds are usually defined might not be optimal for the design of visual displays. A correct response rate of 75% is a common specification for psychophysical thresholds. In a YES/NO task, this corresponds to a 50% of flicker visibility; that is, subjects report perceiving flicker half of the time. Taking this into account, and as we measured the full psychometric function, we also reported the frequency at which flicker was only visible at a rate of 10%, which increased the estimated values by ~5 Hz. Finally, it is important to note that while the estimates offered refer to an average observer given our sample, in practical application more weight might be given to the more sensitive observers, as for the design of visual displays one would want to avoid the visibility of artifacts in the large majority of observers. For this purpose, the estimates obtained through the linear mixed model for individual participants might be a useful contribution.

As modern digital displays continue to increase in brightness, it is important to know how this can affect the visibility of flicker and other temporal artifacts. While models exist that can predict how the CFF will change depending on target size and eccentricity (Barten, 2009; Tyler, 1989), they also assume that the Ferry-Porter Law will continue to hold with increasing log illuminance. However, we find here that the response in fact saturates, decreasing the need for proportional increases in the refresh rates of displays, albeit these would still need to higher than the CFF in order to avoid other temporal artifacts in the image.

Chapter 5. The Effect of Screen Luminance and Ambient Illuminance on Blink Patterns and Visual Discomfort

5.1.Introduction.

Since their introduction, smartphones have become increasingly ubiquitous devices used in many different environments for a multitude of tasks. Their prevalence has grown significantly over the last decade, from 17% of people in the United Kingdom owning a smartphone in 2008 (Ofcom, 2018), to 79% in 2019 and 96% among 16-34 year olds (Ofcom, 2019); with similar trends found worldwide. Despite their popularity, smartphone users often report symptoms of visual fatigue and discomfort, with several studies finding an increase in eyestrain, dryness and blurriness after using these devices or correlated with more frequent use (Long et al., 2017; Golebiowski et al., 2019; Kim et al., 2016). This symptomatology is very similar to that caused by the prolonged use of desktop computers, where most of the research to date has focused and which is known in the literature as Computer Vision Syndrome (CVS).

The collection of short- and long-term symptoms that compose CVS can be broadly classified in three categories: asthenopic, visual, and ocular-surface related (Blehm et al., 2005). Asthenopic symptoms include eyestrain, ache in and around the eyes, tired and sore eyes. Visual symptoms encompass blurred vison, double vision, and slowness of changing focus between distances. These two categories of symptoms are often associated to problems with the accommodation and vergence responses of the visual system. Previous studies have shown that prolonged computer work can lead to increased lag and decreased amplitude of accommodation, recession of the near point of convergence and a shift towards exophoria in near vision (Jaiswal et al., 2019; Blehm et al., 2005; Gowrisankaran & Sheedy, 2015). These symptoms seem to be mostly temporary (Blehm et al., 2005), and not unique to digital displays, but rather a consequence of performing demanding visual tasks at near distances over long periods of time (Iribarren et al., 2001).

Only a small number of similar studies have been done on the use of mobile displays. They seem to show similar results, finding a decrease in accommodative facility after reading on a smartphone for 60 minutes (Golebiowski et al., 2019), and decreased accommodative amplitude and increased lag after watching a video on a smartphone for 30 minutes when compared to reading printed text for the same period of time (Park et al., 2014), indicating that mobile screen use could be more strenuous to the accommodative system than printed text or computer use. However, some other studies have found contradictory results (Jaiswal et al., 2019), and in general more evidence is needed in this area.

The third category of symptoms are those related to the ocular surface, and include dryness, irritation, redness and burning sensation in the eyes. These symptoms result from a lack of proper tear lubrication and consequent desiccation of the eyes. While there can be several factors contributing to this, including environmental conditions and individual characteristics of the users (Blehm et al., 2005), a major cause has been found to be changes in blink patterns while performing computer work (Blehm et al., 2005; Gowrisankaran & Sheedy, 2015).

A reduction in the amount of blinks per minute or blink rate while performing different tasks on a computer monitor has been consistently reported in the literature (Freudenthaler et al., 2003; Schlote et al., 2004; Himebaugh et al., 2009; Cardona et al., 2011). However, these results seem to be influenced by the difference in cognitive demand between the tasks being compared. Most of these studies used the blink rate during easier tasks of conversations or looking at distant targets, as a baseline to compare with more visually demanding tasks performed in a computer, such as reading or playing a video game. When equivalent reading conditions are compared, no differences are found between using a computer display or printed text, with both conditions resulting in a reduced blink rate with respect to baseline levels (Chu et al., 2014; Argilés et al., 2015). Further studies have demonstrated that an increased task difficulty and cognitive load has a greater effect on reducing the blink rate of participants than the format of presentation (Rosenfield et al., 2015; Nielsen et al., 2008).

Another consistent finding in the literature is a reduction in blink amplitude – *i.e*. how much of the ocular surface is covered during a blink–, resulting in a higher number of incomplete blinks during computer display use (Cardona et al., 2011), even when comparing it with equivalent reading tasks of printed text (Chu et al., 2014; Argilés et al., 2015). Task difficulty does not seem to have an effect on blink completeness or amplitude (Cardona et al., 2011; Himebaugh et al., 2009).

A reduction in blink rate and blink amplitude have both been correlated with an increase in dry eye and other CVS symptoms after reading for 15 minutes in a computer display (Portello et al., 2013). This is consistent with the fact that blinking has an important function in the lubrication of the eye. During a blink, the movement of the eyelids spreads the tear fluid evenly over the ocular surface. During incomplete blinks the tear film is not completely replenished, while a reduced blink rate and consequent increase of the interblink time, allows for a greater evaporation of tears (Jaiswal et al., 2019). Another factor that can lead to greater tear evaporation is the gaze angle at which computer displays are used. Studies have found that performing the same task in a computer monitor at a lower gaze angle causes a reduction in blink rate (Nielsen et al., 2008), related to a smaller percentage of the ocular surface being exposed (Cho et al., 2000). Hence, the higher gaze angle at which computer monitors are usually viewed can further affect eye lubrication.

The research on ocular surface discomfort symptoms and smartphone use is so far very limited and shows fewer clear results. Population studies on children and adolescents in South Korea have found that a higher frequency of smartphone use is a risk factor for developing dry eye disease and experiencing a greater number of ocular discomfort symptoms (Kim et al., 2016; Moon et al., 2014, 2016), while stopping smartphone use for four weeks led to an improvement of both objective and subjective indicators of dry eye disease (Moon et al., 2016).

Park et al. (2014, cited in Jaiswal *et al.*, 2019) reported a reduced blink rate after 60 minutes of viewing a video or playing a game on a smartphone, with a concurrent increase in self-reported dry eye symptoms. A more recent study (Golebiowski et al., 2019) found that visual discomfort, tiredness and sleepiness increased after 60 minutes of reading on a smartphone, but found no significant effect on blink rate during the task. They did find however, that the number of incomplete blinks per minute significantly increased during the task. This increase was correlated with a worsening of the overall ocular surface symptoms score.

In summary, as smartphones become increasingly prevalent devices and their frequency of use rises, especially among younger age groups, it is important to investigate the impact they have on ocular health and visual comfort. While the research on the effects of using computer displays to date is extensive with some well-established results (Blehm et al., 2005; Gowrisankaran & Sheedy, 2015), hand-held devices have important differences in their usage and features that might lead to different findings. Smartphones can be used at varying viewing distances and gaze angles, while computer monitors are usually fixed. The latter are also more frequently used indoors, and their luminance is not regularly altered. Smartphones on the contrary are usually used in both indoors and outdoors environments, and the luminance of the screen can vary automatically according to the ambient illuminance, or it can be adjusted manually by the user. Furthermore, the high ambient illumination of outdoor environments will reduce the contrast of an emissive display such as a mobile phone screen and reduce visual acuity, an issue that is not present for reflective visual displays such as paper. However, a high ambient illumination will also constrict the pupil of observers, increasing the depth of focus of the eye and reducing the demands on the accommodative system, as well as improving image sharpness. Thus, it is not clear what the overall effect on visual comfort might be.

Understanding the impact that these different factors have on the ocular health of the user could be valuable in the design of digital hand-held devices that minimise visual discomfort and fatigue. This study aims to evaluate the effect that the interaction of screen luminance and ambient illuminance have on blink rate and subjective symptoms of visual discomfort in healthy subjects.

5.2.Methods.

5.2.1.Participants.

Data were collected from 21 adults with ages between 18 and 45 years old (mean 26.8, SD 7.26), out of which 14 were female and 7 were male. Participants were recruited from students, staff, and the external pool of participants of the Institute of Biosciences of Newcastle University. All but 3 participants were naïve as to the aim of the experiment. The study was approved by Newcastle University Ethics Committee (reference number 15327/2016) and written consent was obtained from each subject.

5.2.2.Apparatus.

Ambient Illuminance. To create the different ambient illumination conditions of the experiment, eleven multi-channel Light Emitting Diode (LED) lamps were used. Two standard illuminants were defined by controlling the output of each individual channel: a D65 illuminant with the highest possible illuminance, and a low-illuminance D65 that was still within photopic levels. For the high ambient illuminance condition, additional lighting was added, including two white LED floodlamps and the three incandescent ceiling lamps. The walls of the room and all objects in it were covered with white cloth to maximise reflectance. Figure 33 shows photos of the experimental setup under both illumination conditions.

Figure 33. Experimental setup in the high ambient illuminance (left) and low illuminance (right) conditions.

Measurements of illuminance and chromaticity under both experimental conditions are shown in Table 13. These were taken by placing the Konica Minolta CL500A illuminance spectrophotometer in the same position of the participant and approximately at eye level.

Smartphone Display. To present the text, a smartphone with a 5.5 inches Active-matrix Organic Light Emitting Diode (AMOLED) screen was used. The white colour of the screen had a luminance of 410.20 cd/m^2 with maximum brightness screen settings, and of 3.64 cd/m^2 with minimum brightness screen settings, as measured in dark conditions with the Konica Minolta LS-100 luminance meter. Being an AMOLED display, the black colour of the screen had a luminance of 0 cd/m^2 under dark conditions. The luminance of the white (at maximum and minimum) and black colours of the screen were also measured under the two conditions of ambient illumination used, to account for any light reflected from the display. All measurements were taken with the luminance meter at 35 cm from the screen, both tilted 45 degrees from the vertical, with the screen pointing upwards and placed in front of the participant's seat, to recreate conditions comparable to those of the experiment. The results can be found in Table 14.

	Illuminance	Chromaticity	
		X	Y
High illuminance	2640.78 lux	0.3160	0.3120
Low illuminance	43.57 lux	0.2943	0.3164

Table 13. Ambient illuminance and chromaticity measurements under the two experimental conditions.

	Low ambient illuminance	High ambient illuminance
White at maximum	412.17 cd/m^2	438.60 cd/m^2
White at minimum	5.32 cd/m^2	22.10 cd/m^2
Black	1.02 cd/m^2	18.24 cd/m^2

Table 14. Luminance measurements of the smartphone screen under the different experimental conditions.

Eye-tracking. To measure the blink rate of participants the Pupil Labs binocular wearable eye-tracker and the Pupil Capture software were used (Kassner et al., 2014). The eye-tracker consisted of two binocular infrared eye cameras (200x200 pixels, 200 Hz) and one world camera (640x480 pixels, 120 Hz). The Pupil Capture software allowed to automatically detect the participant's pupils through a 2D computer vision algorithm. At the start of each session, a calibration procedure was performed to correlate the coordinates of the world camera with both eye cameras, and the parameters of the eye video images (contrast and exposure) and of the 2D pupil detector (minimum and maximum pupil size, and intensity range) were adjusted as necessary to improve pupil detection. An example of images obtained with the eye-tracker are shown in Figure 34.

Questionnaires. To evaluate the subjective experience of visual fatigue and discomfort we selected the Symptoms Questionnaire used by Hoffman, Girshick and Banks (2008), which was

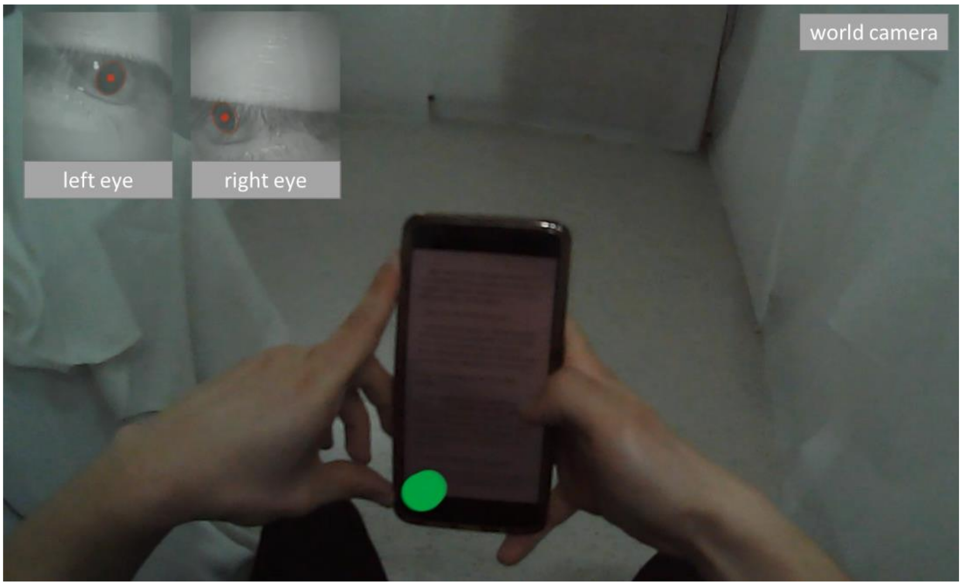

Figure 34. Example of images obtained with the Pupil Labs eye-tracker during the experiment, showing the world camera image with the images from the left and right eye cameras overlaid (top left).

modelled after the one developed by Sheedy & Bergstrom (2002). The questionnaire has five questions, and in each one, participants rated the symptom in a five-point Likert scale (none, mild, modest, bad, severe). The five questions were: *1) How tired are your eyes? 2) How clear is your vision? 3) How tired and sore are your neck and back? 4) How do your eyes feel? 5) How does your head feel?*

In the final session, participants also completed the Sessions Evaluation Questionnaire (Hoffman et al., 2008) , which included four questions: *1) Which session was most fatiguing? 2) Which session irritated your eye the most? 3) If you felt headache, which session was worse? 4) Which session did you prefer?* Both questionnaires are presented in Appendix E.

5.2.3.Design and procedure.

The experiment used a repeated measures two-by-two design where the independent variables were the luminance of the screen (high or low) and the ambient illuminance in the room (high or low), resulting in four different conditions. Each one was done on separate days and their order was randomized between subjects.

Each participant visited the lab on at least four occasions. In the first session they were given the information sheet and consent form to read and sign, and the instructions and procedure of the experiment were explained. The illumination of the room was set previously to the participant's arrival, and the smartphone screen was wiped with a screen cleaner and set to the correct luminance, with the auto-brightness feature turned off. Once participants arrived, they filled in the Symptoms Questionnaire, after which the portable eye-tracker was fitted, adjusted as necessary and calibrated. Participants were then shown a list of digital books, were asked to select one to read during the session and were told to adjust the font size to their preference or leave it at the default 100% if preferred. After reading for a period of 30 minutes, during which their eye activity was recorded, they were asked to fill the Symptoms Questionnaire again. In the final session, they were also given the Sessions Evaluation questionnaire.

5.2.4.Data processing.

Symptoms Questionnaire. To evaluate the effect of each experimental condition on reported symptoms of visual fatigue, each level of the Likert scale was assigned a numerical value from 1 to 5 according to the intensity of the symptom it represented. Then, the differences of the score given for each symptom at the start of the session and at the end was calculated. The sign of the resulting value indicated whether there was an improvement in the symptom (negative values), no difference (zero), or a worsening of the symptom during the session (positive values), while the magnitude represented the intensity of the change.

Blink Detection Algorithm. The eye-tracking data were recorded and exported using Pupil Capture and Pupil Player (Kassner et al., 2014). During the recordings, the pupil of the participants was detected using the 2D pupil detection algorithm of the Pupil Capture software. This algorithm uses computer vision to detect the pupil at each frame and assigns a confidence value. When the eye is closed or occluded, the pupil cannot be reliably detected, resulting in a low confidence value. This was later used to implement an automated blink detection algorithm, followed by a manual validation procedure to exclude false positives.

We firstly inspected each eye-tracking video for quality control. Out of the total 21 participants that took part in the experiment, the eye-tracking data of 8 participants had to be excluded from further processing and analysis. The reasons for exclusion were: 1) frequent and persistent drowsiness and sleepiness during at least three of the sessions for 6 participants, which affected the pupil detection quality for most of the recording, 2) strong light reflections from glasses for 1 participant, which obstructed the pupil from being detected, 3) percentage of incomplete blinks of nearly 100% for 1 participant, in which the pupil was not covered, resulting in almost no blinks being detected. Additionally, of the remaining participants, 1 had the eye-tracking data from one session excluded due to the files being corrupted when storing them, and 1 only completed three of the sessions. In total, the eye-tracking data of 13 participants was used for further analysis, 11 with four completed sessions, and 2 with three sessions.

The pupil detection confidence values that are given by the Pupil Capture 2D detector can be used to identify blinks via a simple but effective algorithm. A moving difference filter is applied to the confidence signal to identify sudden changes that occur within a certain time window (200 ms) and above a specified threshold. This type of filter enhances sharp steps in the signal while reducing high frequency noise. Blinks in the filtered signal present themselves as a positive peak followed by a negative peak, corresponding to the closure and opening of the eyelids causing a sudden drop and gain in the pupil detection confidence, respectively.

While the Pupil Player software uses the confidence values of both eyes to detect blink events, we implemented this algorithm in MATLAB (The MathWorks Inc., 2019) using only the confidence information of the left eye. This is because each eye camera had a different view of their corresponding eye (right camera from above, left camera from below, as seen in Figure 34) and participants kept the smartphone display mostly in downgaze during the experiment. This resulted in better pupil detection in the left eye camera, while the right eye detector would often identify the eye as closed when participants had their gaze in downward positions.

The blink onset and offset thresholds were set to a 25% drop and gain of confidence in pupil detection, respectively. While this is a relatively low value, compared to the default values of the Pupil Player for example (50%), the higher sensitivity to changes in the pupil detection confidence allowed to identify a higher number of blink events, especially those in which the pupil was not completely covered (incomplete blinks). Conversely, this also produced a higher number of false positives, for which a manual check procedure was implemented. For each blink event detected, the corresponding video frames were extracted and saved as an image, which allowed to quickly inspect the results. Most of the events detected by the algorithm were also judged as blinks by the human observer (86.13%). Only 10.68% were identified as false positives and removed from the blink analysis. A small percentage of errors in the blink detection algorithm were corrected, such as multiple blinks in series being detected as one (1.07%), or one blink being detected as two separate events (0.10%). In these cases, the blinks were separated or unified accordingly. Other non-blink eye occlusions were identified and classified, specifically drowsiness (1.94%) and eye-scratching (0.08%). Finally, the blink onset and offset times were set to the nearest zero-crossings that preceded and followed the positive and negative peaks in the signal, respectively.

To calculate the blink rate (BR), the data of each session were divided into time intervals of one minute, and each blink was assigned according to its onset time. Non-blink events (eye-scratching and drowsiness) were on the contrary, considered for their entire duration, and any given one-minute interval during which a non-blink event occurred was excluded from further processing. The total number of blinks that occurred during each interval was counted. Whenever multiple blinks in series occurred, they were counted as separate blinks for the BR calculation but treated as one blink for the interblink time analysis to avoid biasing this variable with multiple zero values. In total, 713 pairs of blinks in series were identified and grouped, of which: 30.9% were in the low Ambient illuminance and high Mobile Phone screen luminance condition (Low A – High MP), 25.5% in the High A – High MP condition, 23.0% in the High A – Low MP condition, and 20.62% in the Low A – Low MP condition. Finally, for the blink duration analysis, cut-off values of 50 ms and 1000 ms were implemented as the minimum and maximum, respectively, which resulted on 0.06% of the blinks detected being excluded.

5.2.5. Statistical analysis.

To analyse the differences in reported symptoms of fatigue between the start and end of the session, a Wilcoxon signed-rank test was used. To analyse the differences in change in scores between conditions, we fitted an ordinal logistic regression on symptom score change with predictors of experimental condition, symptom and their interaction, and random intercept and slopes participants. The model was fitted using the R library ordinal (Christensen RHB, 2019). Post-hoc pairwise comparisons of marginal means on score change for each symptom and in total were performed between all experimental conditions using the emmeans library (Lenth, 2021), with p-values being adjusted for multiplicity using Tukey's method.

We analysed the responses to the session evaluation questionnaire by performing an exact multinomial test of goodness of fit, with the null hypothesis that there was no significant difference between the observed proportion of votes and the expected proportion if the votes for each condition were selected randomly (20%). For the questions where the null hypothesis was rejected, we then performed a post-hoc exact binomial test of the votes given to each condition versus the sum of the votes for the other options in each question, with the null hypothesis that the proportion of votes given to each condition was not significantly different from the expected proportion if choices were random (20%), and the alternative hypothesis that the probability was not equal to 20%. Significance levels were adjusted for multiplicity of testing using the Bonferroni correction method. These tests were performed using the EMT and stats (R Core Team, 2021) R libraries.

To analyse the differences in blink rate (BR), blink duration (BD) and interblink time (IBT) between conditions, different generalized linear mixed effects models (GLMMs) were fitted using the lme4 R library (Bates et al., 2015). Mixed effect models are particularly suited to handle missing and unbalanced data, therefore, the eye-tracking results of the two participants with one missing session were included in the analysis, resulting in a sample of 13 participants. For each response variable, two models were fitted and compared: a simpler model, with the experimental condition as a categorical predictor; and a second, more complex model, with predictors of experimental condition, time-on-task, and their interaction. Both models were compared in each case by calculating their Akaike Information Criterion (AIC), and since these were nested models, by performing a Likelihood Ratio Tests (LRT). For all models, the maximal random-effects structure that did not lead to convergence issues or overfitting was used, which was a random intercept and slope of condition by participant for all response variables (i.e., the effect of each condition could vary randomly among participants).

For BR, the GLMMs were fitted using a Poisson conditional distribution, which is appropriate for this type of data as it consists of counts of events (number of blinks in a one-minute interval), and an identity link. For IBT, we used the raw untransformed data and fitted the GLMMs using a Gamma distribution with a log link. Gamma distributions are appropriate for continuous positive data and allow us to account for the right-skewed nature of chronometric data such as IBT (Lo & Andrews, 2015). Finally, for BD we used the median for each one-minute interval of the experimental sessions and fitted the models using a gaussian distribution with an identity link (i.e., a linear mixed model). All fits and corresponding residuals were visually inspected to verify that assumptions were not violated. Confidence intervals for the fixed effects estimates were calculated using Wald's method, and they were corroborated using parametric bootstrapping and the profile-likelihood based method, obtaining very good agreement in all cases. To assess the effect of time-on-task on the response variables within each experimental condition, the emmeans R library was used to obtain trend estimates of the effect of time within each experimental condition. This library was also used to perform post-hoc pairwise comparisons of marginal means between all experimental conditions at different times in the experiment (minute 0, 15 and 30), with p-values being adjusted for multiplicity using Tukey's method. The significance level was set to 0.05 for all tests performed.

5.3.Results.

To report the results, ambient illuminance will be abbreviated to "A", and mobile phone screen luminance will be shortened to "MP", resulting in four experimental conditions: "High A – Low MP", "High A – High MP", "Low A – High MP", and "Low A – Low MP".

5.3.1. Font size preferences.

In each session participants were given the option to increase or decrease the font size of the text before proceeding with the reading task. Their preferences are shown in Figure 35. Overall, participants kept the default font size (2 mm stroke width) in most conditions, except for the High A – Low MP condition, where the preferred font size increased by almost 1 mm when compared to the High A – High MP condition ($\beta_{HA\text{-}LM} = 0.906$, $t(59) = 7.6$, $p < 0.001$).

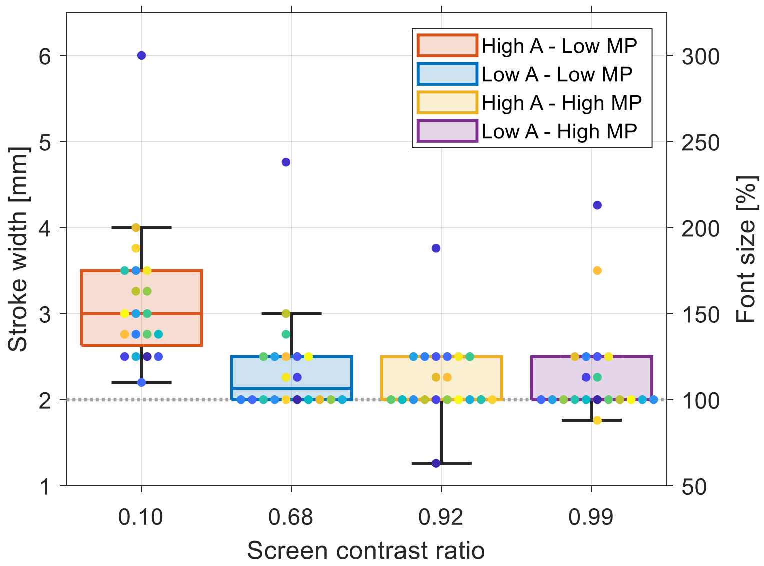

Figure 35. Font sizes selected by participants for each experimental condition. The small markers represent individual data points, with each colour corresponding to one observer. The left ordinate represents the stroke width of the font in millimetres, while the right ordinates represent the font size in percentage as set by the participants, with 100% being the default.

5.3.2. Symptoms Questionnaire.

The results of the Symptoms Questionnaire are illustrated in Figure 36. To analyse the differences in score between the end and start of each experimental condition, a Wilcoxon signed-rank test was performed. Results are shown in Table 15. Overall, there were significant increases in symptom scores for eye tiredness, blurry vision, and eye strain in all conditions, while there were no significant differences in neck and back soreness, and only a significant difference in the Low A – Low MP condition for headache. However, given that 70% of participants reported no difference in in headache in this condition, the latter result can probably be disregarded.

To determine the effect of experimental condition on symptom score increase, we fitted an ordinal logistic regression on the score change values, with fixed-effect predictors of condition, symptom and their interaction, and random effects of participant. The results are shown in Table 16. The intercept of the model was the High A – High MP condition and the blurry vision symptom. As shown the score increase in eye tiredness was worse than in blurry vision in the High A- High MP condition, but no significant interactions between conditions and symptoms were found.

Condition	**Tired eyes**	**Blurry vision**	**Eyestrain**	**Headache**	**Sore neck and back**
High A – Low MP	*0.001*	*0.006*	*0.005*	0.227	0.117
Low A – Low MP	*0.009*	*0.016*	*0.005*	*0.031*	0.273
High A – High MP	*0.001*	*0.047*	*0.020*	0.289	0.063
Low A – High MP	*0.001*	*0.002*	*0.000*	0.148	0.063

Table 15. Wilcoxon signed rank test results for the differences in symptom score between the start and end of the session. The p-values correspond to the null hypothesis that the difference in score comes from a distribution with zero median. Italics represent significance at the 5% level.

Parameter	**Estimate**	**SE**	**z-value**	**p-value**	**RE SD**
condition (HA - LMP)	0.97	0.69	1.39	0.163	1.21
condition (LA - HMP)	0.40	0.85	0.47	0.640	2.55
condition (LA - LMP)	0.40	0.70	0.58	0.563	1.12
Eyestrain	0.58	0.72	0.81	0.418	1.49
Headache	-1.00	0.77	-1.30	0.194	1.75
Sore neck back	-0.59	0.78	-0.76	0.447	1.83
Tired eyes	***1.64***	***0.70***	***2.36***	***0.018***	***1.26***
condition (HA - LMP) * Eyestrain	0.27	0.90	0.30	0.768	-
condition (LA - HMP) * Eyestrain	0.08	0.89	0.09	0.929	-
condition (LA - LMP) * Eyestrain	-0.29	0.90	-0.32	0.748	-
condition (HA - LMP) * Headache	-0.69	0.92	-0.75	0.451	-
condition (LA - HMP) * Headache	-0.20	0.93	-0.22	0.826	-
condition (LA - LMP) * Headache	0.17	0.93	0.19	0.851	-
condition (HA - LMP) * Sore neck back	-0.83	0.94	-0.88	0.377	-
condition (LA - HMP) * Sore neck back	-0.45	0.94	-0.48	0.631	-
condition (LA - LMP) * Sore neck back	-0.78	0.95	-0.82	0.415	-
condition (HA - LMP) * Tired eyes	-0.71	0.90	-0.79	0.432	-
condition (LA - HMP) * Tired eyes	-1.21	0.90	-1.35	0.178	-
condition (LA - LMP) * Tired eyes	-1.37	0.91	-1.51	0.132	-

Table 16. Ordinal logistic regression of symptom score change. Parameter estimates and their standard errors (SE) are shown, as well as z-ratios and p-values, and the random effects

standard deviation (RE SD). The intercept of the model was the High A – High MP condition and the blurry vision symptom

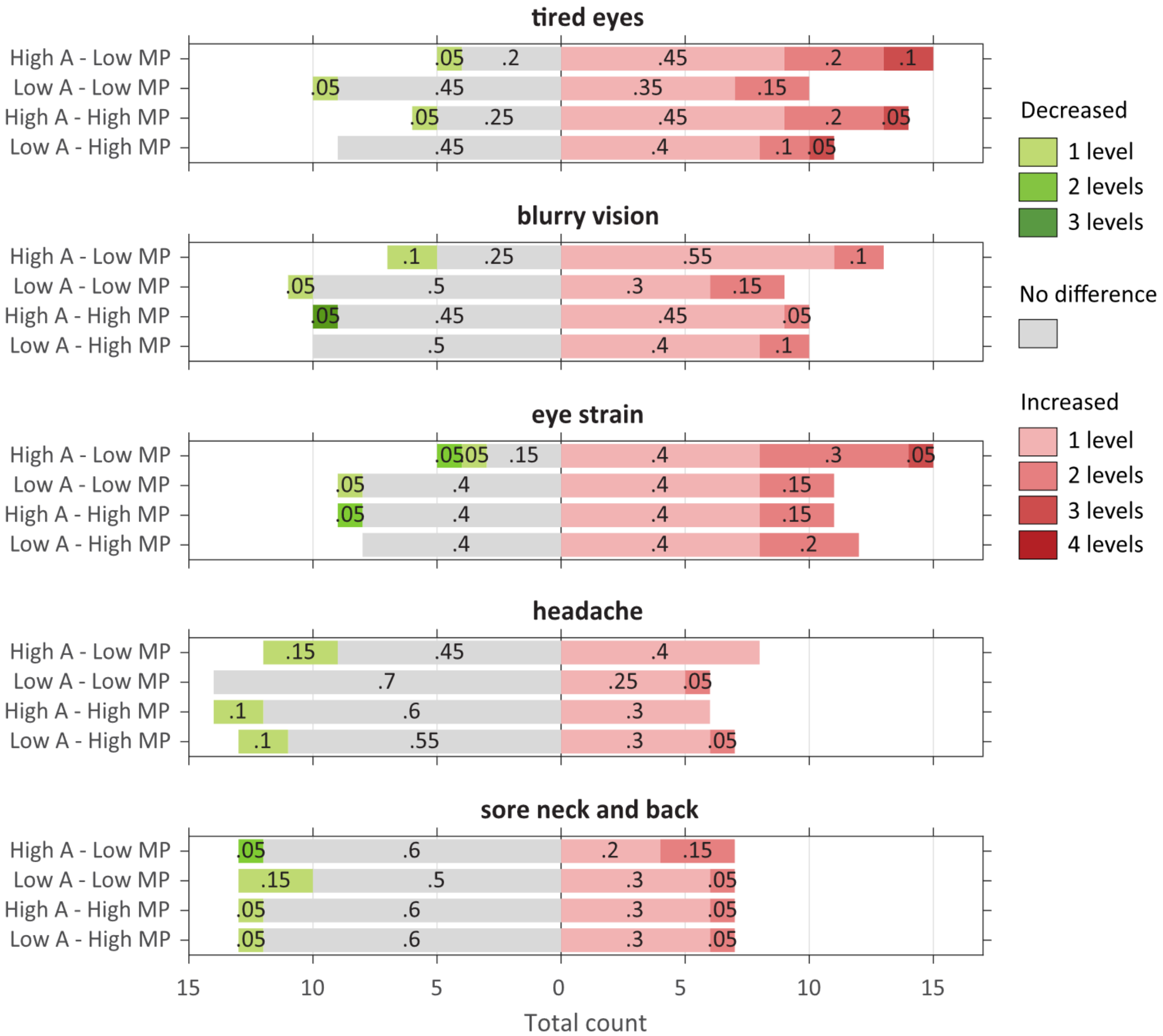

Figure 36. Changes in reported fatigue symptoms between the start and end of the session. The horizontal axis shows the total number of participants that reported either an increase (to the right), no changes or a decrease (to the left) in the severity of the symptoms, while the numbers in the bars show this data as a percentage of the total. The colour of the bars represents of how many levels in the Likert scale was the change in symptom severity.

Post-hoc pairwise comparisons between all pairs of conditions for the score increases of each symptom revealed no significant differences (see Appendix F for full results). No significant differences were found either when averaging across the levels of symptoms and performing pairwise comparisons between conditions. This means that, even twhen taking into account the score changes in all symptoms, the different experimental conditions were not statistically different from eachother.

Qualitatively, however, some trends can be observed in the results shown in Figure 36. The High A – Low MP condition, when compared to the rest, resulted in a larger percentage of increased eyestrain (75% vs 55-60%) and blurry vision (65% vs 45-50%). And both the High A – Low MP and the High A – High MP conditions received a greater proportion of increased eye-tiredness reports (75% and 70%, respectively), when compared to the other two experimental conditions (50-55%).

5.3.3. Sessions Evaluation Questionnaire.

The results of this questionnaire are shown in Figure 37. The High A – Low MP condition received the most votes for fatigue (80%) and eye irritation (50%) and was not selected as their preferred session by any subject. The High A – High MP condition received the second

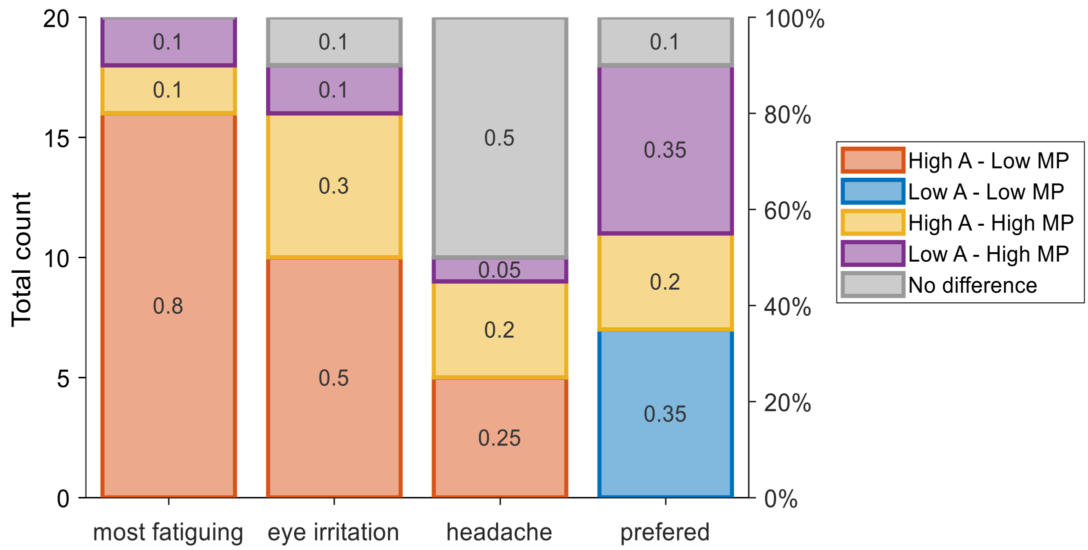

Figure 37. Results of the Sessions Evaluation Questionnaire. Total number of votes received by each experimental condition for: i) being the most fatiguing, ii) causing the most eye irritation, iii) causing the worst headache, and iv) being their preferred session. The left vertical axis represents the total number of votes, while the right vertical axis and the numbers in the bars represent this data as a percentage of the total.

largest proportion of votes for eye irritation (30%) and came in third place as the preferred condition (20%). Most subjects reported no difference between sessions in their headache (50%), with High A – Low MP (25%) and High A – High MP (20%) coming in second and third place, respectively. Low A – High MP and Low A – Low MP received equal number of votes as the preferred session (35%), and interestingly, the latter condition did not receive any votes as being the most fatiguing, causing the most eye irritation or headache.

To analyse this data, we performed an exact multinomial test of goodness-of-fit. If participants were choosing randomly between the options in this survey (i.e., experimental condition did not have an effect in their choice), we would expect a probability of 0.20 for each option in the four questions. Under this assumption, we performed a multinomial goodness of fit test, with the null hypothesis that there is no significant difference between the observed proportion of votes and the expected proportion of votes if participants were choosing randomly (0.20), and the alternative hypothesis that the observed proportion of votes are different from this expected probability. We found significant differences in the most fatiguing, eye irritation and headache questions (p <0.01), thus, we reject the null hypothesis that participants were choosing the options in these questions randomly.

Variable	Condition	Q1	Median	Q2	Mean	SD	SEM
Blink rate [blinks/min]	High A – Low MP	7.61	13.48	30.71	17.98	13.25	3.67
	Low A – Low MP	8.54	21.16	40.29	22.14	15.82	4.39
	High A – High MP	8.48	26.81	34.67	24.85	18.74	5.65
	Low A – High MP	9.23	20.47	29.56	20.60	13.00	3.60
Blink duration [ms]	High A – Low MP	256.3	290.4	323.7	289.5	37.1	10.3
	Low A – Low MP	258.5	278.1	299.4	275.2	35.2	9.8
	High A – High MP	255.4	304.1	314.9	286.4	40.7	12.3
	Low A – High MP	264.6	304.9	320.7	293.1	48.3	13.4
Interblink time [s]	High A – Low MP	1.61	4.18	7.50	5.92	5.69	1.58
	Low A – Low MP	1.24	2.43	7.20	5.13	5.14	1.42
	High A – High MP	1.49	2.05	6.01	5.05	5.67	1.71
	Low A – High MP	1.65	2.27	6.27	5.52	6.42	1.78

Table 17. Summary statistics of the blinking measures for each experimental condition. The median, lower, and upper quartiles (Q1, Q3), mean, standard deviation (SD), and standard error of the mean (SEM) is shown. The data used is the mean blink rate, mean blink duration and mean interblink time per participant and condition.

To determine which answer within these questions significantly deviated from the expected proportion, we performed a post-hoc exact binomial test. Within each of these three questions, we compared the proportion of votes for each option versus the sum of all the other categories, to test which one significantly deviated from the expected ratio (0.2:0.8).

We found that, after significance values were corrected for multiplicity of testing, one option within each of these questions significantly deviated from the expected proportion of votes: the High A – Low MP condition as the most fatiguing (p <0.001, 0.8 proportion of votes, 95% CI from 0.56 to 0.94), the High A – Low MP condition as the most eye irritating (p <0.001, 0.5 proportion of votes, 95% CI from 0.27 to 0.73), and the "no difference" option in the headache question (p <0.001, 0.5 proportion of votes, 95% CI from 0.27 to 0.73). Thus, we can conclude that the High A – Low MP condition was chosen as the most fatiguing and as causing the most eye irritation at a proportion significantly higher than if the options of the survey were chosen at random.

5.3.4. Blink rate.

Summary statistics of blink rate (BR), as well as blink duration (BD) and interblink time (IBT) are provided Table 17. The distributions of BR for each condition and the within-participant mean BR and standard deviation are shown in Figure 38. As expected, there are large idiosyncratic differences in the average BR among participants, as well as variation in the effect caused by each experimental condition.

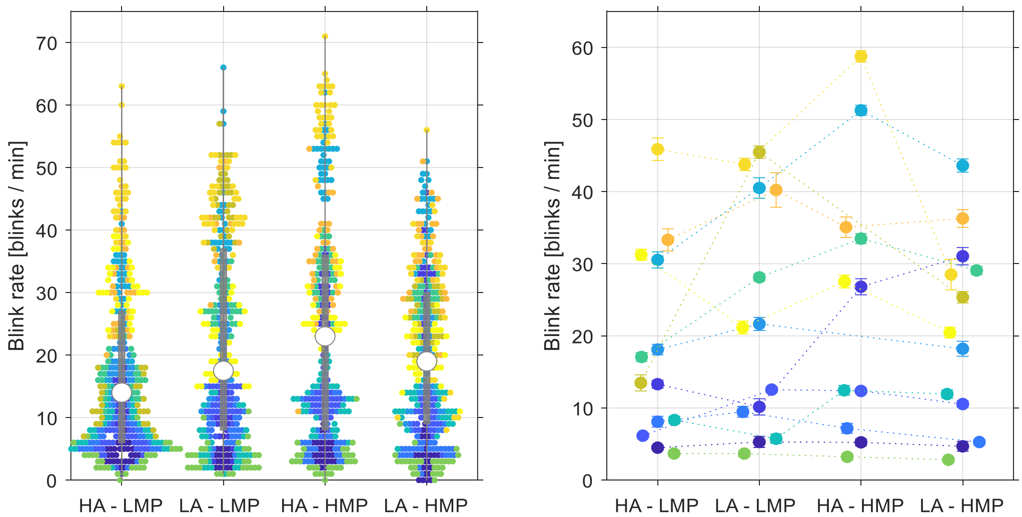

Figure 38. Blink rates for each experimental condition. The left panel shows the distribution of the number of blinks for each minute of the session, with each colour representing one participant. The right panel shows the within-participant mean blink rate and standard error of the mean.

To account for these differences, we fitted two linear mixed models: a reduced model with the experimental condition as a categorical fixed effect, and a more complex model that also included time-on-task and its interaction with the experimental condition as predictor. Results from the LRT and AIC comparison indicated that the second model had greater predictive power (χ^2 (4) = 9.58, p = 0.048; ΔAIC=1.6). The estimated coefficients of this model, as well as confidence intervals, z-values and standard deviations of the random effects are shown in Table 18.

Time-on-task had a negative effect on BR in most of the experimental conditions, with 15 minutes spent on the task causing a decrease of 0.60 blinks/minute in the High A – High MP condition (95% CI from 0.00 to 1.20), a decrease of 0.45 blinks/minute in the High A – Low MP condition (95% from CI -0.34 to 1.24), and a decrease of 0.46 blinks/minute in the Low A – Low MP condition (95% CI from -0.39 to 1.31); while on the Low A – High MP condition, BR increased by 0.24 blinks/minute (95% CI from -0.60 to 1.08) for each 15 minutes of time-on-task. However, in all cases the confidence intervals were wide and included zero, indicating considerable uncertainty in these estimates and insufficient evidence to reject the null hypothesis that time-on-task had no effect on BR (p>0.05). The estimated trends of time within condition and corresponding confidence intervals are shown in Figure 41.

	Blink rate [blinks/min]						
Parameters	**Estimate**	**CI 95%**		**SE**	**z-value**	**p-value**	**RE SD**
Intercept	25.44	16.32	34.56	4.65	5.47	<0.001	16.58
condition (HA – LMP)	***-7.46***	***-12.13***	***-2.79***	***2.38***	***-3.13***	***0.002***	***7.95***
condition (LA – HMP)	***-4.88***	***-9.60***	***-0.15***	***2.41***	***-2.02***	***0.043***	***8.09***
condition (LA – LMP)	-3.37	-7.97	1.23	2.35	-1.44	0.151	7.76
Time	-0.60	-1.20	0.00	0.31	-1.95	0.051	-
Time * (HA – LMP)	0.15	-0.64	0.94	0.40	0.36	0.717	-
Time * (LA – HMP)	0.84	0.00	1.68	0.43	1.95	0.051	-
Time * (LA – LMP)	0.14	-0.71	0.99	0.43	0.33	0.742	-

Participants: 13, Observations: 1474

Table 18. Generalized linear mixed model results of blink rate as a function of experimental condition and time-on-task (Poisson distribution, identity link). Parameter estimates, their 95% confidence intervals (CI 95%), standard errors (SE), z-statistics and p-values are shown, as well as the random effects standard deviation (RE SD). The time-on-task predictor was centred at minute 15 of the experiment and scaled from -1 to 1 (i.e., one unit of time-on-task equals 15 minutes). The intercept of the model is the HA – HMP condition and minute 15 of the experiment. Parameters in bold italics represent significance at the 0.05 level.

There were, however, significant differences between experimental conditions. The highest BR was found in the High A – High MP condition, with an estimate of 25.44 blinks/minute (95% CI from 16.32 to 34.56) at the halfway point of the session (15 minutes). Compared with this condition, BR was significantly reduced in the High A – Low MP condition by 7.46 blinks/minute (95% CI from 2.79 to 12.13, Z = -3.13, p= 0.002), and in the Low A – High MP condition by 4.88 blinks/minute (95% CI from 0.15 to 9.60, Z = -2.02, p= 0.043). The BR in the Low A – Low MP condition was also lower than in the High A – High MP condition by 3.37 blinks/minute, but this difference was not significant (95% CI from -1.23 to 7.97, Z = -1.44, p= 0.151). These differences between conditions remained consistent throughout the duration of the experiment.

5.3.5. Inter-blink time.

The distributions of the log transformed mean IBT for each minute of the experimental conditions for each participant are shown in Figure 39 (left). While for the model fits the unaggregated data were used, here it is displayed in this way to avoid participants with a larger number of observations overtaking the distributions. The within-participants mean log IBT, and corresponding standard errors of the mean are also shown (right).

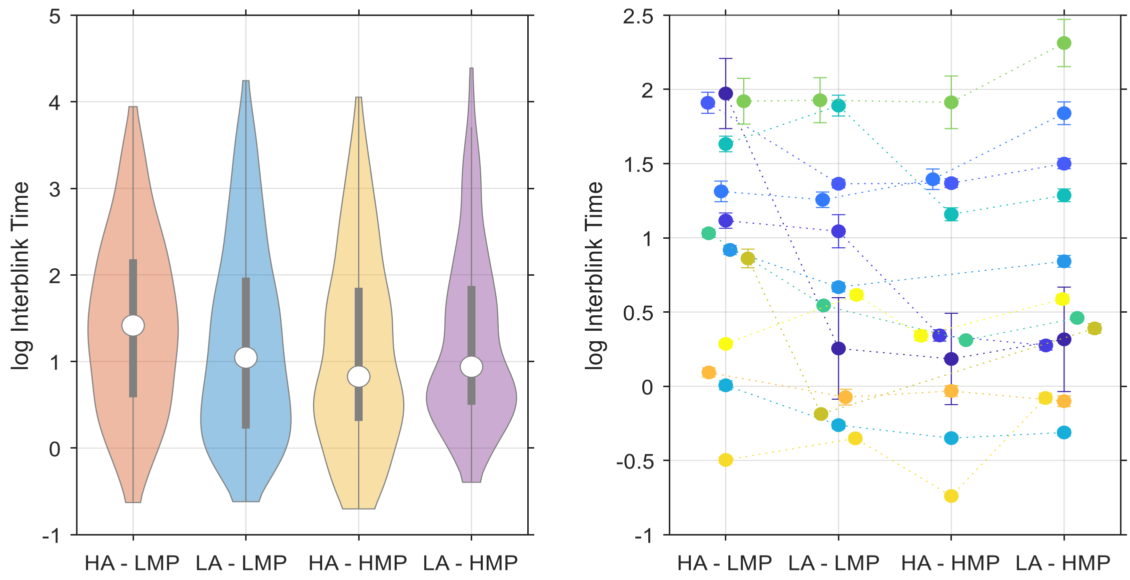

Figure 39. Log transformed interblink times for each experimental condition. The left panel shows the distributions of the mean log-interblink times for each minute of the experimental session. The right panel shows the within-participant mean log-interblink time and standard error of the mean. The data were transformed using natural logarithms, so an IBT of 1 equals 2.7 seconds.

As with the previous response variable, two generalized linear mixed models were fitted. The LRT and AIC comparison showed that the more complex model, with experimental condition, time-on-task, and their interaction as predictors, fitted the data better and had greater predictive power than the simpler model with only experimental condition as a predictor (χ^2 (4) = 14.19, p=0.007; ΔAIC= 6). The results of the full model are shown in Table 19.

In the High A – High MP condition, IBT increased by a rate of 1.03 or 3% for each 15 minutes of time-on-task (95% CI from 1.01 to 1.06, Z = 2.49, p= 0.013); while in the High A – Low MP condition, IBT increased by a rate of 1.04 or 4% for each 15 minutes spent on the task (95% CI from 1.01 to 1.07, Z = 2.61, p= 0.009). Although significant, these effects were small, particularly considering that the experimental sessions had a total duration of 30 minutes. The effects of time on the other two experimental conditions were not significant, with estimated multiplicative changes of 0.98 in the Low A – High MP condition (95% CI from 0.95 to 1.01), and 1.00 in the Low A – Low MP condition (95% CI from 0.97 to 1.03).

	log Interblink time						
Parameters	**Estimates**	**CI 95%**		**SE**	**z-value**	**p-value**	**RE SD**
Intercept	1.02	0.49	1.55	0.27	3.77	<0.001	0.74
condition (HA – LMP)	***0.36***	***0.15***	***0.56***	***0.10***	***3.40***	***0.001***	*0.28*
condition (LA – HMP)	***0.19***	***0.03***	***0.35***	***0.08***	***2.32***	***0.020***	*0.20*
condition (LA – LMP)	0.16	-0.08	0.40	0.12	1.27	0.205	0.33
Time	***0.03***	***0.01***	***0.06***	***0.01***	***2.49***	***0.013***	**-**
Time* (HA – LMP)	0.01	-0.03	0.05	0.02	0.27	0.784	-
Time* (LA – HMP)	***-0.05***	***-0.09***	***-0.01***	***0.02***	***-2.46***	***0.014***	**-**
Time* (LA – LMP)	-0.03	-0.07	0.00	0.02	-1.74	0.082	-
Residual							0.76

Participants: 13, Observations: 30193

Table 19. Generalized linear mixed model results of interblink time as a function of experimental condition and time-on-task (Gamma distribution, log link). Parameter estimates, their 95% confidence intervals (CI 95%), standard errors (SE), z-statistics and p-values are shown, as well as the random effects standard deviation (RE SD). The time-on-task predictor was centred at minute 15 of the experiment and scaled from -1 to 1 (i.e., one unit of time-on-task equals 15 minutes). The intercept of the model is the High A – High MP condition and minute 15 of the experiment. Parameters in bold italics represent significance at the 0.05 level.

When comparing between experimental conditions, we find results consistent with those found in the BR analysis. The lowest IBT was found in the High A – High MP condition, with an estimate of 2.76 seconds at the 15-minute mark of the session (95% CI from 1.63 to 4.69). When compared with this condition, IBT in the High A – Low MP condition was 1.43 times higher (95% CI from 1.16 to 1.75, Z = 3.40, p= 0.001), while in the Low A – High MP condition, it was 1.21 times higher (95% CI from 1.03 to 1.41, Z = 2.33, p= 0.020) at the same 15-minute mark. Due to similar rates of increase in IBT over time, the difference between the High A – High MP and the High A – Low MP condition was maintained constant throughout the experiment. Conversely, due to opposing trends in the effect of time-on-task, the differences in IBT between the High A – High MP condition decreased towards the end of the experimental session. Finally, the IBT in the Low A – Low MP condition was estimated to be 1.17 times higher than in the High A – High MP condition at the 15-minute mark, but this difference was not significant (95% CI from 0.92 to 1.49, Z = 1.27, p= 0.205), and no further differences were found throughout the duration of the experiment.

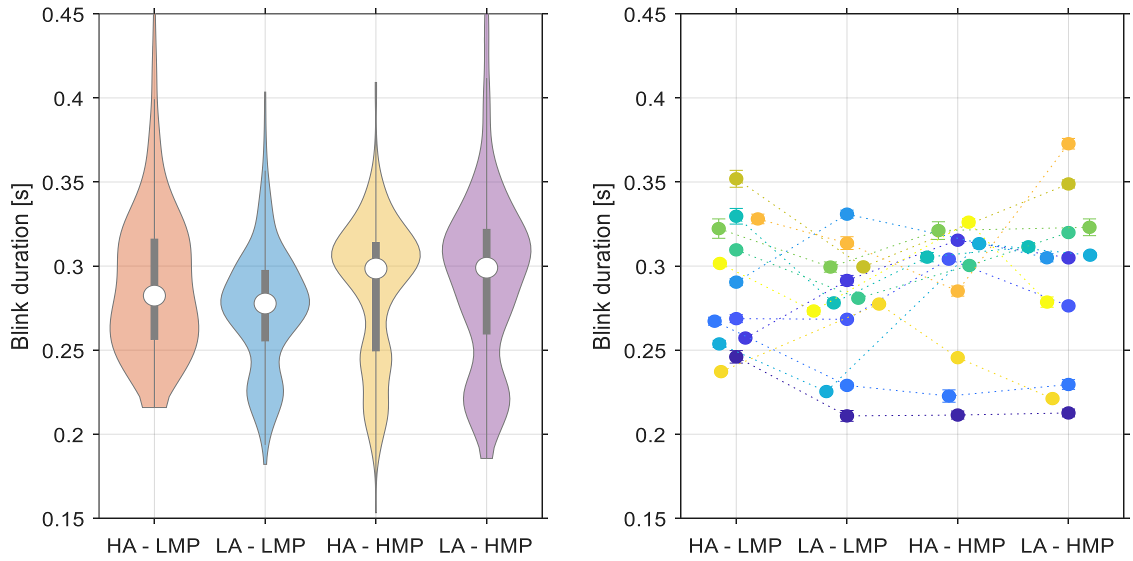

Figure 40. Blink durations for each experimental condition. The left panel shows the distributions of the mean blink duration for each minute of the experimental session for each participant. The right panel shows the within-participant mean blink duration and standard error of the mean.

5.3.6. Blink duration.

The distributions of the mean BD for each minute of the experimental conditions are shown in Figure 40 (left). The data are displayed in this way to avoid participants with a larger number of blinks biasing the distributions. The within-participants mean BD and standard errors of the mean are also shown (right).

As with the previous response variables, two nested mixed effects models were fitted: a reduced model with condition as a categorical predictor, and a full model, with an additional continuous predictor of time-on-task interacting with condition. Results from the AIC comparison and LRT indicated that the more complex model fitted the data better and had greater predictive power ($\chi 2$ (4) = 35.07, p<0.001; ΔAIC= 27). The results of this model fit are presented in Table 20.

	Median Blink Duration [ms]						
Parameters	**Estimates**	**CI 95%**		**SE**	**t-value**	**p-value**	**RE SD**
Intercept	285.63	263.91	307.35	11.08	25.78	<0.001	38.03
condition (HA – LMP)	-1.47	-23.07	20.12	11.02	-0.13	0.896	37.63
condition (LA – HMP)	2.11	-17.63	21.84	10.07	0.21	0.838	33.97
condition (LA – LMP)	-13.05	-31.73	5.63	9.53	-1.37	0.198	31.86
Time	0.52	-2.99	4.02	1.79	0.29	0.773	-
Time * (HA – LMP)	***6.32***	***1.54***	***11.11***	***2.44***	***2.59***	***0.010***	***-***
Time * (LA – HMP)	***5.85***	***0.90***	***10.80***	***2.53***	***2.31***	***0.021***	***-***
Time* (LA – LMP)	-4.86	-9.83	0.11	2.53	-1.92	0.055	-
Residual							19.73
	Participants: 13, Observations: 1467						

Table 20. Linear mixed model fit results of median blink duration as a function of experimental condition and time-on-task. Parameter estimates, their 95% confidence intervals (CI 95%), standard errors (SE), t-values and p-values are shown, as well as the random effects standard deviation (RE SD). The time-on-task predictor was centred at minute 15 of the experiment and scaled from -1 to 1 (i.e., one unit of time-on-task equals 15 minutes). The intercept of the model is the High A – High MP condition and minute 15 of the experiment. Parameters in bold italics represent significance at the 0.05 level.

A significant effect of time was found in three of the experimental conditions, with BD increasing by 6.84 milliseconds per 15 minutes of time-on-task in the High A – Low MP condition (95% CI from 3.57 to 10.11, t(1421) = 4.11, p<0.001), and by 6.37 milliseconds per 15 minutes of time-on-task in the Low A – High MP condition (95% CI from 2.86 to 9.87, t(1422)= 3.56, p<0.001); while in the Low A – Low MP condition BD decreased over time, changing by -4.34 milliseconds per 15 minutes of time-on-task (95% CI from -7.88 to -0.81,

$t(1429)$= -2.41, p= 0.016). No effect of time was found in the High A – High MP condition, and the estimates indicate that median BD remained relatively constant, changing by only 0.52 milliseconds per 15 minutes of time-on-task (95% CI from -2.99 to 4.03).

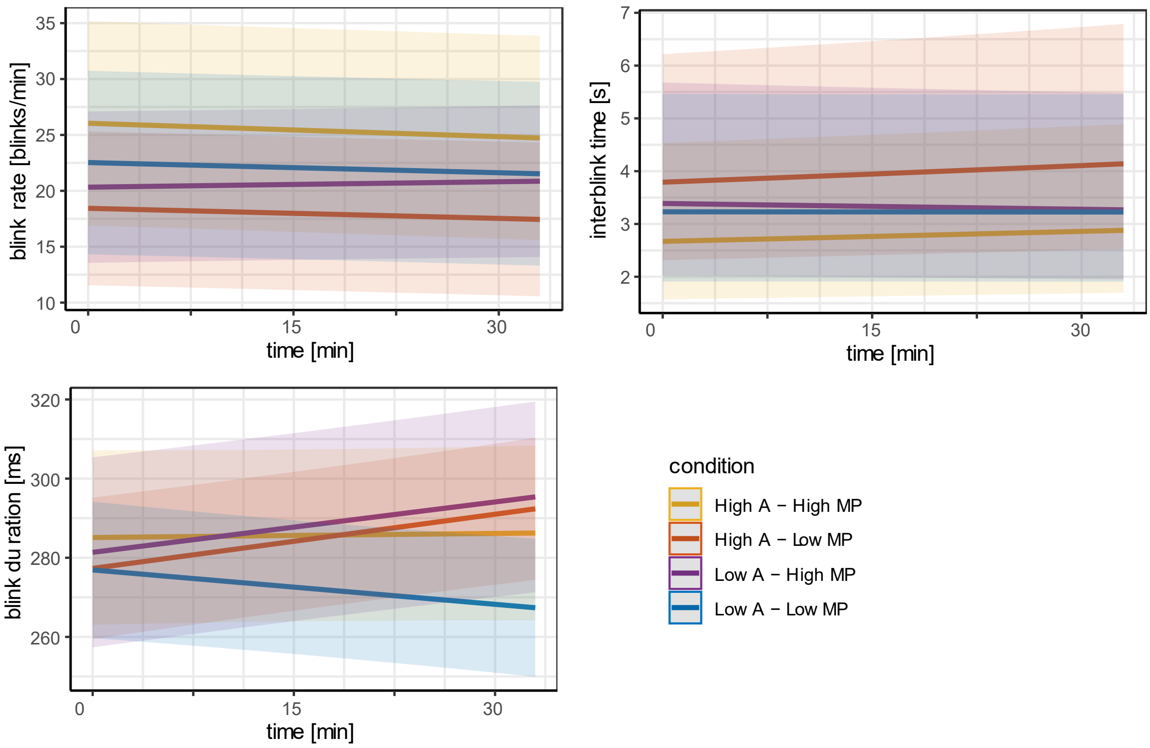

Figure 41. Estimated effects of time-on-task on blink rate (top left), interblink time (top right) and blink duration (bottom left) within each experimental condition. The coloured lines represent the estimated slopes, and the shaded regions, the standard errors of those estimates. The estimates for interblink time have been back transformed to the original response scale.

When comparing between experimental conditions, we see that at the start of the task, BD had similar values in the range of 277-285 ms in all conditions; while at the end of the 30-minute task, BD was lower in the Low A – Low MP condition with an estimate of 268 ms (95% CI from 249 to 288), and higher in the High A – Low MP condition and Low A – High MP condition, with estimates of 291 ms (95% CI from 271 to 311) and 294 ms (95% CI from 267 to 321), respectively. Although these differences were only significant at the 0.10 level, if the task continued for a longer period and the observed effects of time-on-task were maintained, these differences in median BD would become larger.

5.4.Discussion.

In this study we aimed to assess the effect that ambient illuminance and screen luminance have on blinking activity and subjective symptoms of visual discomfort, particularly in mobile displays. The experiment was designed with an emphasis on reproducing conditions as close to real life as possible: participants could hold and position the smartphone display freely, head and body movement were unrestricted, and the eye-tracking was performed with a minimally intrusive wearable device. The high ambient illuminance used was similar to outdoor light levels in a typical overcast day, while the low ambient illuminance was comparable to a dim indoor environment (Engineering ToolBox, 2004). Due to the nature of the design, the four experimental conditions differed not only on the manipulated variables, but also on the screen contrast and possible screen reflections; these are factors that would also be present in real life scenarios.

The analysis of the subjective reports of visual fatigue revealed significant increases in eye tiredness, eye strain and blurry vision in all experimental conditions, and no differences in headache and neck and back soreness. The increase in visual discomfort symptoms is consistent with earlier findings in the literature (Jaiswal et al., 2019). Epidemiological research has found a correlation between the duration and frequency of smartphone use and dry eye symptoms (Moon et al., 2014; Kim et al., 2016; Moon et al., 2016), and that symptoms can improve after a four week period of no use (Moon et al., 2016). Two previous studies have also assessed subjective symptoms after 60 minutes of reading on a smartphone. Long et al., (2017) found a significant increase in eye tiredness, eye discomfort, and blurred vision, and no differences in headache, diplopia, or sore eyes. Similarly, Golebiowski et al., (2019) found a significant increase in eye tiredness, eye discomfort, and sleepiness, and no differences in headache, blurred vision, diplopia, or dry eye symptoms. Our study shows that symptoms can appear even after a shorter duration of 30 minutes of reading on a smartphone.

Eye tiredness and eye strain are common asthenopic symptoms associated with CVS, and evidence points to stress in the accommodative and vergence systems induced by sustained near work as the underlying cause (Sheedy et al., 2003). Blurred vision on the other hand, falls into the category of visual symptoms, and together with diplopia and slowness of changing focus, can be considered as visual consequences of the temporary accommodative and vergence dysfunction (Blehm et al., 2005; Gowrisankaran & Sheedy, 2015). Near work in general correlates with an increase in these symptoms (Iribarren et al., 2001), but emissive visual displays have characteristics that seem to exacerbate them (Rosenfield, 2016; Chu et al., 2014). Studies directly comparing tasks performed with printed text and handheld displays have found with the latter, increased eye tiredness (Hue et al., 2014), worst visual fatigue scores (Benedetto et al., 2013), and a reduced accommodative amplitude and increased lag (Park et al., 2014; Hue et al., 2014).

Headache is sometimes included as an asthenopic symptom in the literature (Sheedy et al., 2003; Rosenfield, 2016), but most of our sample reported no increases in this symptom between the start and end of the sessions, which is a common result with two previous studies on smartphone use (Long et al., 2017; Golebiowski et al., 2019). Neck and back soreness are also a commonly reported extraocular symptom of CVS (Blehm et al., 2005; Gowrisankaran & Sheedy, 2015), but no significant increases were found in our study, possibly due to participants being able to adjust the position of the display and their posture freely, or due to the short duration of the task.

When comparing between the experimental conditions, we did not find any significant differences in the symptoms evaluated. This could indicate that indeed, the different conditions had a similar effect on the subjective symptoms experienced, or that, if any differences existed, the questionnaire used was not sensitive enough to capture them. It is not uncommon in the literature however, to find no differences in subjective evaluations of visual fatigue between tasks performed on visual displays under different illumination conditions (Lee et al., 2011), even when objective measures such as blinking rate indicate there is an effect (Benedetto et al., 2014).

Qualitatively, however, some trends could be observed in the subjective reports: a high ambient illuminance paired with a low screen luminance seemed to cause increased eye strain in a greater proportion of participants, while higher median scores of eye tiredness were observed in the two conditions with high ambient illuminance. When asked to compare between conditions in the final session, the high ambient illuminance with low screen luminance was selected at a significantly higher rate as the most fatiguing and causing the most eye irritation and was not selected as the preferred session by any of the subjects.

The analysis of the blinking activity of the subjects revealed significant differences between experimental conditions in blink rate and interblink time. The lowest interblink time and highest blink rate was found in the high ambient illuminance with high screen luminance session. Compared to this condition, blink rate was significantly lower by 7.46 blinks/min and interblink time was higher by 43% in the high ambient illuminance and low screen luminance condition. Similarly, blink rate was also significantly lower in the low ambient illuminance and high screen luminance condition by 4.88 blinks/min and interblink time higher by 21%. No significant differences were found with the low ambient illuminance and low screen luminance condition in pairwise comparisons, although the estimated blink rate was the second highest. The effects of time-on-task on blink rate and interblink time were negligible in all conditions, meaning that these differences in blinking frequency were present since the start of each reading session and remained mostly stable throughout.

Previous studies have found a decrease in blink rate with reduced luminance contrast, both with printed materials (Gowrisankaran et al., 2007) and visual displays (Nahar et al., 2007; Xie et al., 2021), which could explain the increased interblink time found in the high ambient illuminance with low screen luminance condition. Nahar et al. (2007) found a decrease in blink rate of approximately 4 blinks/min when contrast decreased from 40% to 5%. Similarly, Xie et al., (2021) found a decrease of 5.34 blinks/min when screen contrast changed from 0.97 to 0.47, which is comparable to our results of a 7.46 blinks/min decrease between contrasts of 0.92 and 0.10. Some studies have suggested that cognitive load and not screen contrast, is the determining factor in reducing blinking frequency (Gowrisankaran et al., 2012), with other research offering some support for this idea (Rosenfield et al., 2015). In our study however, participants read fictional novels of their choice, which is a task of low cognitive demand and was shared between all conditions; hence, an unlikely explanation for our findings.

Blinking, while having important physiological functions, interrupts the flow of visual information to the retina. To minimize this, the visual system has the ability to control the timing of blinks in in a way that minimizes the loss of relevant information as much as possible (Fogarty & Stern, 1989; Pivik & Dykman, 2004; Shultz et al., 2011). Our capacity to extract visual information in low contrast is greatly reduced, especially high spatial frequency such as text in a small screen. There is existing evidence of spontaneous blink inhibition in the presence of low contrast stimuli, at least in the short term (Bonneh et al., 2016); thus, it is plausible to think that this inhibition could extend to longer periods of time. This experimental condition was also selected as significantly most fatiguing and eye irritating by participants. This is in line with the fact that a reduced blink rate and increased interblink time allows for a greater evaporation of tears, affecting the lubrication of the eye, and leading to symptoms of discomfort such as eye irritation, dryness, and burning sensation (Gowrisankaran & Sheedy, 2015).

Screen contrast might not be the only relevant factor in maximising blinking rates and visual comfort in displays. We also found an increased interblink time and reduced blink rate in the low ambient illuminance and high screen luminance condition, which had the highest screen contrast of all sessions (0.99). Albeit a smaller effect, this result points to more complex interactions that can affect blinking activity. Not many studies have reported the effect of the interactions between display luminance and surrounding illuminance on blinking rate. In a study with a similar two-by-two design to ours, performed in a computer monitor, Benedetto et al. (2014) found a decreased blink rate in the high screen luminance conditions, independent of the ambient illuminance used. It is important to point out however, that the values of ambient illuminance used in this study (5 lux for low and 85 lux for high) are only comparable to our “low” condition (43.57 lux). Thus, these results could be considered to show some agreement with our findings.

Studies evaluating the subjective preference of observers performing different tasks in visual displays have found that an ambient illuminance more closely matching the display is preferred (Sheedy et al., 2005), lower display brightness is favoured in darker environments (Rempel et al., 2009), and both preference and visual acuity increase as contrast increases up to a certain point (8:1), and then decreases for the highest screen contrasts (Wang & Chen, 2000). However, in these studies the intervals of subjective preference are wide (Kim et al., 2017; Sheedy et al., 2005), and some observers always prefer the maximum screen brightness independent of the ambient illumination (Rempel et al., 2009). These latter findings could explain why this condition was selected as the preferred one by 35% of our sample, and further emphasise the need for objective indicators of visual fatigue, in addition to subjective preference evaluations.

The highest blink rate and lowest interblink time was found in the condition with high ambient illuminance and high screen luminance. While a higher frequency of blinking would allow to keep the eye lubricated and avoid dry eye symptoms, this condition was identified as the most eye irritating by 30% of the sample. It is possible that some subjects experience discomfort from reading at such high ambient illuminance conditions, or that other known detrimental factors such as glare (Gowrisankaran & Sheedy, 2015) might have played a role.

When analysing blinking duration, we found significant effects of time-on-task. While at the start of the experimental sessions the median duration of blinks was similar in all experimental conditions, as time spent on the task increased, blink duration significantly increased in the two conditions where blinking frequency was significantly lower (high– low and low – high) by approximately 13 to 14 ms in total. Conversely, median blink duration significantly decreased with time in the condition with low ambient illuminance and low screen luminance by 9 ms in total, and it remained relatively constant in the condition with high ambient illuminance and low screen luminance.

In contrast with blinking frequency, blink duration has not been an indicator widely studied in the CVS literature. This could be due to methodological difficulties, such as using manual methods for counting blinks or using webcam-based methods where the limited frame rate of the camera might make it difficult to detect small changes in blink duration. At least one previous study (Divjak & Bischof, 2009) reported that an increase in blink duration and eyelid closure time of 25 to 40% was present in subjects with reduced blinking frequency (of 40% or more) when performing tasks in a computer monitor; however, their sample size was limited to three subjects. Other studies have reported consistent increases in blink duration with time-on-task regardless of workload or task modality – auditive vs visual – (Stern & Skelly, 1984; Stern et al., 1984); however, in our study we found this effect in only two of the experimental conditions, and the opposite or no effect in the other two.

Blink duration and associated measurements such as eyelid reopening time, have been reported to be reliable indicators of sleepiness and decreased alertness (Stern et al., 1984; Caffier et al., 2003; Ingre et al., 2006; Schleicher et al., 2008), and it is a commonly used metric in practical applications such as the automated detection of drowsiness in drivers (Benedetto et al., 2011). However, in these studies, the increase in blink duration with increasing drowsiness was preceded by an increase in blinking frequency (Stern et al., 1984; Schleicher et al., 2008), which we did not find in our study. The increase in blinking frequency with sleepiness onset has been postulated to be due to the cessation of the attentional inhibition of blinks that is common when performing visual tasks, which then is followed by an significant increase in blink duration as more severe drowsiness develops and physiological processes such as blinking are slowed down (Schleicher et al., 2008). However, in our study, blinking frequency remained constant with time-on-task and it was significantly lower in the two conditions where blinking duration increased, making this an unlikely explanation for our findings. It is possible that an increase in blink duration with time-on-task accompanied by a decrease in blinking frequency could serve as an indicator of visual fatigue or discomfort, particularly as one of these experimental conditions was identified by subjects as the most fatiguing and causing the most eye irritation. Conversely, the condition with low ambient illuminance and low screen luminance, where blink duration decreased over time, was not selected by any of the subjects as the most fatiguing or eye irritating and was preferred by 35% of the sample. However, the lack of previous research on blink duration and CVS and the methodological limitations of our study do not make it possible to derive strong conclusions from these findings.

On a final note, although the effects on blinking frequency and duration reported here were found after taking into account subject variability, the large individual differences in baseline blinking rate are likely to play a role on visual fatigue and other CVS symptoms (Blehm et al., 2005). Furthermore, we also found some variation in the effect that each experimental condition had for each subject, which points to individual factors possibly playing a role in how ambient illuminance and screen luminance affect blinking activity. This highlights the need for further research in this area with larger sample sizes where individual factors such as refractive error, visual correction, baseline pupil size, among others, could also be considered.

In summary, we found that reading on a smartphone for 30 minutes caused a significant increase in eye tiredness, eye strain and blurred vision. Higher interblink times and lower blink rates were found in conditions where screen luminance and ambient illuminance were mismatched, indicating that screen contrast might not be the only relevant factor affecting visual comfort in digital displays. Subjective reports showed no differences between conditions despite the differences in blinking activity found, further emphasizing the importance of objective indicators of visual discomfort, in addition to subjective reports.

Conclusions.

In this thesis we aimed to investigate the way early properties of the human visual system interact with modern display and illumination technologies, and how this affects the quality of the image perceived. Here we offer a summary of our main findings, as well as possible future areas of research.

Modern digital displays are increasingly using narrowband primaries such as lasers and Light Emitting Diodes (LEDs). This allows for a wider colour gamut to be shown as well as higher energy efficiency; however, it is not clear how this might affect our perception, and in particular, our ability to accommodate and keep the image in focus. The Longitudinal Chromatic Aberration (LCA) of the eye is a very important cue to accommodation, but it is not available in light of reduced spectral bandwidth. Furthermore, the evidence on how light of different wavelengths affects the accommodation response is limited in the existing literature. In Chapter 2 we set out to investigate this topic with a set of experiments where we measured pupil and accommodative responses as well as visual acuity under narrowband illuminants of different peak wavelengths. We found that observers were able to accommodate under narrowband light and correct for the LCA of the eye, with no evidence of differences in the variability of the steady-state accommodation response between narrowband and broadband illuminants. Furthermore, the extent to which people compensate for LCA increases at nearer distances, with a larger difference in accommodation to different wavelengths as the object is placed nearer the observer, causing the slope of the accommodation response curve to become shallower for shorter wavelengths and steeper for longer ones. This means that considering wavelength for accommodative demand would be more relevant for visual displays that are used at nearer distances from the eye. It is important to note however, that we found large individual differences in this effect, and it is not completely clear why observers increasingly compensate for LCA with nearer targets. Investigating both the causes of this phenomenon as well as further exploring individual differences could be a relevant future area of research

We also found in these experiments that within the accommodative range of observers, accommodative errors were small and visual acuity normal. When comparing between illuminants, we found that when accommodation was accurate, visual acuity was worst for blue narrowband light. We propose that this is due to LEDs not being completely monochromatic and LCA causing greater defocus at shorter wavelengths. This effect disappears for larger accommodative errors, due to the increased depth-of-focus of the eye.

While under single narrowband illuminants such as those used in Chapter 2, there is one optimal accommodation response that would bring the object into sharp focus, when the illumination is composed by a mixture of two of these illuminants, no such response exists. In Chapter 3 we presented a set of experiments that explored this question. We found that, when presented with mixtures of two narrowband illuminants, observers accommodate at an intermediate point between the two, weighted by their relative luminance. We hypothesised that observers could be either maximising contrast at lower spatial frequencies, even when this is detrimental to contrast at higher spatial frequencies and these higher frequencies are task relevant; or they could be using LCA as a cue to accommodate, maintaining equivalent blur for both illuminants. Further research would be necessary to elucidate the mechanisms behind this response. For practical applications, this means that mixtures of two narrowband illuminants are not optimal for maximising retinal image quality, particularly at high spatial frequencies.

In Chapter 4 we explored the relationship between luminous intensity and the maximum frequency of flicker that can be detected. This relationship defines the limits of the temporal-resolving ability of the human visual system, and characterizing it has important theoretical and practical applications; particularly for determining the optimal refresh rate for visual displays that would avoid the visibility of flicker and other temporal artifacts. Previous research had shown that this relationship is best described by the Ferry-Porter law, which states that critical flicker fusion (CFF) increases as a linear function of log retinal illuminance. The existing experimental data showed this law holds for a wide range of stimuli and up to 10,000 Trolands; however, beyond this, it was not clear if the CFF continued to increase linearly or if the function saturated. Our aim was to extend the experimental data available to higher light intensities than previously reported in the literature. For this, we measured the peripheral CFF at a range of illuminances over six orders of magnitude. Our results showed that up to 10^4 Trolands, the data conformed to the Ferry-Porter law with a similar slope as previously established for this eccentricity; but at higher intensities, the CFF function flattens and saturates at ~ 90 Hz for a target size of 5.7 degrees, and at ~100 Hz for a target of 10 degrees of angular size. These experimental results could prove valuable for the design of brighter visual displays and illumination sources that are temporally modulated.

Finally, in Chapter 5, we explored the effects of ambient illuminance and screen luminance on symptoms of visual discomfort as well as blink patters, which have been used as objective indicators of visual fatigue. We used a two-by-two design with variations in ambient illuminance (high and low) and screen luminance (high and low), with the high ambience illuminance condition being comparable to outdoor illumination levels. Many modern displays such as smartphone screens are increasingly used in outdoor environments, and the research on the effects this can have on visual fatigue is still very limited. To assess these effects, we asked participants to read on a smartphone for 30 minutes while wearing eye-tracking glasses, as well as to give subjective reports of their symptoms. We found that the reading task caused a significant increase in eye tiredness, eyestrain and blurred vision in all conditions between the start and end of the session, but no differences between conditions were found. However, we did find differences in the blinking patterns of observers. Blinking frequency was significantly lower with high ambient illuminance and low screen luminance, which we proposed could be caused by the reduced screen contrast. Blinking frequency was also reduced with low ambient illuminance and high screen luminance, indicating that a mismatch between screen and ambient illumination might also be detrimental for maintaining an adequate blinking activity and eye lubrication. In these two conditions, we also found that blink duration significantly increased over time during the task, while it remained constant or decreased in the other two experimental conditions. It is possible that an increase on blink duration with time spent on the task could serve as another indicator of visual fatigue together with reduced blinking frequency; but further research would be needed to explore this in more depth. Furthermore, the differences found between reported subjective symptoms and blinking activity emphasize the importance of objective indicators of visual discomfort, in addition to subjective reports.

References.

Aggarwala, K R, Kruger, E.S., Mathews, S. & Kruger, P.B. (1995) Spectral bandwidth and ocular accommodation. *Journal of the Optical Society of America. A, Optics, image science, and vision*. 12 (3), 450–5.

Aggarwala, K. R., Nowbotsing, S. & Kruger, P.B. (1995) Accommodation to monochromatic and white-light targets. *Investigative Ophthalmology and Visual Science*. 36 (13), 2695–2705.

Aggarwala, Karan R., Nowbotsing, S. & Kruger, P.B. (1995) Accommodation to monochromatic and white-light targets. *Investigative Ophthalmology and Visual Science*. 36 (13), 2695–2705.

Anton (2022). powerspectrum.m. MATLAB Central File Exchange. Available at: (https://www.mathworks.com/matlabcentral/fileexchange/24227-powerspectrum-m),.

Del Águila-Carrasco, A.J., Kruger, P.B., Lara, F. & López-Gil, N. (2020) Aberrations and accommodation. *Clinical and Experimental Optometry*. 103 (1), 95–103.

Archer, J. (2018) Why Sony's 8K, 10,000-Nit, 85-inch TV Is The Best I've Ever Seen. *Forbes*. 11 January.

Argilés, M., Cardona, G., Pérez-Cabré, E. & Rodríguez, M. (2015) Blink rate and incomplete blinks in six different controlled hard-copy and electronic reading conditions. *Investigative Ophthalmology and Visual Science*. 56 (11), 6679–6685.

Artal, P. (2017) *Handbook of Visual Optics, Volume One Fundamentals and Eye Optics*.

Artal, P., Manzanera, S., Piers, P. & Weeber, H. (2010) Visual effect of the combined correction of spherical and longitudinal chromatic aberrations. *Optics express*. 18 (2), 1637–48.

Atchison, D.A., Strang, N.C. & Stark, L.R. (2004) Dynamic accommodation responses to stationary colored targets. *Optometry and Vision Science*. 81 (9), 699–711.

Banks, M.S., Akeley, K., Hoffman, D.M. & Girshick, A.R. (2008) Consequences of incorrect focus cues in stereo displays. *Information Display*. 24 (7), 10–14.

Banks, M.S., Hoffman, D.M., Kim, J. & Wetzstein, G. (2016) 3D Displays. *Annual Review of Vision Science*. 2 (1), 397–435.

Barten, P.G.J. (2009) *Contrast Sensitivity of the Human Eye and Its Effects on Image Quality*.

Bates, D., Mächler, M., Bolker, B. & Walker, S. (2015) Fitting Linear Mixed-Effects Models Using lme4. *Journal of Statistical Software*. 67 (1), .

Bedford, R.E. & Wyszecki, G. (1957) Axial Chromatic Aberration of the Human Eye. *Journal of the Optical Society of America*. 47 (6), 2–3.

Benedetto, S., Carbone, A., Drai-Zerbib, V., Pedrotti, M. & Baccino, T. (2014) Effects of luminance and illuminance on visual fatigue and arousal during digital reading. *Computers in Human Behavior*. 41112–119.

Benedetto, S., Drai-Zerbib, V., Pedrotti, M., Tissier, G. & Baccino, T. (2013) E-readers and visual fatigue Kevin Paterson (ed.). *PLoS ONE*. 8 (12), 6–13.

Benedetto, S., Pedrotti, M., Minin, L., Baccino, T., Re, A. & Montanari, R. (2011) Driver workload and eye blink duration. *Transportation Research Part F: Traffic Psychology and Behaviour*. 14 (3), 199–208.

Bharadwaj, S.R., Sravani, N.G., Little, J.-A., Narasaiah, A., Wong, V., Woodburn, R. & Candy, T.R. (2013) Empirical variability in the calibration of slope-based eccentric photorefraction. *Journal of the Optical Society of America. A, Optics, image science, and vision*. 30 (5), 923–31.

Blehm, C., Vishnu, S., Khattak, A., Mitra, S. & Yee, R.W. (2005) Computer vision syndrome: A review. *Survey of Ophthalmology*. 50 (3), 253–262.

Bobier, W.R., Campbell, M.C.W. & Hinch, M. (1992) The influence of chromatic aberration on the static accommodative response. *Vision Research*. 32 (5), 823–832.

Bonneh, Y.S., Adini, Y. & Polat, U. (2016) Contrast sensitivity revealed by spontaneous eyeblinks: Evidence for a common mechanism of oculomotor inhibition. *Journal of Vision*. 16 (7), 1–15.

Branch, O.V. & Arsenal, E. (1986) Biological Cybernetics of Human Visual Accommodation Inputs _ ~ Error Feedback. *Biological Cybernetics*. 194189–194.

Brindley, G.S. (1964) *Physiology of the Eye*. Vol. 49.

Brooke, R.T. (1951) The variation of critical fusion frequency with brightness of various retinal locations. *Journal of the Optical Society of America*. 41 (12), 1010–1022.

Byung-Wook, K. (2022) [CES 2022] Samsung, LG TVs clash again at CES. *The Korean Herald*. 3 January.

Caffier, P.P., Erdmann, U. & Ullsperger, P. (2003) Experimental evaluation of eye-blink parameters as a drowsiness measure. *European Journal of Applied Physiology*. 89 (3–4), 319–325.

Campbell, F.W. (1960) Correlation of Accommodation between the Two Eyes. *Journal of the Optical Society of America*. 50 (7), 1038–1038.

Campbell, F.W. & Gubisch, R.W. (1967) The effect of chromatic aberration on visual acuity. *The Journal of Physiology*. 192 (2), 345–358.

Campbell, F.W. & Westheimer, G. (1960) Dynamics of accommodation responses of the human eye. *Journal of Physiology*. 151285–295.

Campbell, F.W. & Westheimer, G. (1959) Factors influencing accommodation responses of the human eye. *Journal of the Optical Society of America*. 49 (6), 568–571.

Campbell, F.W.W. (1957) The Depth of Field of the Human Eye. *Optica Acta: International Journal of Optics*. 4 (4), 157–164.

Cardona, G., García, C., Serés, C., Vilaseca, M. & Gispets, J. (2011) Blink rate, blink amplitude, and tear film integrity during dynamic visual display terminal tasks. *Current Eye Research*. 36 (3), 190–197.

Charman, W.N. (1989) Accommodation performance for chromatic displays. *Ophthalmic and Physiological Optics*. 9 (March), 459–463.

Charman, W.N. & Heron, G. (1988) Fluctuations in accommodation: a review. *Ophthalmic and Physiological Optics*. 8 (2), 153–164.

Charman, W.N. & Tucker, Jill (1978) Accommodation and color. *Journal of the Optical Society of America*. 68 (4), 459.

Charman, W.N. & Tucker, J. (1978) Accommodation as a function of object form. *Optometry and Vision Science*. 55 (2), 84–92.

Charman, W.N. & Tucker, J. (1977) Dependence of accommodation response on the spatial frequency spectrum of the observed object. *Vision Research*. 17 (1), 129–139.

Chen, Y. (2020) *JBD Showcases Micro LED Display with 3 Million Nits Brightness for AR/VR Applications*. [Online] [online]. Available from: https://www.ledinside.com/news/2020/1/microled_jbd_highbrightness (Accessed 18 June 2022).

Cho, P., Sheng, C., Chan, C., Lee, R. & Tam, J. (2000) Baseline blink rates and the effect of visual task difficulty and position of gaze. *Current Eye Research*. 20 (1), 64–70.

Cholewiak, S.A., Love, G.D. & Banks, M.S. (2018) Creating correct blur and its effect on accommodation. *Journal of Vision*. 18 (9), 1–29.

Cholewiak, S.A., Love, G.D., Srinivasan, P.P., Ng, R. & Banks, M.S. (2017) Chromablur: Rendering Chromatic Eye Aberration Improves Accommodation and Realism. *ACM Transactions on Graphics*. 36 (6), 1–12.

Christensen RHB (2019) *ordinal—Regression Models for Ordinal Data*.

Chu, C.A., Rosenfield, M. & Portello, J.K. (2014) Blink patterns: Reading from a computer screen versus hard copy. *Optometry and Vision Science*. 91 (3), 297–302.

Day, M., Strang, N.C., Seidel, D., Gray, L.S. & Mallen, E.A.H. (2006) Refractive group differences in accommodation microfluctuations with changing accommodation stimulus. *Ophthalmic and Physiological Optics*. 26 (1), 88–96.

DeHoog, E. & Schwiegerling, J. (2007) Position of White Light Best Focus in the Human Eye. *Invest. Ophthalmol. Vis. Sci.* 48 (5), E-Abstract 993.

Divjak, M. & Bischof, H. (2009) Eye blink based fatigue detection for prevention of computer vision syndrome. *Proceedings of the 11th IAPR Conference on Machine Vision Applications, MVA 2009*. 350–353.

Domenech, B., Segui, M.M., Capilla, P. & Illueca, C. (1994) Variation of the visual acuity-luminance function with background colour. *Ophthalmic and Physiological Optics*. 14 (3), 302–305.

Donohoo, D.T. (1985) *Accommodation With Displays Having Color Contrast*. [Online].

Al Enezi, J., Revell, V., Brown, T., Wynne, J., Schlangen, L. & Lucas, R. (2011) A 'melanopic' spectral efficiency function predicts the sensitivity of melanopsin photoreceptors to polychromatic lights. *Journal of Biological Rhythms*. 26 (4), 314–323.

Engineering ToolBox (2004) *Illuminance - Recommended Light Level*. [Online] [online]. Available from: https://www.engineeringtoolbox.com/light-level-rooms-d_708.html.

Feil, M., Moser, B. & Abegg, M. (2017) The interaction of pupil response with the vergence system. *Graefe's Archive for Clinical and Experimental Ophthalmology*. 255 (11), 2247–2253.

Fernandez-Alonso, M., Kaspiris-Rousellis, C., Innes, W. & Read, J.C.A. (2020) Assessment of Psychophysical Methods for Measuring the Critical Flicker Fusion Frequency in Yes / No Tasks. *Proceedings of the European Light Field Imaging Workshop*. 2–6.

Fernandez, E.J., Suchkov, N. & Artal, P. (2020) Adaptation to the eye's chromatic aberration measured with an adaptive optics visual simulator. *Optics Express*. 28 (25), 37450.

Fincham, E.F. (1953) Defects of the colour-sense mechanism as indicated by the accommodation reflex. *The Journal of Physiology*. 3 (121), 570–580.

Fincham, E.F. (1951) The Accommodation Reflex and its Stimulus. *The British journal of ophthalmology*. 35 (7), 381–393.

Fincham, E.F. & Walton, J. (1957) The reciprocal actions of accommodation and convergence. *The Journal of Physiology*. 137 (3), 488–508.

Fisher, S.K. & Ciuffreda, K.J. (1988) Accommodation and apparent distance. *Perception*. 17 (5), 609–621.

Flitcroft, D.I. (1990) A neural and computational model for the chromatic control of accommodation. *Visual neuroscience*. 5 (6), 547–55.

Fogarty, C. & Stern, J.A. (1989) Eye movements and blinks: their relationship to higher cognitive processes. *International Journal of Psychophysiology*. 8 (1), 35–42.

Freudenthaler, N., Neuf, H., Kadner, G. & Schlote, T. (2003) Characteristics of spontaneous eyeblink activity during video display terminal use in healthy volunteers. *Graefe's Archive for Clinical and Experimental Ophthalmology*. 241 (11), 914–920.

Ghahghaei, S., Reed, O., Candy, T.R. & Chandna, A. (2019) Calibration of the PlusOptix

PowerRef 3 with change in viewing distance, adult age and refractive error. *Ophthalmic and Physiological Optics*. 39 (4), 253–259.

Golebiowski, B., Long, J., Harrison, K., Lee, A., Chidi-, N., Asper, L., Golebiowski, B., Long, J., Harrison, K., Lee, A., Chidi-, N., Golebiowski, B., Long, J., Harrison, K., Lee, A., Chidi-egboka, N., Asper, L., Chidi-, N., Asper, L., et al. (2019) Smartphone Use and Effects on Tear Film, Blinking and Binocular Vision. *Current Eye Research*. 00 (00), 1–7.

Gowrisankaran, S., Nahar, N.K., Hayes, J.R. & Sheedy, J.E. (2012) Asthenopia and blink rate under visual and cognitive loads. *Optometry and Vision Science*. 89 (1), 97–104.

Gowrisankaran, S. & Sheedy, J.E. (2015) Computer vision syndrome: A review. *Work*. 52 (2), 303–314.

Gowrisankaran, S., Sheedy, J.E. & Hayes, J.R. (2007) Eyelid squint response to asthenopia-inducing conditions. *Optometry and Vision Science*. 84 (7), 611–619.

Hamer, R.D. & Tyler, C.W. (1992) Analysis of visual modulation sensitivity V Faster visual response for G- than for R-cone pathway? *Journal of the Optical Society of America A*. 9 (11), 1889.

Hecht, S., Verrijp, C.C.D., Selig Hecht & Verrijp, C.C.D. (1933) Intermittent stimulation by light: IV. A theoretical interpretation of the quantitative data of flicker. *The Journal of general physiology*. 17 (2), 269–282.

Hecht, S. & Verrijp, C.D. (1933) Intermittent stimulation by light III. the relation between intensity and critical fusion frequency for different retinal locations. *The Journal of general physiology*. 17 (2), 251–268.

Held, R.T., Cooper, E.A. & Banks, M.S. (2012) Blur and Disparity Are Complementary Cues to Depth. *Current Biology*. 22 (5), 426–431.

Himebaugh, N.L., Begley, C.G., Bradley, A. & Wilkinson, J.A. (2009) Blinking and tear break-up during four visual tasks. *Optometry and Vision Science*. 86 (2), E106–E114.

Hoffman, D.M., Girshick, A.R. & Banks, M.S. (2008) Vergence–accommodation conflicts hinder visual performance and cause visual fatigue. *Journal of Vision*. 8 (3), 1–30.

Howard, I.P. (2012) *Perceiving in Depth: Basic Mechanisms - Volume 1*.

Hue, J.E., Rosenfield, M. & Saá, G. (2014) Reading from electronic devices versus hardcopy text. *Work*. 47 (3), 303–307.

Ingre, M., Åkerstedt, T., Peters, B., Anund, A. & Kecklund, G. (2006) Subjective sleepiness, simulated driving performance and blink duration: Examining individual differences. *Journal of Sleep Research*. 15 (1), 47–53.

Iribarren, R., Fornaciarr, A. & Hung, G.K. (2001) Effect of cumulative nearwork on accommodative facility and asthenopia. *International Ophthalmology*. 24 (4), 205–212.

Ivanoff, A. (1949) Focusing Wave-Length for White Lgith. *Journal of the Optical Society of America*. 39 (8), 718.

Jaiswal, S., Asper, L., Long, J., Lee, A., Harrison, K. & Golebiowski, B. (2019) Ocular and visual discomfort associated with smartphones , tablets and computers: what we do and do not know. *Clinical and Experimental Optometry*. (September), 463–477.

Jaskulski, M., Marín-Franch, I., Bernal-Molina, P., López-Gil, N. & T (2016) The effect of longitudinal chromatic aberration on the lag of accommodation and depth of field. *Ophthalmic and Physiological Optics*. 36 (6), 657–663.

Kassner, M., Patera, W. & Bulling, A. (2014) 'Pupil: An open source platform for pervasive eye tracking and mobile gaze-based interaction', in *UbiComp 2014 - Adjunct Proceedings of the 2014 ACM International Joint Conference on Pervasive and Ubiquitous Computing*. [Online]. 2014 New York, New York, USA: Association for Computing Machinery, Inc. pp. 1151–1160.

Kim, Joowon, Hwang, Y., Kang, S., Kim, M., Kim, T.S., Kim, Jay, Seo, J., Ahn, H., Yoon, S., Yun, J.P., Lee, Y.L., Ham, H., Yu, H.G. & Park, S.K. (2016) Association between Exposure to Smartphones and Ocular Health in Adolescents. *Ophthalmic Epidemiology*. 23 (4), 269–276.

Kim, S.-R., Lee, S.-H., Jeon, D.-H., Kim, J.-S. & Lee, S.-W. (2017) Optimum display luminance dependence on ambient illuminance. *Optical Engineering*. 56 (1), 017110.

Kim, T., Park, J., Lee, S. & Bovik, A.C. (2014) 3D Visual discomfort prediction based on physiological optics of binocular vision and foveation. *2014 Asia-Pacific Signal and Information Processing Association Annual Summit and Conference, APSIPA 2014*. 8 (3), 415–427.

Kingdom, F.A.A.K. & Prins, N. (2016) *Psychophysics: A practical introduction*. Second Edi. Elsevier.

Kleiner, M., Brainard, D. and Pelli, D. (2007) What's new in Psychtoolbox-3? Perception ECVP Abstract Supplement. *PLOS ONE.* (36), .

Kotulak, J.C., Morse, S.E. & Billock, V.A. (1995) Red-green opponent channel mediation of control of human ocular accommodation. *The Journal of Physiology*. 482 (3), 697–703.

Kotulak, J.C. & Schor, C.M. (1986a) Temporal variations in accommodation during steady-state conditions. *Journal of the Optical Society of America A*. 3 (2), 223.

Kotulak, J.C. & Schor, C.M. (1986b) The accommodative response to subthreshold blur and to perceptual fading during the Troxler phenomenon. *Perception*. 15 (1), 7–15.

Krinov, E.L. (1947) Spectral reflectance properties of natural formations. *Tech. Translation TT-439*.

Kruger, P. & Pola, J. (1986) Stimuli for accommodation: Blur, chromatic aberration and size. *Vision Research*. 26 (6), 957–971.

Kruger, P.B., Aggarwala, K.R., Bean, S. & Mathews, S. (1997) Accommodation to stationary and moving targets. *Optometry and vision science : official publication of the American Academy of Optometry*. 74 (7), 505–510.

Kruger, P.B., Mathews, S., Aggarwala, K.R. & Sanchez, N. (1993) Chromatic Aberration and Ocular Focus: Fincham Revisited. *Vision Research*. 33 (10), 1397–1411.

Kruger, P.B., Mathews, S., Aggarwala, K.R., Yager, D. & Kruger, E.S. (1995) Accommodation responds to changing contrast of long, middle and short spectral-waveband components of the retinal image. *Vision Research*. 35 (17), 2415–2429.

Kruger, P.B., Nowbotsing, S., Aggarwala, K.R. & Mathews, S. (1995) Small amounts of chromatic aberration influence dynamic accommodation. *Optometry & Vision Science*. 72 (9), 656–666.

Labhishetty, V., Cholewiak, S.A., Roorda, A. & Banks, M.S. (2021) Lags and leads of accommodation in humans: Fact or fiction? *Journal of vision*. 21 (3), 21.

Lee, D.S., Ko, Y.H., Shen, I.H. & Chao, C.Y. (2011) Effect of light source, ambient illumination, character size and interline spacing on visual performance and visual fatigue with electronic paper displays. *Displays*. 32 (1), 1–7.

Lee, J.H., Stark, L.R., Cohen, S. & Kruger, P.B. (1999) Accommodation to static chromatic simulations of blurred retinal images. *Ophthalmic and Physiological Optics*. 19 (3), 223–235.

Lenth, R. V. (2021) *emmeans: Estimated Marginal Means, aka Least-Squares Means R package version*.

Lo, S. & Andrews, S. (2015) To transform or not to transform: using generalized linear mixed models to analyse reaction time data. *Frontiers in Psychology*. 6 (August), 1–16.

Long, J., Cheung, R., Duong, S., Paynter, R. & Asper, L. (2017) Viewing distance and eyestrain symptoms with prolonged viewing of smartphones. *Clinical and Experimental Optometry*. 100 (2), 133–137.

Lovasik, J. & Kergoat, H. (1988) Accommodative Performance for Chromatic displays. *Ophthalmic and Physiological Optics*. 8 (April), 443–449.

Lovasik, J. V & Kergoat, H. (1988) The effect of optical defocus on the accommodative accuracy for chromatic displays. *Ophthalmic and Physiological Optics*. 8 (4), 450–457.

MacKenzie, K.J., Hoffman, D.M. & Watt, S.J. (2010) Accommodation to multiple-focal-plane displays: Implications for improving stereoscopic displays and for accommodation control. *Journal of Vision*. 10 (8), 1–20.

MacKenzie, K.J. & Watt, S.J. (2010) 'Eliminating accommodation-convergence conflicts in stereoscopic displays: Can multiple-focal-plane displays elicit continuous and consistent vergence and accommodation responses?', in *Stereoscopic Displays and Applications XXI*. [Online]. 2010 p. 752417.

Marcos, S., Moreno, E. & Navarro, R. (1999) The depth-of-field of the human eye from objective and subjective measurements. *Vision Research*. 39 (12), 2039–2049.

Marg, E. & Morgan, M.W. (1950) Further investigation of the pupillary near reflex: The effect of accommodation, fusional convergence and the proximity factor on pupillary diameter. Optometry and Vision Science 27 (5) p.217–225.

Marg, E. & Morgan, M.W. (1949) The pupillary near reflex: The relation of pupillary diameter to accommodation and the various components of convergence. *Optometry and Vision Science*. 26 (5), 183–198.

Marimont, D.H. & Wandell, B.A. (1994) Matching color images: the effects of axial chromatic aberration. *Journal of the Optical Society of America A*. 11 (12), 3113–3112.

Marran, L. & Schor, C.M. (2000) 'Binocular accommodation', in O. Franzén, H. Richter, & L. Stark (eds.) *Accommodation and Vergence Mechanisms in the Visual System*. [Online]. Basel: Birkhäuser. pp. 245–256.

Mather, G. & Smith, D.R.R. (2002) Blur discrimination and its relation to blur-mediated depth perception. *Perception*. 31 (10), 1211–1219.

McLellan, J.S., Marcos, S., Prieto, P.M. & Burns, S.A. (2002) Imperfect optics may be the eye's defence against chromatic blur. *Nature*. 417 (6885), 174–176.

Mon-Williams, M. & Tresilian, J.R. (2000) Ordinal depth information from accommodation? *Ergonomics*. 43 (3), 391–404.

Moon, J.H., Kim, K.W. & Moon, N.J. (2016) Smartphone use is a risk factor for pediatric dry eye disease according to region and age: A case control study. *BMC Ophthalmology*. 16 (1), 1–7.

Moon, J.H., Lee, M.Y. & Moon, N.J. (2014) Association between video display terminal use and dry eye disease in school children. *Journal of Pediatric Ophthalmology and Strabismus*. 51 (2), 87–92.

Morrison, G. (2018) *TVs are only getting brighter, but how much light is enough?* [Online] [online]. Available from: https://www.cnet.com/tech/home-entertainment/tvs-are-only-getting-brighter-but-how-much-light-is-enough/ (Accessed 18 June 2022).

Muggeo, V.M.R. (2003) Estimating regression models with unknown break-points. *Statistics in Medicine*. 22 (19), 3055–3071.

Muggeo, V.M.R. (2017) Interval estimation for the breakpoint in segmented regression: a smoothed score-based approach. *Australian and New Zealand Journal of Statistics*. 59 (3), 311–322.

Nahar, N.K., Sheedy, J.E. & Hayes, J. (2007) Objective Measurements of Lower-Level. *Optometry and Vision Science*. 84 (7), 620–629.

Nakatsuka, C., Hasebe, S., Nonaka, F. & Ohtsuki, H. (2003) *Accommodative Lag Under Habitual Seeing Conditions : Comparison Between Adult Myopes and Emmetropes*. 5155 (03), .

Nielsen, P.K., Søgaard, K., Skotte, J. & Wolkoff, P. (2008) Ocular surface area and human eye blink frequency during VDU work: The effect of monitor position and task. *European Journal of Applied Physiology*. 103 (1), 1–7.

Nicolas P. Cottaris, Haomiao Jiang, Xiaomao Ding, Brian A. Wandell, David H. Brainard; A computational-observer model of spatial contrast sensitivity: Effects of wave-front-based optics, cone-mosaic structure, and inference engine. Journal of Vision 2019;19(4):8. doi: 10.1167/19.4.8.

Niwa, K. & Tokoro, T. (1998) Influence of Spatial Distribution with Blur on Fluctuations in Accommodation. *Optometry and Vision Science*. 75 (3), 227–232.

Nutting, P.G. (1914) Axial chromatic aberration of the human eye. *Proceedings of the Royal Society of London. Series A, Containing Papers of a Mathematical and Physical Character*. 47 (6), 440–443.

O'Neill, W.D. & Stark, L. (1968) Triple-function ocular monitor. *Journal of the Optical Society of America*. 58 (4), 570–573.

Ofcom (2018) *A decade of digital dependency*. [Online] [online]. Available from: https://www.ofcom.org.uk/about-ofcom/latest/features-and-news/decade-of-digital-dependency (Accessed 5 February 2020).

Ofcom (2019) *Communications Market Report (CMR) 2019*. CMR08 (August).

Owens, D.A. (1980) A comparison of accommodative responsiveness and contrast sensitivity for sinusoidal gratings. *Vision Research*. 20 (2), 159–167.

Park, M., Ahn, Y.J., Kim, S.J., You, J., Park, K.E. & Kim, S.R. (2014) Changes in Accommodative Function of Young Adults in their Twenties following Smartphone Use. *Journal of Korean Ophthalmic Optics Society*. 19 (2), 253–260.

Phillips, N.J., Winn, B. & Gilmartin, B. (1992) Absence of pupil response to blur-driven accommodation. *Vision Research*. 32 (9), 1775–1779.

Pivik, R.T. & Dykman, R.A. (2004) Endogenous eye blinks in preadolescents: Relationship to information processing and performance. *Biological Psychology*. 66 (3), 191–219.

Plainis, S., Ginis, H.S. & Pallikaris, A. (2005) The effect of ocular aberrations on steady-state errors of accommodative response. *Journal of Vision*. 5 (5), 7.

Portello, J.K., Rosenfield, M. & Chu, C.A. (2013) Blink rate, incomplete blinks and computer vision syndrome. *Optometry and Vision Science*. 90 (5), 482–487.

Prins, N. & Kingdom, F.A.A. (2018) Applying the model-comparison approach to test specific research hypotheses in psychophysical research using the Palamedes toolbox. *Frontiers in Psychology*. 9 (JUL), .

R Core Team (2021) *R: A Language and Environment for Statistical Computing*.

Ravikumar, S., Akeley, K. & Banks, M.S. (2011) Creating effective focus cues in multi-plane 3D displays. *Optics Express*. 19 (21), 20940.

Read, J.C.A. (2012) Visual perception: Understanding visual cues to depth. *Current Biology*. 22 (5), R163–R165.

Rempel, A.G., Heidrich, W., Li, H. & Mantiuk, R. (2009) Video viewing preferences for HDR displays under varying ambient illumination. *Proceedings - APGV 2009: Symposium on Applied Perception in Graphics and Visualization*. 1 (212), 45–52.

Rosenfield, M. (2016) Computer vision syndrome (a.k.a. digital eye strain). *Optometry in Practice*. 17 (1), 1–10.

Rosenfield, M., Jahan, S., Nunez, K. & Chan, K. (2015) Cognitive demand, digital screens and blink rate. *Computers in Human Behavior*. 51 (PA), 403–406.

Rucker, F.J. & Kruger, P.B. (2006) Cone contributions to signals for accommodation and the relationship to refractive error. *Vision Research*. 46 (19), 3079–3089.

Rucker, F.J. & Kruger, P.B. (2004) The role of short-wavelength sensitive cones and chromatic aberration in the response to stationary and step accommodation stimuli. *Vision Research*. 44 (2), 197–208.

Schleicher, R., Galley, N., Briest, S. & Galley, L. (2008) Blinks and saccades as indicators of fatigue in sleepiness warnings: Looking tired? *Ergonomics*. 51 (7), 982–1010.

Schlote, T., Kadner, G. & Freudenthaler, N. (2004) Marked reduction and distinct patterns of eye blinking in patients with moderately dry eyes during video display terminal use. *Graefe's Archive for Clinical and Experimental Ophthalmology*. 242 (4), 306–312.

Seidemann, A. & Schaeffel, F. (2002) Effects of longitudinal chromatic aberration on accommodation and emmetropization. *Vision Research*. 42 (21), 2409–2417.

Sheedy, J.E., Hayes, J. & Engle, J.O.N. (2003) *Is all Asthenopia the Same ?* 80 (11), 732–739.

Sheedy, J.E., Smith, R. & Hayes, J. (2005) Visual effects of the luminance surrounding a computer display. *Ergonomics*. 48 (9), 1114–1128.

Shibata, T., Kim, J., Hoffman, D.M. & Banks, M.S. (2011) The zone of comfort: Predicting visual discomfort with stereo displays. *Journal of vision*. 11 (8), 1–29.

Shultz, S., Klin, A. & Jones, W. (2011) Inhibition of eye blinking reveals subjective perceptions of stimulus salience. *Proceedings of the National Academy of Sciences of the United States of America*. 108 (52), 21270–21275.

Sivak, J.G. & Millodot, M. (1974) Axial Chromatic Aberration of Eye With Achromatizing Lens. *J Opt Soc Am*. 64 (12), 1724–1725.

Spector, R.H. (1990) 'The Pupils', in HK Walker, WD Hall, & JW Hurst (eds.) *Clinical Methods: The History, Physical, and Laboratory Examinations*. 3rd edition [Online]. Boston: Butterworths. pp. 300–304.

Spitschan, M. (2019a) Melanopsin contributions to non-visual and visual function. *Current Opinion in Behavioral Sciences*. 30 (Figure 1), 67–72.

Spitschan, M. (2019b) Photoreceptor inputs to pupil control. *Journal of Vision*. 19 (9), 1–5.

Sravani, N.G., Nilagiri, V.K. & Bharadwaj, S.R. (2015) Photorefraction estimates of refractive power varies with the ethnic origin of human eyes. *Scientific reports*. 57976.

Stakenburg, M. (1991) Accommodation without pupillary constriction. *Vision Research*. 31 (2), 267–273.

Stark, L.R. & Atchison, D.A. (1997) Pupil size, mean accommodation response and the fluctuations of accommodation. *Ophthalmic and Physiological Optics*. 17 (4), 316–323.

Stark, L.R., Lee, R.S., Kruger, P.B., Rucker, F.J. & Ying Fan, H. (2002) Accommodation to simulations of defocus and chromatic aberration in the presence of chromatic misalignment. *Vision Research*. 42 (12), 1485–1498.

Stern, J.A. & Skelly, J.J. (1984) *THE EYE BLINK AND WORKLOAD CONSIDERATIONS*. 942–944.

Stern, J.A., Walrath, L.C. & Goldstein, R. (1984) The Endogenous Eyeblink. Psychophysiology 21 (1) p.22–33.

Stockman, A., Jägle, H., Pirzer, M. & Sharpe, L.T. (2008) The dependence of luminous efficiency on chromatic adaptation. *Journal of Vision*. 8 (16), 1–26.

Stone, D., Mathews, S. & Kruger, P.B. (1993) Accommodation and chromatic aberration: effect of spatial frequency. *Ophthalmic and Physiological Optics*. 13 (3), 244–252.

Suchkov, N., Fernández, E.J. & Artal, P. (2019) Impact of longitudinal chromatic aberration on through-focus visual acuity. *Optics Express*. 27 (24), 35935.

The MathWorks Inc. (2019) *MATLAB R2019a version 9.6*.

Thibos, L.N., Bradley, A. & López-Gil, N. (2013) Modelling the impact of spherical aberration on accommodation. *Ophthalmic and Physiological Optics*. 33 (4), 482–496.

Thibos, L.N., Ye, M., Zhang, X. & Bradley, A. (1992) The chromatic eye: a new reduced-eye model of ocular chromatic aberration in humans. *Applied Optics*. 31 (19), 3594–3600.

Toates, F.M. (1972) Accommodation Function of the Human Eye. *Physiological Reviews*. 52 (4), 642–652.

Tucker, J. & Charman, W.N. (1987) Effect of Target Content At Higher Spatial Frequencies on the Accuracy of the Accommodation Response. *Ophthalmic and Physiological Optics*. 7 (2), 137–142.

Tucker, J. & Charman, W.N. (1975) THE DEPTH-OF-FOCUS OF THE HUMAN EYE FOR SNELLEN LETTERS. *Optometry and Vision Science*. 52 (1), 3–21.

Tucker, J., Charman, W.N. & Ward, P.A. (1986) Modulation dependence of the accommodation response to sinusoidal gratings. *Vision Research*. 26 (10), 1693–1707.

Tyler, C.W. (1985) Analysis of visual modulation sensitivity II Peripheral retina and the role of photoreceptor dimensions. *Journal of the Optical Society of America A*. 2 (3), 393.

Tyler, C.W. (1987) Analysis of visual modulation sensitivity III. Meridional variations in peripheral flicker sensitivity. *Optical Society of America*. 4 (8), 1612–1619.

Tyler, C.W. (1989) 'The Full Range of Human Temporal Resolution', in *Human Vision, Visual Processing, and Digital Display*. [Online]. 1989 p. 93.

Tyler, C.W. & Hamer, R.D. (1990) Analysis of visual modulation sensitivity IV Validity of the Ferry–Porter law. *Journal of the Optical Society of America A*. 7 (4), 743.

Tyler, C.W. & Hamer, R.D. (1993) Eccentricity and the Ferry–Porter law. *Journal of the Optical Society of America A*. 10 (9), 2084.

Wald, G. & Griffing, D.R. (1947) The change in refractive power of the human eye in dim and bright light. *Journal of the Optical Society of America*. 37 (5), 321–336.

Wang, A.H. & Chen, M. Te (2000) Effects of polarity and luminance contrast on visual performance and VDT display quality. *International Journal of Industrial Ergonomics*. 25 (4), 415–421.

Wang, B. & Ciuffreda, K.J. (2006) Depth-of-focus of the human eye: Theory and clinical implications. *Survey of Ophthalmology*. 51 (1), 75–85.

Ward, P.A. (1987) A Review of Some Factors Affecting Accommodation. *Clinical & Experimental Optometry*. 7023–32.

Ward, P.A. & Charman, W.N. (1985) Effect of pupil size on steady state accommodation. *Vision Research*. 25 (9), 1317–1326.

van der Wildt, G.J. & Bouman, M.A. (1971) An Accommodometer: an Apparatus for Measuring the Total Accommodation Response of the Human Eye. *Applied Optics*. 10 (8), 1950.

Williams, D., Yoon, G.-Y., Porter, J., Guirao, A., Hofer, H. & Cox, I. (2000) Visual Benefit of Correcting Higher Order Aberrations of the eye. *Journal of Refractive Surgery*. 16 (October 2000), 1–7.

Wilson, B.J., Decker, K.E. & Roorda, A. (2002) Monochromatic aberrations provide an odd-error cue to focus direction. *Journal of the Optical Society of America. A, Optics, image science, and vision*. 19 (5), 833–839.

Wilson, D. (1973) A centre for accommodative vergence motor control. *Vision Research*. 13

(12), 2491–2503.

Xie, X., Song, F., Liu, Y., Wang, S. & Yu, D. (2021) Study on the effects of display color mode and luminance contrast on visual fatigue. *IEEE Access*. 935915–35923.

Yao, P., Lin, H., Huang, J., Chu, R. & Jiang, B.C. (2010) Objective depth-of-focus is different from subjective depth-of-focus and correlated with accommodative microfluctuations. *Vision Research*. 50 (13), 1266–1273.

Yoon, G.-Y.G.-Y. & Williams, D.R. (2002) Visual performance after correcting the monochromatic and chromatic aberrations of the eye. *Journal of the Optical Society of America A: Optics and Image Science, and Vision*. 19 (2), 266–275.

Appendix A. Accommodation response curves for individual participants.

In this section, we present the accommodation response curves of individual participants in the three experiments described in Chapter 2. The first three figures present the accommodation response as a function of the distance in dioptres, while the last three figures show the accommodation response as a function of the accommodative demand, which is calculated as the sum of the distance of the target in dioptres and the defocus that the LCA causes for the peak wavelength of the illuminant.

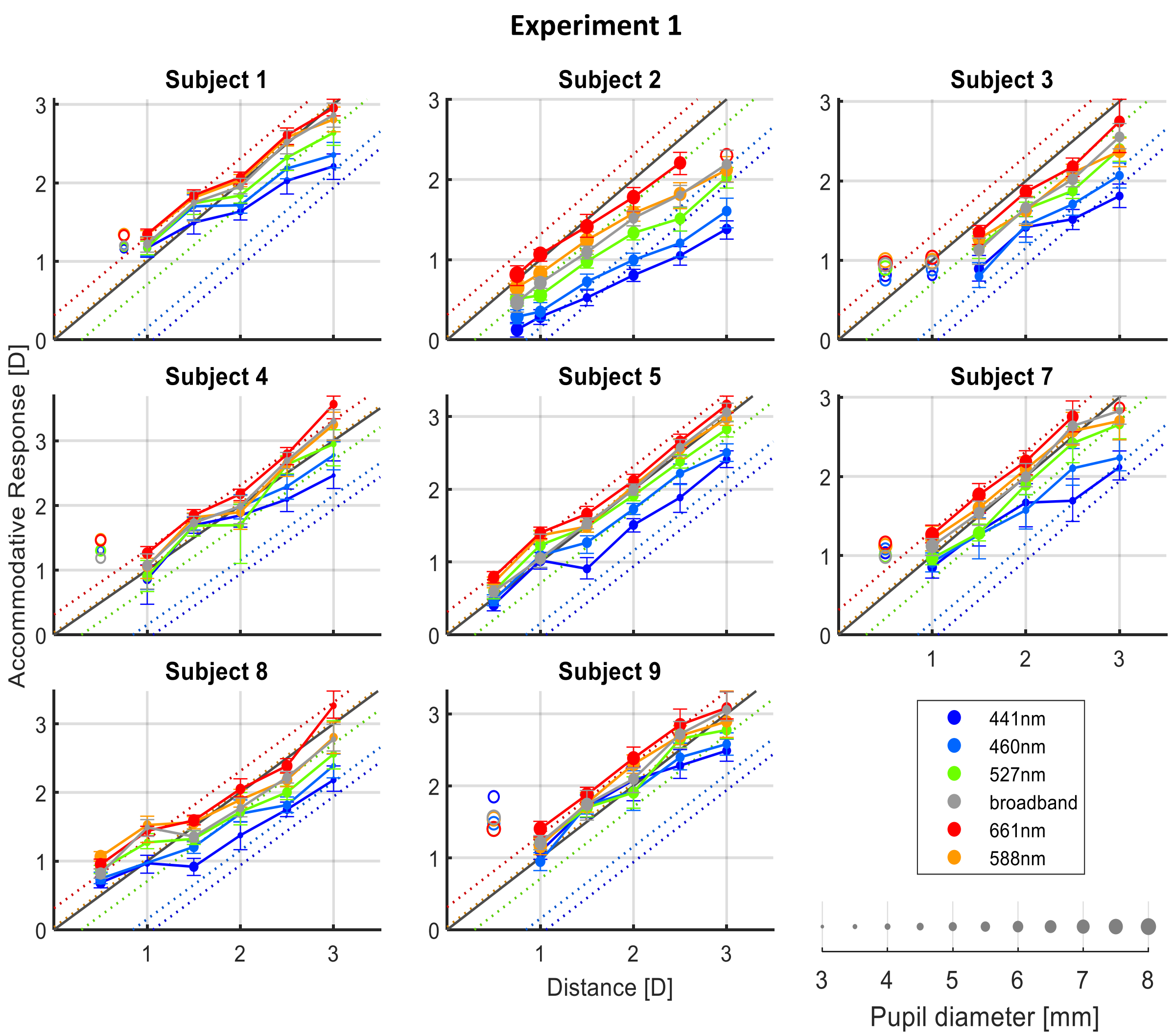

Figure 42. Median accommodation response as a function of distance for individual participants of experiment 1. Each colour represents one illuminant, and the marker sizes represent the median pupil size for each distance and illuminant. The error bars represent the 25th and 75th percentiles of the accommodation response. The filled markers and continuous lines represent the portion of the response curve deemed to be linear, while the unconnected open markers with no error bars represent the portions of the curve identified as saturated. The continuous grey line represents the one-to-one response, while the dotted coloured lines represent the one-to-one response corrected by the LCA defocus for the peak wavelength of each illuminant.

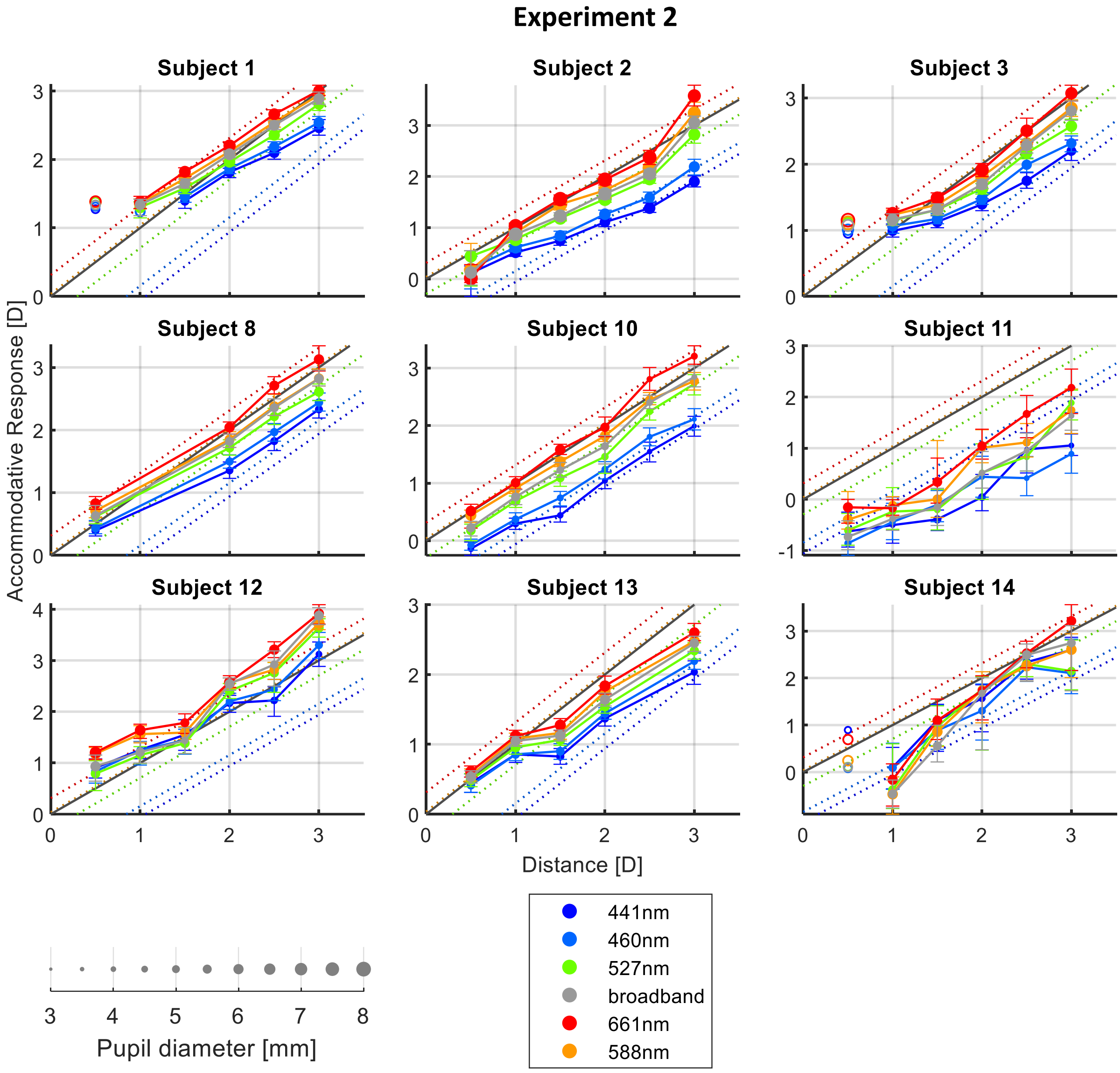

Figure 43. Median accommodation response as a function of distance for individual participants of experiment 2. Each colour represents one illuminant, and the marker sizes represent the median pupil size for each distance and illuminant. The error bars represent the 25th and 75th percentiles of the accommodation response. The filled markers and continuous lines represent the portion of the response curve deemed to be linear, while the unconnected open markers with no error bars represent the portions of the curve identified as saturated. The continuous grey line represents the one-to-one response, while the dotted coloured lines represent the one-to-one response corrected by the LCA defocus for the peak wavelength of each illuminant.

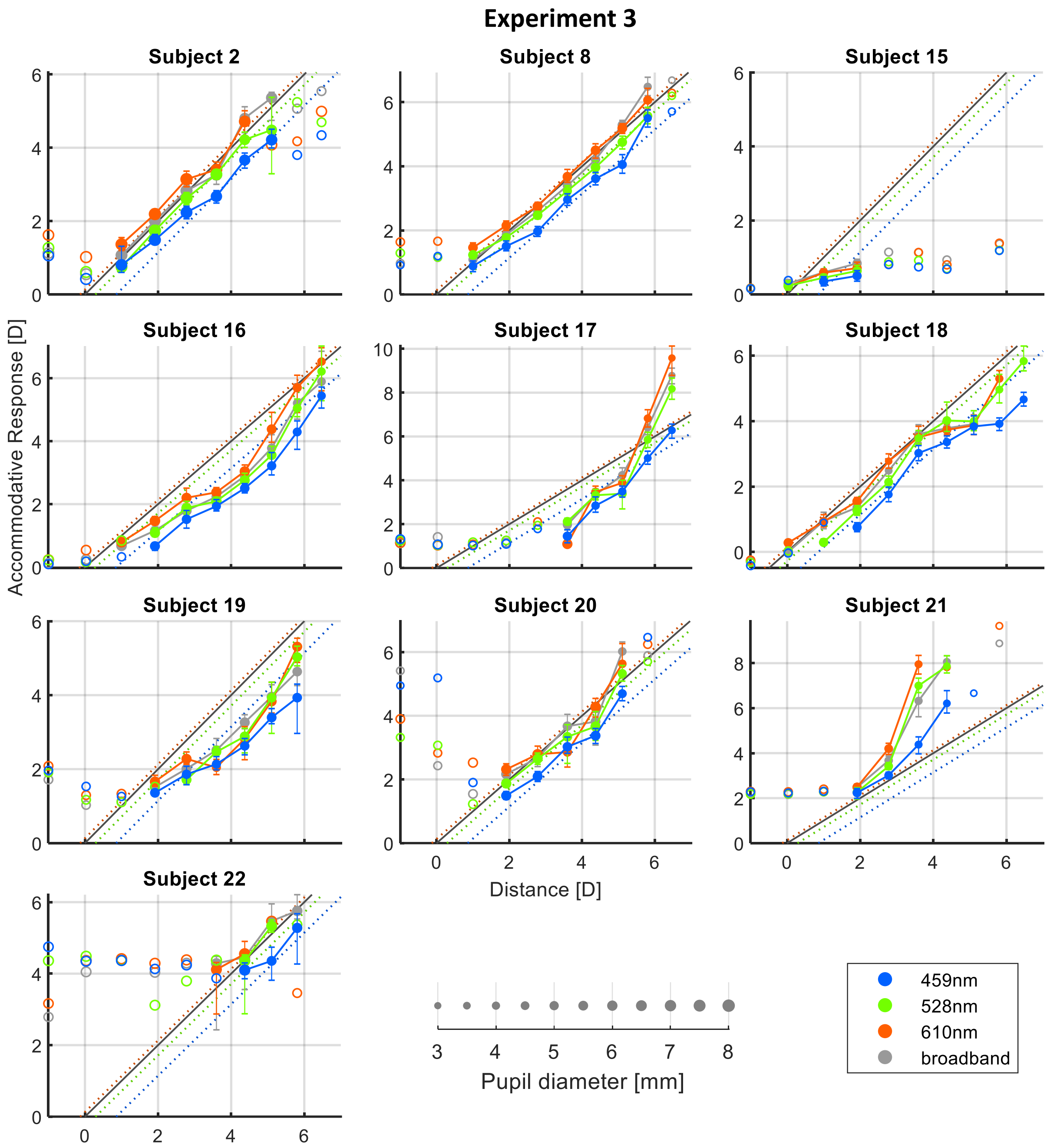

Figure 44. Median accommodation response as a function of distance for individual participants of experiment 3. Each colour represents one illuminant, and the marker sizes represent the median pupil size for each distance and illuminant. The error bars represent the 25th and 75th percentiles of the accommodation response. The filled markers and continuous lines represent the portion of the response curve deemed to be linear, while the unconnected open markers with no error bars represent the portions of the curve identified as saturated. The continuous grey line represents the one-to-one response, while the dotted coloured lines represent the one-to-one response corrected by the LCA defocus for the peak wavelength of each illuminant.

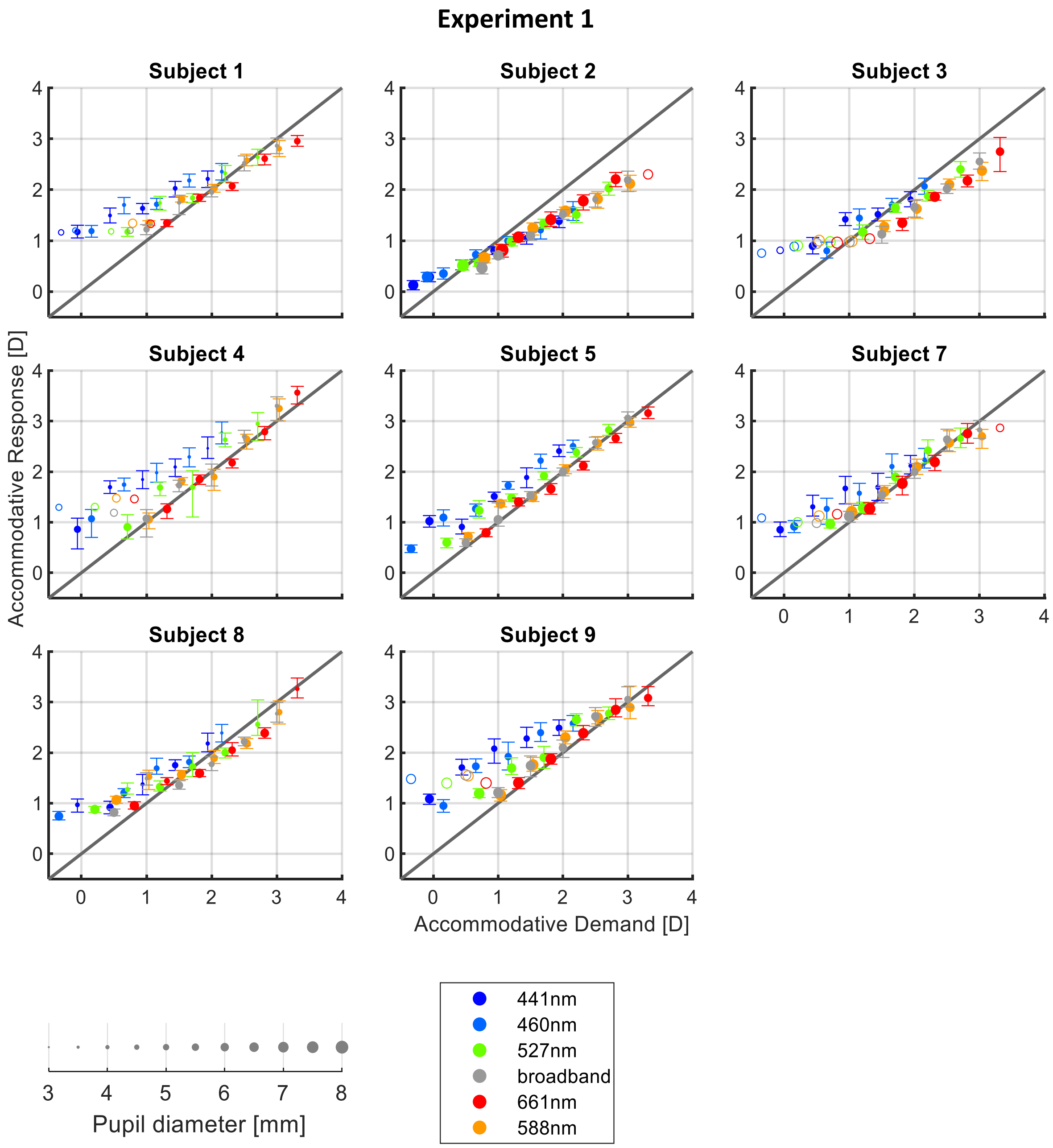

Figure 45. Median accommodation response as a function of the accommodative demand for individual participants of experiment 1. Each colour represents one illuminant, and the marker sizes represent the median pupil size for each distance and illuminant. The error bars represent the 25th and 75th percentiles of the accommodation response. The filled markers represent the portion of the response curve deemed to be linear, while the open markers with no error bars represent the portions of the curve identified as saturated. The continuous grey line represents the one-to-one or ideal response for all the illuminants.

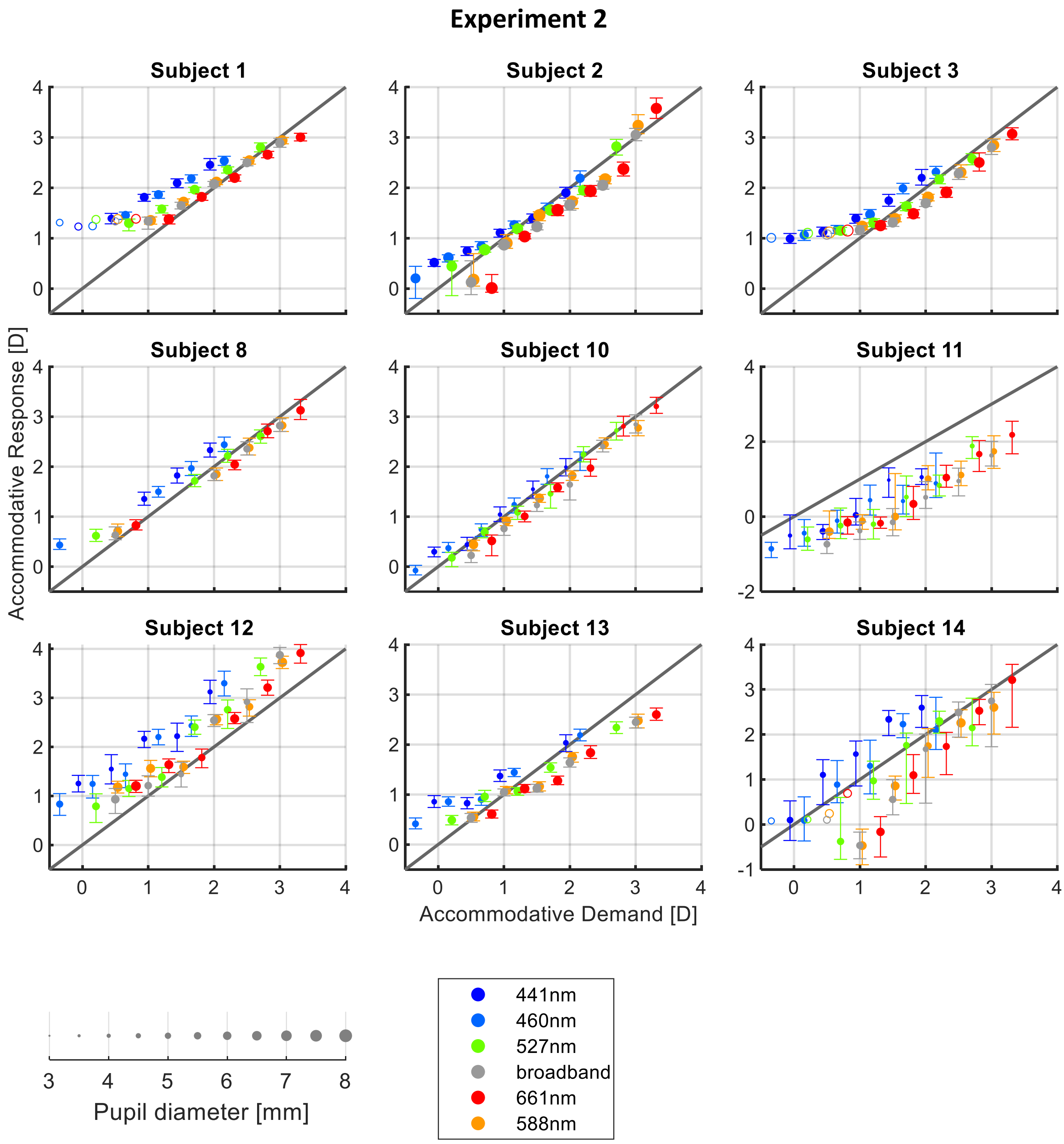

Figure 46. Median accommodation response as a function of the accommodative demand for individual participants of experiment 2. Each colour represents one illuminant, and the marker sizes represent the median pupil size for each distance and illuminant. The error bars represent the 25th and 75th percentiles of the accommodation response. The filled markers represent the portion of the response curve deemed to be linear, while the open markers with no error bars represent the portions of the curve identified as saturated. The continuous grey line represents the one-to-one or ideal response for all the illuminants.

Experiment 3

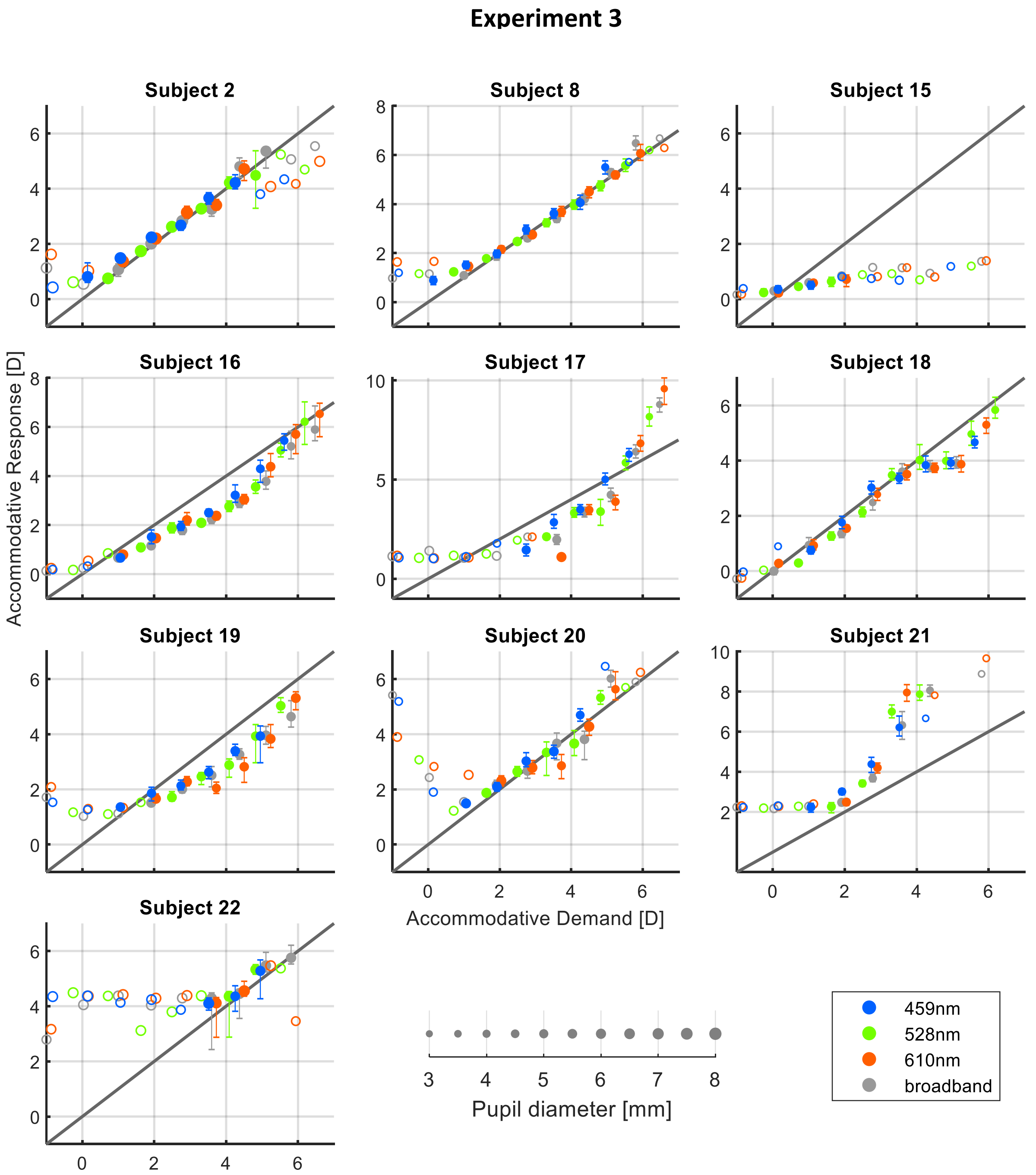

Figure 47. Median accommodation response as a function of the accommodative demand for individual participants of experiment 3. Each colour represents one illuminant, and the marker sizes represent the median pupil size for each distance and illuminant. The error bars represent the 25th and 75th percentiles of the accommodation response. The filled markers represent the portion of the response curve deemed to be linear, while the open markers with no error bars represent the portions of the curve identified as saturated. The continuous grey line represents the one-to-one or ideal response for all the illuminants.

Appendix B. Additional results of the linear mixed models of accommodation.

In this section, we present additional results and post-hoc analyses of the linear mixed models used on the linear portion of the accommodation response curves, as described in Chapter 2. The first table shows the slopes and intercepts estimated for individual participants under each illuminant, which were calculated from the estimated random effects coefficients of the linear mixed models fitted to the data of each experiment. The second table presents the post-hoc pairwise comparisons between the slopes and intercepts estimated for each illuminant in each experiment.

subject	**Experiment 1**					
	broadband	661 nm	588 nm	527 nm	460 nm	441 nm
1	0.89 (0.02) *0.19 (0.02)*	0.81 (0.02) *0.55 (0.03)*	0.81 (0.02) *0.43 (0.03)*	0.79 (0.01) *0.30 (0.03)*	0.68 (0.02) *0.37 (0.05)*	0.62 (0.02) *0.41 (0.06)*
2	0.85 (0.02) *0.06 (0.02)*	0.78 (0.02) *0.22 (0.03)*	0.73 (0.02) *0.35 (0.03)*	0.78 (0.01) *0.06 (0.03)*	0.70 (0.03) *-0.09 (0.04)*	0.65 (0.02) *-0.17 (0.05)*
3	0.97 (0.02) *-0.05 (0.03)*	0.85 (0.03) *0.12 (0.05)*	0.81 (0.02) *0.33 (0.04)*	0.83 (0.02) *0.18 (0.03)*	0.82 (0.03) *-0.05 (0.06)*	0.64 (0.03) *0.27 (0.08)*
4	0.90 (0.02) *0.12 (0.03)*	1.10 (0.02) *0.14 (0.04)*	0.82 (0.02) *0.26 (0.03)*	0.77 (0.02) *0.23 (0.03)*	0.67 (0.03) *0.38 (0.06)*	0.59 (0.03) *0.46 (0.08)*
5	0.92 (0.02) *0.12 (0.02)*	0.94 (0.02) *0.33 (0.03)*	0.82 (0.02) *0.32 (0.03)*	0.80 (0.02) *0.24 (0.03)*	0.75 (0.03) *0.14 (0.05)*	0.70 (0.02) *0.05 (0.06)*
7	0.87 (0.02) *0.16 (0.03)*	0.93 (0.03) *0.34 (0.04)*	0.76 (0.02) *0.40 (0.03)*	0.80 (0.02) *0.16 (0.03)*	0.68 (0.03) *0.18 (0.05)*	0.60 (0.03) *0.25 (0.07)*
8	0.85 (0.02) *0.21 (0.03)*	0.80 (0.02) *0.52 (0.03)*	0.77 (0.02) *0.44 (0.03)*	0.77 (0.02) *0.26 (0.03)*	0.68 (0.03) *0.24 (0.05)*	0.65 (0.03) *0.12 (0.07)*
9	0.91 (0.02) *0.17 (0.03)*	0.95 (0.02) *0.39 (0.04)*	0.82 (0.02) *0.37 (0.03)*	0.79 (0.02) *0.28 (0.03)*	0.70 (0.03) *0.37 (0.05)*	0.60 (0.03) *0.49 (0.07)*
	Experiment 2					
	broadband	661 nm	588 nm	527 nm	460 nm	441 nm
1	1.10 (0.02) *-0.28 (0.05)*	0.84 (0.02) *0.55 (0.05)*	1.00 (0.01) *-0.19 (0.02)*	0.99 (0.03) *-0.28 (0.07)*	0.95 (0.03) *-0.33 (0.08)*	0.89 (0.03) *-0.30 (0.08)*
2	0.89 (0.02) *-0.10 (0.06)*	1.20 (0.03) *-0.41 (0.07)*	0.92 (0.01) *0.00 (0.03)*	0.79 (0.04) *-0.04 (0.09)*	0.62 (0.04) *-0.04 (0.09)*	0.56 (0.04) *-0.11 (0.09)*
3	0.99 (0.02) *-0.18 (0.06)*	0.90 (0.03) *0.24 (0.07)*	1.00 (0.01) *-0.13 (0.03)*	0.92 (0.04) *-0.14 (0.09)*	0.86 (0.04) *-0.20 (0.09)*	0.81 (0.04) *-0.19 (0.09)*
8	1.00 (0.02)	0.92 (0.03)	0.98 (0.01)	0.96 (0.04)	0.91 (0.04)	0.87 (0.04)

	-0.27 (0.06)	*0.30 (0.06)*	*-0.17 (0.03)*	*-0.30 (0.08)*	*-0.42 (0.08)*	*-0.46 (0.08)*
10	0.96 (0.02)	1.20 (0.03)	0.89 (0.01)	0.92 (0.03)	0.78 (0.03)	0.72 (0.04)
	-0.31 (0.05)	*-0.23 (0.05)*	*-0.05 (0.03)*	*-0.37 (0.07)*	*-0.45 (0.07)*	*-0.50 (0.08)*
11	0.92 (0.03)	1.10 (0.03)	0.82 (0.01)	0.90 (0.04)	0.76 (0.04)	0.74 (0.04)
	-0.30 (0.06)	*-1.10 (0.06)*	*0.12 (0.03)*	*-0.26 (0.09)*	*-0.30 (0.09)*	*-0.26 (0.09)*
12	1.10 (0.02)	1.10 (0.03)	0.99 (0.01)	1.10 (0.04)	0.91 (0.04)	0.77 (0.04)
	-0.56 (0.06)	*0.39 (0.07)*	*-0.13 (0.03)*	*-0.51 (0.09)*	*-0.35 (0.09)*	*-0.17 (0.09)*
13	1.00 (0.02)	0.81 (0.03)	0.99 (0.01)	0.96 (0.03)	0.93 (0.03)	0.90 (0.04)
	-0.23 (0.05)	*0.21 (0.05)*	*-0.13 (0.03)*	*-0.22 (0.07)*	*-0.30 (0.07)*	*-0.28 (0.07)*
14	1.00 (0.03)	1.50 (0.03)	0.90 (0.01)	0.76 (0.04)	0.63 (0.04)	0.72 (0.04)
	-0.44 (0.06)	*-1.50 (0.07)*	*-0.09 (0.03)*	*0.22 (0.10)*	*0.47 (0.09)*	*0.35 (0.09)*
	Experiment 3					
	broadband	610 nm		528 nm	459 nm	
2	1.00 (0.01)	0.91 (0.03)		0.92 (0.03)	0.82 (0.03)	
	-1.60 (0.08)	*0.44 (0.11)*		*-1.60 (0.10)*	*-1.60 (0.15)*	
8	1.10 (0.01)	0.96 (0.02)		0.92 (0.02)	0.89 (0.03)	
	-1.60 (0.07)	*0.29 (0.10)*		*-1.40 (0.08)*	*-1.70 (0.14)*	
16	0.98 (0.01)	0.99 (0.03)		1.10 (0.02)	0.95 (0.04)	
	-1.40 (0.08)	*-0.66 (0.11)*		*-1.80 (0.09)*	*-1.80 (0.20)*	
17	2.00 (0.03)	2.60 (0.06)		1.80 (0.03)	1.60 (0.07)	
	1.80 (0.16)	*-8.50 (0.31)*		*2.50 (0.17)*	*3.20 (0.33)*	
18	0.87 (0.01)	0.82 (0.03)		0.96 (0.02)	0.85 (0.05)	
	-1.40 (0.09)	*0.22 (0.11)*		*-1.80 (0.11)*	*-1.90 (0.22)*	
19	0.83 (0.01)	0.82 (0.03)		1.10 (0.02)	0.64 (0.04)	
	-1.20 (0.09)	*-0.18 (0.14)*		*-2.40 (0.09)*	*-1.00 (0.18)*	
20	1.00 (0.01)	0.95 (0.04)		0.92 (0.03)	0.91 (0.04)	
	-1.50 (0.08)	*0.20 (0.14)*		*-1.30 (0.11)*	*-1.70 (0.18)*	

Table 21. Individual slopes and intercepts estimated for the linear portion of the accommodation response curves of each participant to each illuminant used in experiments 1, 2 and 3. For each participant, the first row represents the estimated slopes for each illuminant, and the corresponding conditional standard deviations are shown between parentheses; and the second row in italics represents the estimated intercepts for each illuminant and the corresponding conditional standard deviations between parentheses.

Experiment & Contrasted illuminants		Slope pairwise comparisons				Intercept pairwise comparisons			
		diff.	df	t-ratio	p-value	diff.	df	t-ratio	p-value
1	red - orange	0.10	3.99	7.68	*0.009*	-0.04	3.63	-1.16	0.997
	red - green	0.10	3.66	7.90	*0.011*	0.11	3.83	3.65	0.299
	red - blue	0.18	4.52	13.70	*<0.001*	0.13	5.35	3.62	0.186
	red - violet	0.26	4.09	24.30	*<0.001*	0.09	5.74	2.44	0.554
	red - white	0.00	4.26	-0.16	1.000	0.20	4.03	6.18	*0.049*
	orange - green	0.00	4.05	0.06	1.000	0.15	4.00	5.18	0.095
	orange - blue	0.08	4.49	9.42	*0.003*	0.17	5.39	5.36	*0.035*
	orange - violet	0.16	4.30	18.57	*<0.001*	0.13	5.79	3.43	0.201
	orange - white	-0.10	3.80	-9.32	*0.005*	0.24	3.75	8.21	*0.023*
	green - blue	0.08	3.88	9.45	*0.005*	0.02	4.66	0.72	1.000
	green - violet	0.16	4.20	32.52	*<0.001*	-0.02	5.43	-0.73	1.000
	green - white	-0.10	3.74	-9.85	*0.005*	0.09	3.90	3.28	0.383
	blue - violet	0.08	4.23	10.98	*0.002*	-0.04	4.97	-1.57	0.947
	blue - white	-0.19	3.72	-18.36	*<0.001*	0.07	4.68	2.29	0.685
	violet - white	-0.26	4.52	-29.51	*<0.001*	0.11	5.74	3.23	0.252
2	red - orange	0.12	7.13	3.92	*0.042*	-0.08	6.74	-1.39	0.970
	red - green	0.15	7.57	3.85	*0.042*	0.05	7.60	0.56	1.000
	red - blue	0.25	7.72	5.40	*0.006*	0.05	7.73	0.48	1.000
	red - violet	0.29	7.65	6.99	*0.001*	0.05	7.68	0.52	1.000
	red - white	0.06	7.40	1.93	0.451	0.13	7.23	2.09	0.683
	orange - green	0.03	7.38	0.73	0.972	0.13	7.58	1.47	0.950
	orange - blue	0.13	7.50	3.37	0.078	0.13	7.71	1.24	0.987
	orange - violet	0.17	7.44	4.61	*0.017*	0.13	7.64	1.35	0.974
	orange - white	-0.06	7.17	-1.82	0.510	0.21	7.27	3.10	0.220
	green - blue	0.10	7.12	3.57	0.064	0.00	7.10	0.04	1.000
	green - violet	0.14	7.48	3.98	*0.036*	0.00	7.40	0.02	1.000
	green - white	-0.08	7.36	-2.49	0.238	0.09	7.57	1.06	0.997
	blue - violet	0.04	7.16	1.27	0.794	0.00	6.68	-0.02	1.000
	blue - white	-0.18	7.60	-4.60	*0.017*	0.08	7.77	0.75	1.000
	violet - white	-0.22	7.56	-5.87	*0.004*	0.08	7.76	0.77	1.000
3	red - green	0.07	5.84	0.93	0.790	-0.03	5.88	-0.10	1.000
	red - blue	0.21	5.85	2.68	0.128	-0.23	5.90	-0.62	0.992
	red - white	0.04	5.73	0.82	0.845	-0.18	5.83	-0.73	0.984
	green - blue	0.14	5.13	4.46	*0.023*	-0.20	5.29	-1.35	0.797
	green - white	-0.03	5.35	-0.72	0.884	-0.15	5.29	-1.10	0.901
	blue - white	-0.16	5.26	-5.17	*0.012*	0.05	5.35	0.33	1.000

Table 22. Post-hoc pairwise comparisons of the slope and intercept estimates between illuminants. The estimated differences (diff.), degrees of freedom (df), t-ratios and p-values are shown. The shaded p-values in italics represent significant results at the 0.05 level. The different illuminants have been named according to their colour for easier reading of the

results. For experiments 1 and 2, they represent the 661 nm (red), 588 nm (orange), 527 nm (green), 460 nm (blue) and 441 nm (violet) illuminants; while for experiment 3 they represent the 610 nm (red), 528 nm (green) and 459 nm (blue) illuminants.

Appendix C. Visual acuity results for individual participants.

In this section, visual acuity as a function of accommodative error is plotted for individual participants, as described in Chapter 2.

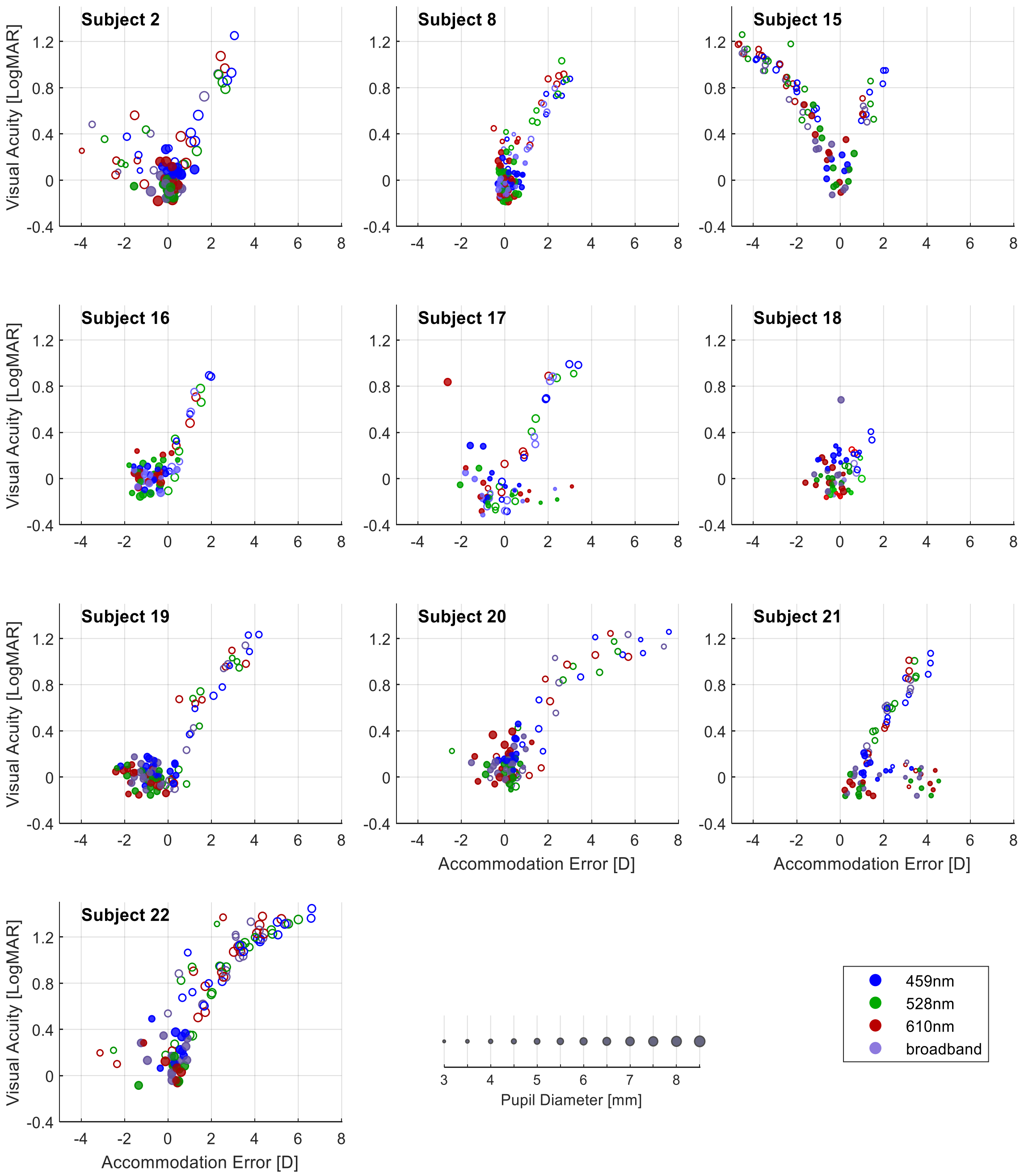

Figure 48. Visual acuity (VA) as a function of the median accommodative error for individual participants of experiment 3. Accommodative error is calculated as the accommodative demand subtracted from the accommodative response. Filled markers correspond to VA measurements over the linear portion of the accommodation response curve, while open markers correspond to measurements at distances where the accommodation function was saturated. The marker colours represent the illuminant used, and the marker sizes the corresponding median pupil size.

Appendix D. Accommodation responses to pairs of narrowband illuminants for individual participants.

In this section, the accommodation responses to pairs of narrowband illuminants are presented for individual participants that took part in Experiments 1, 2 and 3, as described in Chapter 3.

Figure 49. Median accommodation responses of individual participants in Experiment 1 to each pair of narrowband illuminants. Each panel corresponds to one pair of illuminants. The abscissas represent the luminance of the shortest wavelength illuminant within the pair. The luminance of the other illuminant decreased in opposite steps, maintaining the total luminance at 10 cd/m². The coloured markers and error bars represent the median accommodation response, and the 25th and 75th percentiles, respectively. The size of the markers represents the corresponding median pupil diameter. The small grey markers represent the median accommodation response in individual trials, slightly jittered across the abscissas. The dashed lines represent the expected accommodative demand for each illuminant in the pair, calculated as a function of the physical distance of the target (2 dioptres) and the defocus caused by LCA for the peak wavelength of the illuminant.

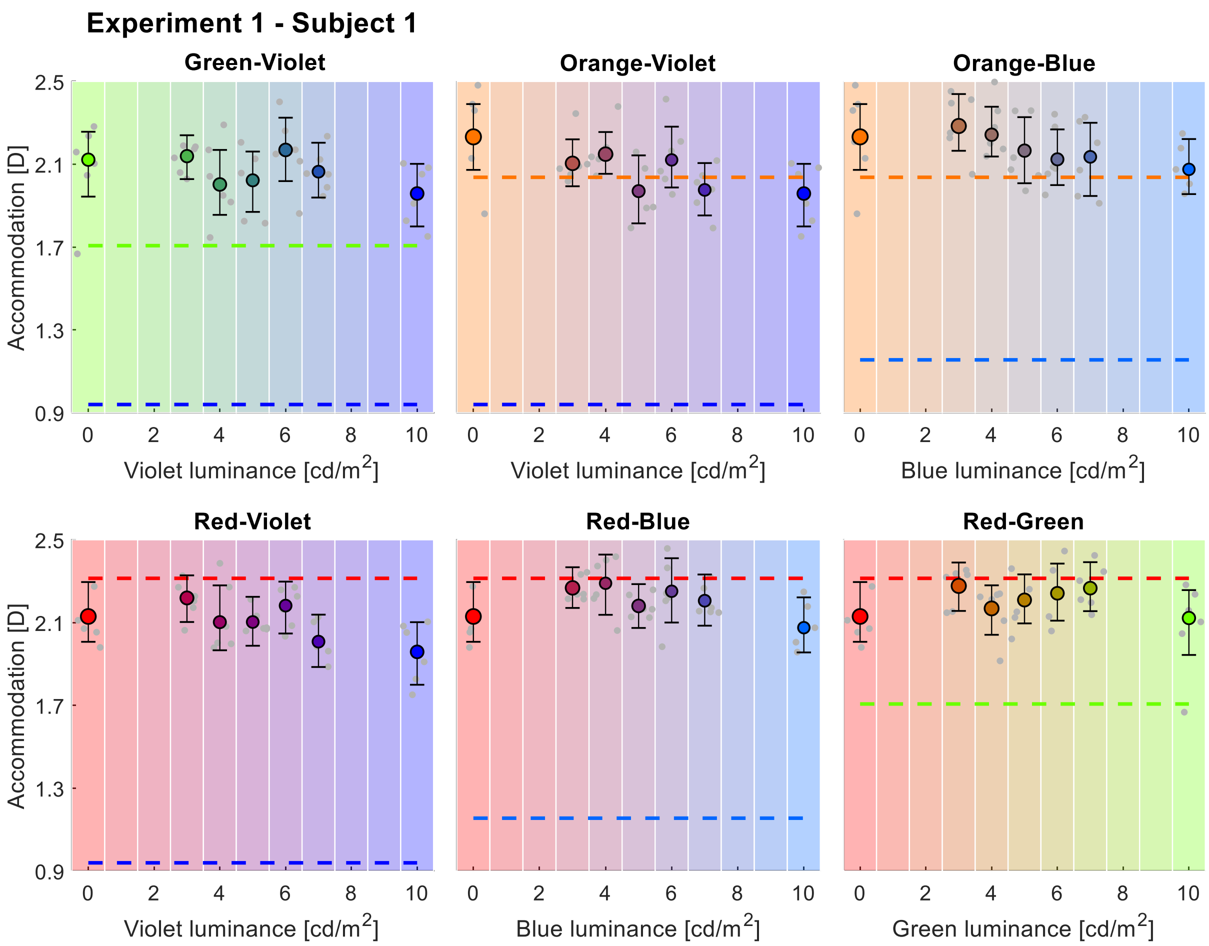

Experiment 1 - Subject 2

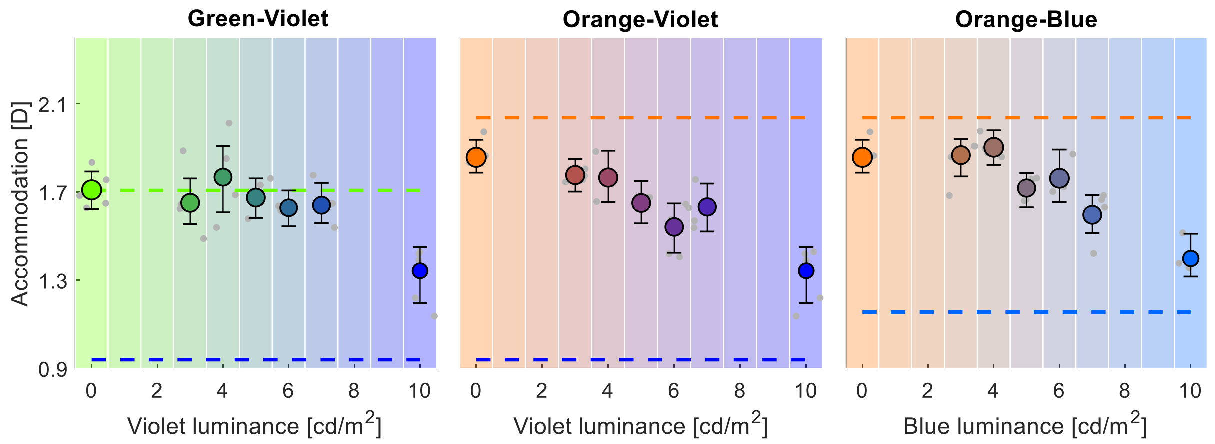

Experiment 1 - Subject 3

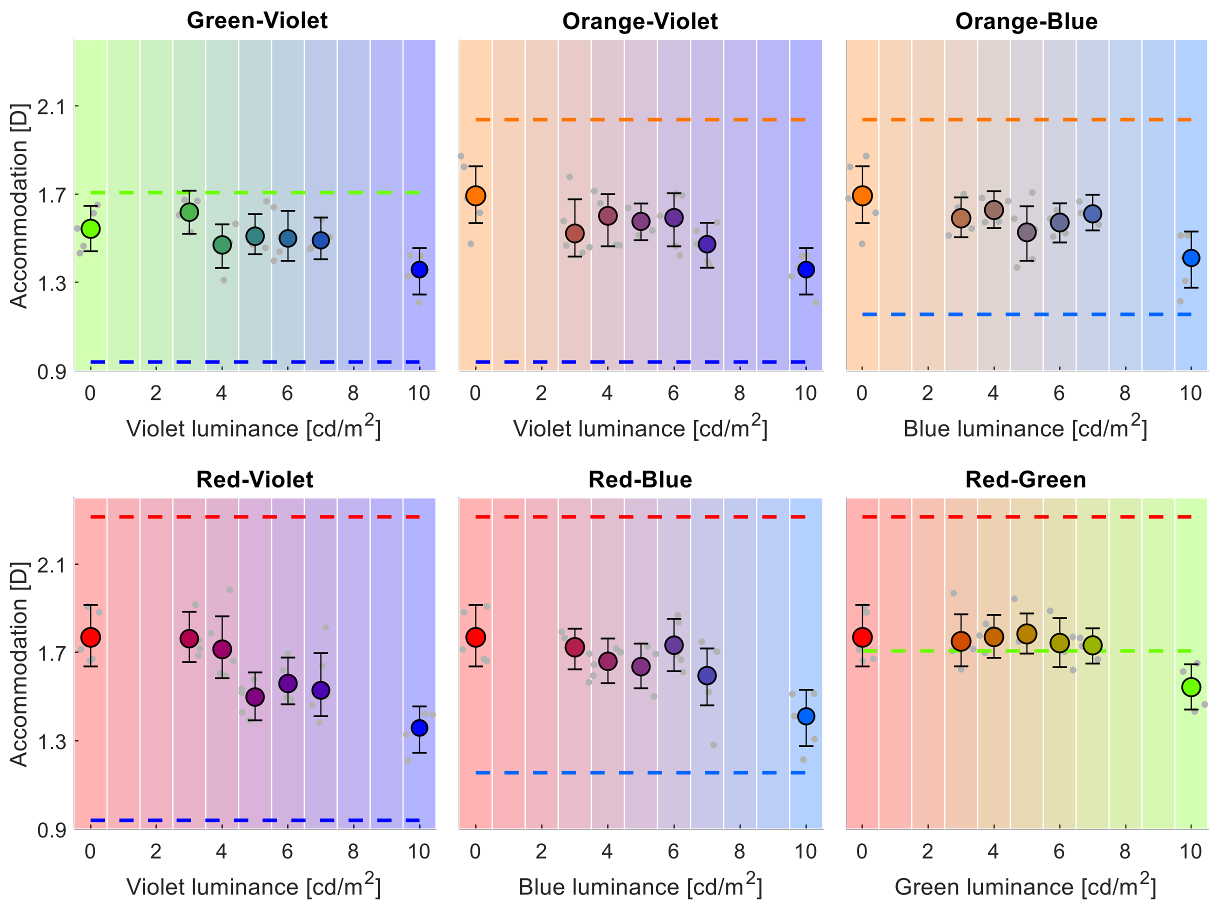

Experiment 1 - Subject 4

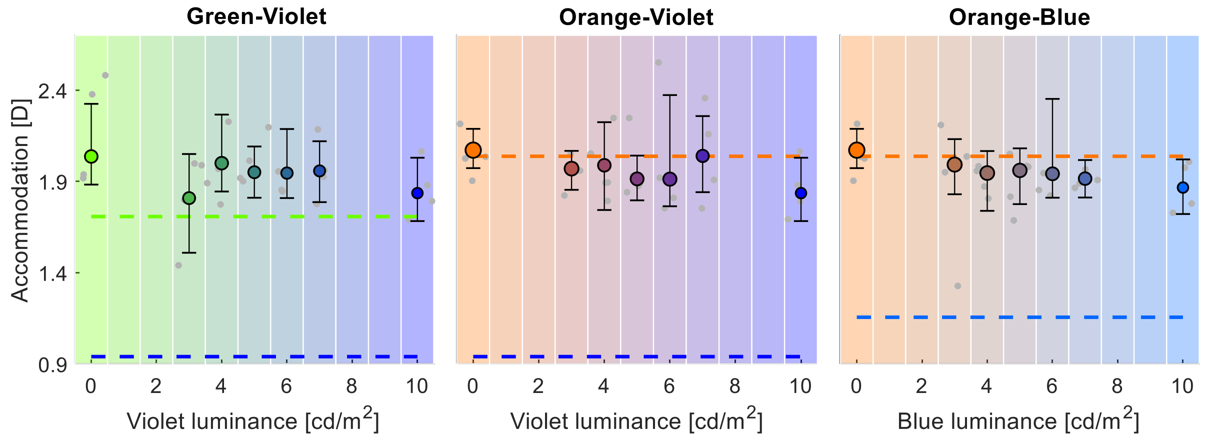

Experiment 1 - Subject 5

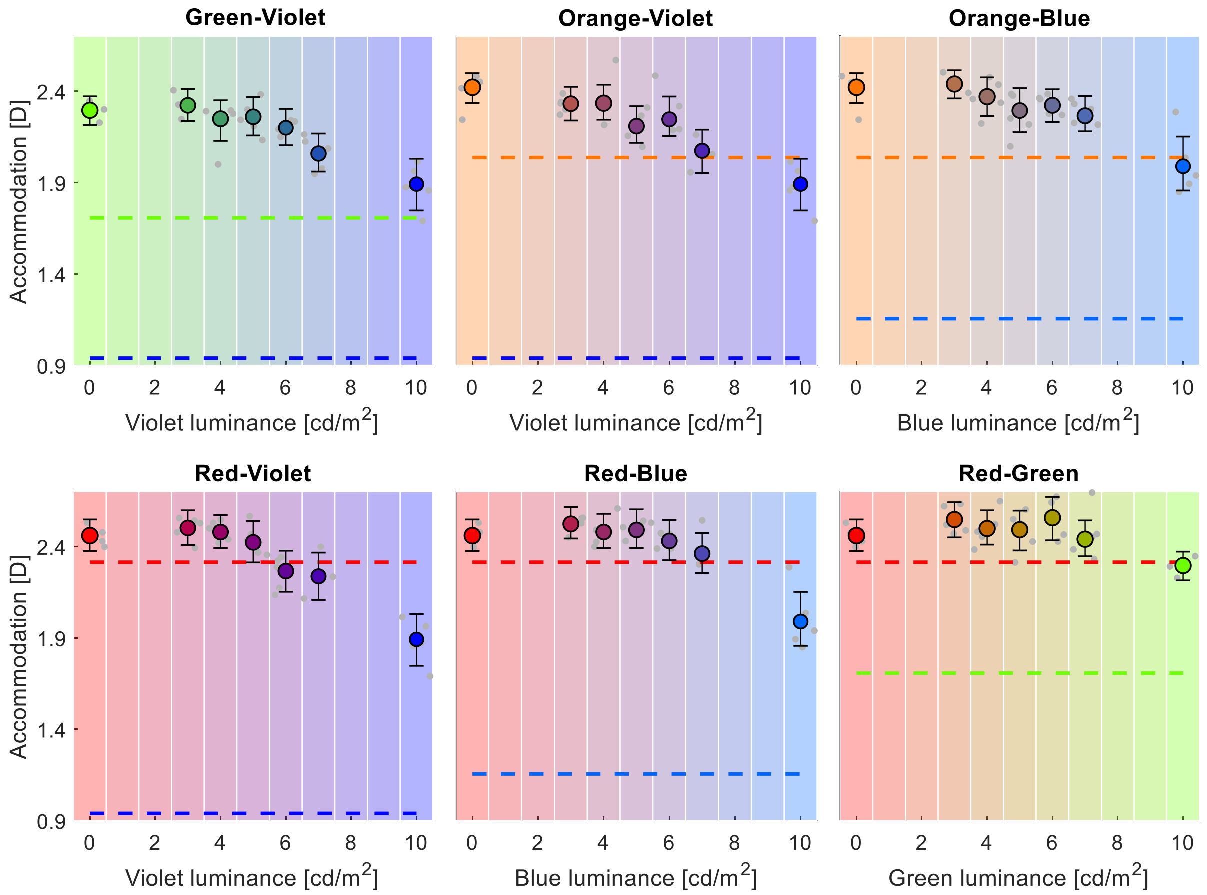

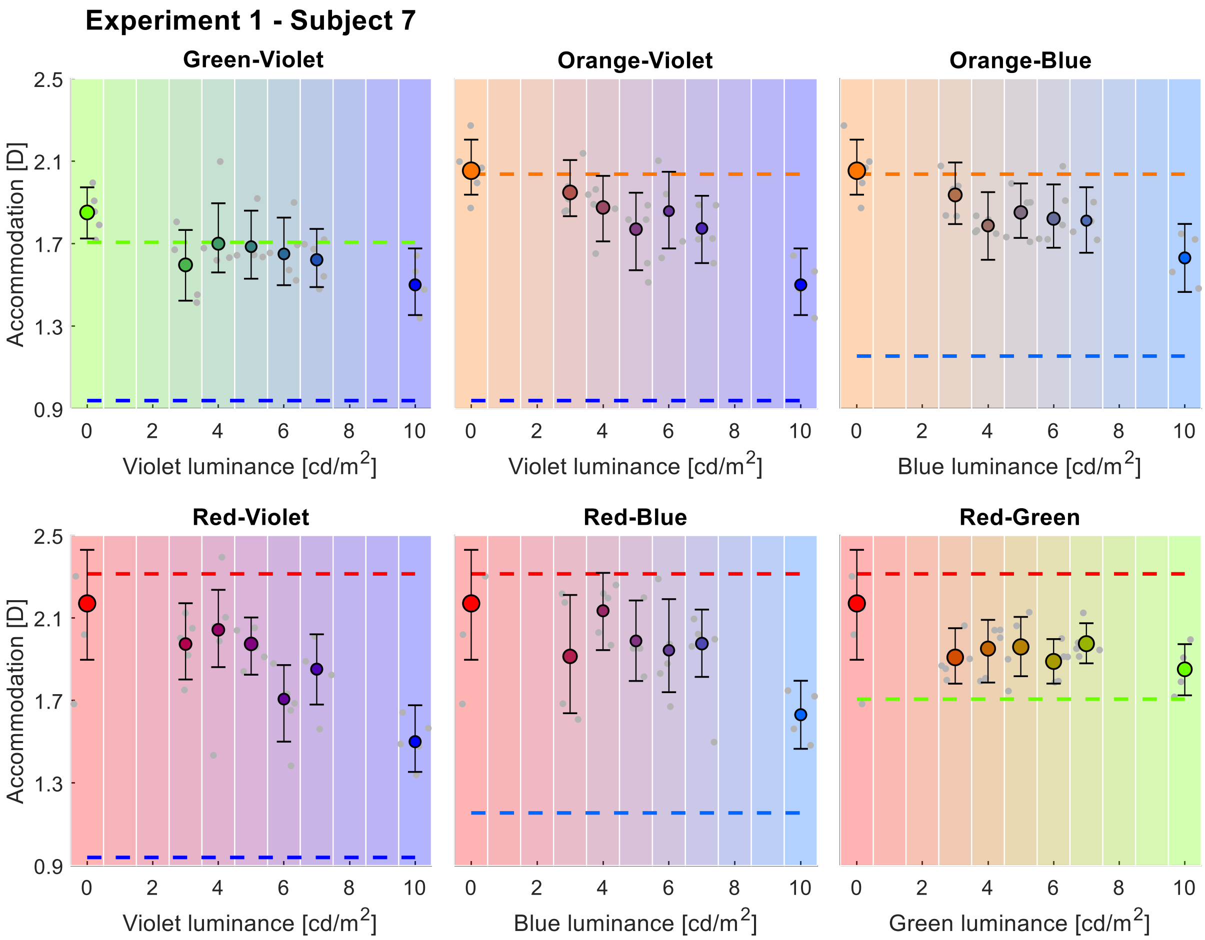
Experiment 1 - Subject 7
Green-Violet
Orange-Violet
Orange-Blue
Red-Violet
Red-Blue
Red-Green
Accommodation [D]
2.5
2.1
1.7
1.3
0.9
0 2 4 6 8 10
Violet luminance [cd/m2]
Blue luminance [cd/m2]
Green luminance [cd/m2]

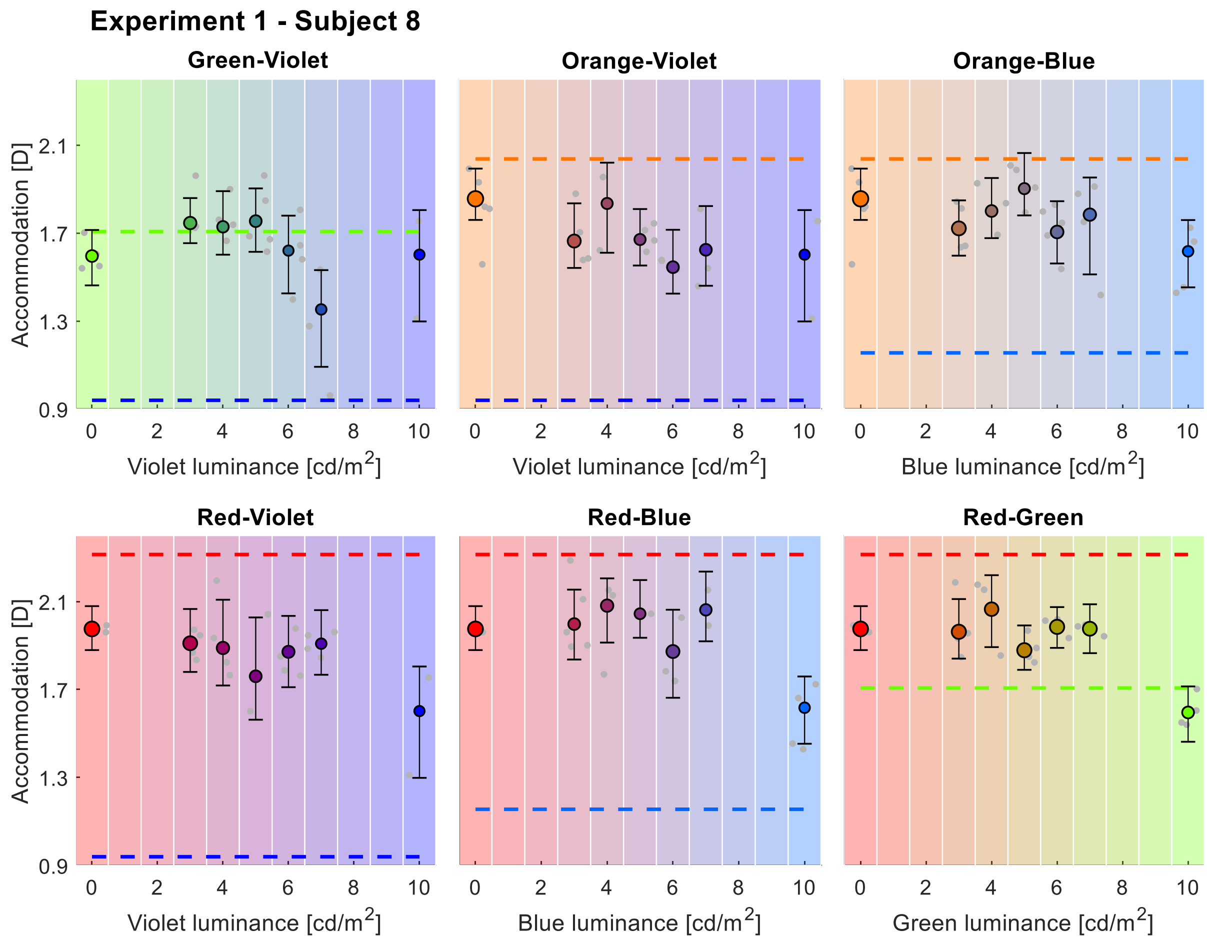
Experiment 1 - Subject 8
Green-Violet
Orange-Violet
Orange-Blue
Red-Violet
Red-Blue
Red-Green
Accommodation [D]
2.1
1.7
1.3
0.9
0 2 4 6 8 10
Violet luminance [cd/m2]
Blue luminance [cd/m2]
Green luminance [cd/m2]

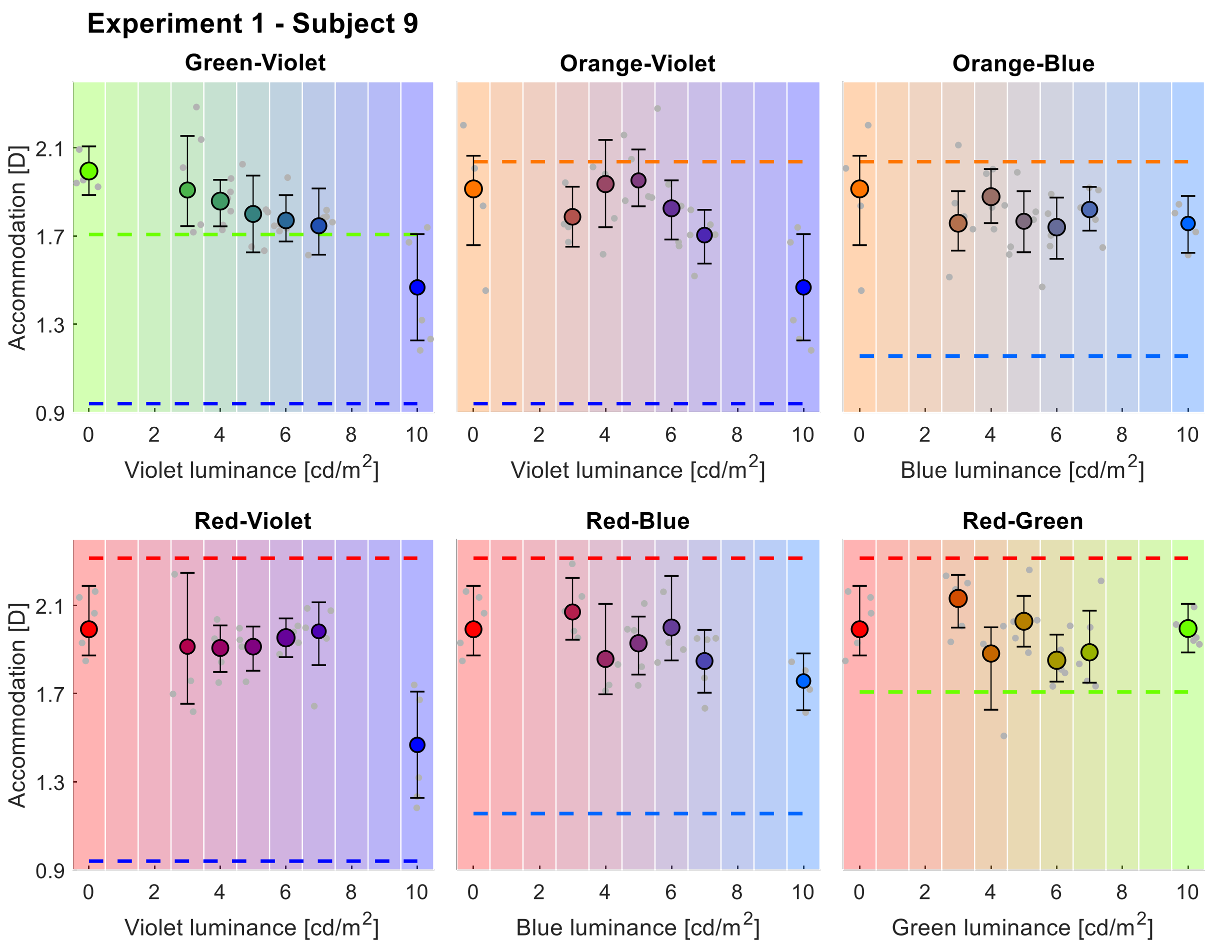

Experiment 1 - Subject 9
Green-Violet
Orange-Violet
Orange-Blue
Red-Violet
Red-Blue
Red-Green
Accommodation [D]
Violet luminance [cd/m2]
Blue luminance [cd/m2]
Green luminance [cd/m2]

Figure 50. Median accommodation responses of individual participants in Experiment 2 to each pair of narrowband illuminants. Each panel corresponds to one pair of illuminants. The abscissas represent the luminance of the shortest wavelength illuminant within the pair. The luminance of the other illuminant decreased in opposite steps, maintaining the total luminance at 10 cd/m^2. The coloured markers and error bars represent the median accommodation response, and the 25th and 75th percentiles, respectively. The size of the markers represents the corresponding median pupil diameter. The small grey markers represent the median accommodation response in individual trials, slightly jittered across the abscissas. The dashed lines represent the expected accommodative demand for each illuminant in the pair, calculated as a function of the physical distance of the target (3 dioptres) and the defocus caused by LCA for the peak wavelength of the illuminant.

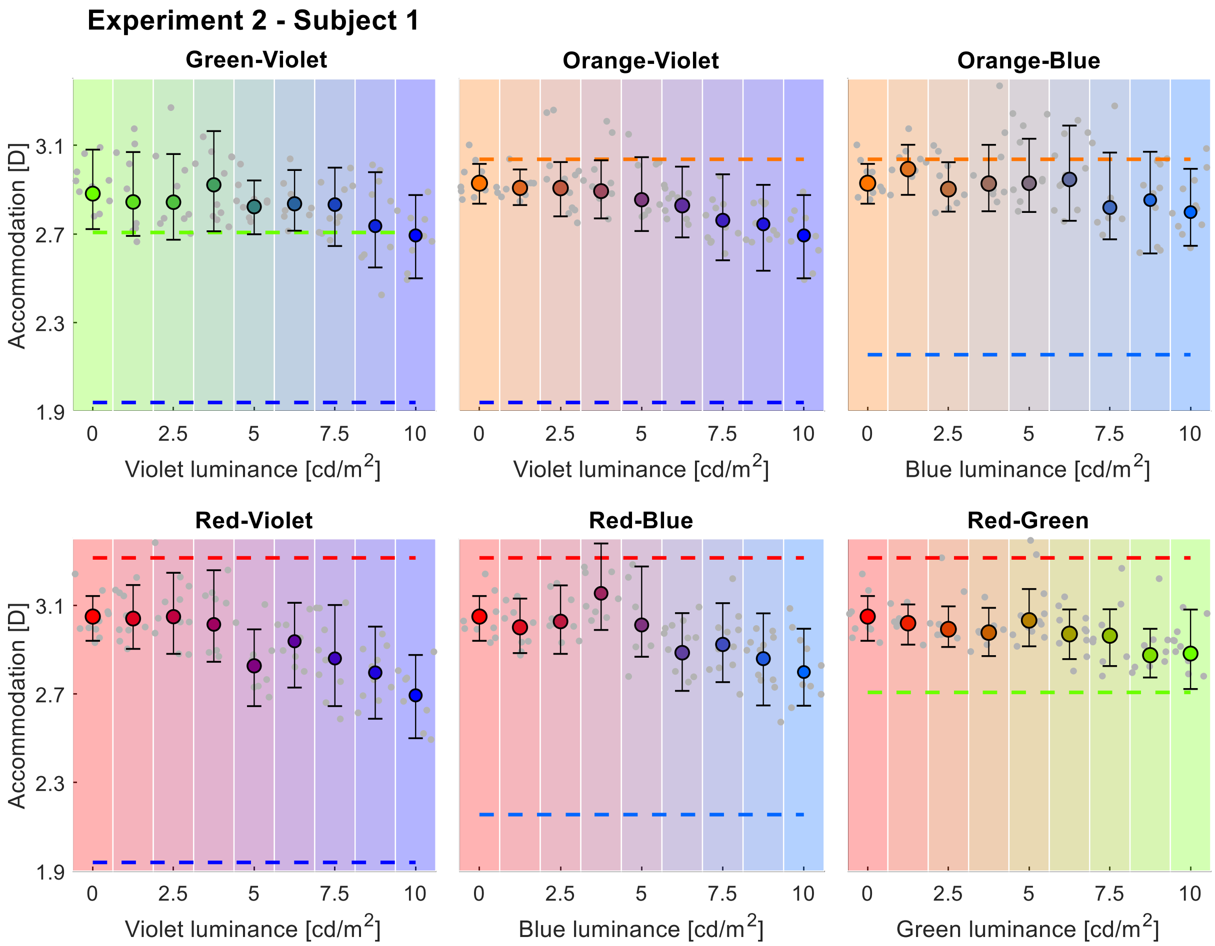

Experiment 2 - Subject 8

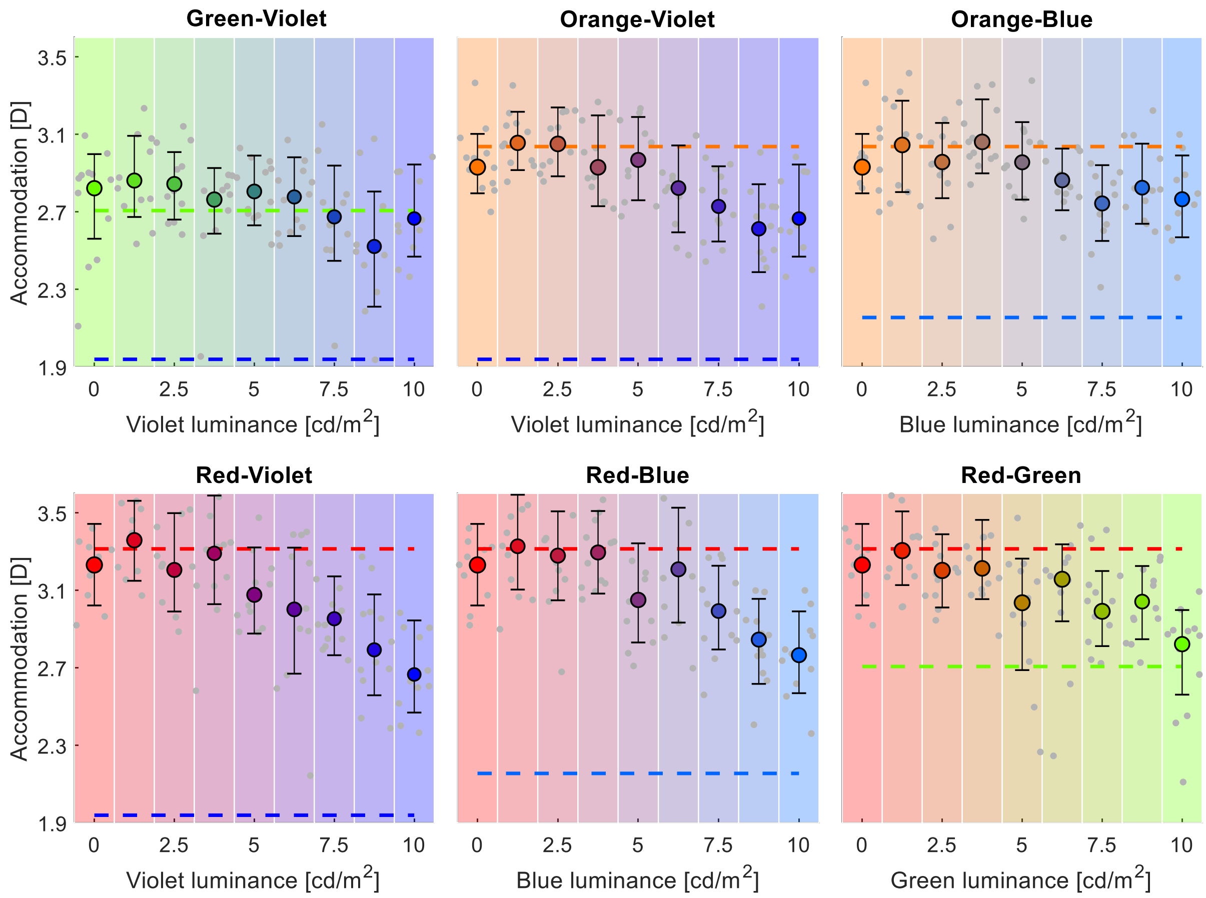

Experiment 2 - Subject 10

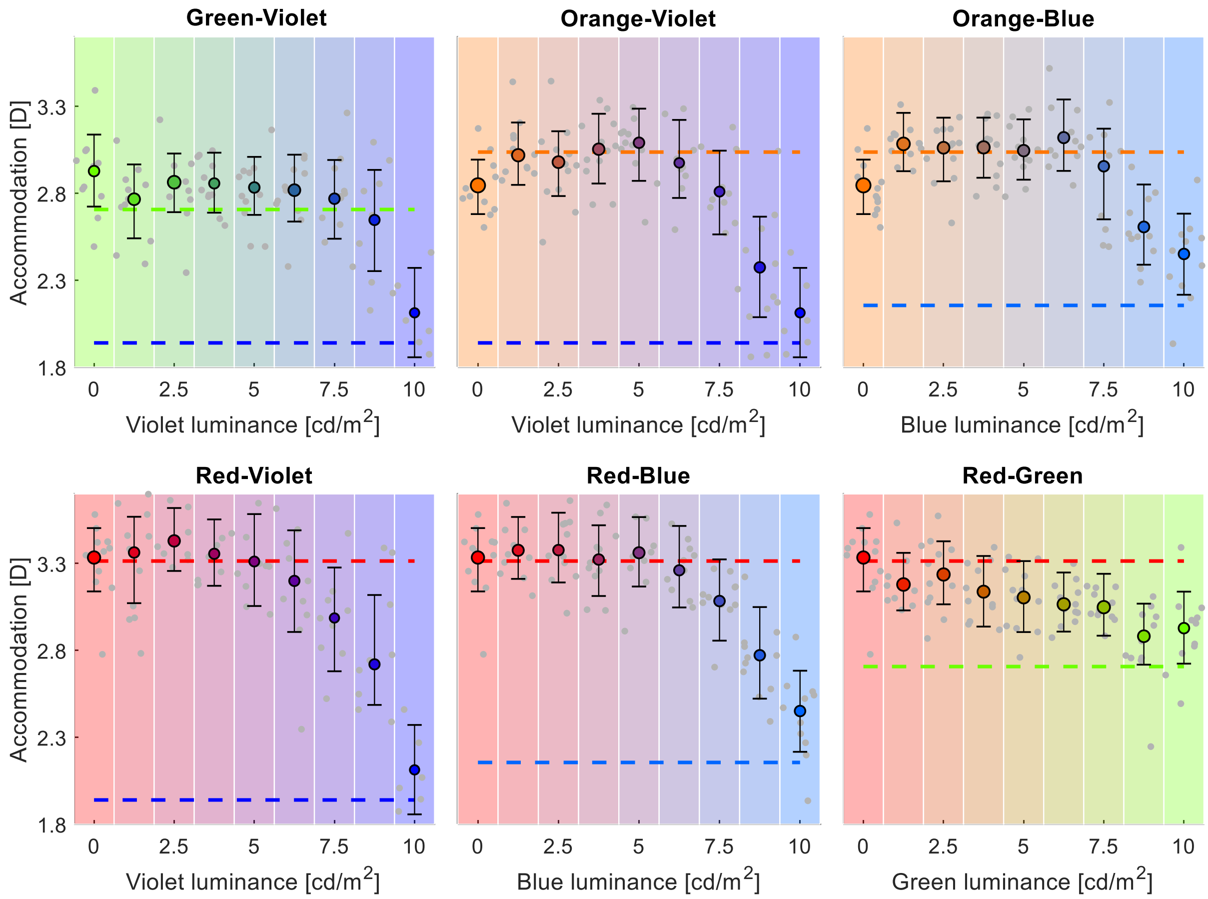

Experiment 2 - Subject 11

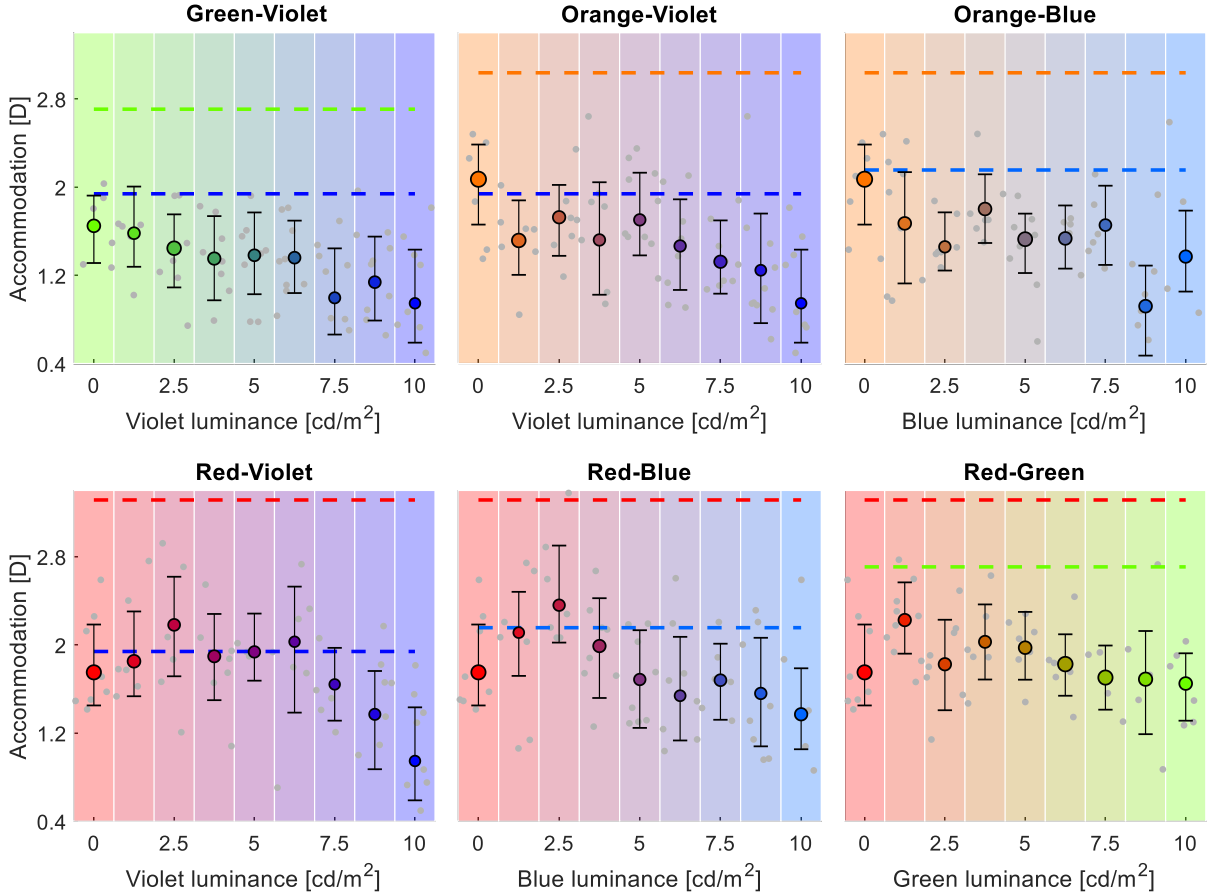

Experiment 2 - Subject 12

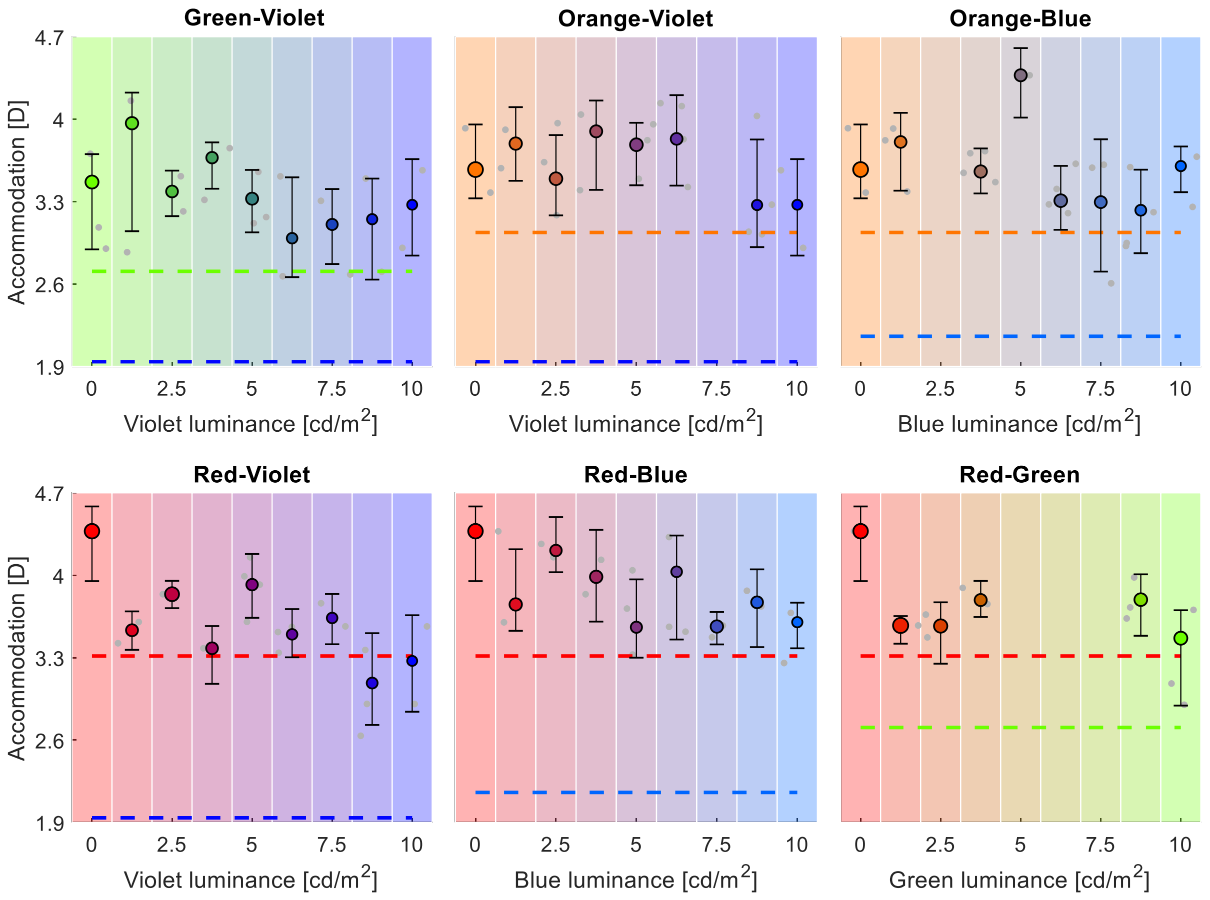

Figure 51. Median accommodation responses of individual participants in Experiment 3 to each accommodative target presented under different pairs of narrowband illuminants. Each column of panels represents one type of accommodative target, and each row corresponds to one pair of narrowband illuminants. The abscissas represent the luminance of the shortest wavelength illuminant within the pair. The luminance of the other illuminant decreased in opposite steps, maintaining the total luminance at 10 cd/m^2. The coloured markers and error bars represent the median accommodation response, and the 25th and 75th percentiles, respectively. The size of the markers represents the corresponding median pupil diameter. The small grey markers represent the median accommodation response in individual trials, slightly jittered across the abscissas. The proportion of correctly identified targets is presented at the corresponding luminance values, only for proportions lower than 1. The dashed lines represent the expected accommodative demand for each illuminant in the pair, calculated as a function of the optical distance of the target (between 3.6 and 5.1 dioptres, as indicated) and the defocus caused by LCA for the peak wavelength of the illuminant.

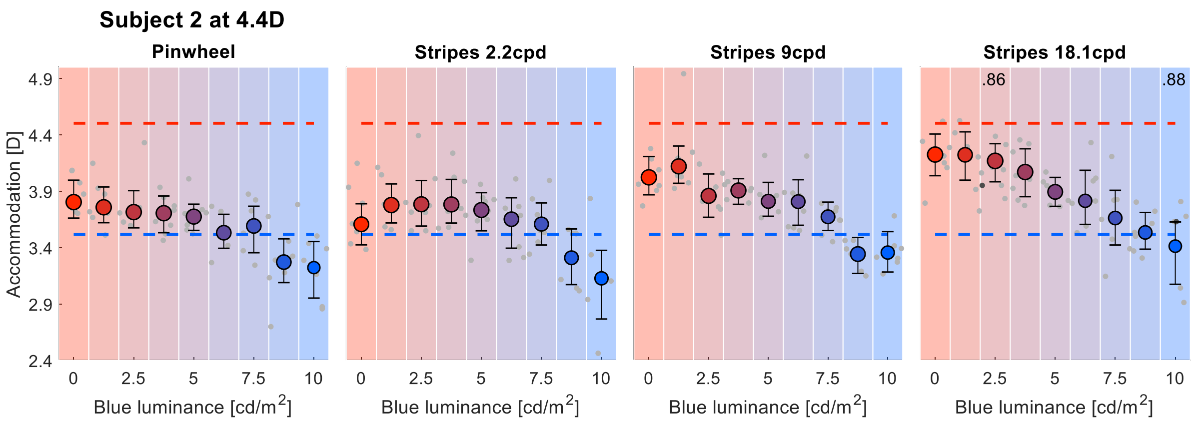

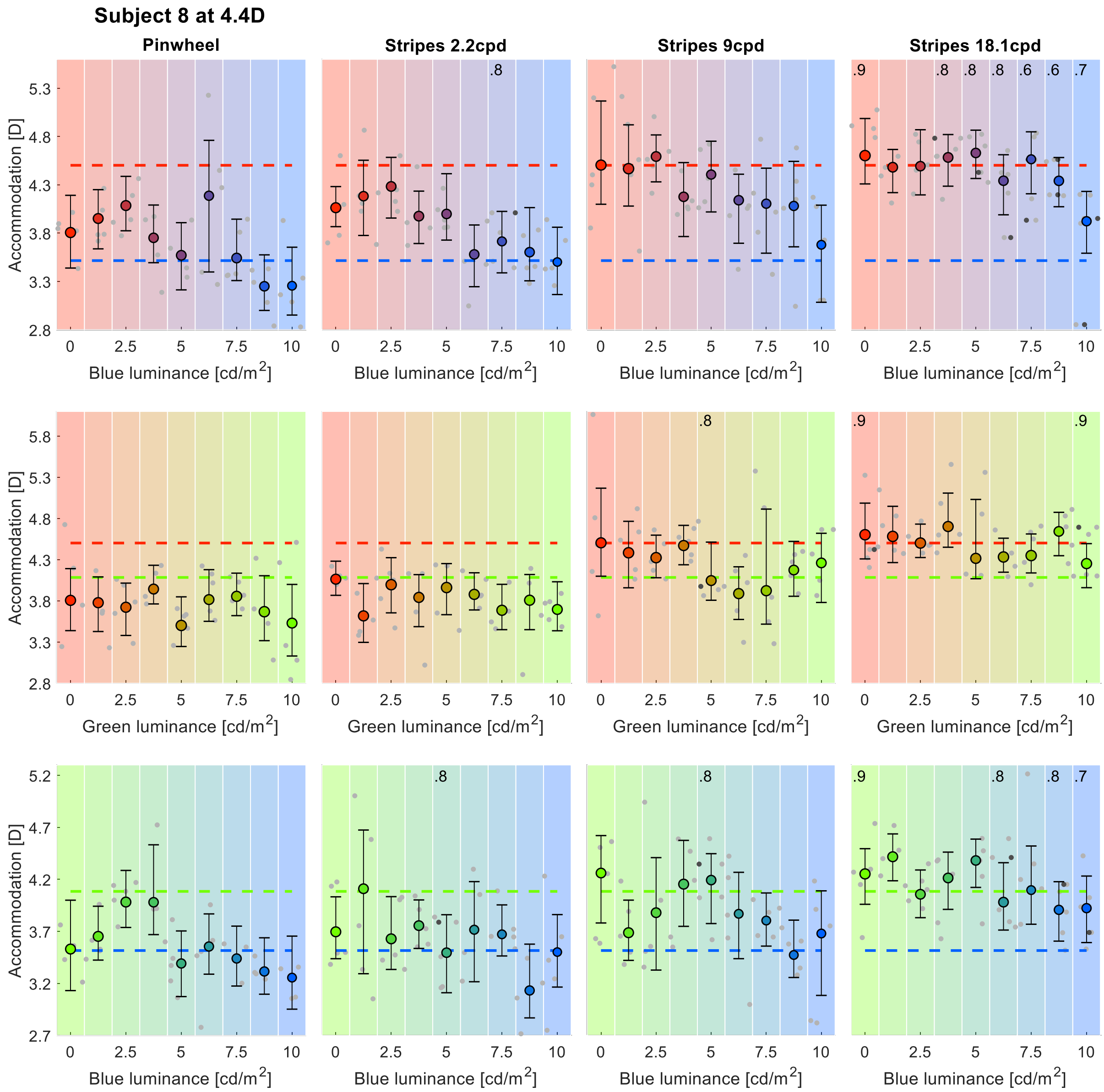
Subject 8 at 4.4D
Pinwheel
Stripes 2.2cpd
Stripes 9cpd
Stripes 18.1cpd
Accommodation [D]
Blue luminance [cd/m2]
Green luminance [cd/m2]

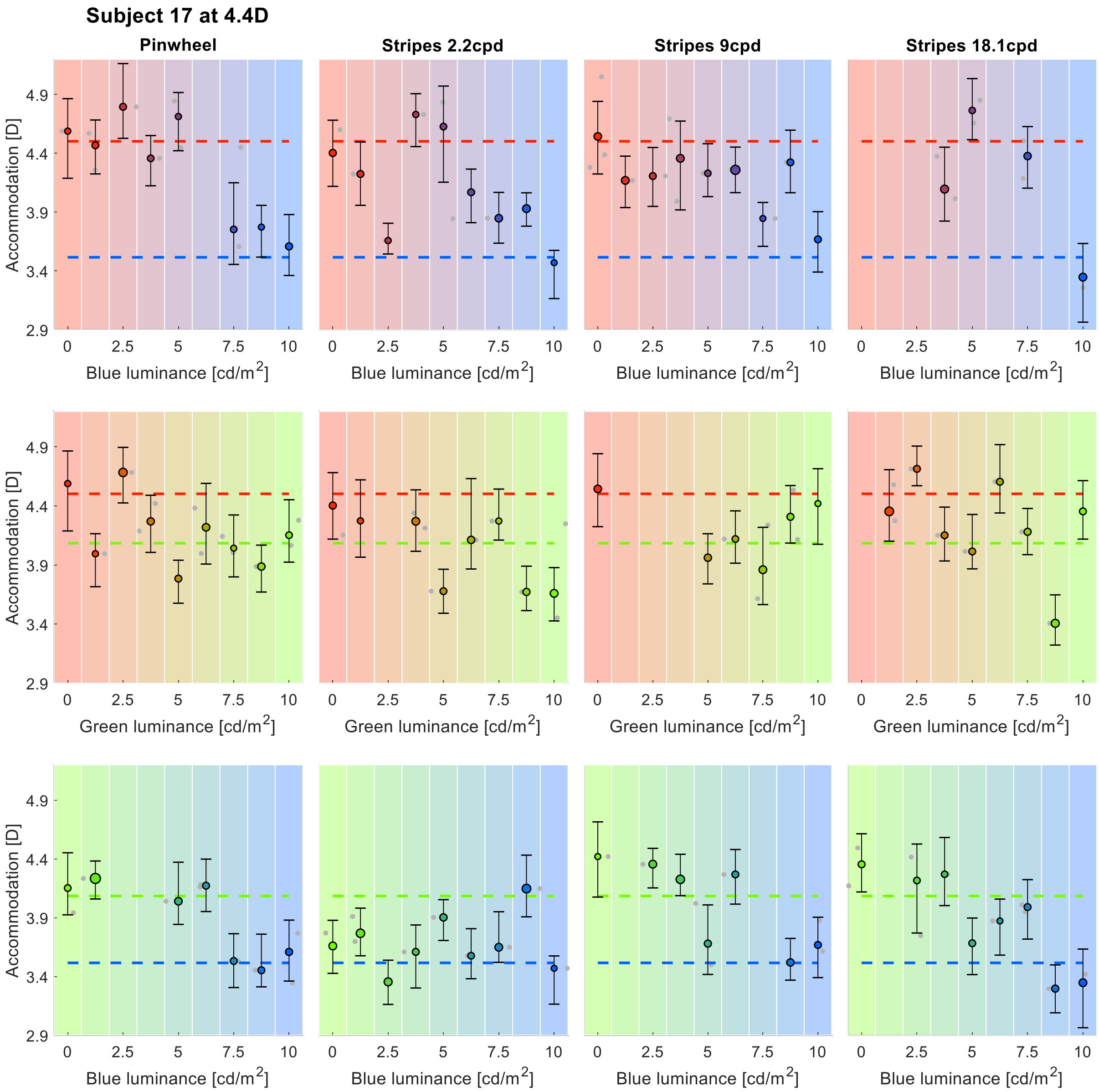

Subject 17 at 4.4D
Pinwheel
Stripes 2.2cpd
Stripes 9cpd
Stripes 18.1cpd
Accommodation [D]
4.9
4.4
3.9
3.4
2.9
0
2.5
5
7.5
10
Blue luminance [cd/m2]
Green luminance [cd/m2]

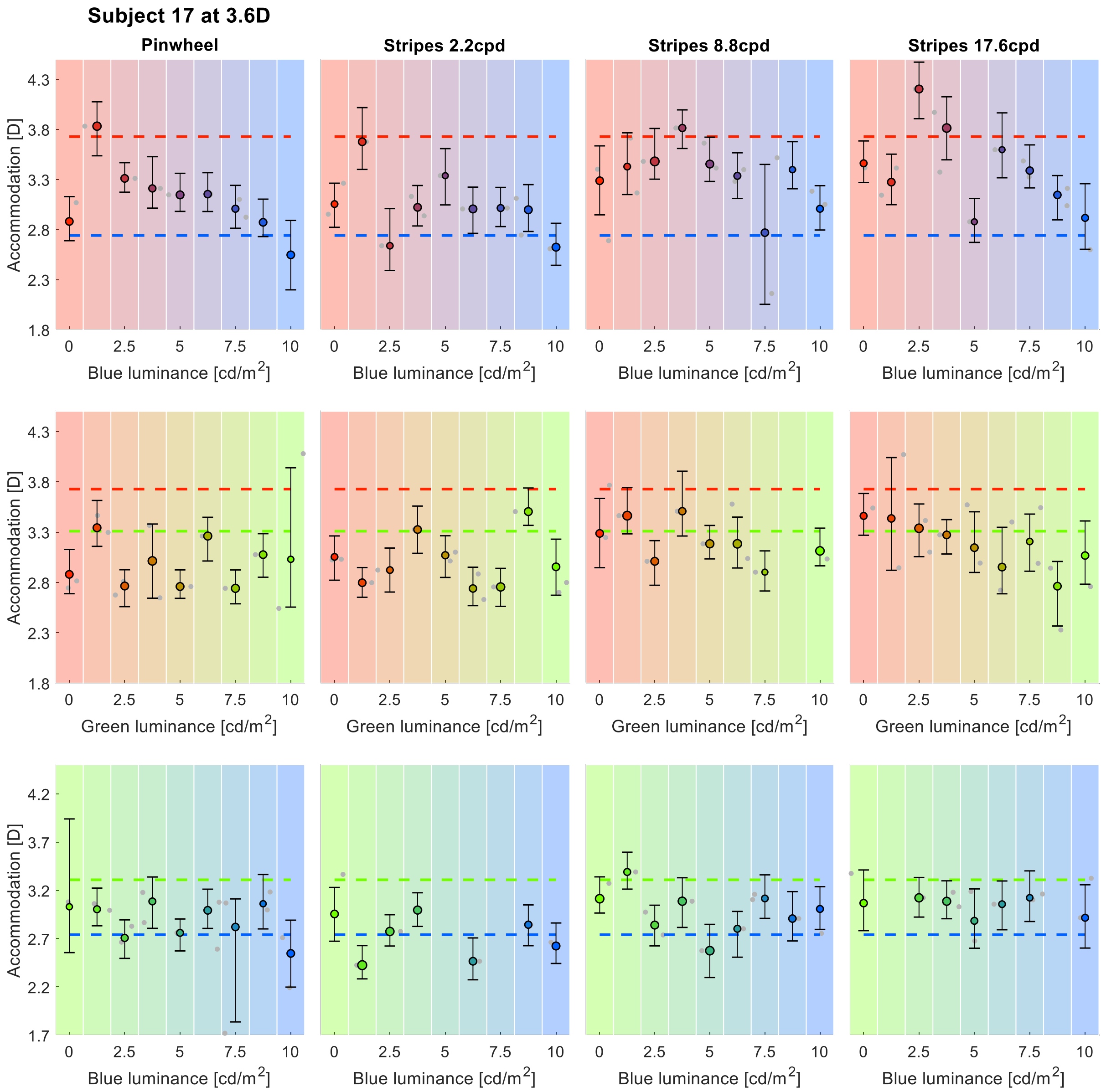
Subject 17 at 3.6D
Pinwheel
Stripes 2.2cpd
Stripes 8.8cpd
Stripes 17.6cpd
Accommodation [D]
4.3
3.8
3.3
2.8
2.3
1.8
4.2
3.7
3.2
2.7
2.2
1.7
0
2.5
5
7.5
10
Blue luminance [cd/m2]
Green luminance [cd/m2]

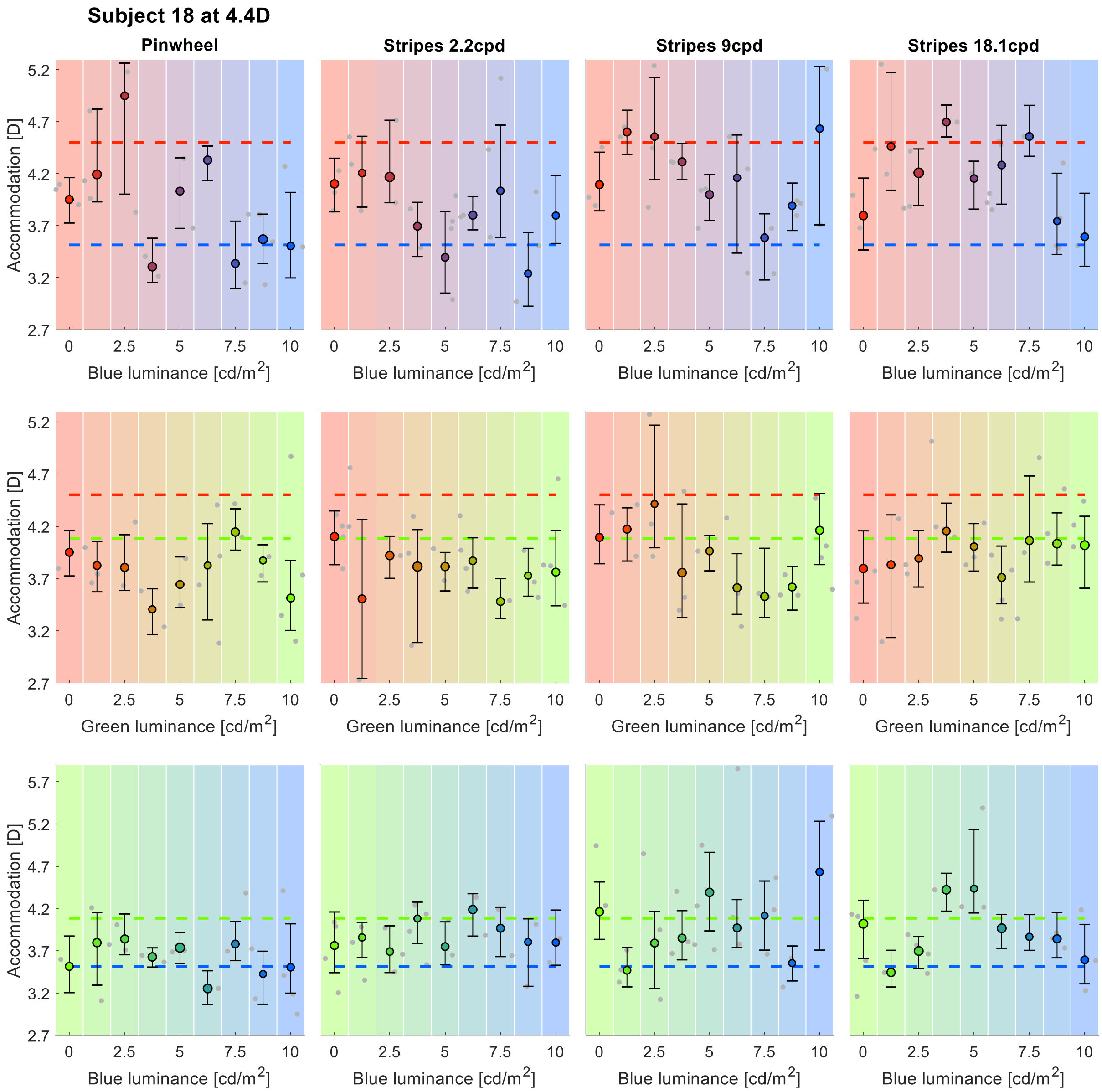

Subject 18 at 4.4D
Pinwheel
Stripes 2.2cpd
Stripes 9cpd
Stripes 18.1cpd
Accommodation [D]
Blue luminance [cd/m^2]
Green luminance [cd/m^2]

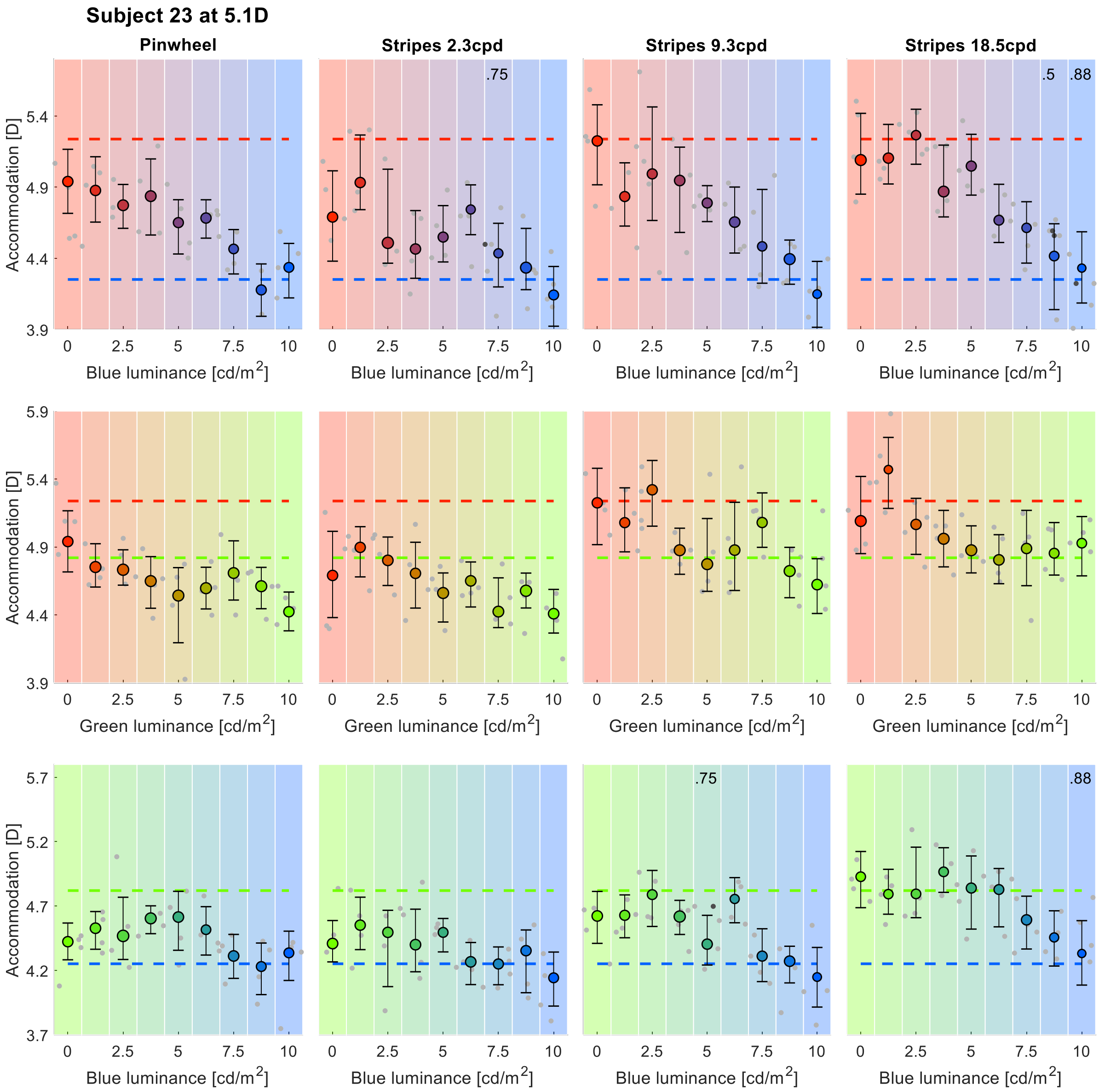
Subject 23 at 5.1D
Pinwheel
Stripes 2.3cpd
Stripes 9.3cpd
Stripes 18.5cpd
Accommodation [D]
Blue luminance [cd/m2]
Green luminance [cd/m2]
.75
.5
.88

Appendix E. Symptoms Questionnaire and Sessions Evaluation Questionnaire.

In this section, we present the Symptoms Questionnaire and the Sessions Evaluation Questionnaire used in the experiment of Chapter 5.

Symptoms questionnaire

*Required

Participant ID *

Your answer

Session number *

1	2	3	4
○	○	○	○

Time of survey *

- ○ Beginning of the session
- ○ End of the session

For each of the following symptoms, select a description that best represents the severity of that symptom at this moment.

Example symptom scale

- ○ None
- ○ Mild
- ○ Modest
- ○ Bad
- ○ Severe

Please rate each of the following symptoms similar to the example above. Rate the severity of each symptom at this moment.

How tired are your eyes? *

- ○ Very fresh
- ○ OK
- ○ Mildly tired
- ○ Moderately tired
- ○ Very tired

How clear is your vision? *

- ○ Very clear
- ○ OK
- ○ Mild blur
- ○ Moderate blur
- ○ Much blur

How tired and sore are your neck and back? *

- ○ Very fresh
- ○ OK
- ○ Mild ache
- ○ Moderate ache
- ○ Severe ache

How do your eyes feel? *

- ○ Very fresh
- ○ OK
- ○ Mild strain
- ○ Moderate strain
- ○ Severe strain

How does your head feel? *

- ○ Very fresh
- ○ OK
- ○ Mild ache
- ○ Moderate ache
- ○ Severe ache

Any comments?

Your answer

Final session evaluation

*Required

Participant ID *

Your answer

Age *

Your answer

Do you wear...? *

- Glasses
- Contact lenses
- None

Eyeglasses prescription (if any)

Your answer

For each of the following questions, select the option that best represents your final impression of all four sessions of the experiment.

Example question

- No difference
- Session 1
- Session 2
- Session 3
- Session 4
- Other:

Please respond to each question similar to the example above. Rate your opinions based on how you felt at the conclusion of each session.

Which session was most fatiguing? *

- No difference
- Session 1
- Session 2
- Session 3
- Session 4
- Other:

Which session irritated your eyes the most? *

- No difference
- Session 1
- Session 2
- Session 3
- Session 4
- Other:

If you felt headache, which session was worse? *

- No difference
- Session 1
- Session 2
- Session 3
- Session 4
- Other:

Which session did you prefer? *

- No preference
- Session 1
- Session 2
- Session 3
- Session 4
- Other:

Any comments?

Your answer

Appendix F. Pairwise comparisons of symptom score between experimental conditions.

In this section, we present the post-hoc pairwise comparisons of the estimated marginal means of symptom score change between experimental conditions, both averaged across all symptoms, and for each individual symptom in the survey. These marginal means were estimated from the fitted ordinal linear regression model, as discussed in Chapter 5.

	Difference	SE	z-ratio	p-value
All symptoms				
(High A - High MP) - (High A - Low MP)	-0.57	0.40	-1.45	0.471
(High A - High MP) - (Low A - High MP)	-0.04	0.63	-0.06	1.000
(High A - High MP) - (Low A - Low MP)	0.05	0.39	0.13	0.999
(High A - Low MP) - (Low A - High MP)	0.53	0.69	0.78	0.864
(High A - Low MP) - (Low A - Low MP)	0.62	0.48	1.31	0.559
(Low A - High MP) - (Low A - Low MP)	0.09	0.56	0.16	0.999
symptom = blurry vision				
(High A - High MP) - (High A - Low MP)	-0.97	0.69	-1.39	0.503
(High A - High MP) - (Low A - High MP)	-0.40	0.85	-0.47	0.966
(High A - High MP) - (Low A - Low MP)	-0.40	0.70	-0.58	0.939
(High A - Low MP) - (Low A - High MP)	0.57	0.88	0.65	0.917
(High A - Low MP) - (Low A - Low MP)	0.56	0.75	0.76	0.874
(Low A - High MP) - (Low A - Low MP)	-0.01	0.80	-0.01	1.000
symptom = eyestrain				
(High A - High MP) - (High A - Low MP)	-1.23	0.69	-1.78	0.282
(High A - High MP) - (Low A - High MP)	-0.48	0.84	-0.57	0.942
(High A - High MP) - (Low A - Low MP)	-0.11	0.67	-0.17	0.998
(High A - Low MP) - (Low A - High MP)	0.76	0.88	0.86	0.828
(High A - Low MP) - (Low A - Low MP)	1.12	0.73	1.53	0.420
(Low A - High MP) - (Low A - Low MP)	0.36	0.78	0.46	0.967
symptom = headache				
(High A - High MP) - (High A - Low MP)	-0.27	0.72	-0.38	0.981

(High A - High MP) - (Low A - High MP)	-0.19	0.87	-0.22	0.996
(High A - High MP) - (Low A - Low MP)	-0.58	0.71	-0.81	0.849
(High A - Low MP) - (Low A - High MP)	0.08	0.90	0.09	1.000
(High A - Low MP) - (Low A - Low MP)	-0.31	0.74	-0.41	0.976
(Low A - High MP) - (Low A - Low MP)	-0.38	0.81	-0.48	0.965
symptom = sore neck back				
(High A - High MP) - (High A - Low MP)	-0.14	0.74	-0.19	0.998
(High A - High MP) - (Low A - High MP)	0.05	0.89	0.06	1.000
(High A - High MP) - (Low A - Low MP)	0.37	0.74	0.50	0.958
(High A - Low MP) - (Low A - High MP)	0.19	0.92	0.21	0.997
(High A - Low MP) - (Low A - Low MP)	0.51	0.79	0.64	0.918
(Low A - High MP) - (Low A - Low MP)	0.32	0.84	0.38	0.982
symptom = tired eyes				
(High A - High MP) - (High A - Low MP)	-0.26	0.69	-0.38	0.981
(High A - High MP) - (Low A - High MP)	0.81	0.85	0.96	0.774
(High A - High MP) - (Low A - Low MP)	0.97	0.68	1.42	0.489
(High A - Low MP) - (Low A - High MP)	1.07	0.90	1.20	0.630
(High A - Low MP) - (Low A - Low MP)	1.23	0.75	1.64	0.357
(Low A - High MP) - (Low A - Low MP)	0.16	0.81	0.20	0.997

Table 23. Pairwise comparisons of estimated marginal means of symptom score change between experimental conditions, for the sum of all symptoms and for each level of symptom. The estimated differences between conditions, their standard errors (SE), z-ratios and p-values are shown.

Appendix G. Effect of time-on-task on blink rate, blink duration and interblink time.

In this section, we present estimated slopes of the effect of time-on-task on blink rate, blink duration and log interblink time within each of the experimental conditions, estimated from the fitted generalized mixed effects models as discussed in Chapter 5.

	Blink Rate [blinks/min]						
Conditions	**Time trend**	**SE**	**95% CI**		**z-ratio**		**p-value**
High A - High MP	-0.60	0.31	-1.20	0.00	-1.95		0.051
High A - Low MP	-0.45	0.26	-0.97	0.06	-1.71		0.086
Low A - High MP	0.24	0.30	-0.35	0.83	0.80		0.424
Low A - Low MP	-0.46	0.31	-1.06	0.15	-1.49		0.137
	log Interblink Time						
Conditions	**Time trend**	**SE**	**95% CI**		**z-ratio**		**p-value**
High A - High MP	***0.034***	***0.014***	***0.007***	***0.061***	***2.49***		***0.013***
High A - Low MP	***0.040***	***0.015***	***0.010***	***0.070***	***2.61***		***0.009***
Low A - High MP	-0.016	0.015	-0.047	0.014	-1.07		0.285
Low A - Low MP	-0.001	0.015	-0.029	0.028	-0.04		0.967
	Blink Duration [ms]						
Conditions	**Time trend**	**SE**	**95% CI**		**t-ratio**	**df**	**p-value**
High A - High MP	0.52	1.79	-2.99	4.03	0.29	1421	0.773
High A - Low MP	***6.84***	***1.67***	***3.57***	***10.11***	***4.11***	***1421***	***<0.001***
Low A - High MP	***6.37***	***1.79***	***2.86***	***9.87***	***3.56***	***1422***	***<0.001***
Low A - Low MP	***-4.34***	***1.80***	***-7.88***	***-0.81***	***-2.41***	***1429***	***0.016***

Table 24. Estimated trends of the effect on time-on-task on blink rate (top), blink duration (middle) and log interblink time (bottom), for each experimental condition. Their standard errors (SE), 95% confidence intervals (95% CI), t-ratios or z-ratios and p-values are shown. Bold italics represent significance at the 0.05 level.

Appendix H. Pairwise comparisons of blink rate, blink duration and interblink time between experimental conditions.

In this section we present the pairwise comparisons of the estimated blink rate, blink duration and log interblink time, between experimental conditions at both the start and end of the experimental sessions (minute 0 and minute 30).

	Blink Rate [blinks/min]							
	Minute 0				**Minute 30**			
Conditions	**Diff.**	**SE**	**z-ratio**	**p-value**	**Diff.**	**SE**	**z-ratio**	**p-value**
(HA-HMP) — (HA-LMP)	***7.61***	***2.42***	***3.14***	***0.009***	***7.31***	***2.41***	***3.04***	***0.013***
(HA-HMP) — (LA-HMP)	*5.72*	*2.45*	*2.33*	*0.092*	4.04	2.45	1.65	0.351
(HA-HMP) — (LA-LMP)	3.51	2.39	1.47	0.455	3.23	2.39	1.35	0.530
(HA-LMP) — (LA-HMP)	-1.89	2.62	-0.72	0.889	-3.28	2.62	-1.25	0.593
(HA-LMP) — (LA- LMP)	-4.09	2.73	-1.50	0.438	-4.09	2.73	-1.50	0.439
(LA-HMP) — (LA-LMP)	-2.20	2.62	-0.84	0.836	-0.81	2.62	-0.31	0.990
	log Interblink time							
	Minute 0				**Minute 30**			
Conditions	**Diff.**	**SE**	**z-ratio**	**p-value**	**Diff.**	**SE**	**z-ratio**	**p-value**
(HA-HMP) — (HA-LMP)	***-0.35***	***0.11***	***-3.28***	***0.006***	***-0.36***	***0.11***	***-3.40***	***0.004***
(HA-HMP) — (LA-HMP)	***-0.24***	***0.08***	***-2.86***	***0.022***	-0.14	0.08	-1.65	0.353
(HA-HMP) — (LA-LMP)	-0.19	0.12	-1.53	0.418	-0.12	0.12	-0.97	0.767
(HA-LMP) — (LA-HMP)	0.11	0.13	0.84	0.834	0.23	0.13	1.69	0.328
(HA-LMP) — (LA- LMP)	0.16	0.14	1.16	0.652	0.24	0.14	1.75	0.298
(LA-HMP) — (LA-LMP)	0.05	0.15	0.32	0.988	0.02	0.15	0.11	1.000
	Blink Duration [ms]							
	Minute 0				**Minute 30**			
Conditions	**Diff.**	**SE**	**z-ratio**	**p-value**	**Diff.**	**SE**	**z-ratio**	**p-value**
(HA-HMP) — (HA-LMP)	7.80	12.10	0.65	0.916	-4.85	12.04	-0.40	0.977
(HA-HMP) — (LA-HMP)	3.74	11.17	0.34	0.987	-7.96	11.13	-0.72	0.890
(HA-HMP) — (LA-LMP)	8.19	10.64	0.77	0.867	17.91	10.62	1.69	0.365
(HA-LMP) — (LA-HMP)	-4.06	8.49	-0.48	0.963	-3.11	8.43	-0.37	0.982
(HA-LMP) — (LA- LMP)	0.39	8.63	0.05	1.000	*22.76*	*8.61*	*2.64*	*0.074*
(LA-HMP) — (LA-LMP)	4.45	9.57	0.46	0.966	*25.86*	*9.58*	*2.70*	*0.067*

Table 25. Pairwise comparisons of blink rate, blink duration and log interblink time, between experimental conditions at the start and end of the experiment (minute 0 and minute 30). The estimated differences (Diff.), their standard errors (SE), and t-tests or z-tests results are shown. Bold italics represent significance at the 0.05 level, and regular italics represent significance at the 0.10 level.